5-2008

A Post-Project Assessment of the Provo River Restoration Project: Channel Design, Reconfiguration, and the Re-Establishment of Critical Physical Processes

Randy Ray Goetz
Utah State University

A POST-PROJECT ASSESSMENT OF THE PROVO RIVER RESTORATION PROJECT: CHANNEL DESIGN, RECONFIGURATION, AND THE RE-ESTABLISHMENT OF CRITICAL PHYSICAL PROCESSES

by

Randy R. Goetz

A thesis submitted in partial fulfillment
of the requirements for the degree

of

MASTER OF SCIENCE

in

Watershed Sciences

Approved:

John C. Schmidt Major Professor	Michael N. Gooseff Committee Member
Michelle A. Baker Committee Member	Byron R. Burnham Dean of Graduate Studies

UTAH STATE UNIVERSITY
Logan, Utah

2008

ABSTRACT

A Post-Project Assessment of the Provo River Restoration Project: Channel Design, Reconfiguration, and the Re-Establishment of Critical Physical Processes

by

Randy R. Goetz, Master of Science

Utah State University, 2008

Major Professor: Dr. John C. Schmidt
Department: Watershed Sciences

A physical assessment of the Provo River Restoration Project was undertaken in order to determine how alterations to the channel were designed, the nature of as-built channel morphology, and the performance of the reconfigured channel in terms of achieving frequent (2-year recurrence) bankfull discharge and increasing transient storage. Measures of channelized and reconfigured channel morphology were obtained using total station survey, digital aerial photography, and pebble counts. Results of geomorphic analysis were compared with similar measurements made by a regional consulting company, and stream channel design data, in order to determine that intended mitigation included reducing channel capacity, increasing sinuosity, decreasing pool spacing, and decreasing the size of bed material. Reconfiguration of the channel resulted in somewhat enlarged cross-sections with reduced mean velocities, increased sinuosity, decreased pool spacing, and decreased bed substrate size.

One-dimensional hydraulic modeling suggests that alterations to channel morphology have increased the bankfull channel capacity in most reaches. Modeling results illustrate the fact that the stage of the 2-year recurrence flood is below bankfull at most cross-sections. This result does not follow the intentions of channel design. However, we have observed floodplain inundation in most years since reconfiguration. The occurrence floodplain inundation is being facilitated by overbank flow at a few point locations illustrating the strengths of incorporating variability into design.

Known geomorphic controls on transient storage were reconfigured in manner to potentially increase in-channel and hyporheic components of transient storage. Stream tracer tests were utilized in order to determine the degree to which these alterations affected transient storage. Numerical analysis of stream tracer tests suggests that while the relative area of transient storage increased, average residence time of water in storage, and the mass transfer rate of solute between storage and the stream did not change. This suggests that an extensive hyporheic zone may not have been established. Correlations between hydrologic and geomorphic parameters indicate that in-stream storage may have been increased, and quick-exchange hyporheic flowpaths may have been created.

(295 pages)

CONTENTS

LIST OF TABLES

Table Page

LIST OF FIGURES

CHAPTER 1

INTRODUCTION

The Provo River, flowing through the Heber Valley of central Utah, is considered an important environmental and recreational resource to the state due its historical status as a prime fishery and wildlife habitat corridor. Resource development aimed at supplying agricultural, municipal, and industrial water for Utah's growing population has resulted in some physical and ecological degradation of the Provo River. The Provo River Restoration Project (PRRP) was initiated in order to improve the ecological value of the system.

Frissell and Ralph [1998] describe the restoration of a stream ecosystem as "the process of returning a river or watershed to a condition that relaxes human constraints on the development of natural patterns of diversity." This definition avoids the implications of describing stream restoration as a complete return to a pre-disturbance condition, which is often unrealistic in light of the highly altered state of many watersheds across the country [*Bradshaw*, 1996]. When applied to the Provo River, the term restoration follows this definition. The modern state of altered hydrology and geomorphology of the Heber Valley prohibits pre-disturbance restoration. Recognizing this, the PRRP attempts to reinstall pre-disturbance processes within the limitations of current geomorphic and hydrologic conditions. Thus, the PRRP stands to serve as a valuable experiment in studying of process and effects of large-scale, process based restoration carried out under common constraints. The scientific community asserts that evaluating projects such as the PRRP can benefit the practice and science of restoration [*Wohl et al.*, 2006, *Kondolf*, 1998].

Here we present the results of a study that utilized the PRRP in order to determine the effects of the project on key physical processes. We utilized geomorphic and hydrologic measurements, design documents, and technical reports in order to determine how the PRRP was conceptualized, designed, and built. From this framework, we determine how effective the as-built PRRP was in re-establishing channel/floodplain connections. This was done in two parts, which are described below.

1.0 STUDY DESCRIPTION

1.1 Chapter 2

Chapter 2 presents a post-project assessment of the design and execution of channel reconfiguration of the PRRP, and the performance of the as-built channel in terms of increasing overbank flooding. PRRP managers specifically targeted re-establishing channel/floodplain connection in restoration design [*Utah Reclamation and Mitigation Commission*, 1997]. Channel cross-sections were based on a design capacity that promotes floodplain inundation on a 2-year recurrence [*Allred*, Personal Communication 2006]. Our own geomorphic measurements, and similar measurements made by *Olsen* [2006] are compared with design estimates of channel morphology. This data set is used to characterize the intended mitigation to impaired channel form, the achieved reconfiguration of the channel, and discrepancies between the two. We then use a one-dimensional hydraulic model to estimate the water surface elevations of several discharges bracketing the 2-year recurrence flood. We use modeling results to compare water surface elevations with as-built channel capacity, and discuss the potential occurrence of overbank flooding in reconfigured reaches.

There are several aspects of the PRRP that make it a potentially successful project The scale of the PRRP is one factor that could increase the chances for successful restoration. *Shields et al.* [2003] suggest that implementing restoration at the reach-scale may be more effective at rehabilitating stream systems than projects that only employ localized treatments. The PRRP falls into the reach-scale restoration category, having reconfigured approximately 16 km of river channel and floodplain in the Heber Valley of northern Utah. Stated goals such as increased frequency of floodplain inundation illustrate a process-based approach taken in PRRP design. *Kondolf* [1998] suggests that a process-based approach to restoration may improve chances for sustained success. There is extensive literature that considers the importance and details involving geomorphic process in stream restoration.

Lane [1955] presents an early insight into this issue. This text introduces the hydraulic engineering community to some basic elements of fluvial geomorphology, emphasizing its importance in relation to hydraulic engineering endeavors. Stream restoration, especially large-scale channel reconfiguration, presents a good example of the marriage of engineering and physical science disciplines. *Morris* [1995] presents a more detailed look at the fundamentally geomorphic aspects of stream restoration. He stresses the importance of hydraulic geometry relationships and models of threshold channel conditions when designing channel cross-section and planform attributes. An overriding theme in recent literature stresses the importance of not only considering process and utilization of geomorphic methods, but doing so at the reach or watershed scale [*Bohn and Kershner*, 2002; *Clarke, et al.,* 2003; *Ward et al.*, 2001]. Important considerations include analysis of basin hydrology such as flood magnitude and frequency, analysis of basin sediment transport regime, and determining a range of channel forming discharges.

Several studies have presented the results of failures to utilize current scientific understanding of geomorphic processes operating watershed and reach scales. *Kondolf et al.* [2001] analyzed a channel reconstruction project in a coastal California stream. The reconstruction failed in less than one year. The authors attributed this to a design process that did not take into account historic channel morphology, and did not address current geomorphic processes. *Smith and Prestegaard* [2005] document a similar project failure on a stream in Maryland. In this case, the project was designed based on morphological measurements, and the subsequent designation of a stable channel type. The restored channel failed at a smaller-than-design discharge. Very little detailed information concerning the hydraulic conditions of the current or proposed channel was generated or evaluated prior to design. The authors saw this as a potential reason for the failure of the design channel. The authors concluded that a consideration of the relationship between channel stability and hydraulic conditions at several discharges could improve channel design.

Every time that a restoration project is monitored and documented, valuable information is passed on to the scientific and professional communities. With the recognition of the usefulness of fluvial geomorphic tools in designing successful restoration projects, assessments of projects that use these techniques become important. Thus, the presentation of the results of the PRRP can provide insight into the conception, design, construction, and performance of a process-based restoration project.

1.2 Chapter 3

Chapter 3 presents a portion of our investigation that addresses the effects channel reconfiguration on transient storage dynamics, which are described in the following several paragraphs. We investigated this process using a combination of geomorphic and hydrologic methods. Total station surveys and aerial photo analysis were used to determine how geomorphic controls on transient storage in the cross-section, planform, longitudinal dimensions have been altered in reconfigured reaches relative to channelized reaches. Pebble counts were used in order to calculate and compare the streambed grain size distribution in each reach. Numerical simulation of hydrologic tracer tests was used to estimate several parameters describing transient storage dynamics, and determine how these parameters differ in reconfigured reaches relative to channelized reaches. The influence of particular geomorphic features over transient storage is estimated using statistical correlations. The correlations are used in order to discuss the potential for restoration design to encourage or inhibit transient storage, and in particular hyporheic flow.

Transient storage is a hydrologic process in which solutes (and water) being transported downstream are temporarily sequestered in areas of low velocity, or transient storage areas. One ecologically important transient storage type is the river's hyporheic zone. The hyporheic zone is the shallow subsurface area surrounding a stream where water is exchanged between stream flow and alluvial ground water (Figure 1-1). The hyporheic zone serves as the biological and hydrological intermediary between stream, riparian, and floodplain habitats [*Biksey and Gross*, 2001].

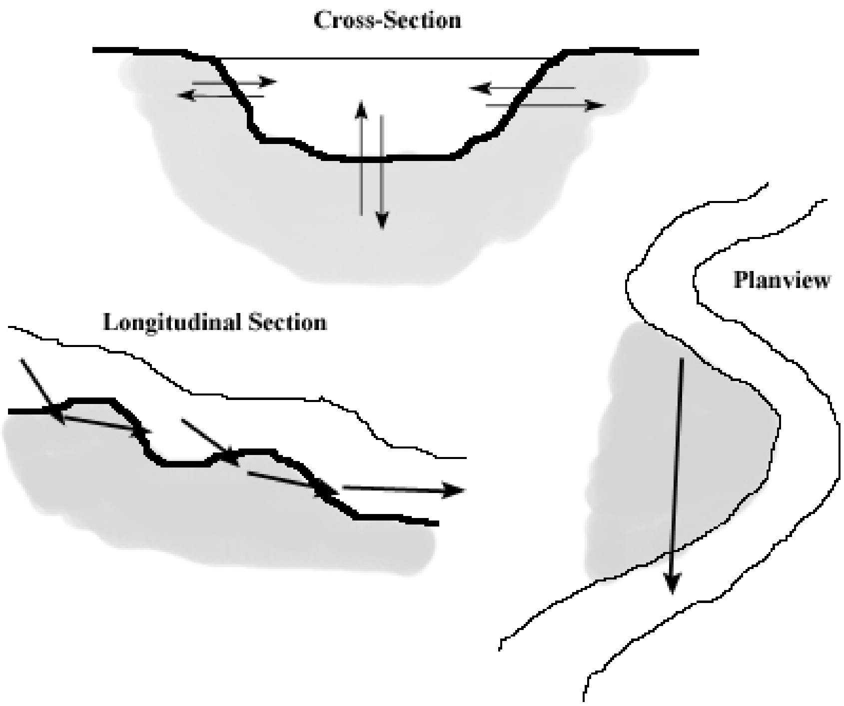

Figure 1-1. Schematic illustrating hyporheic flowpaths in the longitudinal, plan, and cross-sectional views. Geomorphic features controlling these flowpaths are implied. Adapted from Findlay, 1995.

This connection is vital for overall stream ecosystem health, and improved hyporheic function is emerging as a critical metric in evaluating the success of restoration [*Triska et al.*, 1993; *Brunke and Gonser*, 1997; *Fernald et al.*, 2001; *Sophocleus*, 2002].

In the late 1960's and early 1970's, biologists and ecologists became interested in the ecological function provided by stream water moving through subsurface gravels. *Vaux* [1968] speculated that dissolved oxygen required for healthy salmon spawning would be supplied by "intragravel flow" of surface water. He developed equations that predicted that surface water would penetrate the subsurface at streambed convexities, and reemerge at concavities. *Stanford and Gaufin* [1974] presented empirical evidence of hyporheic flow, observing several species of macroinvertebrates, common to streams, in a municipal water supply well. The organisms were found at a depth of 4.2 meters beneath the surface, and about 50 meters lateral to the stream. They concluded that these organisms originated in the stream, and lived some portion of their life-cycle in the gravel interstices of the hyporheic zone.

Concurrently, engineers and physical hydrologists were studying solute transport in surface water. Their research led to the development of a “dead zone” transport model. Conceptually, a dead zone is an area of flow separation, associated with roughness features on the streambed and banks, where surface water is temporarily stored at relatively low velocities [*Thackston and Schnelle*, 1970]. In a text summarizing the state of knowledge of solute transport at the time, *Fischer et al.* [1979] explain that traditional one-dimensional advection-dispersion equations incorporated diffusion, dispersion, and advection of solutes in modeling transport behavior. The use of this type of equation does not accurately simulate solute breakthrough curves obtained by tracer tests in natural systems. Researchers found that concentration data were skewed, with an extended “tail” of observable concentrations at late times. The dead zone model was readily adopted because of its ability to more accurately simulate transport behavior.

Bencala [1983] and *Bencala and Walters* [1983] speculated that the transport of chemically reactive solutes would be significantly affected by intimate contact with reactive sites on streambed sediments. They concluded that this type of contact would require storage of water not only in surface dead zones but in the interstices of cobbles, gravels, and sands of the stream bed. They developed transient storage and kinetic mass transfer models that incorporated these physical concepts. The success of these models in simulating field tracer data supported the concept of subsurface transient storage zones.

Following this research, *Bencala et al.* [1984] used tracer tests to study the interaction of streambed sediment with ions in transport through a small mountain stream. They explicitly invoked “interflow through the sediments” as a transport mechanism, and incorporated it into their experimental design. In order to detect solute in the hyporheic zone, they dug pits from 0.1 to 1.0 meter deep and 0.5 to 5.0 meters from the edge of the stream. By monitoring these wells and hillside inputs, they found the presence of the tracer in several locations outside the stream. They state that, based on their results, the stream channel has “active communication” with the surrounding subsurface.

With the recognition of the hyporheic zone as a distinct component of stream systems, research in the late 80s, and throughout the 90s, continued to improve models, investigate physical controls on hyporheic flow, and study the biogeochemical processes taking place in the hyporheic zone. The disciplines of hydrology and aquatic ecology were often integrated in these studies.

Triska et al. [1989] investigated the role of the hyporheic zone in transporting ecologically important nutrients. By observing uptake of biologically reactive tracers, they concluded that the hyporheic zone was an important component in nutrient transport through the fluvial system. *Duff and Triska* [1990] found that the hyporheic zone facilitated changes in water chemistry. They specifically found that, as water moved away from the channel through the hyporheic zone, dissolved oxygen content decreased, and denitrification potential increased. *Triska at al.* [1993] further investigated nutrient transport and transformation by using tracers to delineate exchange pathways between the hyporheic zone and the riparian zone. They found gradients in concentration and residence time of nutrients, such as nitrate, along these pathways. They concluded that the hyporheic zone is an important link in the ecological continuum of the fluvial system. Research during this period established the hyporheic zone as a crucial ecotone that served to link stream, riparian, and hillslope habitats [*Bencala*, 1993; *Findlay*, 1995]. Current research continues to reveal the ecological importance of the hyporheic zone. *Baxter and Hauer* [2000] recently documented that Bull trout redds were preferentially built in locations of downwelling stream water. *Pepin and Hauer* [2002] have documented streambed algal diversity and abundance differences in relation to upwelling and downwelling locations. *Brunke et al.* [2003] found that the heterogeneity of hyporheic flowpaths creates a patchwork of invertebrate communities that sustains biodiversity in the floodplain. Because hyporheic flow facilitates important ecologic processes, proper hyporheic function is a potential foundation upon which restoration success may depend.

Several researchers have explicitly stated that restoration of hyporheic flow may prove critical for successful improvement of stream restoration's prime motivator: ecological health. *Vervier et al.* [1993] found that hyporheic flow through bends and point bars increased nutrient cycling, and went on to suggest that features conducive to such hyporheic processes should be incorporated into restoration design whenever possible. Stream fauna depend on these nutrient-cycling processes. *Collier et al.* [2004] concluded that restoration of hyporheic function is important to recolonization of certain macroinvertebrate species in degraded streams. *Poole and Berman* [2001] suggests that hyporheic flow may be the most important natural mechanism for attenuation of temperature fluctuations. They suggest that restoration of hyporheic flow should be included in designs intended to mitigate stream temperature degradation. By investigating the influence of channel restoration on hyporheic flow, we can determine the extent to which the PRRP has increased surface water/ground water exchange. Research concerning the physical hydrology, and geomorphic controls of the hyporheic zone, informs and motivates our efforts.

Harvey and Bencala [1993] found that water enters the subsurface at convexities on the streambed often associated with the heads of riffles. Subsurface water returns to the channel at concavities associated with transitions of riffles into pools. They concluded that breaks in the slope of the streambed, and concavities in the water surface profile, generate head gradients that cause the movement of surface water into and out of the streambed.

Kasahara and Wondzell [2003] found that the topographic features responsible for driving hyporheic exchange are dependent on the geomorphic features of the stream in question. They studied several streams of different size. Step-pool units generated hyporheic flow in the relatively straight and steep, second-order stream. These morphologic units created relatively quick exchange along short flow paths. They found that pool-riffle sequences, split channels, meanders, and secondary channels created hyporheic exchange flows in their study streams as well. Hyporheic flow at this scale occurred at longer residence times, as water moves slowly through bars and meander bends.

Anderson et al. [2004] attempted to use bed form size and spacing, and average water surface concavity (AWSC) as metrics to predict the nature of upwelling and downwelling in several geomorphically distinct streams. The lengths of flowpaths scaled positively with the spacing between step-pool units. The greater the AWSC, the greater were the vertical head gradients driving hyporheic exchange. AWSC decreased with basin size, indicating that the magnitude of vertical head gradients decreased also. In general they found that, with increasing basin size, the lengths of flowpaths increases, and the potential for hyporheic flow decreases due to decreased magnitudes in vertical head gradients.

Gooseff et al. [2005] developed relationships between the basin size and streambed morphology in order to predict the importance of bed form size and sequence. They found that for idealized reaches, hyporheic flowpath lengths increased systematically downstream as bed form wavelength increased. For surveyed reaches, they found that a variety of flowpath lengths existed within a single reach. Another aspect of the stream morphology that determines the extent of hyporheic exchange is the nature of the alluvial sediments adjacent to the stream. The amount of water and solute that can enter the subsurface is limited by the hydraulic conductivity of the sediments. Sediment size, distribution, and transport may all interact to influence hyporheic exchange. In a controlled flume experiment, *Packman and McKay* [2002] found that the preferential deposition of clay particles in downwelling regions greatly reduced hyporheic exchange. Streambed clogging by a relatively small amount of fine grain sediment effectively decreased the permeability and porosity of the streambed sediments at the surface-subsurface interface. Clogging essentially isolated deeper streambed sediments from interaction with surface water.

The influence of channel morphology on the function of transient storage has been established through the previously mentioned studies. The PRRP and similar projects are excellent laboratories for testing hypotheses that are based on our understanding of the mechanisms governing transient storage, and the potential effects of restoration on various components of the process. The PRRP provides the opportunity for comparison of pre- and post-project conditions, to assess the details of the physical rearrangement of the channel, and the chance to gain insight into the impacts of common techniques such as compaction through excavation of alluvium. It is our intention to provide results that can increase the success of stream restoration projects whose goals include reestablishing a dynamic connection between the channel, the alluvial aquifer, and the floodplain.

REFERENCES

Anderson, J.K., S.M. Wondzell, M.N. Gooseff, and R. Haggerty (2004), Patterns in stream longitudinal profiles and implications for hyporheic exchange flow at the H.J. Andrews Experimental Forest, Oregon, USA, *Hydrological Processes*, 18, doi:10.1002/hyp.5791.

Baxter, C.V., and F.R. Hauer (2000), Geomorphology, hyporheic exchange, and selection of spawning habitat by Bull Trout (Salvelinus confluentus), *Can. J. Fish. Aquat. Sci.*, 57, 1470-1481.

Bencala, K.E. (1983), Simulation of solute transport in a mountain pool-and-riffle stream with a kinetic mass transfer model for sorption, *Water Res. Res.*, 19 (3), 732-738.

Bencala, K.E. (1993), A perspective on stream-catchment connections, *J. N. Am. Benth. Soc.*, 12, 44-47.

Bencala, K.E. and R.A.Walters (1983), Simulation of solute transport in a mountain pool-and riffle stream: A transient storage model, *Water Resour. Res.*, 19, 718-724.

Bencala, K.E., V.A. Kennedy, G.W. Zellweger, A.P. Jackman, and R.J. Avanzino (1984), Interactions of solutes and streambed sediment 1. An experimental analysis of cation and anion transport in a mountain stream, *Water Resources Research*, 20 (12), 1797-1803.

Biskey, T.M., and E.D. Gross (2001), The hyporheic zone: Linking groundwater and surface water-understanding the paradigm, *Remediation: The Journal of Environmental Cleanup Costs, Technologies, and Techniques*, 12, 55-62.

Bohn, B.A., and J.L. Kershner (2002), Establishing aquatic restoration priorities using a watershed approach, *Journal of Environmental Management*, 64, 355-363.

Bradshaw, A.D. (1996), Underlying principles of restoration, *Can. J. Fish. Aquat. Sci.*, 53 (1), 3-9.

Brunke, M., and T. Gonser (1997), The ecological significance of exchange processes between rivers and groundwater, *Freshwater Biology*, 37, 1-33.

Brunke, M., E. Hoehn, and T. Gonser (2003), Patchiness of river-groundwater interactions within two floodplain landscapes and diversity of aquatic invertebrate communities, *Ecosystems*, 6, 707-722.

Clark, S.J., L. Bruce-Burgess, and G. Wharton (2003), Linking form and function: towards an eco-hydromorphic approach to sustainable river restoration, *Aquatic Conservation: Marine and Freshwater Ecosystems*, 13, 439-450.

Collier, K.J., A.E. Wright-Stow, and B.J. Smith (2004), Trophic basis of production for a mayfly in a North Island, New Zealand, forest stream: Contributions of benthic versus hyporheic habitats and implications for restoration, *N. Z. J. of Marine and Freshwater Res.*, 38, 301-314.

Duff, J.H., and F.J. Triska (1990), Denitrification in sediments from the hyporheic zone adjacent to a small forested stream, *Can. J. Aquat. Sci.*, 47, 1140-1147.

Fernald, A.G., P.J. Jr. Wigington, and D.H. Landers (2001), Transient storage and hyporheic flow along the Willamette River, Oregon: Field measurements and model estimates, *Water Resour. Res.*, 37, 1681-1694.

Findlay, S. (1995), Importance of surface-subsurface exchange in stream ecosystems: The hyporheic zone, *Limnol. Oceanogr.*, 40 (1), 159-164.

Fischer, H.B., E.J. List, R.C.Y. Koh, J. Imberger, and N.H. Brooks (1979), *Mixing in inland and coastal waters*, Academic Press, New York.

Frisell, C.A., and S.C. Ralph (1998), Stream and watershed restoration. In R.J. Naiman and R.E. Bilby (eds.) *River Ecology and Management: Lessons from the Pacific Coastal Ecoregion*, Springer-Verlag, New York, pp. 599-624.

Gooseff, MN, J LaNier, R Haggerty, and K Kokkeler (2005), Determining in-channel (dead zone) transient storage by comparing solute transport in a bedrock channel-alluvial channel sequence, Oregon. *Water Resour. Res.*, 41, W06014, doi:10.1029/2004WR003513.

Harvey, J.W., and K.E. Bencala (1993), The effect of streambed topography on surface-subsurface water exchange in mountain catchments, *Water Resour. Res.*, 29, 89-98.

Kasahara, T., S.M. Wondzell (2003), Geomorphic control of hyporheic exchange flow in mountain streams, *Water Resour. Res.*, 39, 1005-1019.

Kondolf, G.M. (1998), Lessons learned from river restoration projects in California, *Aquatic Conservation: Marine and Freshwater Ecosystems*, 8, 39-52.

Kondolf. G.M., and E.R. Micheli (1995), Evaluating stream restoration projects, *Environmental Management*, 19, 1-15.

Kondolf, G.M., M.W. Smeltzer, and S.F. Railsback (2001), Design and performance of a channel reconstruction project in a coastal California gravel-bed stream, *Environmental Management*, 28 (6), 761-776.

Lane, E.W. (1955), The Importance of Fluvial Morphology in Hydraulic Engineering, *Cons. Hydr. Engr.*, 745, 1-17.

Morris, S.E. (1995), Geomorphic Aspects of Stream-Channel Restoration, *Physical Geomgraphy*, 16 (5), 444-459.

Olsen, D. (2006), Middle Provo River Draft Monitoring Report, *Technical Report*, URMCC, Salt Lake City, UT.

Packman, A.I., and J.S. MacKay (2002), Interplay of stream-subsurface exchange, clay particle deposition, and streambed evolution, *Water Resour. Res.*, 39, 1097-2012.

Pepin, D. M., and F. R. Hauer (2002), Benthic responses to groundwater-surface water exchange in 2 alluvial rivers in northwestern Montana, *Journal of the North American Benthological Society*, 21, 370-383.

Poole, G.C., and C.H. Berman (2001), An ecological perspective on in-stream temperature: natural heat dynamics and mechanisms of human-caused thermal degradation, *Environmental Management*, 27, 787-802.

Shields, F.D. Jr., R.R. Copeland, P.C. Klingeman, M.W. Doyle, and A. Simon (2003), Design for stream restoration, *Journal of Hydraulic Engineering*, 129 (8), 575-584.

Smith, S.M., and K.L. Prestegaard (2005), Hydraulic performance of a morphology-based stream channel design, *Water Resources Research*, 41, doi:10.1029/2004WR003926.

Sophocleous, M. (2002). Interactions between groundwater and surface water: The state of the science, *Hydrogeology Journal*, 10, 52-67.

Stanford, J. A., and A.R. Gaufin (1974), Hyporheic communities of two Montana rivers, *Science*, 185, 700-702.

Thackston, E.L., and K.B. Schnelle, Jr. (1970), Predicting effects of dead zones on stream mixing, *Journal of the Sanitary Engineering Division Proceedings of the American Society of Civil Engineers*, SA2, 319-331.

Triska, F.J., J.H. Duff, and R.J. Avanzino (1993), Patterns of hydrological exchange and nutrient transformation in the hyporheic zone of a gravel-bottom stream: examining terrestrial-aquatic linkages, *Freshwater Biology*, 29, 259-274.

Triska, F.J., V.C. Kennedy, R.J. Avanzino, G.W. Zellweger, and K.E. Bencala (1989), Retention and transport of nutrients in a third-order stream in northwestern California: Hyporheic processes, *Ecology*, 70, 1893-1905.

Utah Reclamation Mitigation and Conservation Commission (1997), Water Resources Technical Report, *FEIS*, US Dept. of the Interior, Washington D.C.

Vaux, W.G. (1968), Intragravel flow and interchange of water in a streambed, *Fishery Bulletin*, 66 (3), 479-489.

Vervier, P., M. Dobson, and G. Pinay (1993), Role of interaction between surface and ground waters in DOC transport and processing: Considerations for river restoration, *Freshwater Biology*, 29, 275-284.

Ward, J.V., K. Tockner, U. Uehlinger, and F. Mallard (2001), Understanding natural patterns and processes in river corridors as the basis for effective river restoration, *Regul. Rivers: Res. Mgmt*, 17, 311-323.

Wohl, E., P.L. Angermeier, B. Bledsoe, G.M. Kondolf, L. MacDonnell, D.M. Merritt, M.A. Palmer, N.L. Poff, and D. Tarboton (2005), River restoration, *Water Resour. Res*., 41, 1-12.

CHAPTER 2

A POST-PROJECT ASSESSMENT OF THE PROVO RIVER RESTORATION PROJECT

ABSTRACT

The complex issues influencing the conception, design, and construction of a large-scale stream restoration project complicate restoration research. We implemented a simple conceptual framework to organize a study of the Provo River Restoration Project Heber Valley, Utah. The investigation assesses the history of project design and construction, thereby providing a context for analysis of the post-construction performance of channel/floodplain connection. We measured cross-section, planform, and longitudinal geometry, and characterized grain size distribution in three channelized and three reconfigured study reaches. Our measurements were combined with those gathered by an independent monitoring group, and used to make comparisons with channel design estimates. We determined the magnitude of potential reconfiguration, the magnitude of reconfiguration that was achieved, and the degree of similarity between design and as-built geomorphology. We then used a one-dimensional hydraulic model (HEC-RAS) to estimate water surface elevations for a range of discharges including the design and actual 2-year recurrence event. We estimated the occurrence of overbank flow, and the performance of the project in terms re-establishing a floodplain connection. Significant alteration was planned in all dimensions, with reduction in channel capacity intended to increase floodplain inundation. On average, reductions in channel capacity were not achieved, and substantial differences were found between design and as-built geomorphology in comparisons of most metrics. The 2-year recurrence flood, which has

been larger than estimated in all reaches since reconfiguration, often did not produce overbank stage at the majority of cross-sections in most reaches. However, varying degrees of floodplain inundation have been observed in each year since the reconfiguration began. Overbank flow occurs at the few low-capacity cross-sections that may exist in a given reach. Constructing a channel with a wide range of geometries may provide a mechanism for the response to unexpected variations in hydrology.

1.0 INTRODUCTION

There is a gap between the science of restoration and the practice of restoration that is hindering advancement on both fronts [*Wohl et. al.*, 2005]. A conspicuous lack of post-project assessment has contributed to this situation [*Kondolf and Micheli*, 1995; *Bash and Ryan*, 2002]. *Bernhardt et al.* [2005] compiled a database of over 37,000 stream restoration projects carried out within the US since 1990 and found that monitoring was an integral component of restoration efforts in only about 10% of the cases. The widespread lack of assessment leaves scientists and restoration professionals unable to quantitatively measure physical alterations and the associated effects provided by carrying out a given restoration design [*Giller*, 2005; *Palmer et al*., 2005].

Effective monitoring can be as challenging as successful restoration, and significant research has been devoted to its study [*Jansson et al*, 2005; *Michener*, 1997; *Woolsey et al.*, 2007; *Ziemer*, 1998]. Several primary components have been mentioned in the restoration literature. It is important that a monitoring program be an integral, rather than extraneous, component of a restoration project [*Ralph and Poole*, 2003]. This suggests that a strong, real-time feedback should exist between the planning and execution of monitoring and restoration activities. The collection of baseline data is critical in the planning process, and in quantifying change [*Kondolf*, 1995]. This indicates that monitoring should begin well in advance of restoration activities. The techniques used in any particular project need to be suited to measuring the success of particular project goals. This implies that programs will vary in their scope, length, and in the particular measurements that are made [*Giller*, 2005; *Frissell and Ralph*, 1998; *Ryder and Miller*, 2005]. Studies that provide data on the performance of particular design methods stand to bridge the perceived gap between science and industry. Such investigations are potentially critical in guiding future research and improving the success of restoration.

There are several examples of post-project assessments in the literature. *Smith and Prestegaard* [2005] assessed the hydraulic performance of a restoration project on a Maryland stream. A review of channel design techniques found that several common methods were employed. A design discharge was computed based on estimates of bankfull discharge. Empirical relationships describing relationships between discharge and channel form were employed. The final design produced a channel that was deemed a stable channel type for a standardized classification system. However, post-restoration field measurements and observations led these researchers to conclude that the channel was hydraulically unstable and prone to failure.

Kondolf et al. [2001] provide a similar case study of a California stream in which a retrospective analysis of the design of an unsuccessful restoration project was performed in order to determine what combination of design, construction, and hydrology contributed to project failure. In design, a stable channel type was chosen based on a set of physical measurements applied to a classification scheme. Researchers concluded that designers had failed to acknowledge the historic morphology of the system, and to take into account the current hydrology and land-use practices operating upstream of the restoration reach. Several case studies also present longer perspectives on the success of habitat improvement structures on channel morphology and fish populations [*Schmetterling and Pierce*, 1999; *Thompson*, 2002; *Champoux et al.*, 2003].

Here we present a post-project assessment of the Provo River Restoration Project (PRRP). We investigate the design and construction of this large-scale stream restoration project, thereby providing a context for assessing project performance in terms of re-establishing geomorphic processes that connect the channel and floodplain. Our assessment is based on measurements of channel cross-section, planform, longitudinal profile, and grain size in channelized, and reconfigured study reaches. These data are supplemented by measurements made by *Olsen* [2006], and compared to the proposed design and objectives of the project. The success of reconfiguration in providing channel-floodplain connection, and active geomorphic processes, is assessed using a combination of hydrologic analysis and HEC-RAS hydraulic modeling.

We develop a conceptual model of the planning, design, and construction process to organize our assessment (Figure 2-1). In this paper, we first revisit the planning and design process, using our conceptual model to frame questions regarding the impetus for restoration, the validity of project goals, and the potential effectiveness of proposed mitigation in achieving goals. We then assess the construction process of the PRRP, using our conceptual model to frame questions regarding the accuracy of design execution, and the actual reconfiguration of the Provo River. Finally, we evaluate the performance of the reconfigured channel in providing floodplain inundation on a

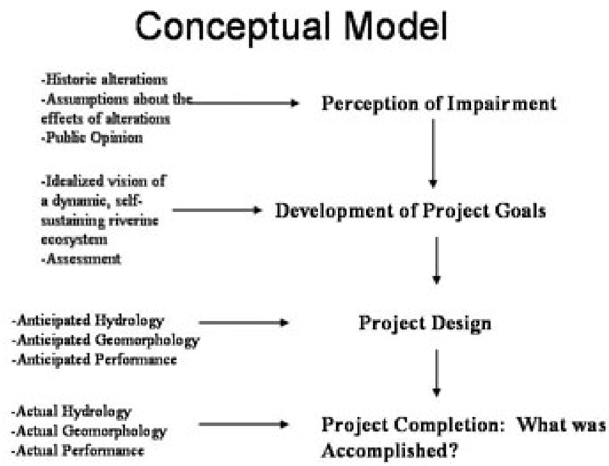

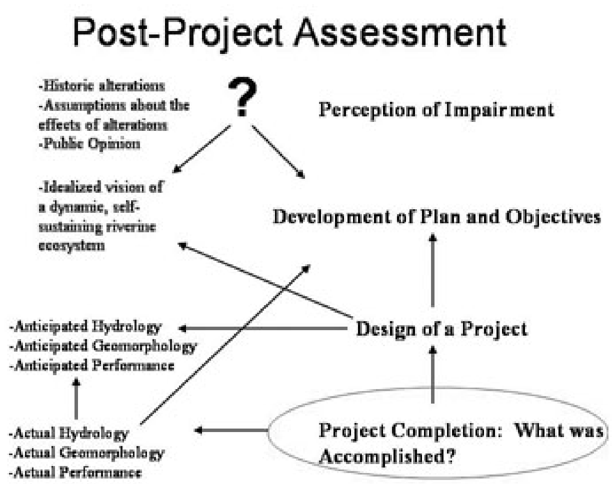

Figure 2-1. The conceptual model used to organize out post-project assessment A), and the reorganization of the model that takes place in asking questions at various levels of the planning, design, build, and performance phases of a project.

recurrence of about 2 years. The challenges facing stream restoration research are apparent in attempting to quantify a process that is influenced socially as well as scientifically, and is subject to the constraints of a large-scale construction project.

2.0 THE PROVO RIVER RESTORATION PROJECT

2.1 Project Area

The PRRP is located in the Heber Valley, an agricultural basin in northern Utah bordered by the Wasatch Mountains to the west and the Uinta Mountains to the east (Figure 2-2). The Provo River ultimately drains to Utah Lake, which in turn drains to the Great Salt Lake. The watershed area draining to the PRRP is 930 km^2 and there are 19 km of channel located in the Heber valley. The mean annual flow and the mean annual flood were 5.3 m^3/s and 35 m^3/s respectively, between 1938 and 1948, before significant water development occurred (USGS gages 10155500 and 10155000). Peak flows typically occurred in late May or June during spring snowmelt.

2.2 Water Resource Development and Associated Environmental Impacts

During the 20th century, two major water resource development projects occurred in the Heber Valley [*Utah Reclamation Mitigation and Conservation Commission*, 1997]. These were the Provo River Project (PRP) and the Central Utah Project (CUP). As part of the PRP, completed between 1938 and 1958, trans-basin diversions from the Weber and Duchesne Rivers were constructed in 1948 and 1952, respectively, causing substantial increases in the magnitudes of both baseflow and peak flow (Figure 2-3).

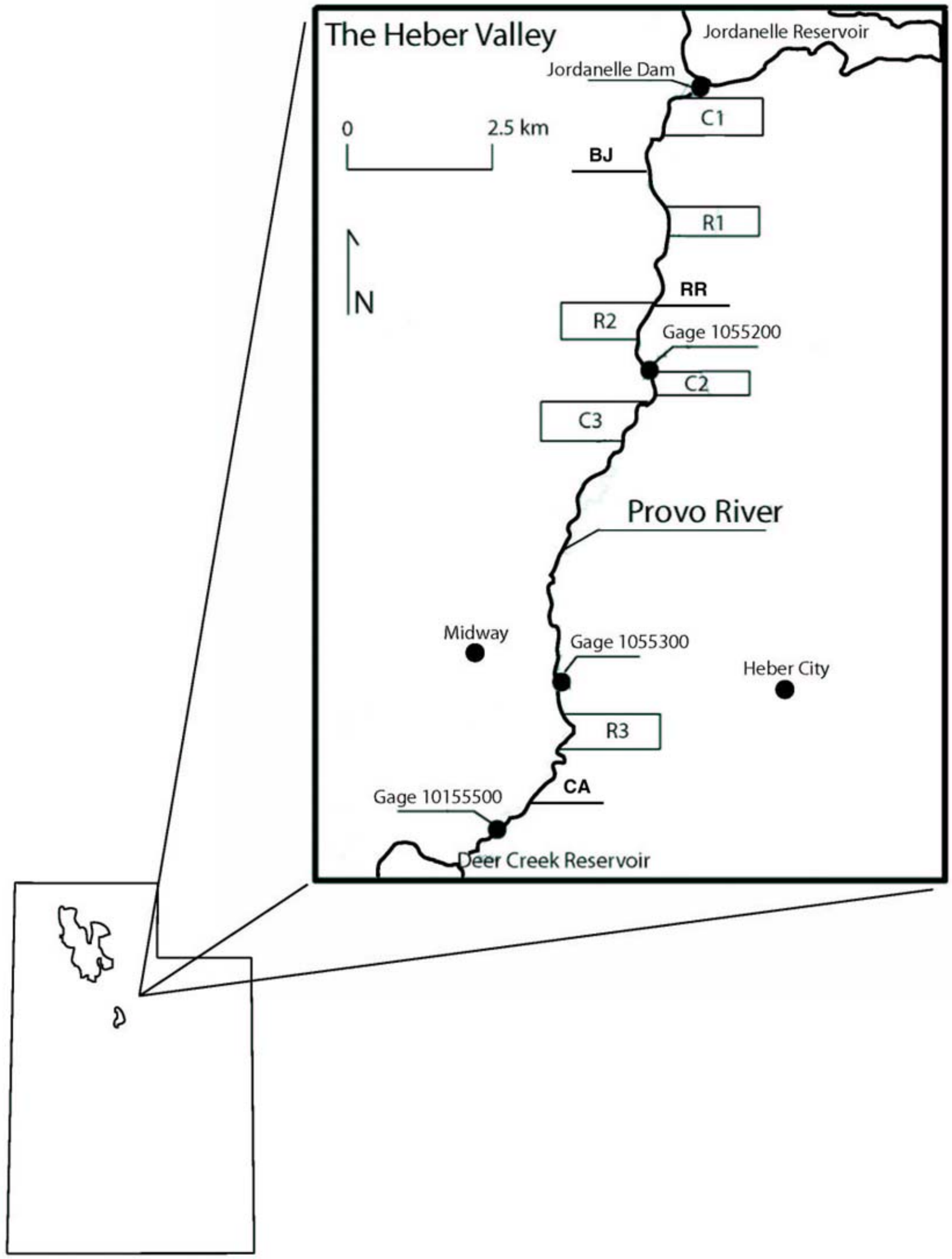

Figure 2-2. Map showing the project area within the Heber Valley, study reaches, the course of the Provo River, water storage facilities, and gages used in hydrologic analysis.

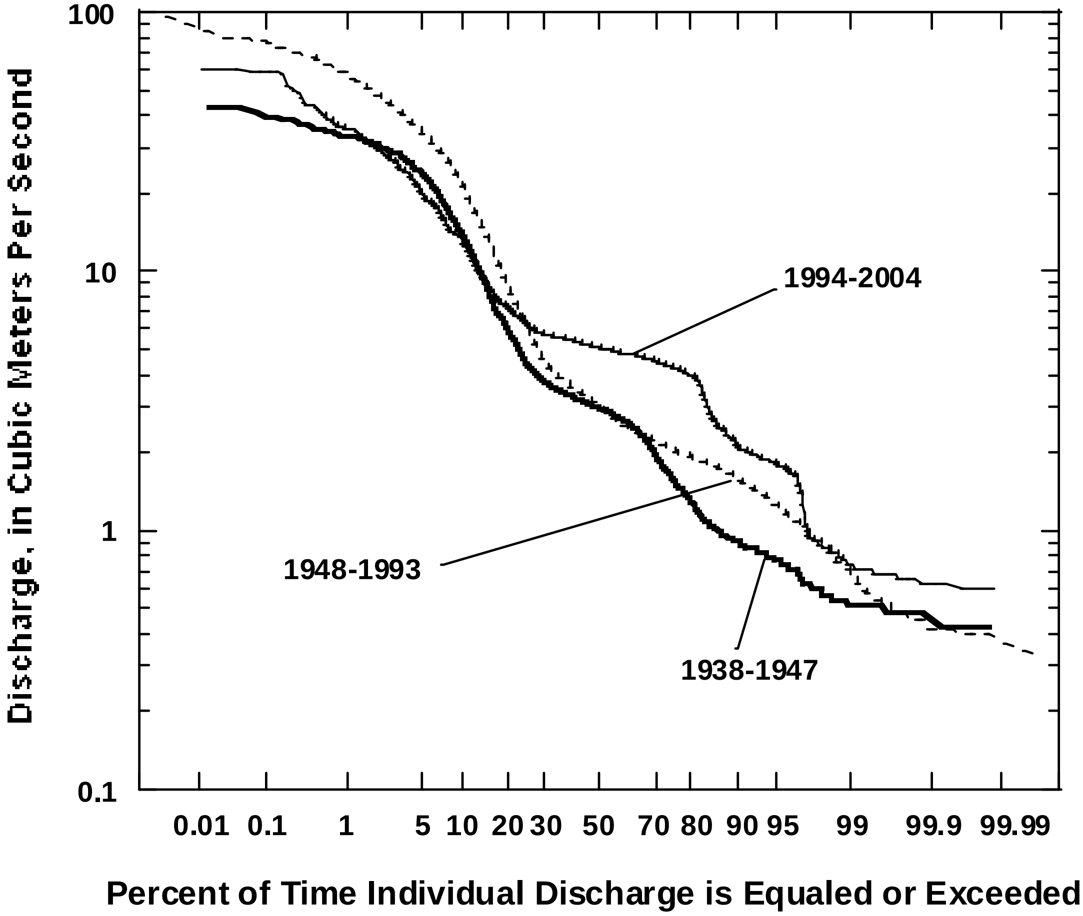

Figure 2-3. Flow duration curves developed from mean daily discharge data gauging stations near Charleston (USGS gage 10155500) and Hailstone (USGS gage 10155000) for the pre-development period (1938-1948), the main development period (1948-1993), and the period following the closure of Jordanelle Dam (1993-2004).

Deer Creek Dam at the downstream end of the Heber Valley was completed in 1941 to store surplus water for subsequent agricultural, municipal, and industrial use [*Central Utah Water Conservancy District*, 1994]. The additional inflow was too large for the existing channel capacity and created significant flood hazards in the Heber Valley. In response, the Bureau of Reclamation initiated the Provo River Channel Revision Project, completed between 1960 and 1965. To mitigate flood hazards, the channel was relocated, straightened, enlarged, and confined between dikes. The revised channel wascapable of containing 122 m^3/s, which was the projected 100-yr flood under the augmented flow regime.

Congress authorized the CUP in 1956 [*Utah Reclamation Mitigation and Conservation Commission*, 1997]. Jordanelle Reservoir, which began to fill in 1993, was constructed as a major component of the Bonneville Unit of the CUP. The reservoir stores water for municipal and industrial use, mainly on the Wasatch Front. The reservoir, located at the upstream end of the Heber Valley, further alters the hydrologic regime and effectively blocks upstream sediment supply to the Provo River in the Heber Valley.

The National Environmental Policy Act (NEPA) of 1969, obligates the federal government to assess the negative environmental impacts of reclamation activities. In 1992, the Central Utah Project Completion Act (CUPCA) was passed in order to authorize mitigation for the CUP. The Utah Reclamation Mitigation and Conservation Commission (URMCC), authorized by the CUPCA, ensures NEPA compliance, and carries out mitigation efforts. The PRRP was a primary tool in this mitigation.

The PRRP was intended to "make modifications to the shape, slope, and alignment of the Provo River between Jordanelle Dam and Deer Creek Reservoir" [*Utah Reclamation Mitigation and Conservation Commission*, 1997]. The high, rip-rap dikes did not allow flow to inundate the floodplain, and confined flow such that depths and velocities in the channel during peak discharge were large. Thus, the channel was laterally disconnected from its floodplain and riparian corridor [*Stromberg et al.*, 1999]. The objective of the modifications was to “create a more naturally functioning river system, and thereby enhance biological productivity and diversity of fish habitat, riparian, and other environmental resources in the Project Area” [*Utah Reclamation Mitigation and Conservation Commission*, 1997].

The Final Environmental Impact Statement [*Utah Reclamation Mitigation and Conservation Commission*, 1997] describes the methods proposed to achieve the desired modifications: “the Proposed Action would reconstruct and realign a majority of the existing river channel and floodplain system into a meandering riffle-pool sequence to re-create a naturally functioning river channel that is re-connected with its floodplain.” The reconstructed Provo River was intended to be subject to natural geomorphic processes resulting in a dynamic channel: “Where possible, the river channel would be allowed to adjust its alignment within the designed meander width in response to changing hydrologic or geomorphic factors.” These statements represent the perception of impairment and objectives of restoration that guided channel design and set standards for success. They are qualitative, and set a wide target for restoration.

2.3 PRRP Channel Design

Allred [Personal Communication, 2006] provided us with values for several channel geometry metrics. These values were used for comparison with measured and supplemental channel geometry values. The following section provides methods for computation of design estimates of channel geometry values. These estimates were used as guidelines in planning potential channel layouts. As channel construction proceeded, designers referenced several viable layout options. Frequently, unrecorded changes were made in the field.

2.3.1 Design Hydrology

The initial step in channel design for the PRRP was determining a design discharge that would provide a basis for determining channel capacity. The release schedule for Jordanelle Dam was developed using modern delivery requirements, and a synthetic 40-year flow history developed from measured mean monthly discharge for a 40-year period between 1950 and 1989. A Log-Pearson type III flood frequency analysis was performed using maximum instantaneous peaks estimated from this synthetic hydrology. The 2-year recurrence flood is estimated to be 40 m^3/s for the upper valley, and 37 m^3/s for the lower valley. Differences in peak flows between the upper and lower portions of the Heber Valley were projected to occur due to irrigation diversions and return flows. These 2-year recurrence discharges were chosen as the design discharges for the reconstructed Provo River (Figure 2-4). The design discharge for this project is intended to overtop the channel banks about every 2 years.

2.3.2 Design Planform

Allred [Personal Communication, 2006] describes the use of several studies empirically relating variables such as slope, or grain size to discharge for a variety of channel patterns [*Leopold and Wolman*, 1957; *Henderson*, 1963; *Alabyan and Chalov*, 1998]. In a relationship between slope and bankfull discharge, the slope and design discharge of the Provo River plotted with braided stream types, or in a transitional zone

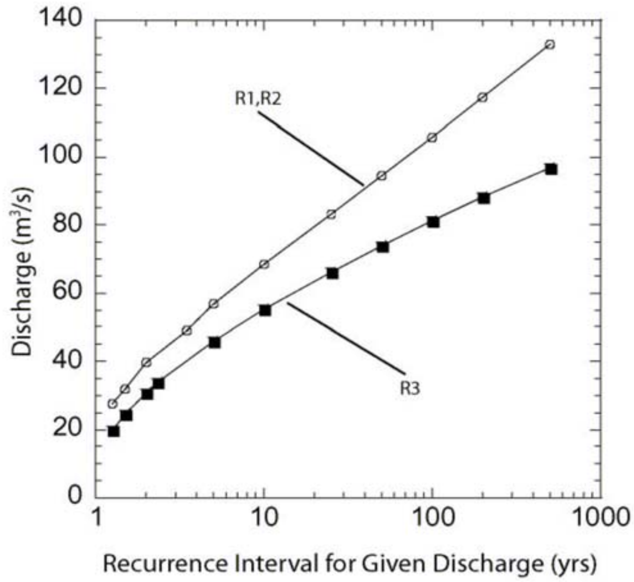

Figure 2-4. Log-Pearson Type-III flood frequency analysis derived from synthetic flow records of the Provo River. Separate analyses were conducted for R1-2, and R3.

between braided and meandering streams. In a similar relationship between bankfull discharge and median grain size, data from the Provo River plotted directly on the line separating meandering and braided stream types. *Allred* [Personal Communication, 2006] found that the Provo River plots between a fairly straight channel with alternating bars, and a fully meandering channel in a relationship between bankfull discharge and stream power.

Given these results, planform design utilized a continuum of channel patterns that incorporated features of braided channels, low sinuosity reaches with alternating bars, and meandering channels (Figure 2-5). In addition to this general planform template, empirical hydraulic geometry relationships compiled by *Williams* [1986] were used to determine more detailed characteristics of meander geometry. He developed many of the relationships independently based on data collected in the field and from maps and

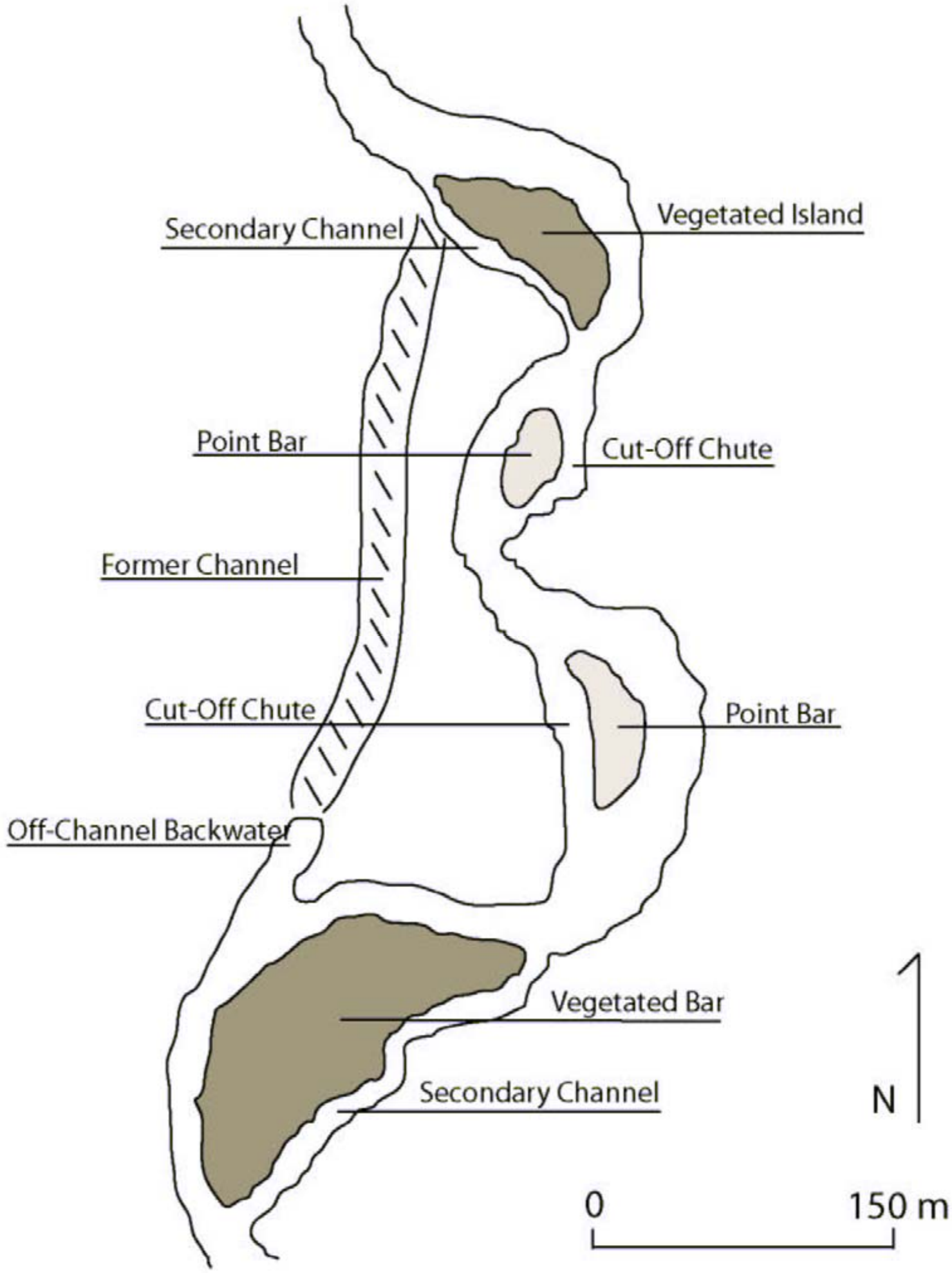

Figure 2-5. Typical planform layout based on the as-built planform of R2. This section includes many features determined to be appropriate in channel design for the PRRP.

diagrams. This framework was used to calculate a range of values for radius of curvature, and meander wavelength. The final pattern chosen for a particular reach depended on the hydraulic feasibility for a particular feature given the local physical constraints.

2.3.3 Design Cross-Section Geometry

Williams [1986] provides empirical relationships between bankfull discharge and characteristics such as width, area, and width-to-depth ratio, and was therefore used to target values for several cross-section parameters. Designers used their design discharge (the 2-year recurrence flood) and calculated a range of values for each parameter. Average values were used as initial inputs into a HEC-RAS hydraulic model in order to simulate flow through the proposed geometry. Thus, cross-section form was iteratively changed until the desired stage/discharge relationships were developed.

2.3.4 Design Longitudinal Profile

The longitudinal profile of the PRRP was designed to conform to the hydraulic framework of the proposed channel pattern and cross-section geometry, and to provide in-stream habitat. The longitudinal profile proposed for the PRRP was a semi-rhythmic riffle-pool pattern. In order to mimic natural riffle-pool sequences, designers located pools at the outside of meander bends and riffles at the shallow inflection points between meanders. The spacing of these features was planned to be 6 times the average bankfull width for the upper valley and as 6.5 times the average bankfull width for the lower valley.

2.3.5 Design Grain Size Distribution

Prior to reconfiguration, two separate grain size distributions were determined using point counts [*Wolman*, 1954]; one for the upper valley, and one for the lower valley. Designers decided that sediment size in reconfigured reaches should be about 10% finer than the measured distributions (Figure 2-6).

2.4 PRRP Monitoring

Monitoring of the PRRP channel was conducted in 2004 and 2005 [*Olsen*, 2006]. Monitoring efforts focused on assessing the post-project physical framework and geomorphic processes that make up the physical template for a restored riverine ecosystem. We incorporated cross-section data in our comparison of channel geometry. Other results of monitoring, such as time series of channel geometry measurements and sediment transport rates, are used to provide context in the discussion of our results.

3.0 METHODS

3.1 Study Reach Designation

We established 3 channelized (C1-C3) and 3 reconfigured (R1-R3) study reaches in fall 2004 (Table 2-1, Figure 2-2). All channelized reaches were reconfigured subsequent to our measurements. Study sites were chosen principally on the basis of accessibility and spatial distribution. Reach lengths were a minimum of approximately 20 bankfull channel widths.

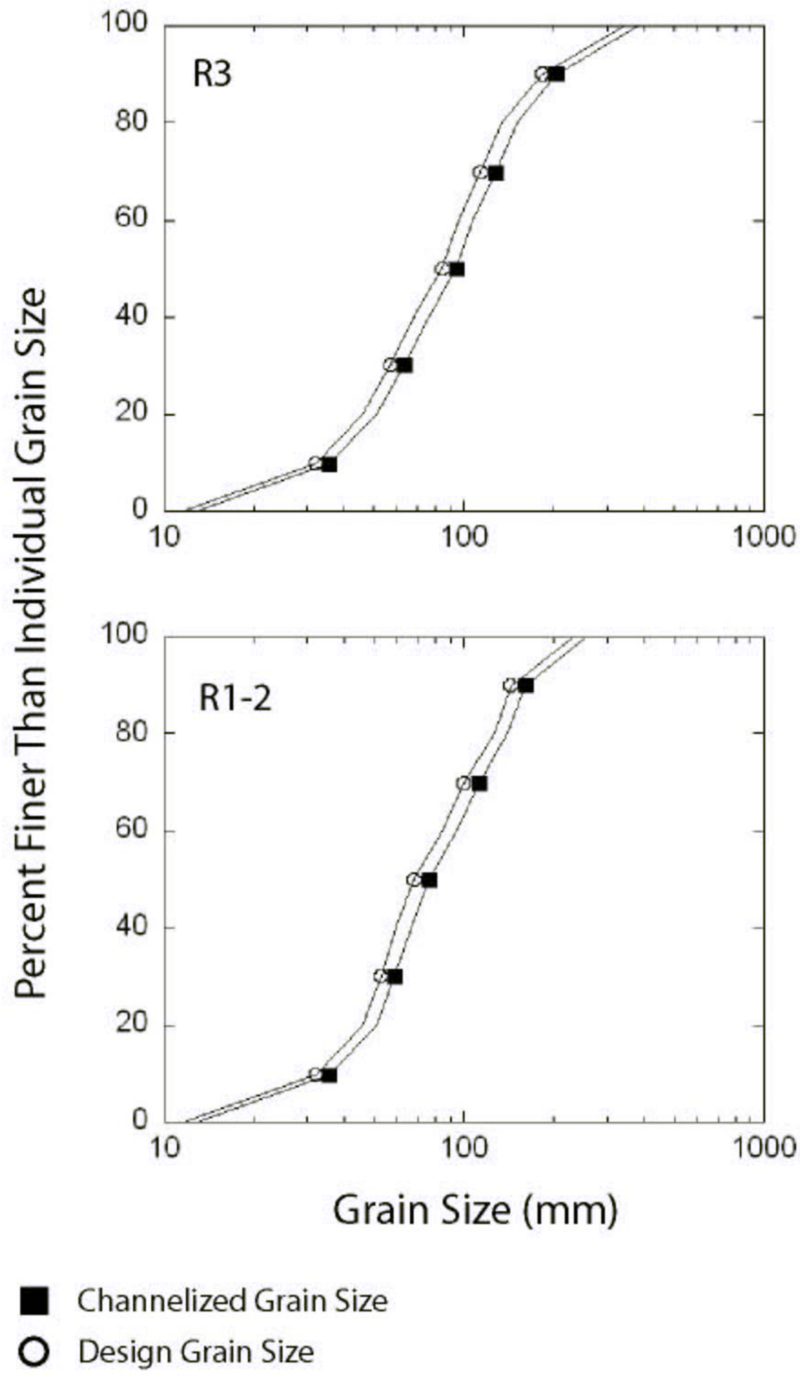

Figure 2-6. Grain size distribution plots generated during the design phase of R1-3. The channelized grain size curves are from field data collected prior to design. Design grain size curves were constructed by reducing the channelized grainsize by 10% at all size fractions.

Table 2-1. Specifications for the three channelized and three reconfigured study reaches.

Reach	Downstream Distance from Jordanelle Dam (km)	Reach Length (m)	Completion Date (yr)	Largest Instantaneous Flow Since Construction (m^3/s, yr)
C1	0.4	534	N/A	N/A
C2	6.5	544	N/A	N/A
C3	7.2	691	N/A	N/A
R1	2.8	639	1999	62, 1999
R2	4.9	872	2000	49, 2004
R3	15.2	632	2003	49, 2004

3.2 Geomorphic Characterization

3.2.1 Measurements of Cross-Section Geometry

It was our intention to determine how cross-section geometry compared in impaired, design, and as-built cross-sections under similar hydraulic conditions. We measured channel cross-sections approximately every bankfull channel width by total station survey. Survey point coordinates can be found in Appendix A, Tables A1-A116. Individual cross-section width typically spanned the levees along channelized reaches or the 2005 high water mark in reconfigured reaches. We simulated the hydraulic conditions for the design discharge in all reaches using HEC-RAS (v. 3.1.3). Channel roughness values were calculated from field measurements using

$$n = \frac{AR^{2/3}S^{1/2}}{v}$$

where n is Manning's roughness coefficient, A is cross-sectional area at the design discharge, R is the hydraulic radius, S is the reach average slope, and v is the cross-section average velocity.

3.2.2 Measurements of Longitudinal Geometry

The longitudinal metrics presented in PRRP design documents are reach average slope and pool spacing. We surveyed channel slope, and used two methods to measure pool spacing. We used the method of *O'Niell and Abrahams* [1984] and *Lisle* [1987] to objectively analyze topographic data and identify significant bedforms. *O'Niell and Abrahams* [1984] evaluated elevation differences between evenly spaced thalweg survey points. We developed a data set of 10-m spaced thalweg points by Kriging the original survey data. We compared cumulative elevation differences between successive points in a series to a pre-determined threshold value of 1.75 times the standard deviation of all elevation differences for a given reach, as suggested by *O'Niell and Abrahams* [1984]. Lengths of thalweg where cumulative elevation differences were in excess of this threshold were designated as significant bedforms. We used the method of *Lisle* [1987] to calculate the spacing between significant pools. We Kriged the original survey data to sub-meter spacing in order to precisely locate elevations at distances separating riffles and pools. We took the length of riffles at minimum pool depth to be the pool spacing. Thalweg survey points coordinates, and data for bed elevations and residual depth analysis can be found in Appendix B, Tables B1-B24.

3.2.3 Measurement of Planform Geometry

Channel pattern was measured using sub-meter resolution, ortho-rectified, digital aerial photos taken in 2004. Within a geographic information system (GIS), we digitized the channel centerline and generated points at a 10-m interval. We determine downstream directional differences between points [*O'Niell and Abrahams*, 1986]. We identified significant meanders objectively by comparing the cumulative directional change of a series of points against a threshold directional change value of 40 degrees as suggested by *O'Niell and Abrahams* [1986]. We calculated the meander wavelength and minimum radius of curvature of significant meanders. Directional differencing data can be found in Appendix C, Tables C1-C12.

3.2.4 Measurement of Sediment Grain Size Distribution

We determined reach-average streambed sediment size using area-weighted grain size distribution. We conducted surface point counts and determined grain size distributions for pool and riffle facies separately [*Wolman*, 1954]. Then we calculated the total area for each facies using digital aerial photos in a GIS. We area-weighted the grain size distributions for each facies and summed the two weighted distributions, creating a single area-weighted grain size distribution for each reach. We used the D_{16}, D_{50}, and D_{84} fractions in reach comparisons. Point count data, and area-weighting data can be found in Appendix D, Tables D1-D12.

3.3 Post-Project Assessment

We used our channel measurements, those of *Olsen* [2006], and the design values provided by *Allred* [Personal Communication, 2006] to quantify each step in our conceptual model and retrospectively analyze the conception, design, construction, and performance of the PRRP (Figure 2-1). *Allred* [Personal Communication, 2006] used a range of values to constrain design geometry. He estimated the arithmetic mean, high, and low value for each metric. High and low values were set as plus or minus one standard deviation of the mean. We mimicked this method in order to generate values for each channelized and reconfigured reach. Using this range of values, we calculated the percent difference between channelized and design, channelized and as-built, and design and as-built geometry.

Each of our as-built study reaches corresponds directly to the design reach of the same name. BJ corresponds to design reach R1, RR corresponds to design reach R2, and CA corresponds to design reach R3. However, channelized study reaches C1-C3 do not correspond directly to any design or as-built reaches. We averaged values and used one set of channelized conditions for comparison with design and as-built geometry. There were no channelized reaches in the lower portion of the Heber Valley at the time of our study. This situation limits our interpretation of comparisons of reconfigured and design study reaches in the lower valley to the average channelized conditions.

3.3.1 Project Conception

Statements regarding the impaired state of the Provo River, and the guiding image for restoration design were qualitative. In order to effectively quantify project performance, a clear picture of the motivations and goals underpinning the PRRP must be presented. We compare our measurements of channelized geomorphology to qualitative statements of impairment to determine how the perceived impairment of the Provo River matches the quantified morphology of channelized reaches.

3.3.2 Project Design

Technical reports and environmental impact statements associated with the PRRP do not quantitatively describe the magnitude of change that was intended through channel reconfiguration. We compute percent differences between channelized and design metrics in order to determine if intended reconfiguration would potentially achieve project goals.

3.3.3 Project Construction

We calculated percent differences between the as-built geometry of our study reaches and those of *Olsen* [2006], to the average channelized condition in order to determine what level of channel reconfiguration was achieved. This comparison allows us to answer questions regarding the actual achievement of the PRRP, and if that achievement has the potential to achieve project goals. We also compare percent differences between as-built and design channel geometry metrics in order to determine the accuracy of construction. This provides context for our assessment of physical processes and the accuracy in construction that is needed to achieve project goals.

3.3.4 Project Performance: Post-Reconfiguration Hydrology and the Occurrence of Bankfull Discharge

In order to determine if the actual hydrology matched the design hydrology, we calculated flow duration curves and recurrence intervals for periods following the completion of restoration in the reconfigured reaches. We used HEC-RAS to model water surface elevations at several discharges bracketing the design and actual 2-yr discharge.

Visual estimates of bankfull water surface elevations were made on each plotted cross-section within every reconfigured reach. We made these estimates by locating geomorphic features, such as abrupt slope breaks, that expressed the minimum bankfull elevation of the channel. For each cross-section, water surface elevations predicted by HEC-RAS were compared to the estimated bankfull elevation. The discharge corresponding to the closest modeled water surface was chosen as the bankfull discharge estimate at that cross-section. With this data, we estimated how many cross-sections would be at or above bankfull stage for a given discharge, and how many days per year a given discharge would last.

4.0 RESULTS

4.1 PRRP Conception and Design

4.1.1 Channelized Geometry and Perceived Impairment

Development of the water resources of the Provo River and adjacent basins was thought to have resulted in a channel that was geomorphically and hydraulically homogeneous, and disconnected from the floodplain. This perceived impairment was the basis for presenting a case for restoration. We tested the perceptions of impairment by quantifying the channelized morphology of the Provo River.

Our measurements suggest that the perception of impairment that led to the restoration was justified. Channel cross-sections were large and relatively simple (Figure 2-7). Reaches were steep, with long continuous riffles and small distantly spaced pools (Figure 2-8). In two of the three channelized reaches, there were not full meanders sequences. Grain size in channelized reaches was coarse and narrowly distributed. This condition was true for both pool and riffle facies (Figure 2-9).

4.1.2 Design Versus Channelized Geomorphology: Trajectory of Potential Change

PRRP goals for restoration of physical form and process included increasing the geomorphic and hydraulic complexity of the channel, and restoring its connection to the floodplain. We compared our measurements of channelized geomorphology to design values in order to determine if project goals might be achieved through potential reconfiguration.

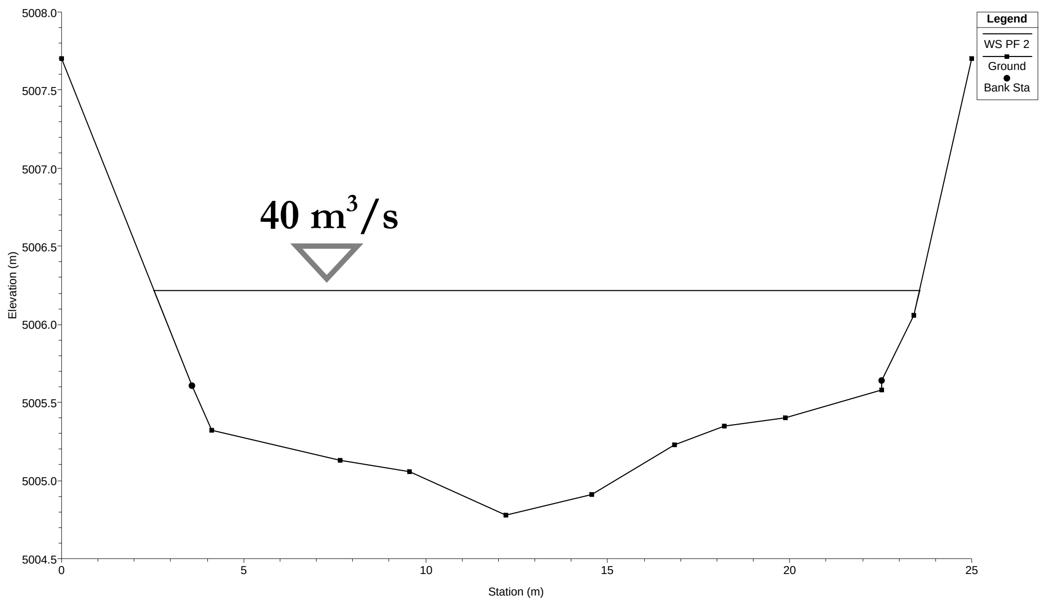

Figure 2-7. A representative channelized cross-section. The estimated 2-year recurrence discharge is contained within the dikes by over a meter.

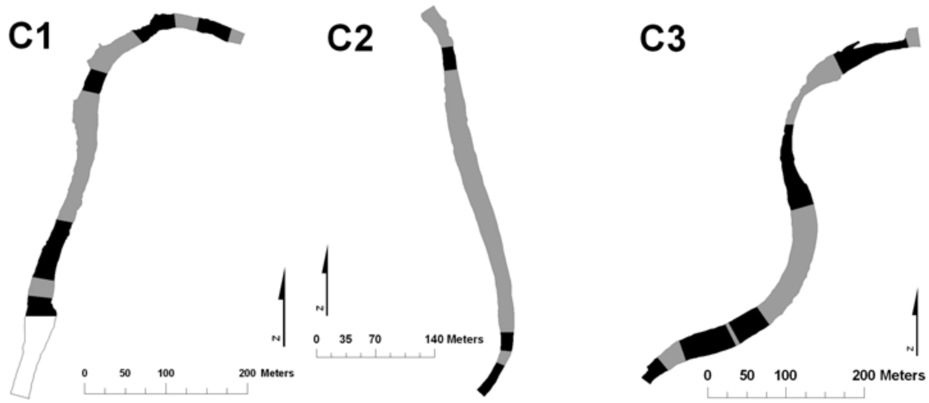

Figure 2-8. Map view of each of the three channelized study reaches. Reaches C1 and C2, are obviously straight, with simplified meander patterns. Grey sections represent riffles, and black sections represent pools. Pools tend to be small, and distantly separated, particularly in C2.

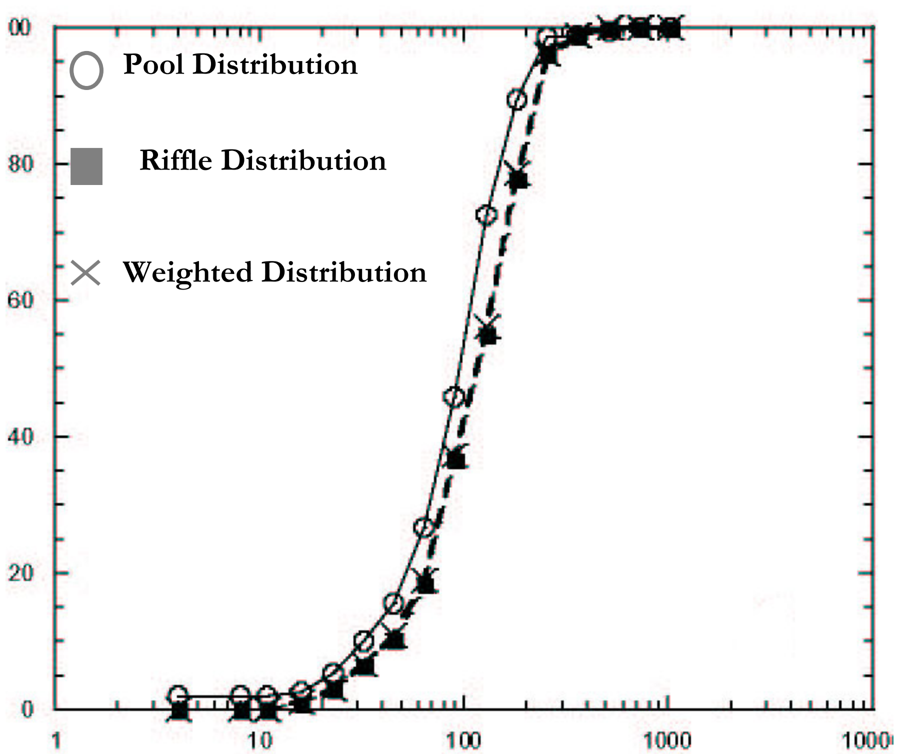

Figure 2-9. A representative grain size distribution for channelized reaches. Distributions between pools and riffles are relatively homogeneous. The predominance of riffles in reach area weights the distribution heavily towards riffles.

Our comparison suggests that the implementation of channel design would produce a channel form that could achieve project goals pertaining to physical processes.

Cross-section design had the potential to decrease bankfull channel capacity relative to the average channelized river, increasing the likelihood of frequent floodplain inundation (Figure 2-10). In R1 and R2 design alterations to the channelized river increased mean depth and roughness, and reduced width, area, hydraulic radius, and velocity relative to the average channelized condition (Table 2-2). Proposed changes for average values were often less than 30% of channelized values in these reaches. However, substantial changes were proposed in the width-to-depth ratio (59.8% to 71.1% reductions for the range of values), and in the low estimates of hydraulic roughness and hydraulic radius (62.1% increase and a 42.4% decrease respectively). In R3 potential alteration to average width, depth, velocity, and roughness values were similar to R1 and R2, though with larger percent decreases in width (47.5%), and smaller percent decreases in depth (9.8%). However, design cross-section area and hydraulic radius had the potential to increase average values in R3 relative to the average channelized condition.

Longitudinal design had the potential to decrease reach average gradient and pool spacing relative to the average channelized condition (Figure 2-11). These potential alterations could have achieved project goals of decreased average velocities at bankfull, and increased habitat complexity at lower flows. In R1 and R2, potential alteration would reduce channel slope of approximately 9.3 % compared to the average channelized slope (Table 2-3). R3 was designed with a slope of 0.0045, a potential 82.2% reduction in slope compared to the average channelized river. It is important to recall that

Table 2-2. Values for cross section metrics in an average channelized condition, design estimates, and percent differences between the two sets of values. Negative percent differences indicate a percent decrease in a design value relative to the average channelized value.

Average Channelized Condition

Parameter	Average	High	Low
Width (m)	31.0	39.7	22.2
Mean Depth (m)	0.7	0.9	0.6
Width/Depth	45.6	65.6	25.7
Bankful Area (m^2)	22.2	27.8	16.6
Manning's Roughness	0.03	0.05	0.01
Hydraulic Radius (m)	0.7	0.8	0.6
Velocity (m/s)	2.1	2.5	1.7

Design Values

	R1			R2			R3		
Parameter	**Average**	**High**	**Low**	**Average**	**High**	**Low**	**Average**	**High**	**Low**
Width (m)	24.4	30.5	19.8	24.4	30.5	19.8	21	27	18
Mean Depth (m)	0.9			0.9			0.8		
Width/Depth	29	40	15	29	40	15	27	40	15
Bankful Area (m^2)	19.0	27.8	13.3	19.0	27.8	13.3	25	42	17
Manning's Roughness	0.04	0.05	0.033	0.04	0.05	0.033	0.04	0.05	0.033
Hydraulic Radius (m)	0.6	0.9	0.4	0.6	0.9	0.4	1	1.8	0.6
Velocity (m/s)	2	2.7	1.4	2	2.7	1.4	1.7	2	1.4

Percent Difference Between Design and Average Channelized Values

	R1			R2			R3		
Parameter	**Average**	**High**	**Low**	**Average**	**High**	**Low**	**Average**	**High**	**Low**
Width (m)	-27.0	-30.4	-12.1	-27.0	-30.4	-12.1	-47.5	-47.2	-23.3
Mean Depth (m)	15.4			15.4			9.8		
Width/Depth	-59.8	-64.1	-71.1	-59.8	-64.1	-71.1	-69.1	-64.1	-71.1
Bankful Area (m^2)	-17.3	-0.2	-25.3	-17.3	-0.2	-25.3	11.1	33.8	2.1
Manning's Roughness	27.8	9.5	62.1	27.8	9.5	62.1	27.8	9.5	62.1
Hydraulic Radius (m)	-18.2	5.7	-42.4	-18.2	5.7	-42.4	29.1	52.9	5.1
Velocity (m/s)	-4.3	9.2	-22.7	-4.3	9.2	-22.7	-22.7	-22.6	-22.7

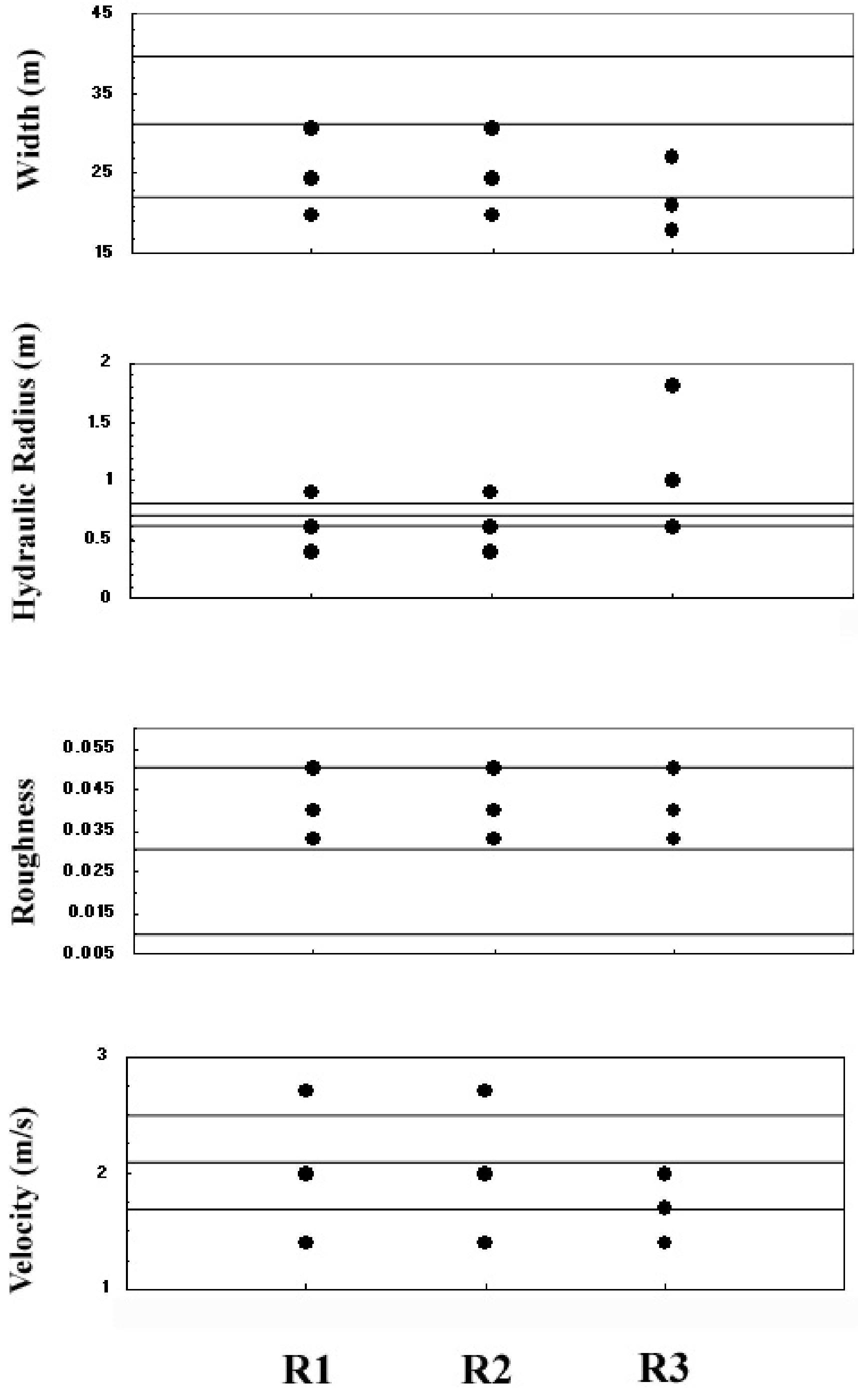

Figure 2-10. Plots displaying the relationship between select design and channelized cross-section values. Design values are represented by solid dots at high, average, and low value positions for each design reach. Solid horizontal lines display channelized conditions with high, average, and low value positions.

measurements in channelized reaches were made in the upstream, higher gradient portion of the Heber Valley. Therefore, the decrease in slope in R3 is a potential overestimate of reductions relative to the average channelized condition. Design pool spacing was set as a multiple of the average bankfull width. Average pool spacing in the channelized river was 4.8 times larger than the average bankfull width. The longitudinal design for R1 proposed an average pool spacing of approximately 6 times the average design bankfull width for this reach. This was the same spacing proposed for R2. R3 was designed with an average pool spacing of 6.5 times the average design bankfull width.

The majority of channelized reaches lacked a statistically significant number of planform features. C1 and C2 were mainly straight channels with a single sharp bend at the upstream end. We used the reach length of C1 and C2 as a minimum meander wavelength to calculate average channelized values. However, use of the single bend radius values resulted in smaller than realistic average channelized minimum radius of curvature, so this comparison was not made. Substantial decreases in average meander wavelength were proposed for all study reaches (Figure 2-12). In R1, the average design wavelength of about 280.4 m represented a potential decrease of approximately 45% compared to the average channelized condition (Table 2-4). For R2, the same average design wavelength was used. For R3, which is at the downstream, lower gradient end of the valley, the average design wavelength of 241 m represented a potential decrease of about 68.7% from the average channelized condition.

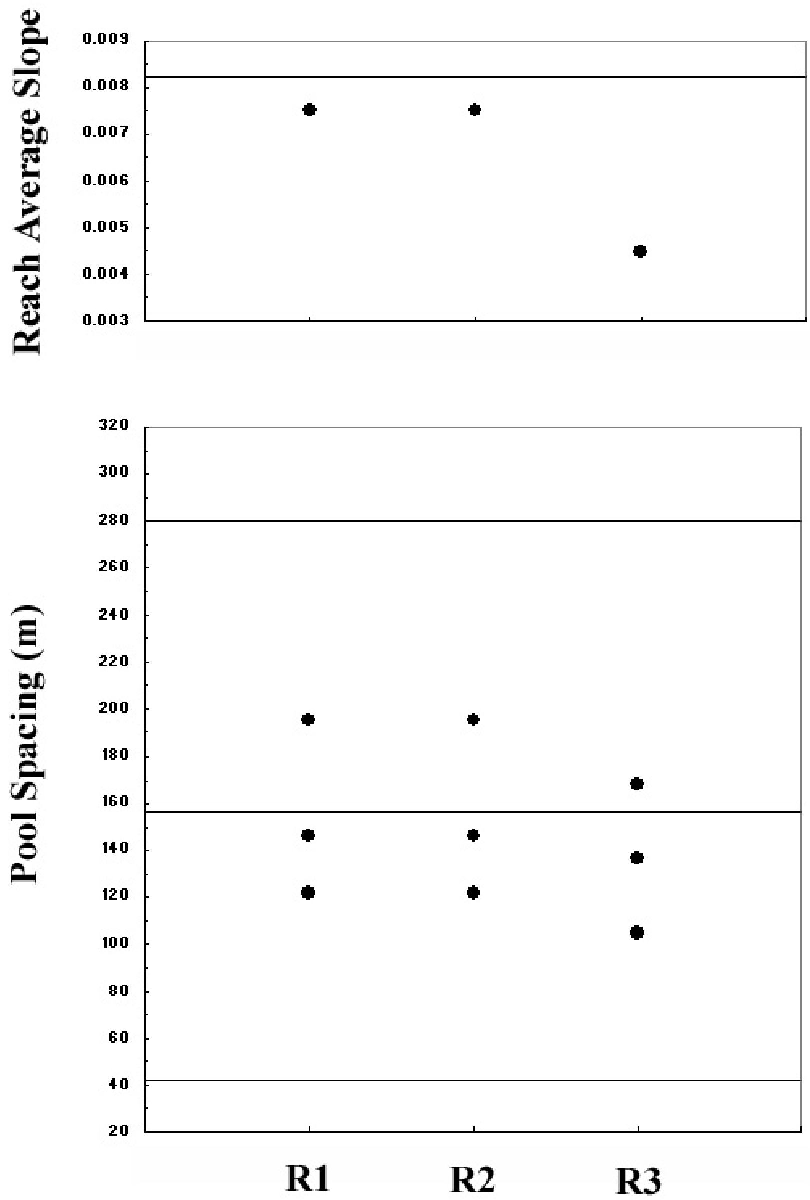

Figure 2-11. Plots displaying the relationship between design and channelized longitudinal values. Design values are represented by solid dots at high, average, and low value positions for each design reach. Channelized values are represented by horizontal lines at high, average, and low positions where applicable. For reach average slope, only average values are presented for both design and channelized reaches.

Table 2-3. Average channelized and design values for longitudinal metrics, and percent differences from a comparison of design values to average channelized values. Negative values represent percent decreases in proposed channel geometry relative to channelized values.

Average Channelized Condition

Parameter	Average	Low	High
Channel Slope	0.0082		
Pool-to-Pool Spacing (m)	156.8	41.2	280.8

Design Values

	R1			R2			R3		
Parameter	**Average**	**Low**	**High**	**Average**	**Low**	**High**	**Average**	**Low**	**High**
Channel Slope	0.0075			0.0075			0.0045		
Pool-to-Pool Spacing (m)	146.3	121.9	195.1	146.3	121.9	195.1	136.5	105	168

Percent Difference Between Design and Average Channelized Values

	R1			R2			R3		
Parameter	**Average**	**Low**	**High**	**Average**	**Low**	**High**	**Average**	**Low**	**High**
Channel Slope	-9.3			-9.3			-82.2		
Pool-to-Pool Spacing (m)	-7.2	66.2	-43.9	-7.2	66.2	-43.9	-14.9	60.8	-67.1

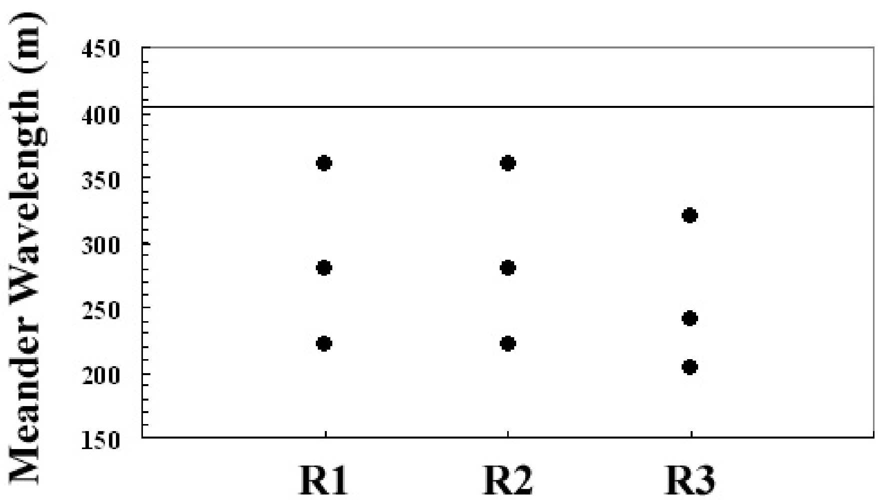

Figure 2-12. Plot displaying the relationship between design and channelized meander wavelength. Design values are represented by solid dots at high, average, and low value positions for each design reach. The average channelized value is represented by the horizontal line.

Table 2-4. Average channelized and design values for planform metrics, and percent differences from a comparison of design values to average channelized values. Negative values represent percent decreases in proposed channel geometry relative to channelized values.

Average Channelized Condition

Parameter	Average	Low	High
Wavelength	406.6	N/A	N/A
Radius	53.7	38.8	135.9

Design Values

	R1			R2			R3		
Parameter	**Average**	**Low**	**High**	**Average**	**Low**	**High**	**Average**	**Low**	**High**
Wavelength	280.4	222.2	360.0	280.4	222.2	360.0	241	203	320
Radius	61.9	49.1	79.6	61.9	49.1	79.6	53	45	71

Percent Difference Between Design and Average Channelized Values

	R1			R2			R3		
Parameter	**Average**	**Low**	**High**	**Average**	**Low**	**High**	**Average**	**Low**	**High**
Wavelength	-45.0			-45.0			-68.7		
Radius	13.1	21.0	-70.8	13.1	21.0	-70.8	-1.5	13.8	-91.4

Increased flows, and decreased sediment flux were believed to have armored the bed of most reaches, leaving a coarse and immobile bed. PRRP designers proposed a 10% reduction to the grain size distribution they measured prior to reconfiguration (Table 2-5; Figure 2-6). The proposed D_{16}, D_{50}, and D_{84} potentially achieved greater reductions in grain size when compared to the measured channelized grain size we measured (Figure 2-13). In reaches R1 and R2, a potential 27.7% decrease in the D_{16} fraction would have resulted from achieving design values, with successively smaller reductions at the D_{50} and D_{84} fractions. Larger percent reductions were proposed for R3, with the largest reduction proposed for the D_{50} fraction.

Table 2-5. Average channelized and design values for planform metrics, and percent differences from a comparison of design values to average channelized values. Negative values represent percent decreases in proposed channel geometry relative to channelized values.

Average Channelized Condition

D_{16} (mm)	D_{50} (mm)	D_{84} (mm)
54.0	96.7	163.4

Design Reaches

Reach	D_{16} (mm)	D_{50} (mm)	D_{84} (mm)
R1	42.3	84.6	153
R2	42.3	84.6	153
R3	42.3	69	135

Percent Differences Between Design and Average Channelized Values

Reach	D_{16} (mm)	D_{50} (mm)	D_{84} (mm)
R1	-27.7	-14.3	-6.8
R2	-27.7	-14.3	-6.8
R3	-27.7	-40.1	-21.0

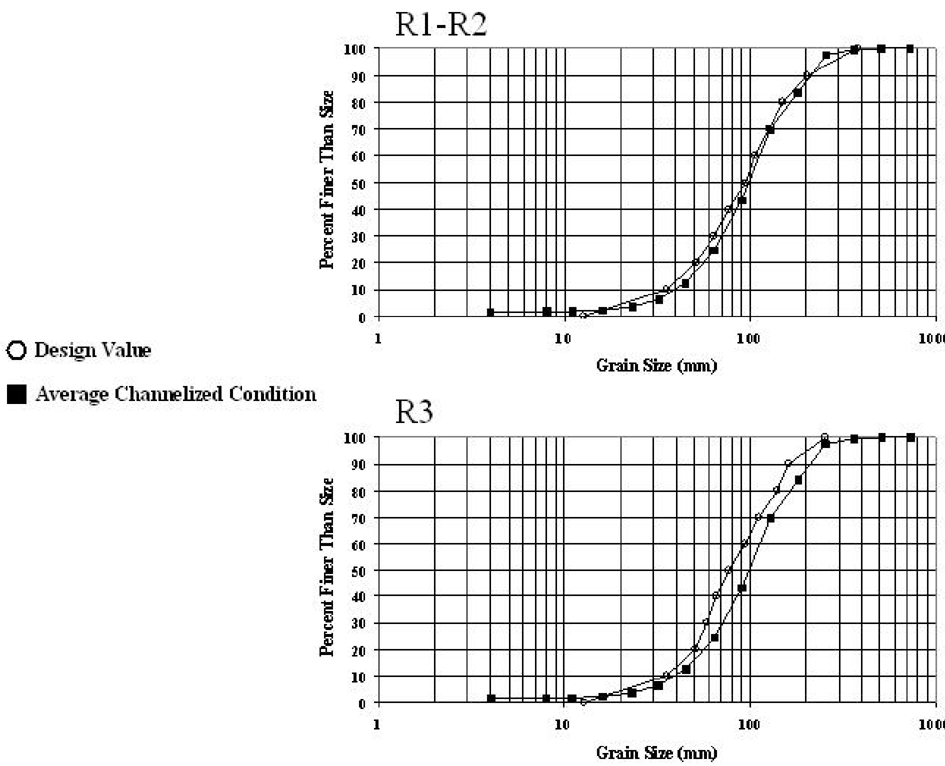

Figure 2-13. Plots of grain size distribution illustrating the difference between the average channelized distribution, and potential alterations proposed in channel design.

4.2 PRRP Construction

4.2.1 As-Built Geomorphology: Achieved Reconfiguration

After assessing plans for reconfiguring the Provo River, we characterized actual channel reconfiguration. We compared reconfigured geomorphology to average channelized conditions in order to determine if desired changes had been achieved (Figure 2-14). Measured cross-sections in R1 and R2 showed increases of less than 20 % relative to the average channelized condition for most metrics over the range of values (Table 2-6). For mean depth and roughness increased values were the desired trajectory. Substantial decreases in velocity in R1 and R2 also follow design objectives. For measurements of reconfigured area, width, and hydraulic radius, increased values failed to follow design potential. In R3, reconfiguration of the channel achieved many of the potential design alterations. The width-to-depth ratio was decreased, as were velocities. Increases were measured in the mean depth, area, hydraulic roughness, and hydraulic radius. Achievement of potential design alteration in BJ includes large percent increases in mean depth that led to a decrease in the width-to-depth ratio, increased mean depth, increased roughness, and decreased velocity. In RR, actual alterations followed a similar trajectory. All proposed changes to cross-section geometry were achieved in CA. Percent reductions in width, width-to-depth ratio, and velocity were measured. Values of the other metrics were increased. As-built longitudinal reconfiguration achieved most of the potential design alterations (Figure 2-15). Channel slope in R2 was reduced by about 18.8% relative to the average channelized slope (Table 2-7).

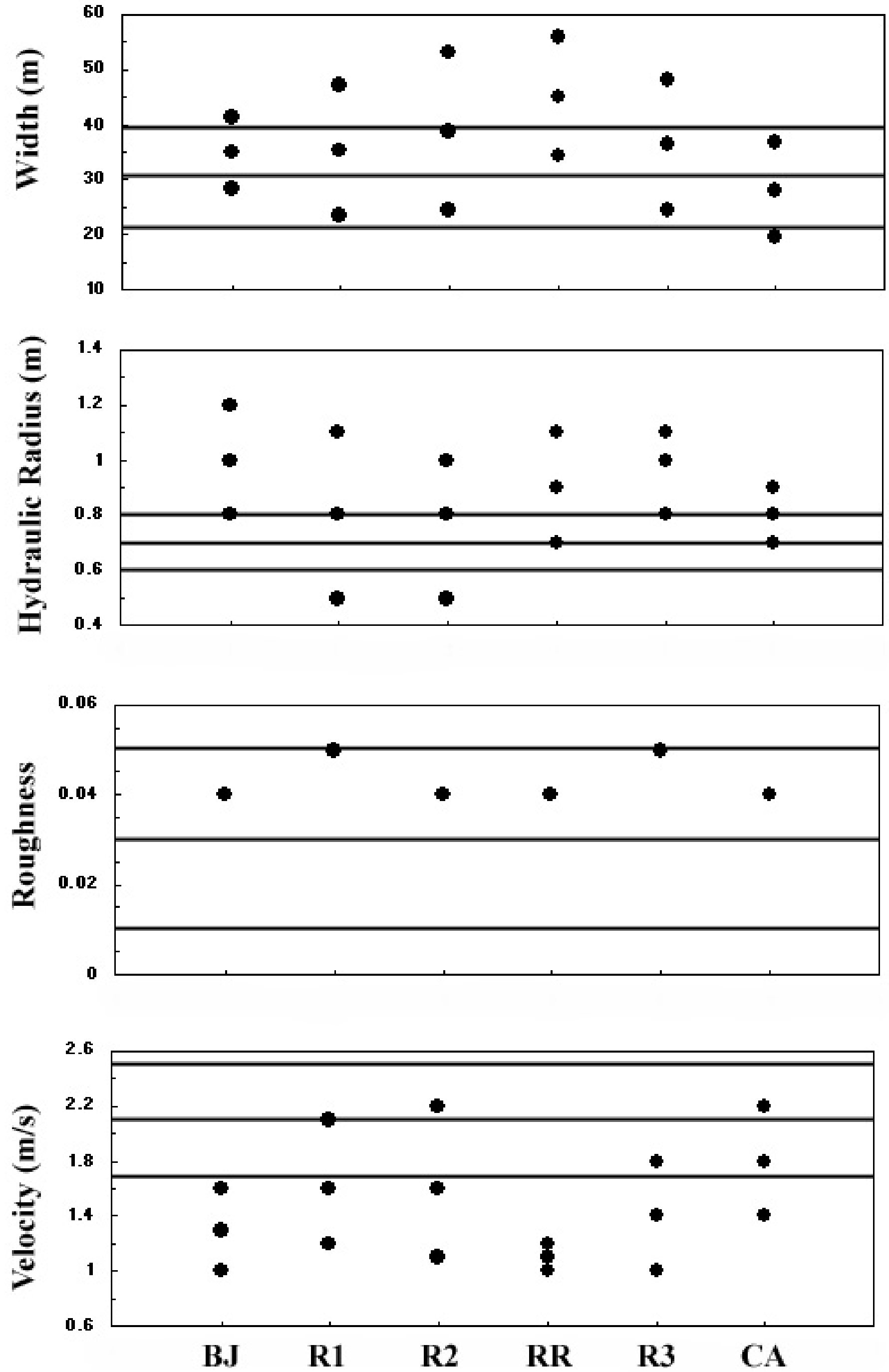

Figure 2-14. Plots displaying the relationship between as-built and channelized cross-section measurements. As-built values are represented by solid dots at high, average, and low value positions for each study reach. Channelized valued are represented by horizontal lines at high, average, and low value positions.

Table 2-6. Average channelized and as-built values for cross-section metrics, and percent differences from a comparison of as-built values to average channelized values. Negative values represent percent decreases in achieved channel geometry relative to channelized values.

As-Built Values

	R1			R2			R3		
Parameter	**Average**	**Low**	**High**	**Average**	**Low**	**High**	**Average**	**Low**	**High**
Width (m)	35.4	47.1	23.6	38.8	53.0	24.6	36.3	48.1	24.5
Mean Depth (m)	0.9	1.2	0.6	0.8	1.0	0.5	1.0	1.2	0.8
Width/Depth	49.7	80.1	19.2	53.1	75.3	31.0	40.5	66.1	14.9
Bankful Area (m^2)	28.5	38.7	18.3	31.1	51.2	10.9	35.0	46.2	23.7
Manning's Roughness	0.05			0.04	0.05	0.03	0.05	0.06	0.04
Hydraulic Radius (m)	0.8	1.1	0.5	0.8	1.0	0.5	1.0	1.1	0.8
Velocity (m/s)	1.6	2.1	1.2	1.6	2.2	1.1	1.4	1.8	1.0

As-Built Values as Measured by Bio-West

	BJ			RR			CA		
Parameter	**Average**	**Low**	**High**	**Average**	**Low**	**High**	**Average**	**Low**	**High**
Width (m)	34.9	41.3	28.4	45.1	55.9	34.3	28.2	36.6	19.8
Mean Depth (m)	1.0	1.2	0.8	0.9	1.1	0.7	0.9	0.9	0.8
Width/Depth	35.0	44.8	25.3	53.4	75.8	31.1	33.2	44.4	22.0
Bankful Area (m^2)	36.0	46.6	25.4	39.7	45.4	34.1	24.0	30.6	17.5
Manning's Roughness	0.04			0.04			0.04		
Hydraulic Radius (m)	1.0	1.2	0.8	0.9	1.1	0.7	0.8	0.9	0.8
Velocity (m/s)	1.3	1.6	1.0	1.1	1.2	1.0	1.8	2.2	1.4

Percent Differences Between As-Built and Average Channelized Values

	R1			R2			R3		
Parameter	**Average**	**Low**	**High**	**Average**	**Low**	**High**	**Average**	**Low**	**High**
Width (m)	12.5	15.7	6.1	20.1	25.0	9.6	14.6	17.4	9.3
Mean Depth (m)	15.5	25.4	-5.3	8.0	15.7	-6.6	27.2	26.9	27.6
Width/Depth	8.1	18.1	-33.7	14.1	12.8	17.1	-12.7	0.7	-72.0
Bankful Area (m^2)	21.9	28.1	8.8	28.4	45.6	-52.2	36.4	39.8	29.9
Manning's Roughness	35.8			27.4	8.8	58.3	40.3	19.6	69.1
Hydraulic Radius (m)	14.6	23.6	-3.7	7.5	14.7	-5.7	26.4	25.9	27.1
Velocity (m/s)	-28.2	-17.8	-46.5	-27.5	-12.1	-58.4	-44.5	-32.8	-65.3

Percent Differences Between As-Built (Bio-West) and Average Channelized Values

	BJ			RR			CA		
Parameter	**Average**	**Low**	**High**	**Average**	**Low**	**High**	**Average**	**Low**	**High**
Width (m)	11.1	3.9	21.8	31.3	29.0	35.2	-9.9	-8.7	-12.2
Mean Depth (m)	30.0	30.7	28.9	21.6	24.4	17.0	16.1	7.2	26.6
Width/Depth	-30.3	-46.4	-1.6	14.6	13.4	17.4	-37.4	-47.8	-16.5
Bankful Area (m^2)	38.2	40.3	34.4	44.0	38.7	51.2	7.5	9.1	4.8
Manning's Roughness	27.8			27.8			27.8		
Hydraulic Radius (m)	29.8	30.6	28.7	21.1	23.4	17.3	15.9	6.4	27.0
Velocity (m/s)	-54.8	-48.8	-64.4	-88.7	-100.6	-74.0	-16.6	-12.0	-23.9

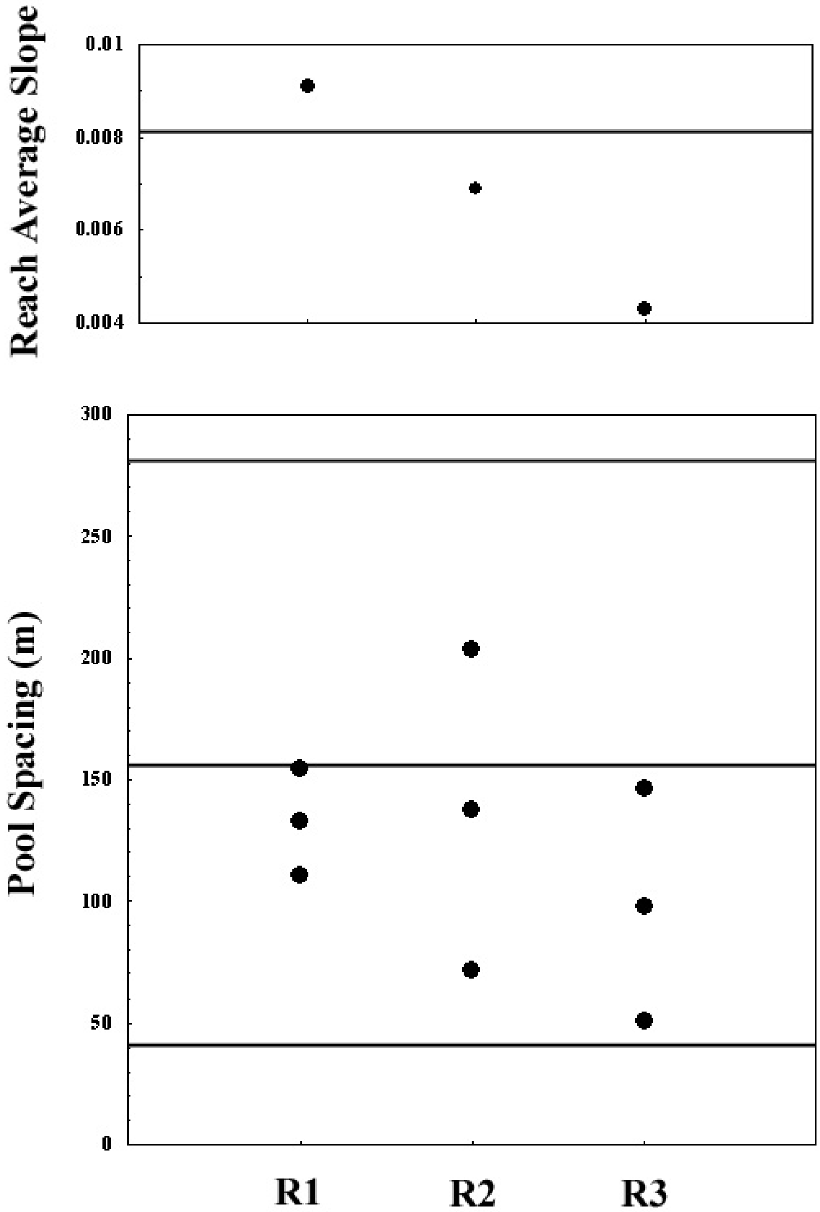

Figure 2-15. Plots displaying the relationship between measurements of as-built and channelized longitudinal profile. As-built values are represented by solid dots at high, average, and low value positions for each study reach where applicable. Design values are represented by horizontal lines at high, average, and low value positions where applicable. For reach average slope, only average values are presented.

Table 2-7. Average channelized and as-built values for longitudinal metrics, and percent differences from a comparison of as-built values to average channelized values. Negative values represent percent decreases in achieved channel geometry relative to channelized values.

Average Channelized Condition

Parameter	Average	Low	High
Channel Slope	0.0082		
Pool-to-Pool Spacing	156.8	41.2	280.8

As-Built Values

	R1			R2			R3		
Parameter	**Average**	**Low**	**High**	**Average**	**Low**	**High**	**Average**	**Low**	**High**
Channel Slope	0.0091			0.0069			0.0043		
Pool-to-Pool Spacing	132.9	111.2	154.7	137.8	72.1	203.4	98.0	50.4	146.2

Percent Differences Between As-Built and Average Channelized Values

	R1			R2			R3		
Parameter	**Average**	**Low**	**High**	**Average**	**Low**	**High**	**Average**	**Low**	**High**
Channel Slope	9.9			-18.8			-47.6		
Pool-to-Pool Spacing	-18.0	62.9	-81.5	-13.8	42.9	-38.0	-37.5	22.3	-47.9

In R3 slope was reduced by about 47.6%. Pool spacing was reduced in all reaches relative to the average channelized condition. In R1 and R2, the average spacing was reduced by less than 20%. In R3, the average reduction was greater, around 37.5%. The one design alteration that was not achieved was a slope reduction in R1. In that reach, slope was increased about 9.9% relative to the average channelized slope.

Design reconfiguration of channel planform, relative to the average channelized condition, had the potential to decrease meander wavelength. Reductions in wavelength were achieved in all measured study reaches (Figure 2-16). The as-built wavelength in R1 of about 200.5 m represents a decrease of 102.8% relative to the average channelized condition (Table 2-8). The average as-built wavelength for R2 was reduced by about 32.1% relative to the average channelized condition. The average as-built wavelength for R3 achieved an approximate 118.9% decrease over the average channelized condition.

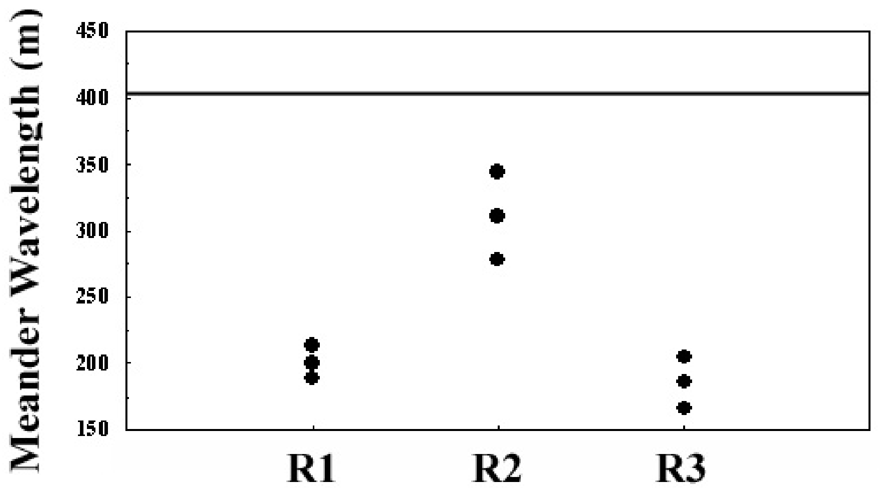

Figure 2-16. Plot displaying the relationship between as-built and channelized meander wavelength. As-built values are represented by solid dots at high, average, and low value positions. The average channelized value is represented by the horizontal line.

Table 2-8. Average channelized and as-built values for planform metrics, and percent differences from a comparison of as-built values to average channelized values. Negative values represent percent decreases in achieved channel geometry relative to channelized values.

Average Channelized Condition

Parameter	Average	Low	High
Wavelength	406.6		
Radius	53.8	38.8	135.9

As-Built Values

	R1			R2			R3		
Parameter	**Average**	**Low**	**High**	**Average**	**Low**	**High**	**Average**	**Low**	**High**
Wavelength	200.5	188.2	212.8	310.2	277.1	343.4	185.7	166.5	204.9
Radius	28.5	21.2	35.8	28.0	25.1	30.9	24.8	19.5	30.1

Percent Differences Between As-Built and Average Channelized Values

	R1			R2			R3		
Parameter	**Average**	**Low**	**High**	**Average**	**Low**	**High**	**Average**	**Low**	**High**
Wavelength	-102.8			-31.1			-118.9		
Radius	-88.7	-83.2	-279.3	-92.1	-54.8	-339.1	-116.8	-98.6	-352.0

Potential design alterations to grain size were consistent reductions in all size fractions (Table 2-9). As-built grain size succeeded in achieving a reduction in grain size distribution compared to the average channelized distribution (Figure 2-17). In as-built reaches, the largest reductions were in the D_{16} size fraction. There was a particularly large decrease in R3 (660.6%). R3 consistently displayed the largest percent reductions in grain size.

4.2.2 Accuracy in Design Execution

We compared design values to as-built measurements of channel morphology in order to determine discrepancies and similarities between the design and construction of the PRRP. Using this comparison, we provide a basis for discussing potential successes or shortcomings in re-establishing physical processes. We see large percent differences when comparing many of the average cross-section values (Table 2-10). As-built cross-section values for area, width, hydraulic radius and the width-to-depth ratio were often substantially larger than design metrics (Figure 2-18). This result is consistent between our study reaches and those of Olsen [2006]. As-built values for roughness were greater than design values in R1 and R3. The average value for roughness in R2 was less than a percent different from design specification. As-built velocities (estimated in HEC-RAS) were less than design estimates in all six reconfigured study reaches. A reduction in bankfull channel capacity will ultimately be determined by the interaction of the actual hydrology with larger than anticipated cross-section geometry, larger roughness values, and smaller velocities.

In comparison of as-built and design longitudinal profile, we found substantial differences in slope in R1, and pool spacing in R3 (Figure 2-19). The channel slope achieved in R1 reach is about 21.3% steeper than the proposed slope (Table 2-11). As-Built R2 is about 8% lower gradient than the design slope for the reach. As-built R3 is within about 4.4% of the design slope for that reach. All three as-built reaches displayed an average pool spacing of about 3 times their respective measured bankfull widths. For R1, this spacing is about 9.1% shorter than the design spacing, with high and low values smaller in as-built R1 as well. For R2, average pool spacing is about 5.8% shorter than the average design spacing. However, the high value was slightly larger in as-built R2. The average pool spacing in as-built R3 is about 28.2% shorter than the design spacing for that reach. Both the high and low values were smaller as well.

Table 2-9. Average channelized and as-built values for grain size metrics, and percent differences from a comparison of as-built values to average channelized values. Negative values represent percent decreases in achieved channel geometry relative to channelized values.

Average Channelized Condition

D_{16} (mm)	D_{50} (mm)	D_{84} (mm)
54.0	96.7	163.4

As-Built Values

Reach	D_{16} (mm)	D_{50} (mm)	D_{84} (mm)
R1	35.3	77	123.7
R2	23.1	66.8	125.1
R3	7.1	52.8	97.2

Percent Differences Between As-Built and Average Channelized Values

Reach	D_{16} (mm)	D_{50} (mm)	D_{84} (mm)
R1	-53.0	-25.5	-32.1
R2	-133.8	-44.7	-30.6
R3	-660.6	-83.1	-68.1

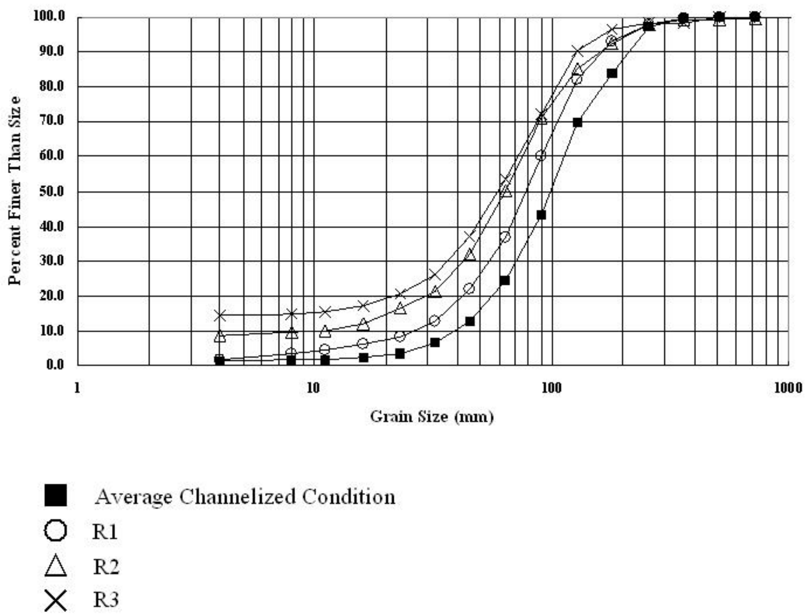

Figure 2-17. Plots of grain size distribution illustrating the difference between the average channelized distribution, and as-built alterations to the Provo River.

Table 2-10. Percent differences from a comparison of cross-section design and as-built values. Negative values represent the percent to which a design value was smaller than achieved channel geometry.

Percent Differences Between As-Built and Design Values

	R1			R2			R3		
Parameter	**Average**	**Low**	**High**	**Average**	**Low**	**High**	**Average**	**Low**	**High**
Width (m)	-45.1	-54.7	-19.3	-59.0	-73.9	-23.9	-72.8	-78.1	-36.0
Mean Depth (m)	-0.1			8.1			-23.9		
Width/Depth	-73.8	-100.4	-28.0	-86.0	-88.2	-106.5	-50.0	-65.2	0.5
Bankful Area (m^2)	-50.2	-39.2	-37.4	-63.9	-84.3	17.7	-39.9	-10.1	-39.6
Manning's Roughness	-12.5			0.5	0.8	9.2	-20.9	-12.5	-22.5
Hydraulic Radius (m)	-38.3	-23.4	-37.3	-27.8	-10.5	-34.7	3.7	36.4	-30.1
Velocity (m/s)	18.6	22.9	16.2	18.2	19.0	22.5	15.1	7.6	25.8

Percent Differences Between As-Built (Bio-West) and Design Values

	BJ			RR			CA		
Parameter	**Average**	**Low**	**High**	**Average**	**Low**	**High**	**Average**	**Low**	**High**
Width (m)	-42.9	-35.6	-43.2	-85.0	-83.5	-73.0	-34.2	-35.4	-10.0
Mean Depth (m)	-20.8			-7.8			-7.6		
Width/Depth	-22.6	-12.0	-68.4	-87.0	-89.5	-107.1	-23.0	-11.0	-46.8
Bankful Area (m^2)	-89.8	-67.7	-91.0	-109.6	-63.3	-156.7	3.8	27.2	-2.8
Manning's Roughness	12.5	30.0	-6.1	12.5	30.0	-6.1	12.5	30.0	-6.1
Hydraulic Radius (m)	-68.3	-35.7	-99.6	-49.7	-23.1	-72.2	15.7	49.6	-30.0
Velocity (m/s)	32.6	38.9	25.3	44.8	54.7	29.5	-5.2	-9.5	0.9

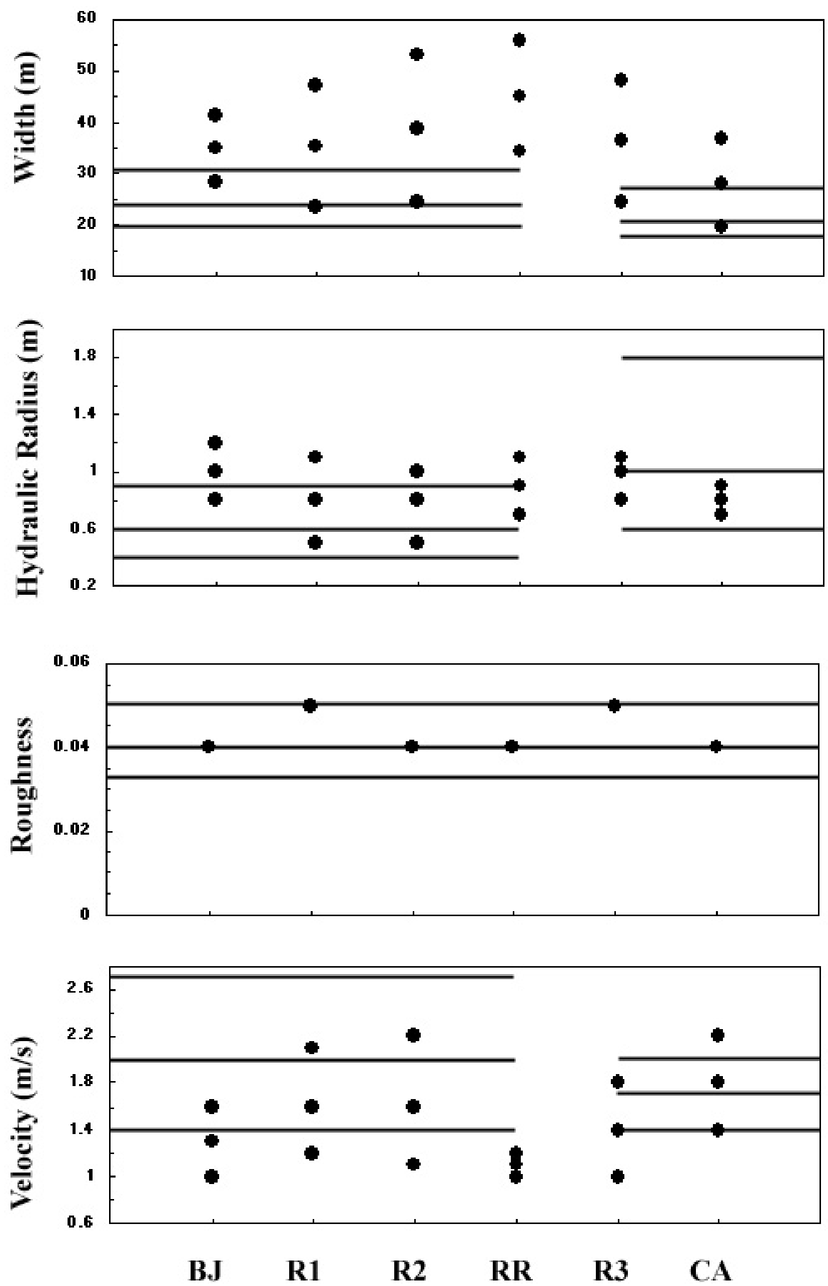

Figure 2-18. Plots displaying the relationship between as-built and design values for cross-section measurements. As-built values are represented by solid dots at high, average, and low value positions for each study reach. Design values are represented by horizontal lines at high, average and low value positions. The break between RR and R3 in design values represents the two separate set of design values generated for upstream and downstream reaches. Only one set of design and as-built values was used for roughness.

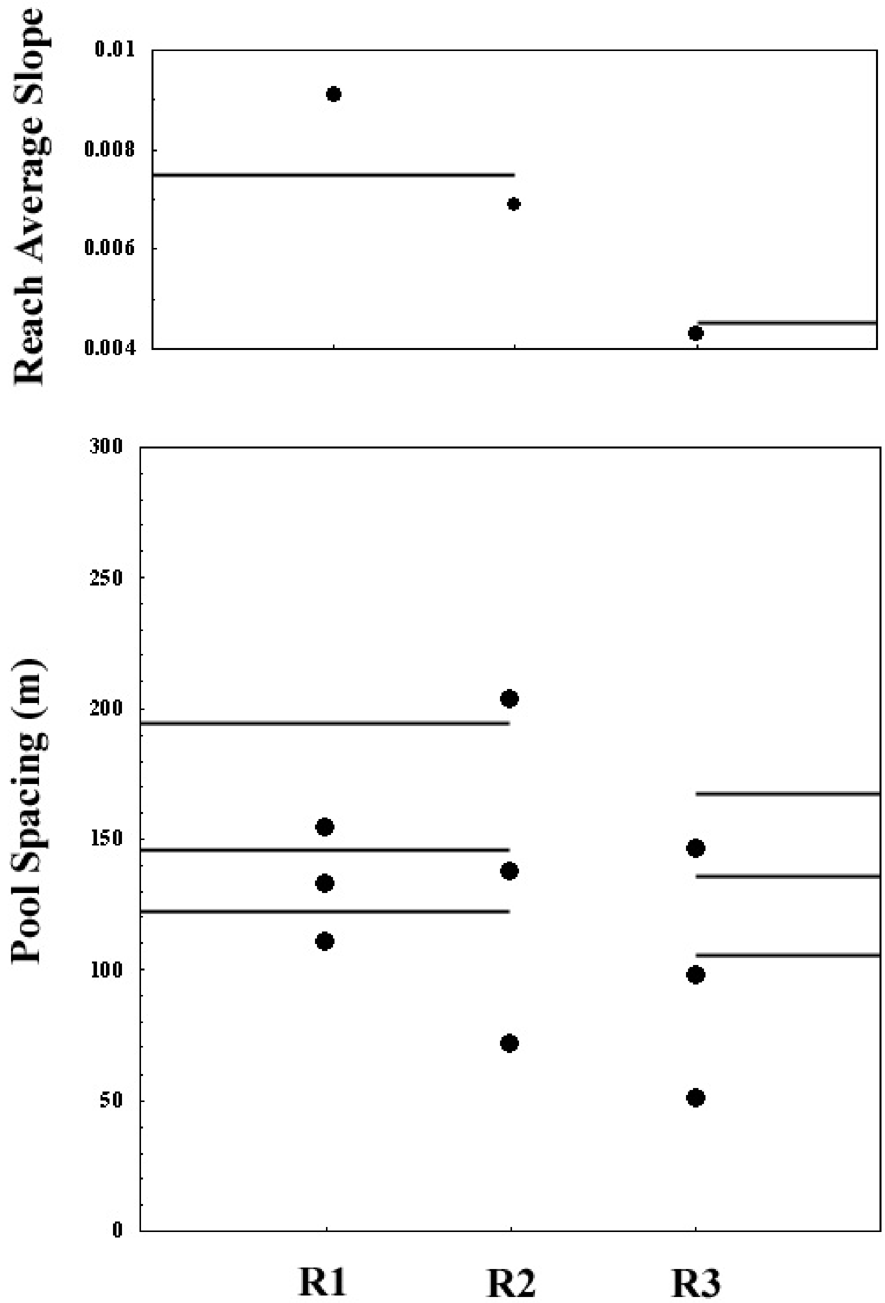

Figure 2-19. Plots displaying the relationship between as-built and design values of longitudinal profile measurements. As-built values are represented by solid dots at high, average, and low value positions for each study reach. Design values are represented by horizontal lines at high, average, and low value position where applicable. Breaks in design values represent separate sets of design values for upstream and downstream reaches. For reach average slope, average values are presented.

Table 2-11. Percent differences from a comparison of longitudinal design and as-built values. Negative values represent the percent to which a design value was smaller than achieved channel geometry.

Percent Difference Between Design and As-Built Values

	R1			R2			R3		
Parameter	**Average**	**Low**	**High**	**Average**	**Low**	**High**	**Average**	**Low**	**High**
Channel Slope	-21.3			8.0			4.4		
Pool-to-Pool Spacing	9.1	8.8	20.7	5.8	40.8	-4.3	28.2	52.0	13.0

In comparison of as-built and design planform features, we found that accuracy in construction was variable (Figure 2-20). As-built values of meander wavelengths were all within about 28.5% of design values (Table 2-12). For R1 and R3, the as-built wavelengths were smaller than design values. This results in an increased frequency in meander forms in those reaches. In R2, as-built wavelengths were about 10.6 percent larger than design. In this reach, the frequency of meanders is greater than design. As-built alterations to grain size exceeded the reductions intended in design (Table 2-13; Figure 2-21). The most substantial differences are in the D_{16} fraction, where design estimates of grain size were up to 83.2% coarser than achieved.

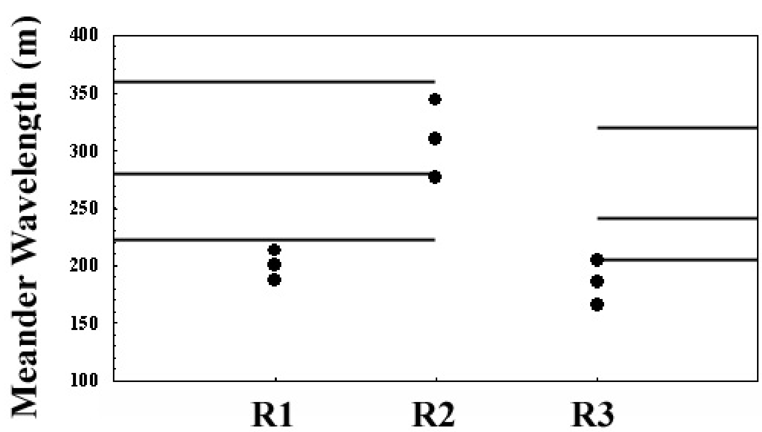

Figure 2-20. Plot displaying the relationship between as-built and design meander wavelength. As-built values are represented by solid dots at high, average, and low value positions. Design values are represented by horizontal lines at high, average, and low value positions. The break in design values at R2 represents the two separate sets of design values for upstream and downstream reaches.

Table 2-12. Percent differences from a comparison of planform design and as-built values. Negative values represent the percent to which a design value was smaller than achieved channel geometry.

Percent Difference Between Design and As-Built Values

	R1			R2			R3		
Parameter	**Average**	**Low**	**High**	**Average**	**Low**	**High**	**Average**	**Low**	**High**
Wavelength	28.5	15.3	40.9	-10.6	-24.7	4.6	22.9	18.0	36.0
Radius	53.9	56.9	55.0	54.7	48.9	61.1	53.2	56.6	57.7

Table 2-13. Percent differences from a comparison of grain size design and as-built values. Negative values represent the percent to which a design value was smaller than achieved channel geometry.

Design v. As-Built

Reach	D_{16} (mm)	D_{50} (mm)	D_{84} (mm)
R1	16.5	9.0	19.2
R2	45.4	21.0	18.2
R3	83.2	23.5	28.0

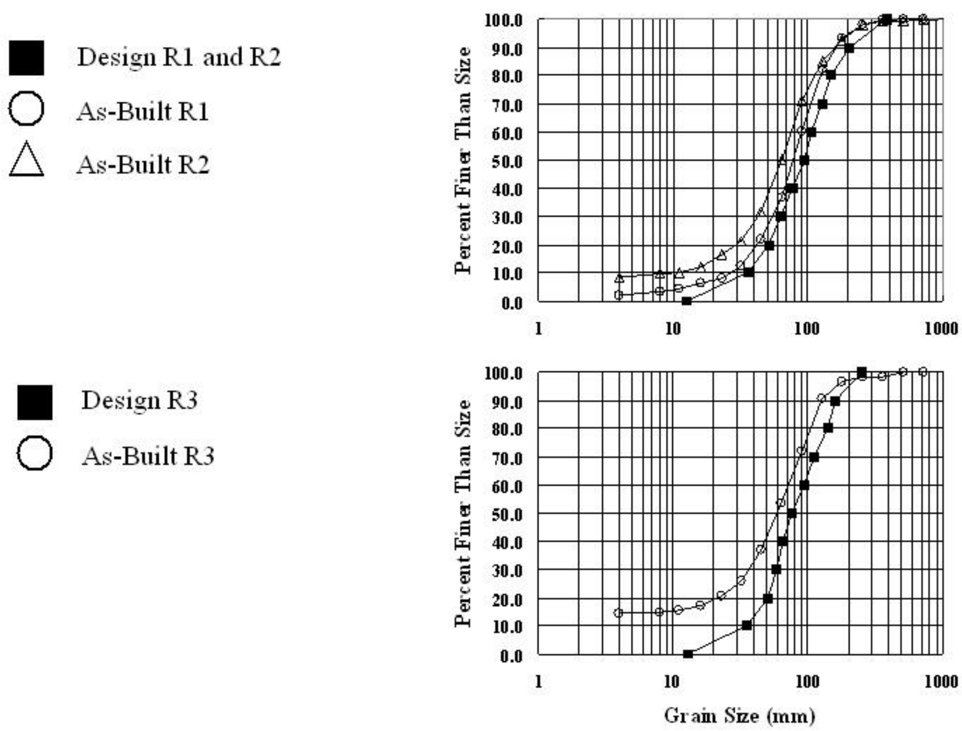

Figure 2-21. Plots of grain size distribution illustrating the differences between potential design alterations, and as-built alterations.

There appears to be a downstream trend in increasing differences between design estimates and achieved grain size. In R3, design sediment size is no less than 23.5% larger than achieved for any size fraction. This is in contrast to R1, where design sediment size is no more that 19.2% larger than achieved. These results are somewhat contradictory when compared to as-built roughness, which was generally increased. This would most naturally correspond to increased grain size, not decreased. However, there are other forms of energy loss in a stream that could increase overall roughness values.

4.3 Project Performance Evaluation: Post-Reconfiguration Hydrology and the Occurrence of Bankfull Discharge

Flow duration curves were calculated for each reconstructed study reach for the period of time since construction was complete in that reach (Figure 2-22). Also, we used a Log-Pearson Type III flood frequency analysis to estimate the actual 2-year flood for each reach, and compared this to the design 2-year flood (Table 2-14). Our results suggest that values used for the design discharge (about 2-year recurrence) were underestimates. Floods recurring on a 2-year interval have exceeded the design discharge in each study reach. The discrepancy between design estimates and actual 2-year floods is particularly pronounced in R3 and CA.

A significant goal of the PRRP was to construct a channel whose capacity would allow for naturalized overbank flooding. Cross-sections were sized so that the design discharge would inundate the flood plain about every two years. In each reach we estimated the number of cross-sections that would be at, or above, bankfull for several discharges bracketing the actual 2 year event, and the duration of these high flows (Figure 2-23). In R1, 7 cross-sections (about 39%) are at bankfull discharge during the 2-

year event. This flow lasts for about 1.9 days a year in this reach. There are 8 cross-sections in R1 (about 44%) whose capacity exceeds the largest instantaneous discharge recorded since reconfiguration. In R2, 10 cross-sections (about 43%) are bankfull at the

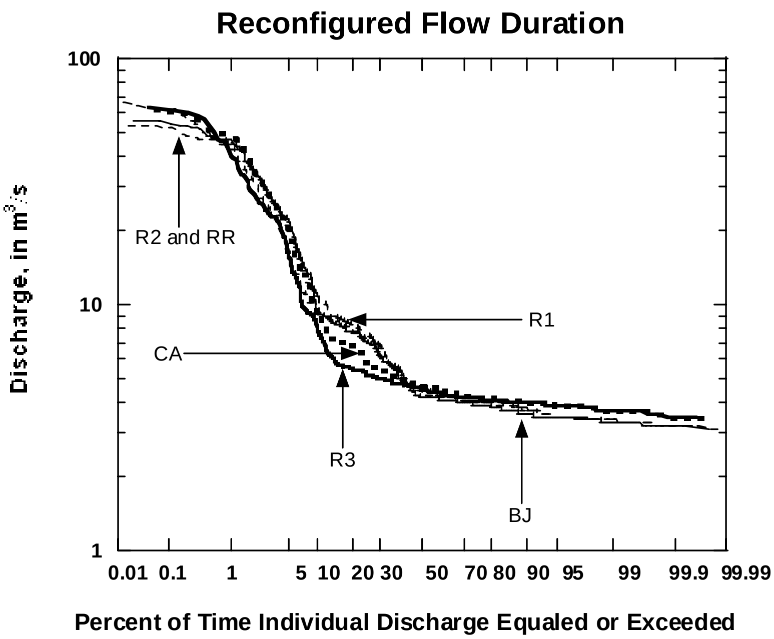

Figure 2-22. Flow duration curves for reconfigured study reaches using daily streamflow records since completed reconfiguration. Flow duration for R1, R2, BJ, and RR were derived from the record of USGS gage 1055200. Flow duration for R3 was derived from the record of USGS gage 1055300, and 10155500 for CA.

Table 2-14. Design and actual discharges at a 2-year recurrence interval for each reconfigured reach.

Reach	Design 2-year Event (m3/s)	Actual 2-year Event (m3/s)
BJ	40	49
R1	40	49
R2	40	47
RR	40	47
R3	37	53
CA	37	52

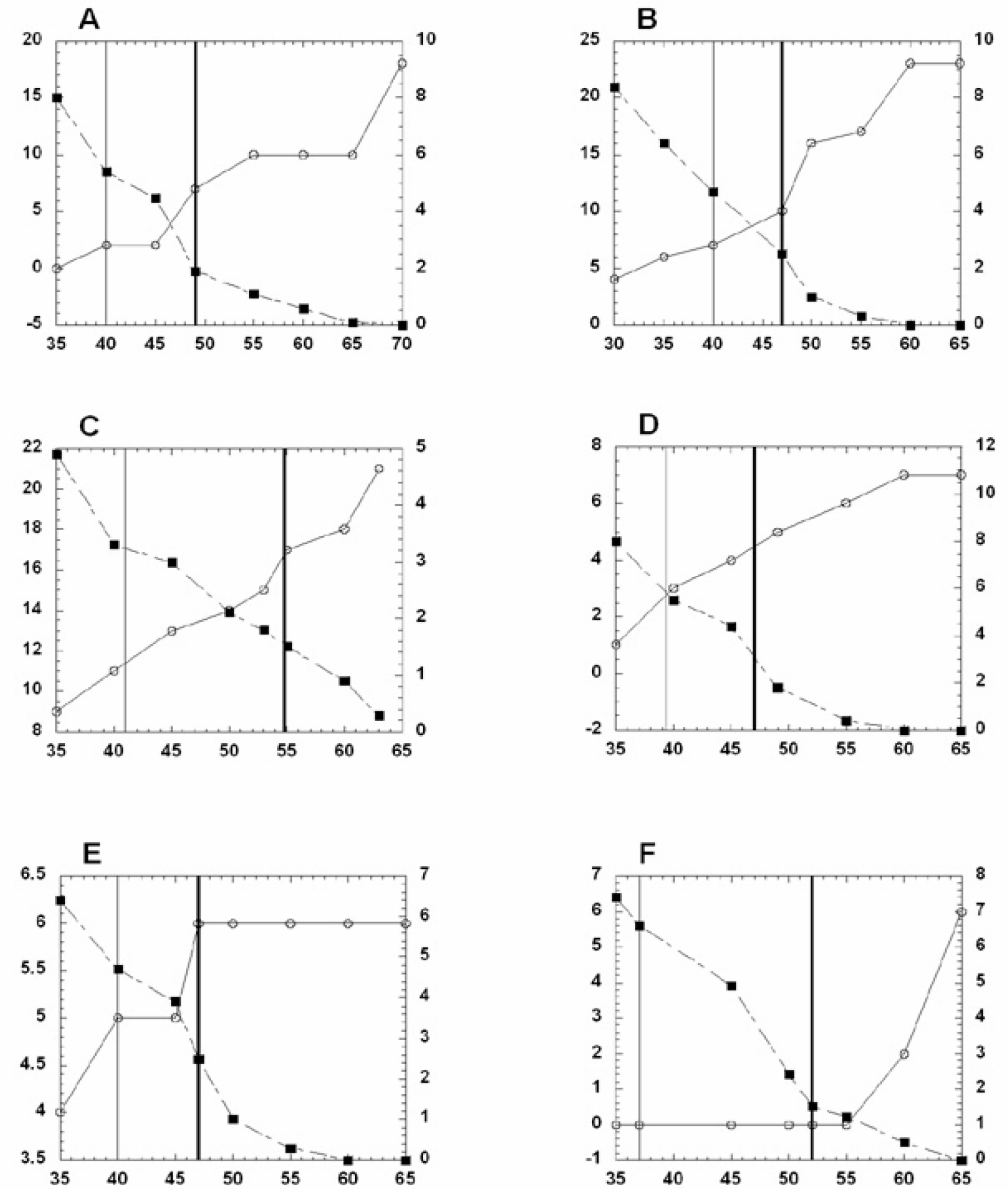

Figure 2-23. Plots illustrating relationships between discharge (in cubic meters per second on all X axis), number of cross-sections at or above bankfull discharge (open curcles, all left Y axis), and duration of inundation (black squares, in days discharge equaled or exceeded on all right y axis). Plot A represents data from R1, B from R2, C from R3, D from BJ, E from RR, and F from CA. The thin vertical line is set at the design discharge for a given reach, and the thick vertical line is set at the actual 2-year event.

2-year event. This discharge lasts for about 2.5 days a year in this reach since completion. About 6 cross-sections (23%) have a bankfull capacity that exceeds the largest instantaneous discharge recorded in this reach since completion. In R3, 15 cross-sections (about 71%) are bankfull at the 2 year event. The 2 year recurrence discharge lasts for about 1.8 days in this reach. Almost 67% of the cross-sections in this reach are bankfull at discharges below the 2 year event. Flows in this range are estimated to last for at least about 5 days a year. About 14% of cross-sections had estimated bankfull water surface elevations that exceeded the largest instantaneous flow recorded since completion.

In BJ, 5 cross-sections (about 71%) are at bankfull during the 2-year event, which lasts for about 1.8 days a year in this reach. One cross-section had a bankfull capacity that exceeded the largest recorded instantaneous peak since completion. In RR, 100% of cross-sections are bankfull at the 2-year event, which lasts for about 1.8 days. About 83% of cross-sections in this reach had bankfull capacities less than the 2-year event. In CA, no cross-sections were found to be bankfull during the 2-year event. A discharge of 60 m^3/s brought 2 cross-sections (about 30%) to a bankfull water surface elevation. Water surface elevations estimated for the largest recorded instantaneous peak discharge since completion were below bankfull for the remaining cross-sections in CA.

These results suggest that there is substantial variability in channel capacity within a given reconfigured reach and between reaches. Even though a single design discharge was used in channel design for several reaches, the channel was not constructed so that the 2-year event was bankfull in all locations. In some reconfigured reaches, the majority of cross-sections are not at bankfull stage during the 2-year event, and many cross-sections in the reach have capacities that exceed the largest recorded event. In other reconfigured reaches, most cross-sections are at or above bankfull during the 2-year event, and many cross-sections in the reach are bankfull at much smaller discharges.

5.0 DISCUSSION: A POST-PROJECT ASSESSMENT OF THE PRRP

Stream restoration is a widely implemented technique in mitigating the degradation of our national water resources. Often, restoration is employed at great cost, but with uncertain benefits. One of the hindrances to quantifying the benefits of restoration is a lack of project monitoring. Here we discuss the results of a post-project assessment of the design and build process, and geomorphic performance of the PRRP.

5.1 Assessing Project Conception and Design

PRRP managers viewed the channelized Provo River as oversized and disconnected from its floodplain, and hydraulically simple with a coarse, armored bed. Thus the Provo River did not provide adequate aquatic habitat. Reconstruction was primarily focused on increasing hydraulic complexity for habitat, decreasing the grain size distribution, and decreasing the bankfull capacity of the channel for floodplain connection. The design of channel planform and longitudinal profile were the primary means to increase hydraulic complexity. Decreased meander wavelength and decreased pool spacing were intended to provide in-channel habitat for fish species. Design alterations that were meant to re-establish the channel’s connection to the floodplain focused on reducing the bankfull channel capacity through decreased cross-sectional area and hydraulic radius, and reduced mean velocities. Decreases in velocity were to be achieved by intended increases in roughness, and decreases in channel slope. Design intentions also included reductions in grain size that would allow for an adequate rate of sediment transport. This was seen as important in allowing geomorphic processes and the maintenance of channel form to be self-sustaining.

Our measurements of reconfigured reaches, as well as those of *Olsen* [2006], suggest that the achievement of intended mitigation was somewhat variable. In terms of reducing the channel capacity, it seems that in many cases reconfigured channels had somewhat larger cross-sectional areas and hydraulic radii than the average channelized condition. However, increases in roughness, decreases in channel slope in most reaches, and decreases in velocity were achieved. Most of the measures intended to increase habitat complexity were achieved, though not to design specifications. Pool spacing and meander wavelength were decreased in all reaches. We observed decreases in grain size that were substantially larger than intended.

5.2 The Accuracy of Design Execution and Implications for Target Processes

Our measurements suggest that as-built channel geometry differs substantially from design geometry. The as-built geometry of planform, longitudinal, and as-built grain size distributions are all generally smaller than design estimates, and the as-built geometry of the majority of cross-sections is larger than design estimates. Here we will discuss possible explanations for these discrepancies.

Self-forming alluvial channels adjust their geometry according to fluxes of sediment and water. Larger than anticipated floods could be responsible for the differences between design and as-built geomorphology that we observed. In R1 the maximum annual instantaneous flow has equaled or exceeded the design discharge 4 times since its completion in 1999. BJ has experienced peak flows that exceeded its design discharge every year since its completion in 2002. R2 and RR have experienced peak annual flows exceeding the design discharge 3 years since their completion in 2000. *Olsen* [2006] reports repeat cross-section measurements that show no significant changes in channel geometry in BJ and RR between 2004 and 2005. This would seem to suggest that channel adjustments would not be responsible for discrepancies between design and as-built dimensions. Field observations in R1 and R2 of limited channel dynamics support this conclusion. R3 and CA, completed in 2003, have experienced flows in excess of their design discharge in 3 years. Repeat cross-section measurements in reach CA show significant alteration to cross-section shape took place between measurements in 2004 and 2005. Field evidence for channel adjustment in R3 includes cut-bank erosion of up to 2 meters, exposing rock barbs that had been buried in the bank during construction. Large gravel bars are being deposited opposite these cut-banks.

Another potential reason for discrepancies between design and as-built channel geometry could be a lack of adherence to design layout during construction. This could have been inadvertent or deliberate. The design values for channel geometry used in this study were obtained from preliminary documents. Personal communication with *Allred* [Personal Communication, 2006] suggests that several iterative changes to channel design can take place before construction is complete. The option to exploit the entire range of geometry values, and change layout specifications on site, was inherent in the planning process and utilized during construction. Unrecorded alterations could produce the discrepancies we observe. Also, design values were applied to the construction of miles of river. We made measurements in small subsections of these design reaches that could have been areas where geometry values at the high or low end of the design range were used in construction. If this is not the case, then it is a matter of error in carrying out the physical construction of the channel.

5.3 Performance Assessment

Regardless of the accuracy of construction relative to design, or the reason for discrepancies between the two, it is the re-establishment of targeted physical processes that determines the ultimate effectiveness of reconfiguration. If inundation of the floodplain occurs about every two years, then restoration of that aspect of the physical template could be deemed a success in the short-term. Our estimates of the occurrence of bankfull discharge suggest that in most reaches, the majority of cross-sections are below bankfull at the 2-year recurrence flood. However, relatively extensive inundation of the floodplain has been observed in each year since reconfiguration. A physical connection to the floodplain does seem to have been achieved despite lower than bankfull stage at the majority of cross-sections. Inundation of the floodplain appears to be occurring through overbank flow at point locations along the river (Figure 2-24). The methods used in construction seem to have allowed the as-built channel to respond to a range of discharges near the design discharge. However, the range of discharges that can achieve bankfull, or overbank, flow on the PRRP appear to be shifted toward flows larger than the design discharge in most reaches. If a period of reduced flood peaks were to occur, the channel could be disconnected from the floodplain.

6.0 CONCLUSION

Monitoring is a neglected aspect of stream restoration. An integrated monitoring program has the potential to enhance the ability of practitioners to successfully manage a project, and the ability of researchers to advance the science of stream restoration. We performed a post-project assessment of the PRRP by using a conceptual model of the restoration process as a framework to analyze the steps taken in the PRRP. We assessed the validity of the project conception, the potential of channel design, and the effectiveness of construction on re-establishing floodplain inundation about every two years.

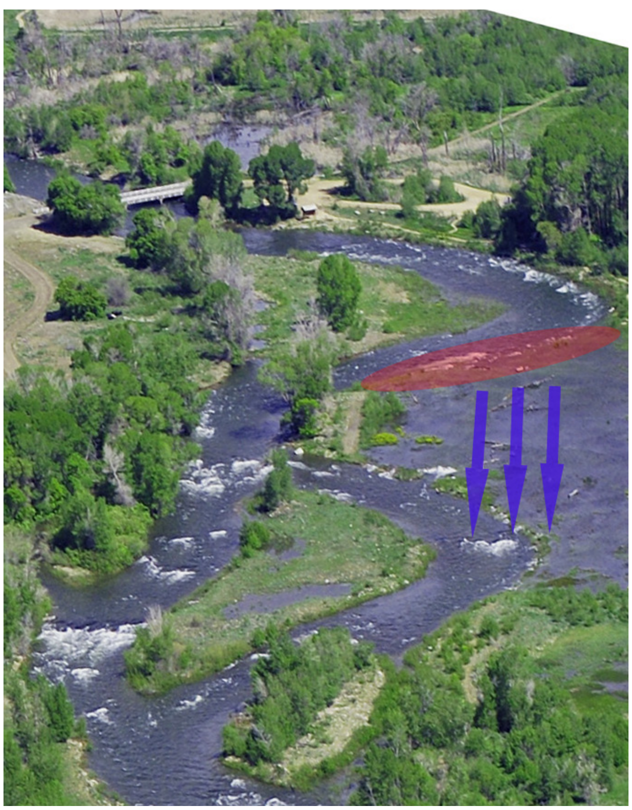

Figure 2-24. Aerial image of R1 illustrating how a small section of lower capacity (red area) allows significant floodplain inundation (blue arrows indicate direction of flow). In most other locations, this discharge of about 50 m^3/s in May 2005, is at or below bankfull stage. Photo courtesy of Allred Restoration.

Prior to this study, no reports of the geomorphology of the channelized river had been produced. Our measurements of channelized geomorphology suggest that perceptions of impairment were justified. The river was straightened, simplified, had a coarse homogeneuos bed, and a capacity designed to contain 122 m^3/s. PRRP design had the potential to increase channel sinuosity, complexity of the longitudinal profile, decrease grain size, and reduce channel capacity compared to the average channelized condition. These alterations were planned in order to make adjustments to channel geometry that were physically appropriate for a hydrologic system estimated to have a 2-year recurrence discharge of 40 m^3/s. Potential reductions to channel capacity were meant to produce bankfull stage at this design discharge. The success of channel reconfiguration appears to be variable. The achievements of reconfiguration include reductions in meander wavelength, reductions in slope and pool spacing, and reductions in grain size, though actual changes were often substantially different than design potential. Reconfiguration was not as successful in reducing cross-section capacity. Results of hydraulic modeling suggest that the majority of cross-section capacities exceed the 2 year flood, despite the fact that post reconfiguration floods have been slightly larger than anticipated. However, inundation of the floodplain has been observed in several years since reconstruction. The flooding has been the result of overbank flow at point locations. The fact that this project goal has been met, despite as-built geomorphology that differs substantially from design, could be the result of incorporating a range of design values when constructing the channel. Incorporating a range of channel geometries in construction may provide a mechanism for the reconstructed channel to respond to a range of flows rather than a single design discharge. However, if flood peaks are reduced in the future, there is the potential for floodplain connections to be lost. A study of this nature must deal with inherent uncertainties of a large-scale construction project. Any research concerning stream restoration should be aware of the history of a project and the methods used in design and construction.

REFERENCES

Alayban, A.M., and R.S. Chalov (1998), Types of river channel patterns and their natural controls, *Earth Surf. Processes Landforms*, 23, 467-474.

Bash, J.S., and C.M. Ryan (2002), Stream restoration and enhancement projects: is anyone monitoring, *Environmental Manag.*, 29, 877-885.

Bernhardt, E.S., M.A. Palmer, J.D. Allen, G. Alexander, K. Barnas, S. Brooks, J. Carr, S. Clayton, C. Dahm, J. Follstad-Shah, D. Galat, S. Gloss, P. Goodwin, D. Hart, B. Hassett, R. Jenkinson, S. Katz, G.M. Kondolf, P.S. Lake, R. Lave, J.L. Meyer, T.K. O'Donnell, L. Pagano, B. Powell, and E. Sudduth (2005), Synthesizing U.S. river restoration efforts, *Science*, 38, 636-637.

Central Utah Water Conservancy District (1994), Provo River Restoration Project, *Technical Report*, Central Utah Water Conservancy District, Orem, UT.

Champoux, O., P.M. Biron, and G.R. Andre (2003), The long-term effectiveness of fish habitat restoration practices: Lawrence Creek, Wisconsin, *Annals of the Association of American Geographers*, 93 (1), 42-54.

Frisell, C.A., and S.C. Ralph (1998), Stream and watershed restoration, In R.J. Naiman and R.E. Bilby (eds.) *River Ecology and Management: Lessons from the Pacific Coastal Ecoregion*, Springer-Verlag, New York, pp. 599-624.

Giller, P. S. (2005) River restoration: seeking ecological standards, Editor's introduction, *J. App. Eco.*, 42, doi: 0.1111/j.1365-2664.2005.01020.x.

Henderson, F.M. (1963). Stability of alluvial channels, *Trans. Am. Soc. Civ. Eng*., 128, 657-686.

Jansson, R., H. Backx, A.J. Boulton, M. Dixon, D. Dudgeon, F.M.R. Hughes, K Nakamura, E.H. Stanley, and K. Tockner (2005), Stating mechanisms and refining criteria for ecologically successful river restoration: a comment on Palmer et al. (2005), *J. Applied Ecology*, 42, 218-222.

Kondolf, G.M. (1995), Five elements for effective evaluation of stream restoration, *Restoration Ecology*, 3, 133-136.

Kondolf. G.M., and E.R. Micheli (1995), Evaluating stream restoration projects, *Environmental Manage.*, 19, 1-15.

Kondolf, G.M., M.W. Smeltzer, and S.F. Railsback (2001), Design and performance of a channel reconstruction project in a coastal California gravel-bed stream, *Environmental Manage.*, 28 (6), 761-776.

Leopold, L.B., and M.G. Wolman (1957), River channel pattern: braided, meandering, and straight: Physiographic and hydraulic studies of rivers, *US Geol. Surv. Prof. Paper*, 282-B.

Lisle, T.E. (1987), Using “residual depths” to monitor pool depths independently of discharge, *Res. Note PSW-394*, 4 p, USDA, Berkeley, Calif.

Michener, W.K. (1997), Quantitatively evaluating restoration experiments: research design, statistical analysis, and data management consideration, *Restoration Ecology*, 5 (4), 347-337.

Olsen, D. (2006), Middle Provo River Draft Monitoring Report, *Technical Report*, URMCC, Salt Lake City, Utah.

O’Neill, M.P., and A.D. Abrahams (1984), Objective identification of pools and riffles, *Water Resour. Res.*, 20, 921-926.

O’Neill, M.P., and A.D. Abrahams (1986), Objective identification of meanders and bends, *J.l of Hydrology*, 83, 337-353.

Palmer M.A., E.S. Bernhardt, J. D. Allan, P.S. Lake, G. Alexander, S. Brooks, J. Carr, S. Clayton, C. N. Dahm, J. Follstad Shah, D. L. Galat, S. Loss, G. P. Goodwin, D.D. Hart, B. Hassett, R. Jenkinson, G.M. Kondolf, R. Lave, J.L. Meyer, T.K. O'Donnell, L. Pagano, and E. Sudduth (2005), Standards for ecologically successful river restoration, *J. of Applied Ecology*, 42, doi:10.1111/j.1365-2664.2005.01004.x.

Ralph, S. C., and G.C. Poole, 2003. Putting monitoring first: Designing accountable ecosystem restoration and management plans. *In:*Restoration of Puget Sound Rivers, D. R. Montgomery, S. Bolton, D. B. Booth, and L. Wall (Editors). University of Washington Press, Seattle, Wash.

Ryder, D.S., and W. Miller (2005), Settings goals and measureing success:linking patterns and processes in stream restoration, *Hydrobiologia*, 552, 147-158.

Schmetterling, D.A., R.W. and Pierce (1999), Success of instream habitat structures after a 50-year flood in Gold Creek, Montana, *Restoration Ecology*, 7(4), 369-375.

Smith, S.M., and K.L. Prestegaard (2005), Hydraulic performance of a morphology-based stream channel design, *Water Resources Research*, 41, doi:10.1029/2004WR003926.

Stromberg, J.C., S.J. Lite, and D.T. Patten (1999), Provo River Restoration Project: riparian vegetation final version, *Technical Report*, URMCC, Salt Lake City, Utah.

Thompson, D.M. (2002), Long-term effect of instream habitat-improvement structures on channel morphology along the Blackledge and Salmon Rivers, Connecticut, USA, *Environmental Manage.*, 29 (1), 250-265.

Utah Reclamation Mitigation and Conservation Commission (1997), Provo River Restoration Project, *FEIS*, US Dept. of the Interior, Washington, D.C.

Williams, G.P. (1986), River meanders and channel size, *J. of Hydrology*, 88, 147-164.

Wohl, E., P.L. Angermeier, B. Bledsoe, G.M. Kondolf, L. MacDonnell, D.M. Merritt, M.A. Palmer, N.L. Poff, and D. Tarbton (2005), River restoration, *Water Resour. Res*., 41, 1-12.

Wolman, M.G. (1954), A method of sampling coarse river-bed material, *Trans. Amer. Geo. Union*, 35, 951-9.

Woolsey, S., F. Capelli, T. Gonser, E. Hoehn, M. Hostman, B. Junker, A. Paetzold, C. Roulier; S. Schweizer; S.D. Tiegs, K. Tockner; C. Weber, and A. Peter (2007), A strategy to assess river restoration success, *Freshwater Biology*, 52 (4), 752-769.

Ziemer, R.R. (1998), Monitoring watersheds and stream, USDA Forest Service Gen. Tech. Rept. PSW-GTR-168, Arcata, Calif.

CHAPTER 3

THE EFFECTS OF LARGE-SCALE CHANNEL RECONFIGURATION ON TRANSIENT STORAGE DYNAMICS: THE POTENTIAL FOR HYPOREIC REHABILITATION ON THE PROVO RIVER, HEBER VALLEY, UTAH [1]

ABSTRACT

The Provo River Restoration Project has reconfigured 19-km of the Provo River, Heber Valley, Utah. Channel geomorphology was measured and transient storage parameters estimated in three reconfigured and three channelized stream reaches to determine the relative effects of channel reconfiguration on reach-integrated transient storage, a process that may be important to restoring stream ecosystem function. Channel morphology was measured using total station equipment, a GIS, and streambed pebble counts. Transient storage parameters were estimated from Rhodamine-WT breakthrough curves using a numerical solution to a modified one-dimensional advection-dispersion equation (STAMTT-L). Despite substantial channel alterations, we found that estimates of solute residence time in storage, and mass transfer rates were not significantly different between reconfigured and channelized reaches. However, there was a significant increase (186%) in estimates of relative storage capacity (β_{tot}). Statistical correlation between geomorphic parameters and β_{tot} suggests that reconfiguration may have resulted in increased in-channel storage in larger, more frequent reconstructed pools, and increased hyporheic exchange through shallow, quickly exchanging flowpaths in steep reconstructed riffles.

---

[1] Coauthored by Randy R. Goetz, John C. Schmidt, and Michael N. Gooseff

1.0 INTRODUCTION

Development of rivers and streams to meet the needs of human society has adversely transformed some of these valued ecosystems. Recently, society has been inspired to improve management, protection, and rehabilitation of some degraded rivers and streams [*NRC*, 1992; *FISRWG*, 1998; *Graf* 2001; *Gleick*, 2003; *Nilsson et al.*, 2005]. The term rehabilitation in this context refers to projects employing a wide range of techniques applied over varying spatial scales that share the common goal of reversing undesired impacts to riverine ecosystems. Over $15 billion has been spent in the U.S. on stream and wetland rehabilitation since 1990 [*Bernhardt et al.*, 2005]. However, due to a common lack of explicit project goals, and poor post-project monitoring, there is relatively little known about the effectiveness of rehabilitation techniques [*Kondolf and Micheli*, 1995; *Bash and Ryan*, 2002]. Recently, there has been a call to quantitatively assess the degree of ecological improvement gained by various stream rehabilitation techniques, and to increase general scientific understanding of the effects of rehabilitation on key physical and ecological processes [*Giller*, 2005; *Palmer et al.*, 2005; *Wohl et al.*, 2005].

Stream water flux through the hyporheic zone is increasingly viewed as one of the physical processes critical to riverine rehabilitation success [*Triska et al.*, 1993; *Brunke and Gonser*, 1997; *Fernald et al.*, 2001; *Sophocleus*, 2002]. The hyporheic zone is the shallow subsurface area surrounding a stream where water is exchanged between the stream channel and saturated alluvial sediment [*White*, 1993]. This subsurface region is one component of transient storage, which is the term applied to all low-velocity regions in the channel and hyporheic zone [*Bencala and Walters*, 1983].

The hyporheic component of transient storage is of particular ecological importance. Hyporheic exchange locations have been shown to influence trout spawning patterns and algal diversity and abundance [*Baxter and Hauer*, 2000; *Pepin and Hauer*, 2002]. Transport of ecologically important nutrients, such as nitrate and dissolved organic carbon (DOC), through the hyporheic zone contributes to their biogeochemical processing [*Triska et al.*, 1989; *Duff and Triska*, 1990; *Biskey and Gross*, 2001]. This ecotone is a biological and hydrological link along the habitat continuum that includes streams, riparian forests, floodplains, and hillslopes [*Bencala*, 1993; *Brunke et al.*, 2003].

Hyporheic exchange processes are largely governed by channel morphology. Planform geometry, bed material organization, and slope control hydraulic head gradients that drive surface water into (downwelling), and out of (upwelling), the subsurface [*Harvey and Bencala*, 1993; *Marion et al.*, 2002; *Kasahara and Wondzell*, 2003]. The size and spacing of channel and bar forms influence the spatial distribution of upwelling and downwelling zones [*Anderson et al.*, 2004; *Gooseff et al.*, 2006]. The grain size distribution and hydraulic conductivity of alluvial deposits controls the magnitude of flux and exchange rates between the stream and hyporheic zone [*Cardenas and Zlotnik*, 2003; *Storey et al.*, 2003]. Thus, rehabilitation that includes significant channel and floodplain reconfiguration might be expected to have a proportionally greater impact on hyporheic exchange than rehabilitation efforts that do not involve reconfiguration.

Some studies have suggested that explicitly addressing the hyporheic zone in stream rehabilitation could assist in achieving goals such as processing of DOC, re-establishing macroinvertebrate populations, and regulating stream temperature [*Vervier et al.*, 1993; *Poole and Berman*, 2001; *Collier et al.*, 2004]. However, little research has targeted the effects of stream rehabilitation efforts on hyporheic function. *Hancock and Boulton* [2005] studied the effects of an environmental flow release from a dam on the Hunter River in Australia. They monitored dissolved oxygen (DO) and nitrate concentrations at three upwelling and three downwelling locations in order to detect hyporheic “flushing effects” they expected to see from increased stream flow. High flows produced a temporary reduction in the concentration of interstitial nitrate-nitrite concentrations, and a temporary increase in the concentration of DO at two of their study sites. No lasting effects were observed in hyporheic chemistry. *Kasahara and Hill* [2005] recognized that channel design elements commonly employed in stream rehabilitation, such as constructed step-pool and riffle-pool sequences, should induce greater hyporheic exchange. Their detailed hydrometric data, collected at the scale of individual riffles, suggested that reconstructed riffles created more spatially extensive hyporheic zones than a pre-project riffle. However, DO concentrations decreased more than expected with depth, leading them to also conclude that streambed interstices became clogged with fine sediment, reducing hydraulic conductivity, and the depth of penetration of stream water into the hyporheic zone.

Here, we investigate the effects of channel construction and reconfiguration on reach-scale transient storage of the Provo River in Utah. We compare the geomorphic and transient storage characteristics of three channelized reaches prior to reconstruction, with three reconstructed reaches during summer and fall baseflow conditions. We characterize transient storage using reach-representative solute residence time distribution, exchange rate between the stream and transient storage zones, and relative transient storage capacity. Planform, longitudinal, cross-sectional, and grain size characteristics are used to describe stream morphologic controls on transient storage. We show that the geomorphology of the Provo River was altered along a trajectory that might be expected to increase stream water flux through the hyporheic zone, thereby affecting transient storage characteristics. However, we found that transient storage processes in reconfigured reaches of the Provo River operated with similar exchange rates and residence time distributions as channelized reaches, but with significantly increased capacity.

2.0 STUDY AREA AND RESOURCE DEVELOPMENT HISTORY

The study area is that portion of the Provo River in the Heber Valley, a structurally controlled basin in northern Utah bordered by the Wasatch Mountains to the west and the Uinta Mountains to the east (Figure 3-1). The dominant sediments of the Heber Valley are Pleistocene glacial outwash from the Uinta and Wasatch Mountains, and Holocene alluvium of the Provo River and local tributaries [*Woodward et al.*, 1976; *CUWCD*, 1994; *Willis and Willis*, 2003]. The Provo River ultimately drains to Utah Lake, which in turn drains to the Great Salt Lake. The drainage basin upstream from Jordanelle Dam is 653 km^2. There are 19 km of channel within the valley, and the watershed area increases to 930 km^2 at gage 1055500. The mean annual flow and the mean annual flood were 5.3 m^3/s and 35 m^3/s, respectively, before significant water development, determined for the period 1938-1948 at gage 10155500. Unregulated peak flows in the region typically occur in late May or June during spring snowmelt.

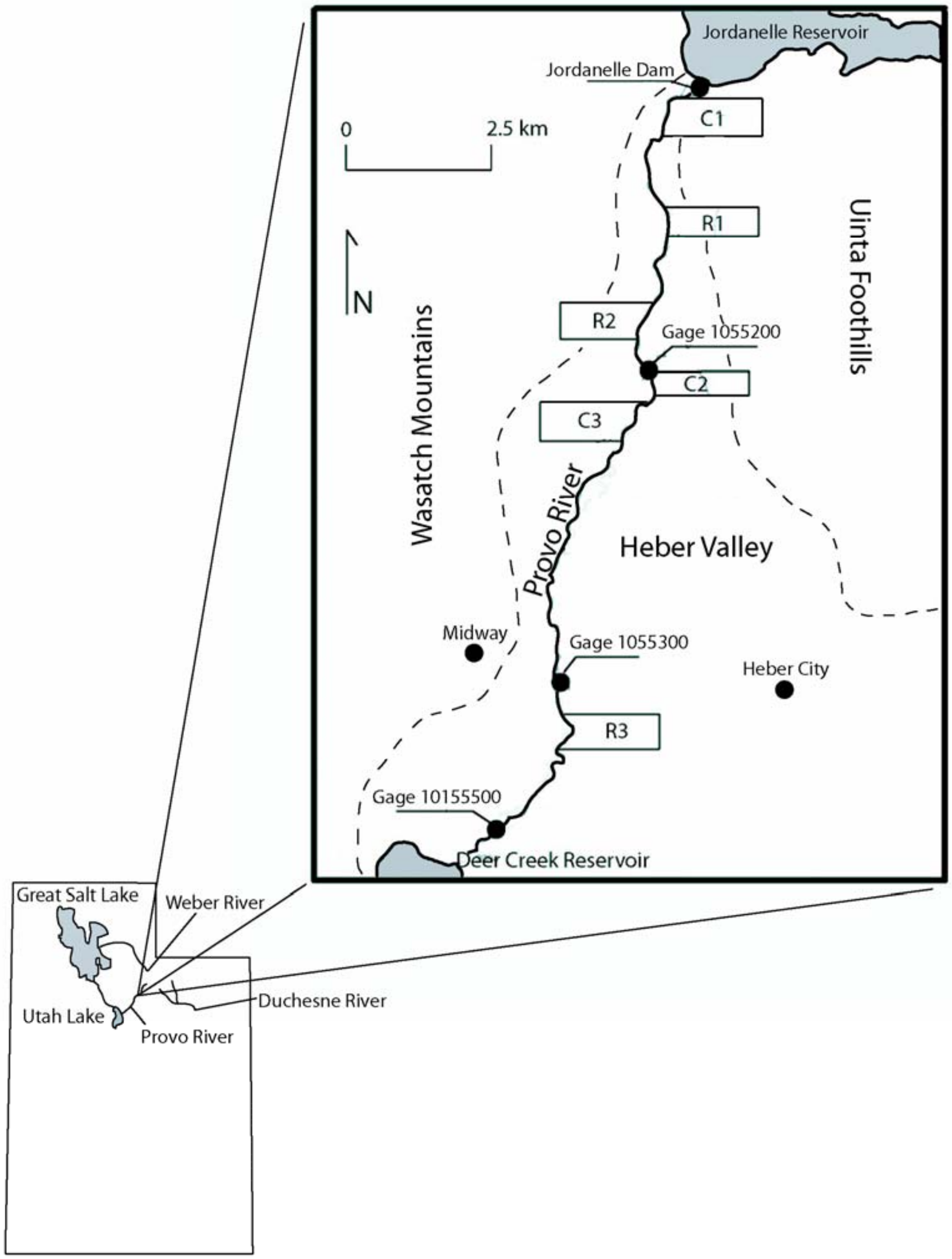

Figure 3-1. Area map showing the study area, study reach locations, and stream gage locations. Study reaches designated with C are channelized, and study reaches designated with R are reconfigured. Gages locations are 10155200 (Provo River at River Road Bridge), 10155300 (Provo River near Midway), and 10155500 (Provo River near Charleston). Dashed lines represent the approximate topographic boundary separating the valley floor from uplands.

As evidenced by differential stream gaging we performed during our stream tracer tests, all study reaches gain ground water discharge on the order of 1 m^3/s over a typical reach length (~ 650 m).

Between the late 1930's and the 1990's, various resource development projects augmented the flow regime (Figure 3-2). Trans-basin diversions from the Weber and Duchesne Rivers in 1948 and 1952, respectively, increased the mean annual flow of the Provo River by about 5%, and annual peak flows by about 15%. Deer Creek Dam at the downstream end of the Heber Valley was completed in 1941 to store surplus water for subsequent agricultural, municipal, and industrial use. The river in the study area was channelized and diked in the 1960's to accommodate the post-development 100-yr flood. Jordanelle Dam, completed in 1993, further altered the flow regime, and also eliminated the upstream sediment supply. The present hydrology of this managed and altered river includes unusually high baseflow and reduced flood-peaks relative to the hydrology before construction of Jordanelle Dam [*CUWCD*, 1994]. In 1992, national legislation authorized mitigation of the adverse impacts of these water development activities, thereby establishing the Provo River Restoration Project (PRRP).

3.0 PRRP DESIGN AND CONSTRUCTION

The goal of the PRRP is "to help mitigate environmental impacts…on riverine environments…increase biological productivity and diversity…improve fish habitat", and to "create a diversity of wetland and aquatic habitats" [*URMCC*, 1997]. The PRRP is somewhat unique in the freedom available to incorporate relatively active geomorphic processes into channel design.

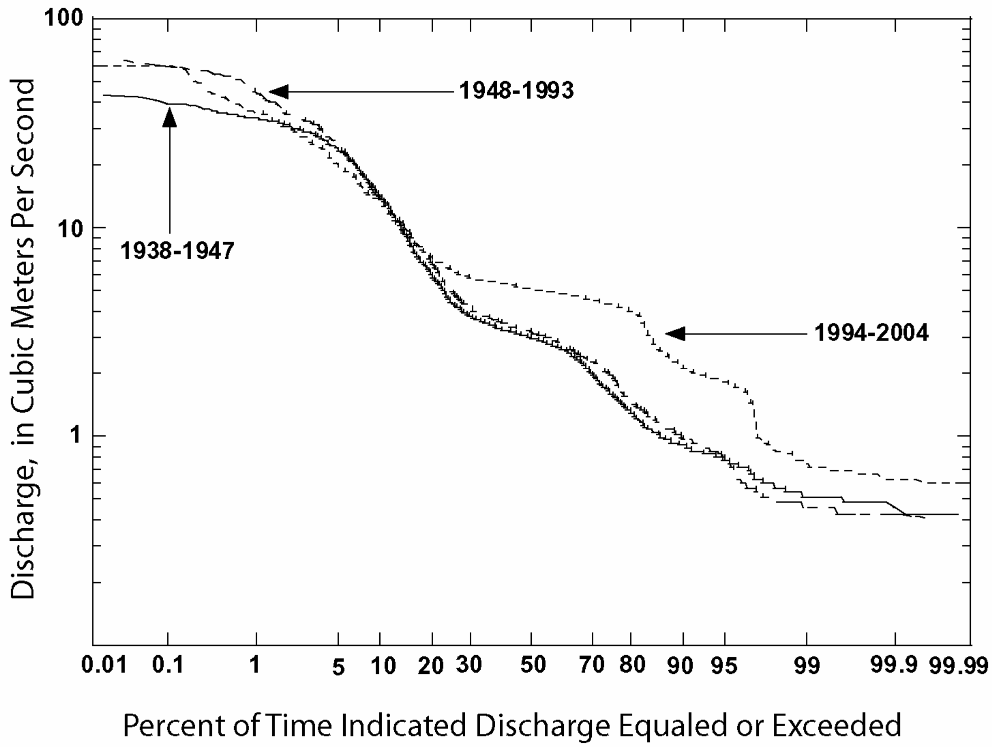

Figure 3-2. Flow duration curves developed from mean daily discharge data at the gaging station near Charleston (USGS 10155500) for the pre-development period (1938-1948), the main development period (1948-1993), and the period following the closure of Jordanelle Dam (1993-2004).

The proposed rehabilitation created a dynamic physical template that accommodated channel migration within a relatively wide alluvial corridor where land was purchased.

The first step in design was determination of the discharge that would just fill the banks of the channel. Flow duration and flood frequency were estimated from a synthetic 40-yr flow record modeled from gaging records, and from estimates of the operational rules of Jordanelle Dam that accounted for downstream irrigation demands. The 1.5-yr recurrence flood was estimated to be 40 m^3/s, and channel design sought to allow overbank flows when dam releases exceeded this value.

Regional hydraulic geometry relationships were applied as guidelines to determine channel planform and cross-section geometry [*Allred*, Personal Communication, 2006]. Relationships developed by *Leopold and Wolman* [1957], *Henderson* [1963], and *Alabyan and Chalov* [1998] were used to determine the appropriate planform characteristics. The reconstructed channel design based on these relationships had a meandering pattern including secondary channels, medial bars, and cut-off chutes at point bars (Figure 3-3). Values for parameters such as radius of curvature, meander belt width, channel width, depth, and velocity were estimated using empirical relationships compiled by *Williams* [1986]. Constrained by the proposed layout and cross-section geometry, the proposed longitudinal profile included a semi-rhythmic riffle-pool pattern with a proposed pool spacing of about 6.5 times the bankfull channel width. Overall channel morphology was intended to maximize the distribution of velocity and habitat conditions, and establish a diverse template for ecosystem processes to proceed.

Increased transient storage was not an explicit goal of the PRRP, but reestablishment of meandering planform with pools and riffles could be expected to increase transient storage. However, some construction techniques may have adversely affected the hyporheic component of transient storage, thereby limiting the ecological effectiveness of the project. For instance, heavy equipment working in the old channel introduced fine sediment into suspension. Downstream deposition of fines has the potential to "clog" interstitial space in the streambed, effectively isolating the subsurface from hyporheic exchange [*Kasahara and Hill*, 2005; *Rehg et al.*, 2005]. During excavation, the new channel was used as a roadway for heavy equipment in order to minimize compaction and damage to flora in the floodplain (Figure 3-4). This may have led to compaction of the alluvium underlying the new streambed. Compaction can decrease the porosity and hydraulic conductivity of sediment to various degrees dependent upon grainsize distribution and water content [*Terzhagi et al.*, 1996]. These conditions could necessitate the need for specific considerations of hyporheic function in channel design and construction.

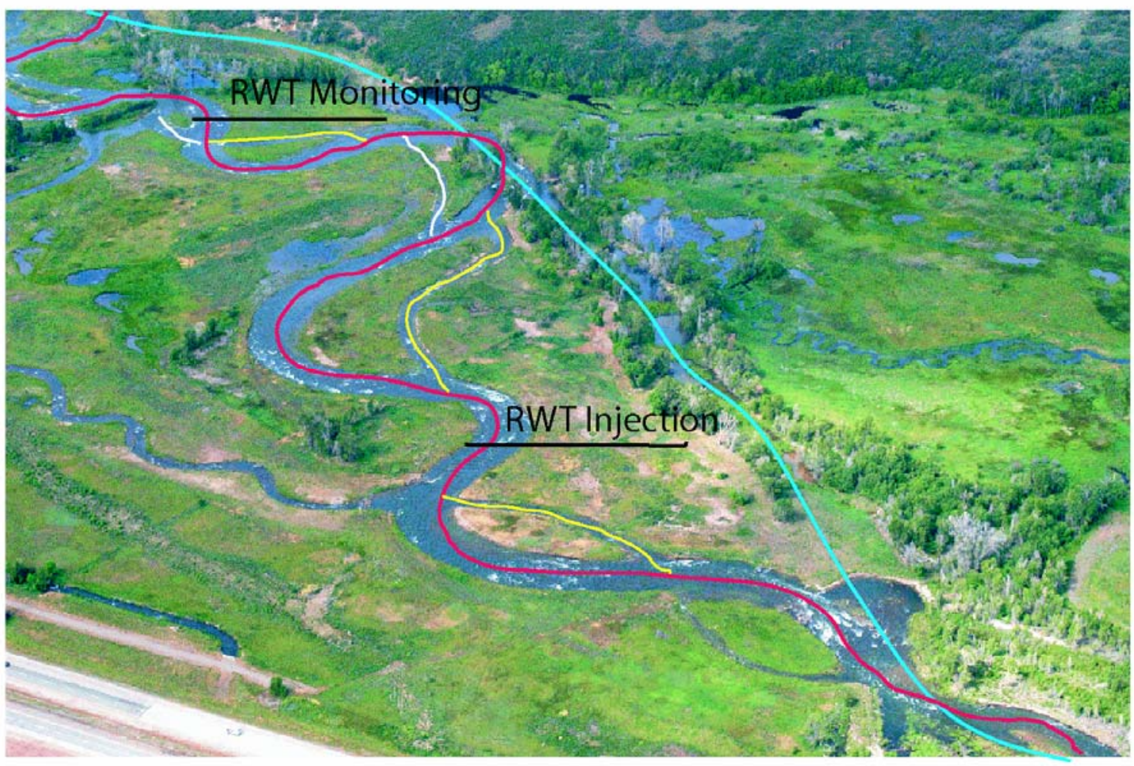

Figure 3-3. Oblique aerial photo of study reach R2. Flow is from the bottom right, to the upper left corner. The photo is taken at the approximate design bankfull stage of 40 m^3/s, in late spring 2003. Some design features are highlighted including the meandering main channel (red), split channels (yellow), and secondary high-flow channels (white). The path of the channelized river prior to reconstruction is delineated in blue. The upstream tracer injection site and downstream monitoring location for R2 tracer tests are also indicated. Photo courtesy of Tyler Allred.

Figure 3-4. This truck, common amongst equipment used in construction of the PRRP, is shown transporting excavated material via the bed of the reconfigured channel that is under construction.

4.0 METHODS

4.1 Study Site Selection and Description

Three channelized (C1-3) and 3 reconfigured (R1-3) study reaches were established in fall 2004 (Table 3-1, Figure 3-1). Subsequent to this study, all channelized reaches were reconfigured, and the PRRP was completed in fall 2006. Study sites were chosen principally on the basis of accessibility and spatial distribution. Reach lengths were a minimum of approximately 20 bankfull channel widths. This metric is approximate, because bankfull characteristics do not exist in channelized reaches and are not yet geomorphically expressed in rehabilitated reaches. This study reach length ensured proper mixing during tracer injections, and statistically significant geomorphic characterization [*Fisher et al.*, 1979]. Reach length was also constrained by the divergence and return of secondary channels (Figure 3-3). Avoiding net inflow or outflow of surface discharge allowed the assumption of minimal loss of tracer mass during injections, and essentially steady stage during topographic surveys.

Table 3-1. Study reach details including location relative to Jordanelle Dam, reach length, date of construction completion, and the largest discharge to date.

Reach	Downstream Distance from Jordanelle Dam (km)	Reach Length (m)	Completion Date (yr)	Largest Instantaneous Flow Since Construction (m^3/s, yr)
C1	0.4	534	N/A	N/A
C2	6.5	544	N/A	N/A
C3	7.2	691	N/A	N/A
R1	2.8	639	1999	62, 1999
R2	4.9	872	2000	49, 2004
R3	15.2	632	2003	49, 2004

Since the inception of the PRRP, release schedules at Jordanelle Dam have been altered in order to produce a naturalized hydrograph within the constraints of the prevailing water delivery requirements. Since construction was complete on the first reconfigured study reach, stream discharge has exceeded the design 1.5 year flood discharge approximately 1.2% of the time (Figure 3-5). Annual peak discharges equaled, or exceeded 40 m^3/s in 1999, 2003, 2004, and 2005.

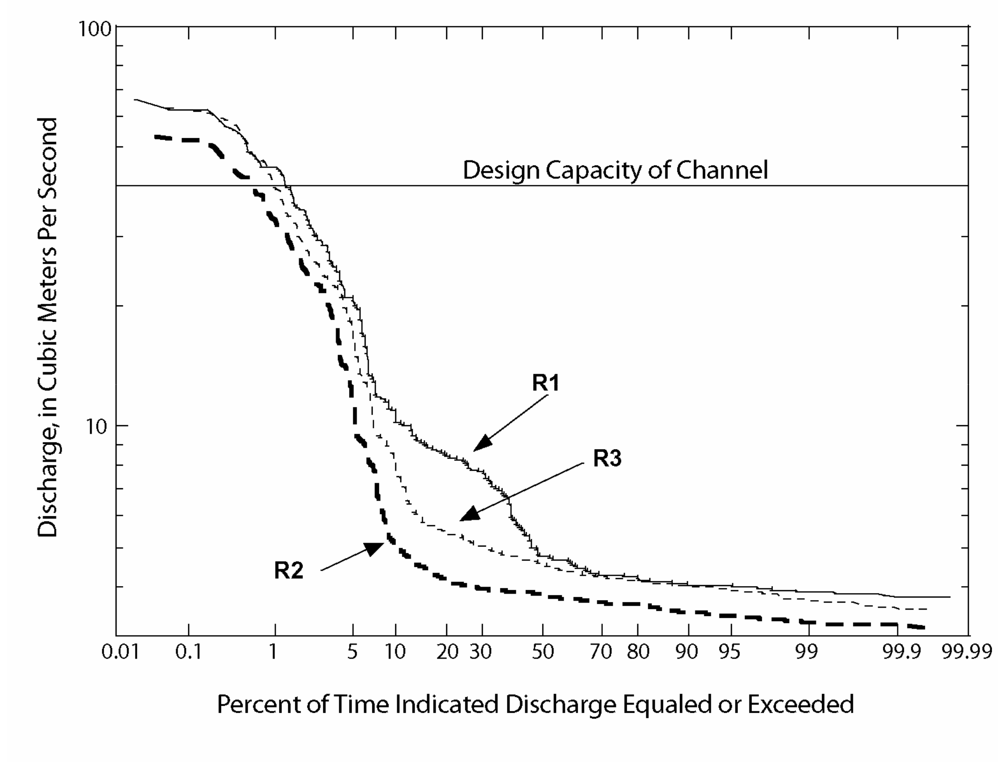

Figure 3-5. Flow duration curves developed for the 3 reconfigured reaches illustrating hydrology in each reach since their respective completion dates, based on mean daily discharge at the nearest gage. Periods of record are 1999-2004 (R1), 2001-2006 (R2), and 2003-2006 (R3). Note that 40 m^3/s is the design bankfull discharge.

4.2 Geomorphic Measurements

We measured channel topography and surface bed material, and made comparisons between channelized and reconfigured reaches that quantify reach-average alterations to the physical controls of transient storage.

4.2.1 Cross-Section Geometry

Channel cross-sections were measured approximately every channel width. Individual cross-section width typically spanned the levees in channelized reaches, or the 2005 high water mark in reconfigured reaches. The width of the channel at peak stage in spring 2005 was used as a proxy for bankfull width, because this discharge was approximately 40 m^3/s. Several standard measures of cross-section form were calculated. Wetted perimeter (P), area (A), hydraulic radius (R), width (W), mean depth (D), the width-to-depth ratio (W/D), velocity (v), and flow resistance were determined from the survey data. Flow resistance was estimated by calculating Manning's roughness coefficient (*n)* derived from reach-average values of *A*, *R*, and slope (*S*).

$$n = \frac{R^{(2/3)} S^{(1/2)} A}{Q} \qquad (1)$$

Cross-section metrics were calculated using baseflow stage. This water level defined channel geometry during field tracer tests. Thus, the baseflow channel accommodated all in-channel transient storage, and controlled head distributions that drove hyporheic flux.

4.2.2 Longitudinal Geometry

The methods of *O'Niell and Abrahams* [1984] and *Lisle* [1987] were employed to objectively analyze streambed topography data, and to determine the reach average lengths of pools and riffles, the fraction of the reach composed of pools and riffles, and the reach average spacing of pools and riffles. Those metrics with dimensions of length were normalized by baseflow and bankfull channel width. Other longitudinal metrics included the reach average bed slope, and the rugosity of the bed profile expressed as the r^2 value of a linear least-squares regression to the bed profile. Riffle-specific metrics were the length-weighted mean slope of riffles and the relative slope of riffles in relation to the reach average slope.

The method of *O'Niell and Abrahams* [1984] is centered on evaluating elevation differences between evenly spaced thalweg survey points. Original survey points were unevenly spaced, therefore we interpolated points by kriging. Qualitative assessment of 5-, 10-, and 20-m point spacing indicated that 10-m spacing provided a superior portrayal of the longitudinal profile, and a manageable amount of data. Cumulative elevation differences between a series of points were compared to a pre-determined threshold value. We used a suggested value of 1.75 times the standard deviation of all elevation differences. Cumulative elevation differences in excess of this threshold are designated as significant bedforms.

The method of *Lisle* [1987] was used to calculate the lengths of, and spacing between, significant features, using minimum pool depth to determine feature length. Original survey data was interpolated at sub-meter spacing in order to precisely locate points separating riffles and pools. Pool lengths were calculated as the linear distance from a riffle crest to the next point upstream at an equal elevation. The straight line between these two points represents the water surface at minimum pool depth. Pool spacing was calculated as the linear distance between pools. With lengths and elevation differences determined, slopes were calculated for individual riffles.

4.2.3 Planform Geometry

Channel pattern characteristics were measured using sub-meter resolution, ortho-rectified, digital aerial photos within a geographic information system (GIS). The channel centerline was digitized, and points generated along the centerline at a 10-m interval. The spatial coordinates of these points were used to determine downstream directional differences along the channel centerline after the method of *O'Niell and Abrahams* [1986]. Comparison of cumulative directional change against a threshold directional change value (30 degrees) allowed the objective identification of meanders.

Once significant meanders, inflection points, and apex points were established, several metrics were calculated. Sinuosity was calculated as the length of the channel centerline divided by the straight-line distance from the upstream end of the reach to the downstream end of the reach. Meander wavelength was determined by measuring the distance between successive apex points. The half-meander sinuosity is the centerline distance between successive inflection points, divided by the straight-line distance between those points [*Howard and Hemberger*, 1991]. Minimum radius of curvature was measured by creating a circle tangential to the channel centerline trace for a distance of 10 m upstream and downstream from the meander apex. All of these metrics except sinuosity were normalized by baseflow and bankfull channel width.

4.2.4 Bed Sediment Size

Streambed sediment was characterized using area-weighted grain size distribution. We conducted surface point counts in several individual pool and riffle features in each reach accumulating about 300 counts for each facies [*Wolman*, 1954]. The proportion of each facies in each reach was determined from digital aerial photos in a GIS. Planform polygons were created for each riffle and pool delineated using the method of *Lisle* [1987]. The total area was calculated for each facies. Facies grain size distributions were weighted by the fraction of planform area composed of that facies and area-weighted grain size distributions were calculated. The percent smaller than 4 mm, D_{16}, D_{50}, and D_{84} fractions were determined graphically from plots of distribution and used to compare channelized and reconfigured reaches.

4.3 Hydrology

4.3.1 Stream Tracer Experiments

We performed slug injections of Rhodamine WT (RWT) fluorescent dye in each study reach. The injection location was across the center of a section of narrow, turbulent flow that promoted rapid mixing across the entire channel width [*Fisher et al.*, 1979; *Moore*, 2005]. No significant inflow or outflow points occurred in the study reaches, though all reaches gained about 1 m^3/s of ground water discharge. In-stream RWT concentration was measured continuously on a 5-s interval at a single downstream location using a Turner 10 AU automated field fluorometer equipped with a flow-through cell. The stream water intake of the flourometer was fixed near the channel center. The time series of in-stream RWT concentration was represented as a breakthrough curve (BTC), and BTCs were analyzed numerically in order to characterize transient storage in each reach.

RWT is known to sorb to streambed substrate [*Bencala et al.*, 1983], and is therefore not a perfectly conservative hydrologic tracer. However, for the size of the river reaches studied here, neither salt tracers, nor continuous drip experiments were feasible. Recently, Haggerty (personal communication, 2006) has proposed that RWT desorption may be a rate-limiting transport process, though his experimental platform consisted of only sand and finer size sediment. The Provo River is a gravel and cobble bed stream with a small fraction of material less than 2 mm.

4.3.2 Solute Transport Modeling

We used a one-dimensional solute transport model, STAMMT-L, to analyze RWT breakthrough curves [*Haggerty and Reeves*, 2002; *Haggerty et al.*, 2002]. This model provides a semi-analytical solution to a one-dimensional, dual-porosity, advection-dispersion transport equation (2).

$$\frac{\partial C}{\partial t} = -v\frac{\partial C}{\partial x} + D_L\frac{\partial^2 C}{\partial x^2} - \beta_{tot}\frac{\partial}{\partial t}\int_0^t C(\tau)g^*(t-\tau)d\tau \quad (2)$$

We used both exponential and power-law distributions of residence time in an attempt to compare fits and minimize error (3, 4). The term for exponential residence time distribution was

$$g^*(t) = \alpha\ e^{-\alpha t} \quad (3)$$

The term for power-law residence time distribution was

$$g^*(t) = \frac{(k-2)}{(\alpha_{\max}^{k-2} - \alpha_{\min}^{k-2})}\int_{\alpha_{\min}}^{\alpha_{\max}} \alpha^{k-2}e^{-\alpha t}d\alpha \quad (4)$$

In all cases, C is the solute concentration in the stream (mg L^{-1}), v is the mean velocity of the stream water, D_L is the dispersivity (m), β_{tot} is the ratio of the immobile zone size to the mobile zone size, α is an exchange rate coefficient (s^{-1}), k is the power-law coefficient (slope of tail at late time), t is time (s), and x is the distance downstream (m). Mean storage residence time (t_{stor}) was computed as $1/\alpha$ for exponential simulations, and as the inverse of the harmonic mean of α_{min} and α_{max} for power-law simulations. In order to reduce error in fitting the observed BTC, the model iterates the values of β_{tot}, t_{stor}, and k. Root mean squared error (RMSE) values are computed as an indication of simulation fit to the data, with smaller values indicating better model fit to data. The model simulates mass transfer between mobile (stream) and immobile (transient storage) domains. STAMMT-L represents the immobile zone as a diffusive volume with one of several prescribed geometries. We used an infinite layered geometry. Other user inputs include the length of the system, the advective velocity, measured mobile domain BTCs, upstream concentration boundary conditions, initial conditions, and the ratio of injection mass to discharge. We used a Marsh-McBirney Flowmate 2000 in order to measure discharge at the top and bottom of each study reach for each test.

4.4 Statistical Analysis

Values derived for geomorphic metrics and transient storage parameters were statistically analyzed in order to assess trends in geomorphic and hydrologic change accomplished by the reconfiguration process. This analysis allowed us to better understand how physical reconfiguration specifically affected controls on transient storage, and transient storage parameters. Significant change was quantitatively determined using parametric independent sample t-tests [*Hayter*, 1996]. The null hypothesis for t-tests was: channelized reaches are the same as reconfigured reaches. P-values less than or equal to 0.1 indicate that the null hypothesis was false. For the various metrics, there was a wide range of sample populations, the lowest of which was 3. P-values for tests with small populations carry less statistical power than those with large populations.

We also attempted to correlate trends in physical attributes with trends in transient storage parameters, because we sought to understand the relation between attributes of channel reconstruction and changes in transient storage function. Correlations were performed using a linear regression Pearson correlation test. We focused on correlating geomorphic metrics with β_{tot} estimates derived from the numerical simulations of our BTCs, because β_{tot} was the only transient storage parameter that was significantly different between channelized and reconfigured reaches.

5.0 RESULTS

5.1 Comparison of Channelized and Reconfigured Reaches

5.1.1 Geomorphic Measurements

Reconfiguration of the middle Provo River has produced channel morphology that can be expected to increase transient storage (Figure 3-6). The channel and bed features created by reconfiguration have been shown to drive hyporheic exchange [*Kasahara and Wondzell*, 2003] as well as create low velocity in-channel storage zones. Features controlling these aspects of transient storage have been positively enhanced.

5.1.1.1 Cross-Section Geometry

Because hydrologic tracer tests were carried out during baseflow conditions, we compared cross-section geometry at baseflow stage (Table 3-2). Despite large-scale channel reconstruction, only one geomorphic attribute was significantly altered. Other attributes were altered to lesser degrees. The reach-average R was the only measured variable that was significantly altered by rehabilitation, increasing by 15% in reconfigured reaches (p=0.01). A substantial alteration also occurred in W/D. The reach average value of W/D decreased 20% in reconfigured reaches (p=0.20). These reconfigurations created relatively deeper, narrower average cross-sections at baseflow.

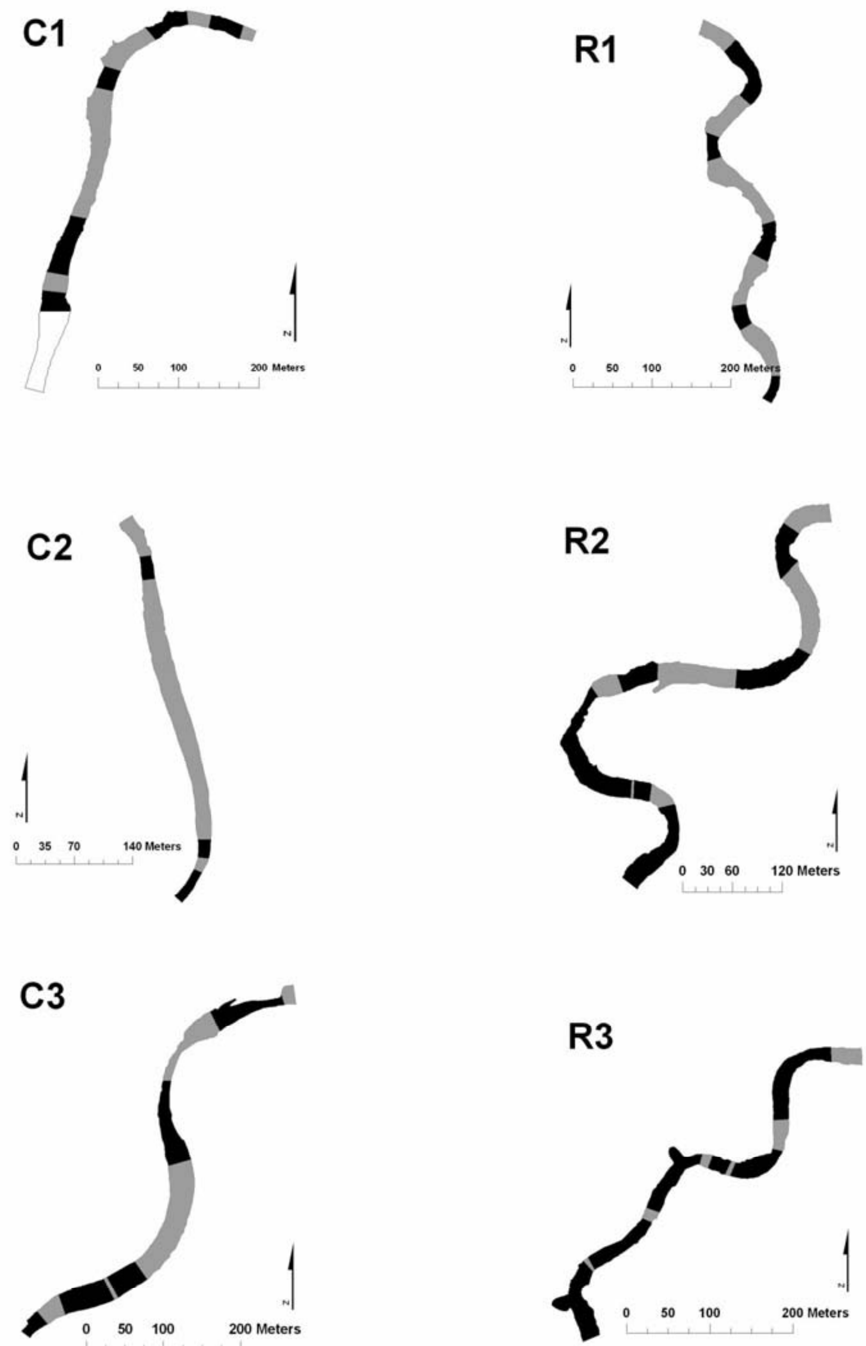

Figure 3-6. Detailed maps of each study reach. Reaches are divided into their respective riffle (gray) and pool (black) facies. The longitudinal profile of the unshaded portion of C1 was not analyzed. Flow is from top to bottom in all cases.

Table 3-2. Summary table for reach-average baseflow cross-section metrics.

Reach	Discharge (m^3/s)	Wetted Perimeter (m)	Area (m^2)	Hydraulic Radius (m)	Velocity (m/s)	Mannings Roughness Coefficient	Width (m)	Width/Mean Depth Ratio
C1	6.90	24.49	9.63	0.40	0.78	0.07	24.25	64.54
C2	4.56	20.54	7.24	0.37	0.66	0.07	20.33	55.38
C3	4.56	29.18	11.52	0.39	0.45	0.08	28.97	75.14
R1	7.80	27.84	11.66	0.44	0.75	0.08	26.51	68.45
R2	4.64	30.98	13.24	0.44	0.39	0.14	28.86	68.85
R3	5.78	17.35	7.68	0.46	0.83	0.04	18.21	40.13

5.1.1.2 Longitudinal Geometry

In general, reconfigured reaches were composed of longer, more closely spaced pools separated by shorter, steeper riffles (Figure 3-7). Although the null hypothesis was not rejected in any statistical test of longitudinal metrics, differences in the mean values of some metrics for reconfigured reaches were relatively large compared to channelized reaches (Table 3-3). The reach-average length of pools (normalized to bankfull width) increased by 50% (p=0.18) in reconfigured reaches; there was a 49% increase in the mean value of the fraction of total reach length composed of pools (p=0.22); reach-average pool spacing (normalized by bankfull width) decreased 36% (p=0.10). There was a 32% decrease in the mean value of the fraction of total reach length composed of riffles (p=0.23). The relative length-weighted slope of riffles increased by 80% (p=0.24).

5.1.1.3 Planform Geometry

Reconfigured reaches are more sinuous than channelized reaches with closely spaced meanders whose individual bends have smaller radii of curvature (Figure 3-6). Although the null hypothesis was not rejected in any statistical test, however comparison of mean values suggests that reconfigured reaches are different from channelized reaches (Table 3-4). Sinuosity increased by 20% (p=0.17). There was a 51% decrease in the

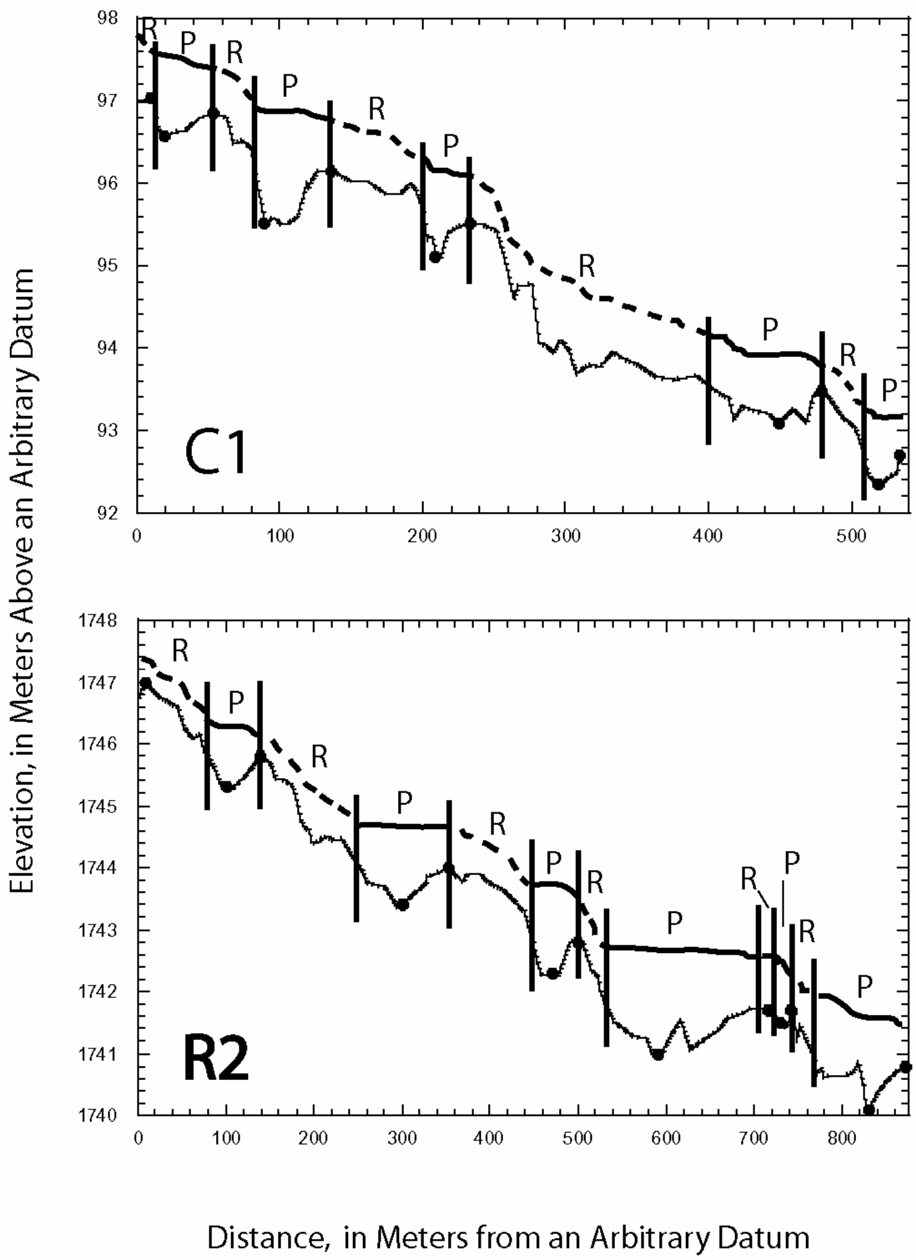

Figure 3-7. Representative longitudinal profiles for channelized (C1) and reconfigured (R2) reaches. Points on bed surface represent threshold elevations delineating significant pool (low points) and riffle (high points) facies. Pools (P) are represented by a solid water surface and riffles (R) are represented with a dashed water surface. Individual unit lengths are delineated by vertical bars and coincide with facies division in Figure 3-4.

Table 3-3. Summary table for reach-average longitudinal metrics. W_{bf} is bankfull width, and W_{ac} is active, or baseflow, width.

Metric	Reach					
	C1	C2	C3	R1	R2	R3
r^2	0.93	0.97	0.95	0.96	0.94	0.88
Reach Average W_{bf}	29.90	29.70	35.78	43.22	36.01	36.41
Reach Average W_{ac}	24.06	20.33	29.85	22.44	25.78	18.83
POOLS						
Average Length (Normalized to W_{bf})	1.52	1.76	1.93	1.18	2.39	2.36
Average Length (Normalized to W_{ac})	1.89	2.57	2.32	2.28	3.34	4.56
Fraction of Total Reach Length in Unit Type	0.43	0.29	0.50	0.40	0.59	0.82
Average Wavelength (Normalized to W_{bf})	4.15	6.54	4.25	3.08	3.83	2.70
Average Wavelength (Normalized to W_{ac})	5.16	9.55	5.10	5.92	5.34	5.22
RIFFLES						
Fraction of Total Reach Length in Unit Type	0.55	0.69	0.48	0.59	0.40	0.18
Length Weighted Mean Slope	0.0029	0.0032	0.0056	0.0031	0.0029	0.0038
Reach Slope	0.0086	0.0081	0.0081	0.0091	0.0073	0.0048
Relative Riffle Slope	1.68	1.18	2.08	1.74	2.40	4.73

mean meander wavelength normalized to bankfull width (p=0.03), and a 51% decrease when normalized to baseflow channel width (p=0.06). Half-meander sinuosity increased by 17% in reconfigured reaches (p=0.33). Reach-average minimum radius of curvature (normalized by bankfull discharge) was reduced by 45% (p=0.23), and by 42% when normalized by baseflow channel width (p=0.14).

Table 3-4. Summary table of reach-average planform metrics. N/A refers to the lack of a particular feature that would allow measurement. In statistical tests, the reach length was used as a minimum value for absent features. W_{bf} is bankfull width, and W_{ac} is active, or baseflow, width.

Metric	Reach					
	C1	C2	C3	R1	R2	R3
Total Length (m)	534.3	543.8	691	639.1	873	632
Sinuosity	1.19	1.04	1.16	1.21	1.61	1.26
Mean Full-Meander Wavelength (normalized to W_{bf})	N/A	N/A	11.29	6.75	8.7	5.10
Mean Full-Meander Wavelength (normalized to W_{ac})	N/A	N/A	13.62	8.93	12.0	9.86
Mean Half-Meander Sinuosity (pathlength/straight length)	N/A	N/A	1.14	1.15	1.65	1.15
Mean Minimum Radius of Curvature (Normalized to W_{bf})	1.00	1.02	2.43	0.96	0.78	0.68
Mean Minimum Radius of Curvature (Normalized to W_{ac})	1.25	2.16	2.92	1.27	1.09	1.32

5.1.1.4 Bed Sediment Size

Reconfigured reaches have finer bed material at all fractions compared to channelized reaches, and the difference in distribution between pools and riffles is greater in reconfigured reaches than in channelized reaches except at the largest fractions (Figure 3-8). The null hypothesis was not rejected in statistical tests of grainsize distribution. However, large relative differences in grain size are apparent, particularly in the finer size fractions (Table 3-5). The percent of material smaller than 4 mm increased for reconfigured reaches. The mean value of the area-weighted D_{16} was reduced by 60% in reconfigured reaches (p=0.02). The mean value of the area-weighted D_{50} was reduced by 32% in reconfigured reaches (p=0.03). The mean value of the area-weighted D_{84} was reduced by 29% in reconfigured reaches (p=0.05).

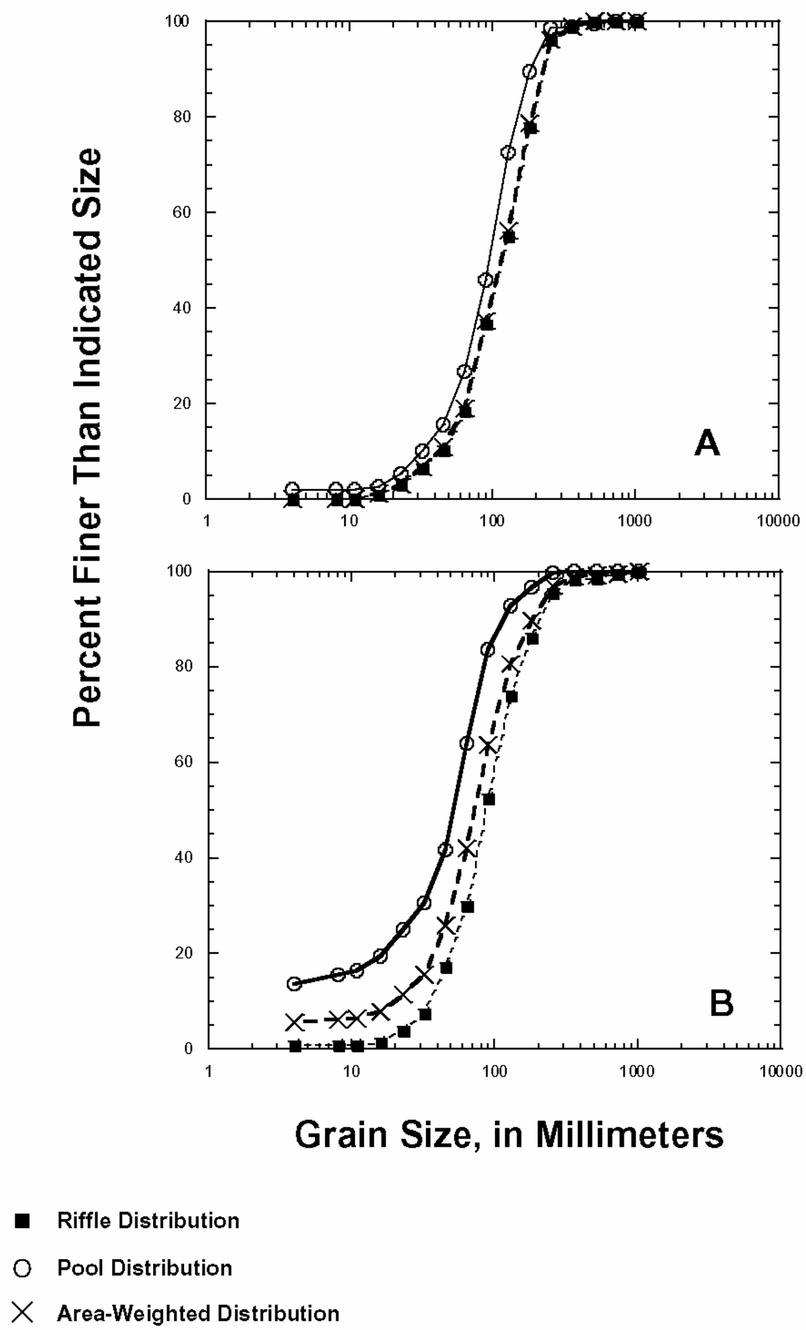

Figure 3-8. Representative plots of grainsize distribution for a A) channelized and B) reconstructed reaches. Plots for pools, riffles, and the area-weighted average of pools and riffles are shown in order to illustrate the differences in distribution between facies, and the result of producing a reach-average distribution.

Table 3-5. Summary table of reach average grainsize analysis.

Reach	Percent finer than 4mm	Area-Weighted D_{16} (mm)	Area-Weighted D_{50} (mm)	Area-Weighted D_{84} (mm)
C1	0.94	54	102	192
C2	0.98	58	103	148
C3	2.3	50	85	150
R1	1.5	35	77	124
R2	7.4	23	67	125
R3	14.2	7	53	97

5.1.2 Tracer Tests and Numerical Simulation

Power-law distributions of residence time produced the best fits to field data in all numerical simulations (Figure 3-9). The results of simulations of measured BTCs suggest limited differences in transient storage dynamics between reconfigured and channelized reaches, which is contradictory to our expectations of transient storage comparisons for the PRRP (Table 3-6). While β_{tot} increased 186 % (p=0.0094) in reconfigured reaches, t_{stor} and k were not significantly affected by reconfiguration. On average, water moved through storage zones at a similar rate, and for similar amounts of time in both reconfigured and channelized reaches. However, water was retained in storage at greater capacity in reconfigured reaches.

5.2 Correlation Between Geomorphic Conditions and Transient Storage Processes

5.2.1 Transient Storage Metric Correlation with Longitudinal Metrics

In the longitudinal direction, the size, spacing, and gradient of pool and riffle features provide first order controls on transient storage (Table 3-7). In channelized reaches, the β_{tot} parameter showed strong positive correlation (r = 0.99) with the reach

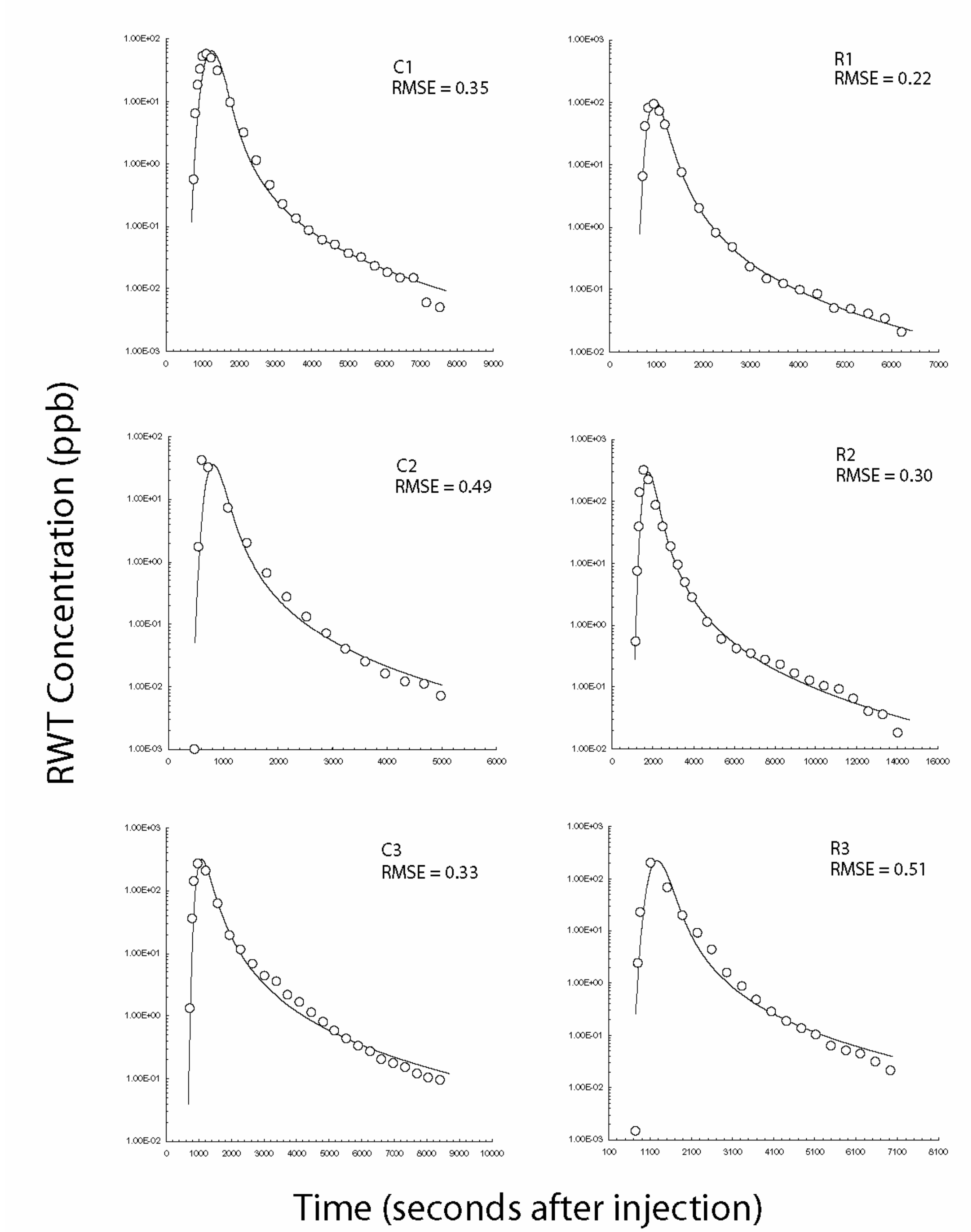

Figure 3-9. RWT BTC plots for stream tracer tests displaying in-stream concentration through time. Open circles are field data (culled for clarity), and solid lines are STAMMT-L power-law fits to field data. RMSE values are statistical error in the fit of the simulated curve with lower numbers representing better fits.

average pool length normalized to the bankfull width, a strong positive correlation with length weighted mean riffle slope (r = 0.93), and a strong negative correlation with the mean reach slope (r = -0.83).

Table 3-6. Summary table of reach-representative parameters from numerical modeling of tracer test BTC's.

Reach	β_{tot} (-)	t_{stor} (s)	k (-)
C1	0.36	186	2.39
C2	0.49	239	2.34
C3	0.66	306	2.22
R1	1.15	192	2.38
R2	1.41	291	2.35
R3	1.77	112	2.48

Table 3-7. β_{tot} correlated to longitudinal metrics using a linear regression. Table displays resulting r values. W_{bf} is bankfull width, and W_{ac} is active, or baseflow, width.

	r Values by Reach Type		
Metric	Reconfigured	Channelized	Combined
r^2	-0.98	0.44	-0.63
POOLS			
Average Length (Normalized to Wbf)	0.8	0.99	0.56
Average Pool Length (Normalized to Wac)	1	0.57	0.87
Total Fraction of Reach Length in Unit Type	1	0.4	0.82
Average Spacing (Normalized to Wbf)	-0.41	-0.03	-0.71
Average Spacing (Normalized to Wac)	-0.9	-0.08	-0.38
RIFFLES			
Total Fraction of Reach Length in Unit Type	-1	-0.4	-0.81
Length Weighted Mean Slope	0.79	0.93	-0.08
Reach Slope	-1	-0.83	-0.73
Relative Riffle Slope	0.98	0.51	0.82

The β_{tot} parameter was also strongly correlated with several longitudinal metrics in reconfigured reaches. There was a perfect (r = 1.0) positive correlation with the average pool length normalized to baseflow channel width, and the fraction of the total reach composed of pools. There was a perfect (r = -1.0) negative correlation with the fraction of the total reach composed of riffles, and with the mean reach slope. Other metrics that showed strong positive correlations were the average pool length normalized to the bankfull width (r = 0.80), the length-weighted mean riffle slope (r = 0.79), and the relative riffle slope (r = 0.98). Other strong negative correlations with β_{tot} in reconfigured reaches were found for the bed rugosity, represented as the reach r^2 (r = -0.98), and the average pool spacing normalized to baseflow channel width (r = -0.90).

With the complete dataset, β_{tot} displayed strong positive correlations with the average pool length normalized to both bankfull and baseflow channel widths (r = 0.87, 0.82 respectively) and with the relative riffle slope (r = 0.82). There were strong negative correlations with the fraction of the total reach in riffles (r = -0.81).

5.2.2 Transient Storage Metric Correlation with Planform Metrics

In the planform dimension, meander geometry is a first-order control on transient storage (Table 3-8). β_{tot} values in channelized reaches showed strong positive correlations with the mean minimum radius of curvature normalized to both the bankfull and baseflow channel widths (r = 0.90, 0.99, respectively). There were strong negative correlations with the mean full-meander wavelength normalized to the bankfull width (r = -0.92). In reconfigured reaches, there were no strong positive correlations between β_{tot} and planform metrics. A strong negative correlation did result with the mean minimum radius of curvature normalized to the bankfull width (r = -0.97). With the full data set, there were no strong positive correlations. Strong negative correlations resulted with the mean full-meander wavelength normalized to the bankfull and baseflow channel width (r = -0.90, -0.79, respectively).

Table 3-8. β_{tot} correlated to planform metrics using linear regression. Table displays resulting r values. W_{bf} is bankfull width, and W_{ac} is active, or baseflow, width.

	r Values by Reach Type		
Metric	Reconfigured	Channelized	Combined
Total Length (m)	-0.12	0.92	0.55
Sinuosity	0.02	-0.14	0.59
Mean Full-Meander Wavelength (normalized to W_{bf})	-0.54	-0.92	-0.90
Mean Full-Meander Wavelength (normalized to W_{ac})	0.21	-0.69	-0.79
Mean Half-Meander Sinuosity (pathlength/straight length)	-0.10	-0.27	0.41
Mean Minimum Radius of Curvature (Normalized to W_{bf})	-0.97	0.90	-0.46
Mean Minimum Radius of Curvature (Normalized to W_{ac})	0.28	0.99	-0.48

5.2.3 Transient Storage Metric Correlation with Cross-Section Metrics

Cross-section form has not been shown to be a primary control on transient storage, and correlations in this dimension may be related to other aspects of channel morphology (Table 3-9). β_{tot} values in channelized reaches showed strong positive correlation with the Manning's *n* (r = 0.91). There were no strong negative correlations for channelized reaches. In reconfigured reaches, a strong positive correlation was made with the hydraulic radius (r = 0.98). Strong negative correlations were made with the wetted perimeter (r = -0.79), the area (r = -0.76), and with the width-to-depth ratio (r = -0.84). With the combined dataset, a strong positive correlation was made with the hydraulic radius (r = 0.92).

Table 3-9. β_{tot} correlated to baseflow cross-sectional metrics using linear regression. Table displays resulting r values.

	r Values by Reach Type		
Metric	Reconfigured	Channelized	Combined
P (m)	-0.79	0.6	-0.13
A (m^2)	-0.76	0.5	0.14
R	0.98	-0.19	0.92
n	-0.51	0.91	0.05
W (m)	-0.59	0.65	-0.34
D (m)	0.95	0.99	0.83
W/D	-0.84	0.72	-0.64

5.2.4 Transient Storage Metric Correlation with Bed Sediment Size

Grain size distribution controls hydraulic properties of sediments (Table 3-10). β_{tot} values in channelized reaches were strongly negatively correlated with the area weighted D_{50} (r = -0.89) and area weighted D_{84} (r = -0.81). In reconfigured reaches, β_{tot} values showed perfect negative correlation with the area weighted D_{16} and D_{50}. A strong negative correlation was produced for the area weighted D_{84} as well (r = -0.89). With the combined dataset, strong negative correlations were found for all three sizes (r = -0.99, -0.98, -0.91, respectively).

Table 3-10. β_{tot} correlated to grainsize distribution using a linear regression. Table displays resulting r values.

	r Values by Reach Type		
Metric	Reconfigured	Channelized	Combined
Percent Finer than 4 mm	1	0.82	0.77
Area-Weighted D_{16} (mm)	-1	-0.63	-0.99
Area-Weighted D_{50} (mm)	-1	-0.89	-0.98
Area-Weighted D_{84} (mm)	-0.89	-0.81	-0.91

6.0 DISCUSSION

The PRRP was intended to re-establish natural riverine processes, with the ultimate goal of enhanced ecological function. The PRRP is not uncommon in this respect. Thousands of projects are implemented to reverse undesired changes to riverine systems. Thus, the PRRP is unique primarily in the scale of channel reconfiguration and the freedom with which natural processes are allowed to operate within the river corridor. We hypothesized that a project of this scale would result in significant differences between the morphology of channelized and reconstructed reaches. We anticipated that the direction of change would be towards increased geomorphic complexity and a corresponding increase in the function of transient storage, an ecologically critical process.

6.1 Reconfiguration of Physical Controls on Transient Storage

Distinguishing between in-channel and hyporheic portions of transient storage is of primary concern in tracer hydrology [*Harvey and Wagner*, 2000; *Gooseff et al.*, 2005]. Some physical parameters arguably exert more control over one component of the transient storage process than others. We used statistical correlations to differentiate between the particular effects of reconfiguration on control mechanisms of hyporheic exchange and in-channel storage in the PRRP. However, establishing the statistical significance of change was difficult given the small population of values for each metric. Small population sizes limit measures of significance, but comparisons of mean values do illustrate trends.

6.1.1 Longitudinal Controls

Statistical correlation suggests that the length, spacing, and total aerial extent of pools, and the relative slope of riffles appear to be primary controls on β_{tot}. β_{tot} increased with pool length, and decreased with pool spacing. Reconfigured reaches incorporated relatively larger, closely spaced pools possibly facilitating this increase in β_{tot}. β_{tot} correlations suggest that reconfigured reaches with shorter, steeper riffles have increased storage capacity. These steep riffles are constructed using high conductivity gravel and cobble with the capacity for a large volume of quick hyporheic exchange [*Kasahara and Wondzell*, 2003].

6.1.2 Planform Controls

Meander wavelength and minimum radius of curvature appear to have had the most significant effect on β_{tot}. For reconfigured channels, both of these metrics display a negative correlation with β_{tot}. This suggests that a channel design that incorporates more closely spaced, tighter meanders would increase transient storage capacity. Hyporheic flowpaths through meander bends would be positively affected by decreasing the spacing and radius of curvature of individual bends. However, hyporheic flow induced by these features would tend to be along longer flowpaths, increasing the mean residence time. Residence time did not increase in reconfigured reaches in this study. This implies that increased storage correlated to meander geometry is not related to long hyporheic flowpaths. Three possible explanations for this correlation are proposed. The effects of meander morphology on storage capacity could be cross-correlated to more obvious longitudinal controls. Reconfigured reaches with larger pools and steeper riffles also have more closely spaced and tighter bends. Also, in many locations, the old channel of the impaired Provo River bypasses meanders (Figure 3). The former channel is filled with spoil from excavation that includes some gravel and larger material. This could create high conductivity flowpaths in relict channels that increase capacity while having negligible affect on residence time. Thirdly, the slug injection method may not have sufficiently labeled longer flow paths with tracer, removing their influence from our BTC's.

6.1.3 Cross-Section Controls

Analysis of the cross-sectional dimension gives us important information about the average capacity of the channel, its roughness, and water velocities. A positive relationship between β_{tot} and hydraulic radius in reconfigured reaches suggests that deeper average cross-sections facilitate increased storage. Similarly, there is a negative relationship with the width/depth ratio. These trends may reflect aspects of pool morphology that are likely to control in-stream transient storage.

6.1.4 Grain Size Controls

β_{tot} correlated strongly with all grainsize metrics. Correlations between β_{tot} and grain size indicate that as sediment size decreases, storage capacity increases. Also, as the percent of grains finer than 4 mm increases, β_{tot} increases. This is somewhat counterintuitive. Fine-grain sediment is often thought to impede the penetration of surface water into the hyporheic zone. However, D_{16} values in reconfigured reaches are still in the gravel size range, and percentages of material smaller than 4 mm are relatively low. The increase in β_{tot} associated with decreased grainsize could also be reflective of the tendency for pools (in-channel storage) to have a finer overall grainsize distribution.

6.2 Alterations to Transient Storage Dynamics

Numerical simulation of BTCs yielded some parameter values that contradicted our original hypothesis. The lack of significant differences in t_{stor} and k between channelized and reconfigured reaches is perhaps the most interesting result of this investigation, especially when compared to the large increase in β_{tot} in reconfigured reaches. The situation sets boundaries on transient storage processes imparted through reconfiguration.

If a significant amount of this increased storage could be attributed to hyporheic flowpaths in the floodplain or at significant depths below the streambed, one would expect to see a relative shift of t_{stor} towards longer time, because of the tortuous flowpaths characteristic of subsurface flow. This expectation assumes increased hyporheic flowpath lengths through meander bends and gravel bars, or increased depth of penetration of surface water into the hyporheic zone caused by enhanced longitudinal controls in reconfigured reaches, compared to channelized reaches. Tracer particles traveling these paths would experience longer travel times, thereby increasing t_{stor} estimates. As stream water accessed flowpaths deeper in the subsurface and farther into the adjacent floodplain, one could also expect that the exchange rate between the immobile and mobile zones would decrease. This would be due mainly to the fine-grain floodplain deposits that one would expect to encounter in these regions. This material would result in lower hydraulic conductivities, and slower exchange rates.

Significant alteration of transient storage residence times and mass transfer rates were not apparent in our results, however we did see a significant increase in storage capacity. If we assume that a laterally extensive and substantially deep hyporheic zone was not created by reconfiguration, then in-channel storage or a hyporheic zone with quick-exchange flow paths would have to accommodate the increase in storage capacity. Our geomorphic measurements and correlations support this conclusion. Increased pool size and abundance could increase in-channel storage, and short, steep riffles composed of coarse material could induce a large amount of quick hyporheic exchange.

6.3 Transient Storage Restoration

Our original hypothesis, that large-scale stream reconfiguration would inevitably alter the size, residence times, and exchange dynamics of both in-channel and hyporheic components of transient storage, was not demonstrated. This implies that if the rehabilitation of hyporheic function is to be a specified goal of rehabilitation, design parameters may need to more specifically target that goal. This presents a complicated engineering challenge, and suggestions about possible solutions are beyond the scope of this study. We can, however, discuss several potential constraints that exist for the PRRP. These are common physical conditions that could apply to many stream restoration projects.

One naturally imposed limitation is the regional ground water regime [*Woessner*, 2000]. The Provo River gains on the order of 1 m^3/s of flow per 650 m of channel length. The prevalent ground water gradient toward the stream could limit hyporheic flow from extending laterally any significant distance into the adjacent floodplain. There could be anthropogenic boundary conditions imposed through various construction techniques as well.

We observed that as a new channel is constructed, large machinery is repeatedly moving over the freshly excavated alluvium composing the valley floor. Though heterogeneous, the general sediment composition observed in the PRRP construction reach is matrix-supported floodplain alluvium, and is very poorly sorted from large cobble to fine sand and silt. This is the substrate into which the reconfigured channel is carved. There is some potential for compaction of this material as heavy equipment works in the channel. Regardless of compaction, when the sorted cobble is added to the channel as bed substrate, a high conductivity layer is created over a relatively low conductivity material. If the contrast in hydraulic conductivity is high enough, surface water may preferentially travel through the large bed material. The total flux would depend on the thickness of the added cobble.

Another example of a channel construction process affecting the nature of transient storage is in the occurrence of streambed "clogging." Construction typically proceeds from the downstream end of a reach to the upstream end. As construction progresses, fine sediment is introduced to the channel downstream. Fine-grain sediment deposited in the interstitial space of the streambed, below the surface armor layer, may create a barrier to hyporheic flow [*Rehg et al.*, 2005]. This could effectively decrease the penetration of surface water into the streambed and limit transient storage to its in-channel component.

6.4 Limitations of the Stream Tracer Technique

Some aspects of the stream tracer technique limit the extent of interpretation of tracer test results with regard to hyporheic processes. Stream tracers have a "window of detection" that sets spatial and temporal limits on their characterization of transient storage processes [*Harvey and Wagner*, 2000]. Of the total possible set of flowpaths that might exist in a river system, there exists a subset of flowpaths that can be measured using stream tracers. Stream tracers have decreasing utility in characterizing transient storage flowpaths with large spatial extents and long residence times. Thus, the usefulness of stream tracer tests in measuring hyporheic interaction may be limited to near-stream flowpaths that are short, and have relatively low residence times.

The relative interaction of downstream transport and transient storage can also set limits on the interpretation of tracer test results. An expression of the balance of these processes known as the Damkohler number, *DaI*, is used to quantify the balance between advection and storage, determine the potential sensitivity of a particular tracer test to storage processes, and the reliability of parameter estimates derived from a particular tracer test [*Harvey and Wagner*, 2000].

$$DaI = \frac{\alpha(1 + A/A_s)L}{v}$$

where α is the harmonic mean of maximum and minimum diffusion rate coefficients in units of per second, A/A_s is equivalent to B_{tot}, L is the reach length in meters, and *v* is the reach average velocity in meters per second [*Wagner and Harvey, 1997*]. *Harvey and Wagner* [2000] used data from several tracer tests to calculate *DaI* and determine the range of values that still produce reliable parameter estimates. They found that *DaI* values much less or greater than 1 introduced unacceptable uncertainty into parameter estimates. We generated *DaI* values for each of our tests and found a range of values from about 0.95 to about 7.39. These *DaI* values suggest that our parameter estimates are within an acceptable range of reliability.

7.0 CONCLUSION

Large-scale channel reconfiguration associated with the PRRP altered the physical controls on transient storage in a way that would tend to create hyporheic exchange flowpaths through riffle-pool sequences and meander bends. However, tracer studies did not provide evidence of the creation of these flowpaths. Though β_{tot} was substantially increased, t_{stor}, and k were unaltered. The increase in storage capacity may be due to quick exchange hyporheic flow and in-channel storage. Though restored hyporheic function was not a stated goal of the PRRP, we expected that such large-scale channel reconfiguration would promote this process and add to an enhanced, rehabilitated river ecosystem in the Provo River. Stream restoration projects that wish to include increased hyporheic flow as an objective may need to develop specialized design parameters to engineer a hyporheic zone within imposed and practical constraints.

Studies of this nature are currently under-represented in the literature. Pressure is increasing for the scientific community to advance its understanding of the effects of ecological restoration on transient storage processes. Field studies that are incorporated into restoration projects during the planning and design phase stand to contribute significantly. Future research would also benefit by using detailed hydrometric data at the reach scale. In this way, direct physical evidence of hyporheic exchange could be gathered, and a more detailed picture of the interplay between channel reconfiguration and transient storage could be presented. Hydrometric data would complement the stream tracer approach, and eliminate some of the potential limitations of the tracer technique.

REFERENCES

Alayban, A.M., and R.S. Chalov (1998), Types of river channel patterns and their natural controls, *Earth Surf. Processes Landforms*, 23, 467-474.

Anderson, J.K., S.M. Wondzell, M.N. Gooseff, and R. Haggerty (2004), Patterns in stream longitudinal profiles and implications for hyporheic exchange flow at the H.J. Andrews Experimental Forest, Oregon, USA, *Hydrological Processes*, 18, doi:10.1002/hyp.5791.

Bash, J.S., and C.M. Ryan (2002), Stream restoration and enhancement projects: is anyone monitoring, *Environmental Management*, 29, 877-885.

Baxter, C.V., and F.R. Hauer (2000), Geomorphology, hyporheic exchange, and selection of spawning habitat by Bull Trout (Salvelinus confluentus), *Can. J. Fish. Aquat. Sci.*, 57, 1470-1481.

Bencala, K.E. (1993), A perspective on stream-catchment connections, *J. N. Am. Benth. Soc.*, 12, 44-47.

Bencala, K.E., R.E. Rathbun, A.P. Jackman, V.C. Kennedy, G.W. Zellweger, and R.J. Avanzino (1983), Rhodamine WT dye loses in a mountain stream environment. *Water Resor. Bull., 19*, 943-950.

Bencala, K.E. and R.A.Walters (1983), Simulation of solute transport in a mountain pool-and riffle stream: A transient storage model, *Water Resour. Res.*, 19, 718-724.

Bernhardt, E.S., M.A. Palmer, J.D. Allen, G. Alexander, K. Barnas, S. Brooks, J. Carr, S. Clayton, C. Dahm, J. Follstad-Shah, D. Galat, S. Gloss, P. Goodwin, D. Hart, B. Hassett, R. Jenkinson, S. Katz, G.M. Kondolf, P.S. Lake, R. Lave, J.L. Meyer, T.K. O'Donnell, L. Pagano, B. Powell, and E. Sudduth (2005), Synthesizing U.S. river restoration efforts, *Science*, 38, 636-637.

Biskey, T.M., and E.D. Gross (2001), The hyporheic zone: Linking groundwater and surface water-understanding the paradigm, *Remediation: The Journal of Environmental Cleanup Costs, Technologies, and Techniques*, 12, 55-62.

Brunke, M., and T. Gonser (1997), The ecological significance of exchange processes between rivers and groundwater, *Freshwater Biology*, 37, 1-33.

Brunke, M., E. Hoehn, and T. Gonser (2003), Patchiness of river-groundwater interactions within two floodplain landscapes and diversity of aquatic invertebrate communities, *Ecosystems*, 6, 707-722.

Cardenas, M.B., and V.A. Zlotnik (2003), Three-dimensional model of modern channel bend deposits, *Water Resour.Res.*, 39, 1141-1153.

Collier, K.J., A.E. Wright-Stow, and B.J. Smith (2004), Trophic basis of production for a mayfly in a North Island, New Zealand, forest stream: Contributions of benthic versus hyporheic habitats and implications for restoration, *New Zealand Journal of Marine and Freshwater Research*, 38, 301-314.

Central Utah Water Conservancy District (1994), Provo River Restoration Project, *Technical Report*, Central Utah Water Conservancy District, Orem, UT.

Duff, J.H., and F.J. Triska (1990), Denitrification in sediments from the hyporheic zone adjacent to a small forested stream, *Can. J. Aquat. Sci.*, 47, 1140-1147.

Federal Interagency Stream Restoration Working Group (1998), Stream corridor restoration: principles, processes, and practices, National Technical Information Service, Washington D. C.

Fernald, A.G., P.J. Jr. Wigington, and D.H. Landers (2001), Transient storage and hyporheic flow along the Willamette River, Oregon: Field measurements and model estimates, *Water Resour. Res.*, 37, 1681-1694Findlay, S. (1995), Importance of surface-subsurface exchange in stream ecosystems: The hyporheic zone, *Limnology and Oceanography*, 40, 159-164.

Fischer, H.B., E.J. List, R.C.Y. Koh, J. Imberger, and N.H. Brooks (1979), *Mixing in inland and coastal waters*, Academic Press, New York.

Giller, P. S. (2005) River restoration: seeking ecological standards, Editor's introduction, *J. App. Eco.*, 42, doi: 0.1111/j.1365-2664.2005.01020.x.

Gleick, P.H. (2003), Global freshwater resources: soft-path solutions for the 21st century, *Science*, 302, 1524-1528.

Gooseff, M.N., J.K. Anderson, S.M. Wondzell, J. LaNier, and R. Haggerty (2006), A modelling study of hyporheic exchange pattern and the sequence, size, and spacing of stream bedforms in a mountain stream network, Oregon, USA, *Hydrological Processes*, 20, 2443-2457.

Gooseff, MN, J LaNier, R Haggerty, and K Kokkeler (2005), Determining in-channel (dead zone) transient storage by comparing solute transport in a bedrock channel-alluvial channel sequence, Oregon. *Water Resour. Res.*, 41, W06014, doi:10.1029/2004WR003513.

Graf, W. L. (2001), Damage control: restoring the physical integrity of America’s rivers, *Annals of the Association of American Geographers*, 91, 1-27.

Haggerty, R., and P.C. Reeves (2002), STAMMT-L version 1.0 user’s manual, Sandia National Laboratories, Albuquerque, New Mexico.

Haggerty, R., S.M. Wondzell, and M.A. Johnson (2002), Power-law residence time distribution in the hyporheic zone of a 2nd-order mountain stream, *Geophysical Research Letters*, 29, doi: 10-1029/2002GL014743.

Hancock, P.J., and A.J. Boutlon (2005), The effects of an environmental flow release on water quality in the hyporheic zone of the hunter river, Australia, *Hydrobiologia*, 552, 75-85.

Harvey, J.W., and K.E. Bencala (1993), The effect of streambed topography on surface-subsurface water exchange in mountain catchments, *Water Resour. Res.*, 29, 89-98.

Harvey, J.W., and B.J. Wagner (2000), Quantifying hydrologic interactions between streams and their subsurface hyporheic zones, from *Streams and Groundwaters*, J.A. Jones, and P.J. Mulholland, eds., 33-44.

Hayter, A.J. (1996), *Probability and statistics for engineers and scientists*, PWS Publishing Company, Boston MA.

Henderson, F.M. (1963). *Stability of alluvial channels, Trans. Am. Soc. Civ. Eng*., 128, 657-686.

Howard, A.D., and A.T. Hemberger (1991), Multivariate characterization of meandering, *Geomorphology*, 4, 161-186.

Kasahara, T., and A.R. Hill (2005), Effects of riffle-step restoration on hyporheic zone chemistry in N-rich lowland streams, *Can. J. Fish. Aquat. Sci*., 63, 120-133.

Kasahara, T., and S.M. Wondzell (2003), Geomorphic control of hyporheic exchange flow in mountain streams, *Water Resour. Res*., 39, 1005-1019.

Kondolf. G.M., and E.R. Micheli (1995), Evaluating stream restoration projects, *Environmental Management*, 19, 1-15.

Leopold, L.B., and M.G. Wolman (1957), River channel pattern: braided, meandering, and straight: Physiographic and hydraulic studies of rivers, *US Geol. Surv. Prof. Paper*, 282-B.

Lisle, T.E. (1987), Using “residual depths” to monitor pool depths independently of discharge, *Res. Note PSW-394*, 4 p, USDA, Berkeley CA.

Marion, A., M. Bellinello, I. Guymer, A. Packman (2002), Effect of bed form geometry on the penetration of non-reactive solutes into a streambed, *Water Resour. Res*., 38, doi:10.1029/ 2001WR000264.

Moore, D.M. (2005), Slug injection using salt in solution, *Streamline Watershed Management Bulletin*, 8, 1-6.

National Research Council, 1992, Restoration of aquatic ecosystems, 552 p, National Academy Press, Washington, D. C.

Nilsson, C., C.A. Reidy, M. Dynesius, and C. Revenga (2005), Fragmentation and flow regulation of the world's large river systems, *Science*, 308, 405-408.

O'Neill, M.P., and A.D. Abrahams (1984), Objective identification of pools and riffles, *Water Resour. Res.*, 20, 921-926.

O'Neill, M.P., and A.D. Abrahams (1986), Objective identification of meanders and bends, *Journal of Hydrology*, 83, 337-353.

Palmer M.A., E.S. Bernhardt, J. D. Allan, P.S. Lake, G. Alexander, S. Brooks, J. Carr, S. Clayton, C. N. Dahm, J. Follstad Shah, D. L. Galat, S. Loss, G. P. Goodwin, D.D. Hart, B. Hassett, R. Jenkinson, G.M. Kondolf, R. Lave, J.L. Meyer, T.K. O'Donnell, L. Pagano, and E. Sudduth (2005), Standards for ecologically successful river restoration, *Journal of Applied Ecology*, 42, doi:10.1111/j.1365-2664.2005.01004.x.

Pepin, D. M., and F. R. Hauer (2002), Benthic responses to groundwater-surface water exchange in 2 alluvial rivers in northwestern Montana, *Journal of the North American Benthological Society*, 21, 370-383.

Poole, G.C., and C.H. Berman (2001), An ecological perspective on in-stream temperature: natural heat dynamics and mechanisms of human-caused thermal degradation, *Environmental Management*, 27, 787-802.

Rehg, K.J., A.I. Packman, and J. Ren (2005), Effects of suspended sediment characteristics and bed sediment transport in streambed clogging, *Hydrological Processes*, 19, 413-427.

Sophocleous, M. (2002). Interactions between groundwater and surface water: The state of the science, *Hydrogeology Journal*, 10, 52-67.

Storey, R.G., K.W.F Howard, and D.D. Williams (2003), Factors controlling riffle-scale hyporheic exchange flows and their seasonal changes in a gaining stream: A three-dimensional groundwater flow model, *Water Resour. Res.*, 39, 1034-1050.

Terzaghi, K., R.B. Peck, and G. Mesri (1996), *Soil mechanics in engineering practice*, 3rd ed., 549 p, Wiley and Sons, New York NY.

Triska, F.J., J.H. Duff, and R.J. Avanzino (1993), Patterns of hydrological exchange and nutrient transformation in the hyporheic zone of a gravel-bottom stream: examining terrestrial-aquatic linkages, *Freshwater Biology*, 29, 259-274.

Triska, F.J., V.C. Kennedy, R.J. Avanzino, G.W. Zellweger, and K.E. Bencala (1989), Retention and transport of nutrients in a third-order stream in northwestern California: Hyporheic processes, *Ecology*, 70, 1893-1905.

Utah Reclamation Mitigation and Conservation Commission (1997), Provo River Restoration Project, *FEIS*, US Dept. of the Interior, Washington D.C.

Vervier, P., M. Dobson, and G. Pinay (1993), Role of interaction between surface and ground waters in DOC transport and processing: Considerations for river restoration, *Freshwater Biology*, 29, 275-284.

Wagner, B.J., and J.W. Harvey (1997), Experimental design for estimating parameters of rate-limited mass transfer: Analysis of stream tracer studies, *Water Resour. Res*., 33, pp. 1731-1741.

White, D.S. (1993), Perspective on defining and delineating hyporheic zones, *Journal of the North American Benthological Society*, 12, 61-69.

Williams, G.P. (1986), River meanders and channel size, *Journal of Hydrology*, 88, 147-164.

Willis, J.B., and G.C. Willis (2003), Geology of Wasatch Mountain State Park, in *Geology of Utah's Parks and Monuments*, 2nd ed., edited by D.A. Sprinkle, T.C. Chidsey Jr., and P.B. Anderson, pp. 495-516, Utah Geological Association and Bryce Canyon Natural History Association Publication.

Woessner, W.W. (2000), Stream and fluvial plain ground water interactions: Rescaling hydrogeologic thought, *Ground Water*, 38, 423-429.

Wohl, E., P.L. Angermeier, B. Bledsoe, G.M. Kondolf, L. MacDonnell, D.M. Merritt, M.A. Palmer, N.L. Poff, and D. Tarbton (2005), River restoration, *Water Resour. Res*., 41, 1-12.

Wolman, M.G. (1954), A method of sampling coarse river-bed material, *Trans. Amer. Geo. Union*, 35, 951-9.

Woodward, L., E.H. Jensen, and J.L. Harvey (1976), Soil survey of the Heber Valley area, Utah; Parts of Wasatch and Utah counties, *Soil Survey*, United States Department of Agriculture, Washington, D.C.

CHAPTER 4

CONCLUSION

Ecosystem conservation and restoration are important applications of geomorphology, hydrology, engineering, and biology. These scientific disciplines provide the primary knowledge and tools used to develop stream restoration plans [*Federal Interagency Stream Restoration Working Group*, 1998; *Wohl et al.*, 2005]. It is critical for practitioners, managers, and researchers to collaborate on integrated monitoring studies in order to facilitate increased restoration success and scientific progress [*England et al.*, 2007; *Giller*, 2005; *Kondolf*, 1998]. The research presented here is the product of collaboration between professionals involved with the PRRP, and researchers interested in the process of large-scale stream restoration and its effects on transient storage dynamics and channel/floodplain connectivity. We developed a simple and adaptable conceptual model outlining the primary steps in a large-scale restoration project from inception to completion. Within the structure of this conceptual model, we analyzed technical documents and made measurements in order to retrospectively quantify pre- and post- project channel morphology, floodplain inundation, and transient storage on the Provo River.

Our post-project evaluation of the PRRP revealed that many of the physical conditions of the impaired system were only qualitatively described. The guiding vision for the PRRP was based on moving toward a self-sustaining system both physically and biologically [*Utah Reclamation Mitigation and Conservation Commission (A)*, 1997]. Several studies collected ecological baseline data during the planning phase, detailing existing habitat quality, as well as habitat requirements, populations, and distributions of many aquatic and riparian species [*Belk and Ellsworth*, 2000; *Ross and Peterson*, 1998; *Shiozawa et al.*, 2002; *Stromberg et al.*, 1999]. However there was an apparent lack of geomorphic measurements made in existing channelized portions of the river prior to project design. The main baseline physical analysis was focused on surface and groundwater resources in the area [*Utah Reclamation Mitigation and Conservation Commission (B)*, 1997]. There were no baseline measurements of existing channel geometry, hydraulics, sediment flux, or groundwater/surface water dynamics reported. From a research perspective, such baseline measurements are critical to understanding how the system was altered by, and reacts to, the restoration process. Our retrospective analysis of the planning and design procedures of the PRRP coupled with physical measurements in channelized and reconfigured reaches provided us with the information necessary to quantitatively assess these physical alterations and functional responses.

In quantifying the channelized condition of the Provo River we found that the perceptions of physical impairment that led to the PRRP were justified. Our measurements suggest that the channelized river was relatively simple in planform, with a uniformly steep gradient and distantly spaced pools. The streambed substrate was coarse, with little difference in grain size distribution amongst pool and riffle facies. Cross-section measurements characterize a channel that is capable of conveying the 100-yr flood, as it was designed to do by the Bureau of Reclamation during the Provo River Project.

Channel design, though based primarily on qualitative assessment of the impaired physical form the Provo River, was intended to introduce geomorphic complexity appropriate to the anticipated hydrology. A range of values was developed using standard hydraulic geometry relationships. These values were used to guide design and construction. Initial calculations of channel geometry values went through an iterative design and build process. The logistical necessities of construction, which often supersede planned alterations, led to further changes to initial design values that were often not reported. The intended alterations put forward in design documents were such that, when compared to existing impaired conditions, goals of increased floodplain inundation, and increased hydraulic complexity would have been achieved. However, we found that the as-built channel often differed substantially from initial designs. It is important to consider these discrepancies between design alterations and as-built conditions when measuring the effectiveness of the PRRP in producing intended functional changes to the system.

We analyzed cross-section form and channel hydraulic parameters such as velocity and flow resistance in order to estimate the magnitude of floodplain inundation for the post-reconfiguration 2-year recurrence discharge. An estimation of the 2-year recurrence flow was the design discharge upon which design estimates were based. In measurements of channel morphology, increases to hydraulic roughness were greater than intended, as were reductions to velocity, but slopes were somewhat steeper than designed. We also found that reconfigured channels had somewhat larger cross-sectional areas and hydraulic radii than the average channelized condition. Cross-section design had intended reductions in these metrics. One-dimensional hydraulic modeling results suggest that in many reaches, a substantial percentage of as-built cross-sections had capacities in excess of the actual 2-year flood. This result suggests that a primary project goal, the occurrence of bankfull discharge at a 2-year recurrence interval, may not be met. However, overbank flow has been observed in most reaches in most years since their respective reconfigurations. This apparent contradiction might be resolved by observing that overbank flow is not occurring throughout a given reach, but instead overbank flow occurs at relatively few point locations where cross-section capacity is smaller than the 2-year flood. In light of this situation, it is significant that we found the post-reconfiguration 2-year flood to be larger than estimated in all reaches. This is something that was not previously quantified. The combination of facts that floods have been larger than expected, and that floodplain inundation is currently achieved by overbank flow at only a few cross-sections indicates a disconnection of the channel and floodplain with any future decreases in the magnitude of 1 to 2 year floods. Thus the interpretation of project success in terms of channel/floodplain connections is strengthened with the results of our analysis of the design and construction process.

Our investigation of physical changes imparted by the design and build process of the PRRP also assisted in our analysis of transient storage and hyporheic exchange on the Provo River. By comparing as-built conditions to channelized conditions we determined that reconfiguration of the Provo River altered geomorphic controls on transient storage in a manner that would be expected to increase transient storage capacity (β_{tot}) and residence time (t_{stor}), and decrease the exchange rate between the stream and storage zones (k). Reconfigured reaches tended to be composed of long pools separated by short, relatively steep, riffles. On average, cross-sections were made deeper, and velocities were slowed. Reconfigured reaches achieved increased frequency of meanders, and reduced radii of curvature achieving an overall increase in sinuosity. Grain size distributions in reconfigured reaches displayed reductions in all grain size fractions. In fact, the magnitude of these alterations, which would be expected to increase transient storage, exceeded most design intentions. This was true in particular of pool spacing, average depth, and average velocities. However, through numerical analysis of hydrologic tracer tests, we found that the β_{tot} parameter was the only transient storage metric that was substantially increased, while t_{stor}, and k were unaltered. These results do not provide conclusive evidence of the establishment of an extensive hyporheic zone, which is contrary to our original hypothesis. Surface water flux through a laterally, or vertically, extensive hyporheic zone would tend to increase mean residence time, and decrease the exchange rate of solute between storage and the channel. In-channel storage may have been increased through the construction of long, deep pools that would account for the increase in β_{tot}. More detailed hydrometric data may be needed to substantiate these results, but it appears that stream restoration projects that wish to include increased hyporheic flow as an explicit project goal may need to attempt to design and construct a hyporheic zone. Again, this is a conclusion that would not be reached with some detailed knowledge concerning the methods of design and construction of a particular project. We know through our post-project assessment that transient storage was not explicitly addressed in design, and certain construction techniques may have resulted in streambed compaction thereby limiting hyporheic exchange.

The results of this case study in post-project evaluation show that many assumptions were made along the route from the perception of a problem, to formulating project goals, channel and floodplain design, and eventual construction of the PRRP. Assumptions were made regarding the physical impairment to the system. Though these assumptions were made based on a scientific understanding of naturally functioning river systems, no data was collected to quantify the nature of physical impairment. These perceptions guided the formation of project goals. Our measurements suggest that perceptions of impairment were likely correct, and design efforts were on track to achieve goals of re-establishing dynamic physical processes. However, with no evaluation of the result, managers were left to assume design objectives were achieved and that the techniques were effective. Our measurements suggest that what was constructed was often very different than design, and the functional response of the Provo River to channel and floodplain re-alignment was not as expected.

REFERENCES

Belk, M.C., and C.M. Ellsworth (2000), Fish diversity and abundancem and availability and use of aquatic habitats in the Provo River between Deer Creek and Jordanelle Reservoirs, 1997-1999: Pre-restoration baseline report, *Utah Reclamation Mitigation and Conservation Commission*, 18 pp.

England J., K.S. Skinner, and M.G. Carter (2007), Monitoring, river restoration and the Water Framework Directive, *Water and Environmental J.*, dio: 10.1111/j.1747-6593.2007.00090.x, 1-8.

Federal Interagency Stream Restoration Working Group (1998), Stream corridor restoration: principles, processes, and practices, National Technical Information Service, Washington, D. C.

Giller, P. S. (2005) River restoration: seeking ecological standards, Editor's introduction, *J. App. Eco.*, 42, doi: 0.1111/j.1365-2664.2005.01020.x.

Kondolf, G.M. (1998), Lessons learned from river restoration projects in California, *Aquatic Conservation: Marine and Freshwater Ecosystems*, 8, 39-52.

Ross, D.A., and C.R. Peterson (1998), A review of the habitat requirements of the Columbia Spotted Frog (Rana luteiventris) in the intermountain region and recommendations for the restoration of the Columbia Spotted Frog habitat along the middle Provo River, *Utah Reclamation Mitigation and Conservation Commission*, 51 pp.

Shiozawa D.K., B.J. Weibell, and E. McLaughlin (2002), The investigation of the macrobenthos of the Provo River between Jordanelle and Deer Creek Reservoirs, *Utah Reclamation Mitigation and Conservation Commission*, 45 pp.

Stromberg, J.C., S.J. Lite, and D.T. Patten (1999), Provo River Restoration Project: Riparian vegetation, *Utah Reclamation Mitigation and Conservation Commission*, 250 pp.

Utah Reclamation Mitigation and Conservation Commission (A) (1997), Provo River Restoration Project, *FEIS*, US Dept. of the Interior, Washington, D.C.

Utah Reclamation Mitigation and Conservation Commission (B) (1997), Water Resources Technical Report, *FEIS*, US Dept. of the Interior, Washington D.C.

Wohl, E., P.L. Angermeier, B. Bledsoe, G.M. Kondolf, L. MacDonnell, D.M. Merritt, M.A. Palmer, N.L. Poff, and D. Tarboton (2005), River restoration, *Water Resour. Res*., 41, 1-12.

APPENDIXES

APPENDIX A: POINT COORDINATES OF ALL CROSS-SECTIONS IN EACH REACH

STUDY REACH C1

Table A-1. Reach C1, cross-section 1 point coordinates and descriptions.

Cross-Section 1				
N (m)	**E (m)**	**Z (m)**	**X (m)**	**Description**
4981.43	5042.17	100.92	0.00	XS1-LEP
4981.47	5042.08	100.71	0.10	TOPO
4985.05	5034.05	100.54	8.89	TOPO
4987.36	5028.85	98.38	14.58	TOPO
4987.75	5027.99	98.18	15.53	TOPO
4987.99	5027.46	97.72	16.11	LEW
4987.88	5027.70	97.65	16.38	OS
4988.21	5026.94	97.12	17.21	OS
4988.79	5025.65	97.05	18.62	OS
4989.53	5024.00	97.05	20.43	OS
4990.76	5021.23	97.04	23.46	OS
4992.40	5017.55	97.38	27.49	OS
4992.69	5016.89	97.34	28.21	OS
4993.55	5014.97	97.37	30.32	OS
4994.30	5013.29	97.58	32.16	OS
4994.39	5013.09	97.67	32.37	REW
4994.58	5012.65	97.84	32.85	TOPO
4995.09	5011.53	98.18	34.09	TOPO
4995.75	5010.04	99.16	35.72	TOPO
4996.66	5007.99	99.66	37.95	TOPO

Table A-2. Reach C1, cross-section 1-A point coordinates and descriptions.

Cross-Section 1A				
N (m)	**E (m)**	**Z (m)**	**X (m)**	**Description**
4967.80	5025.46	99.47	0.00	TOPO
4969.12	5022.69	98.95	3.07	TOPO
4971.00	5018.75	97.46	7.44	LEW
4971.73	5017.23	96.97	9.11	OS
4972.03	5016.59	96.62	9.83	OS
4972.80	5014.99	96.58	11.60	OS
4973.49	5013.54	96.71	13.21	OS
4974.02	5012.42	96.85	14.45	OS
4974.80	5010.79	96.97	16.26	OS
4977.43	5005.29	97.18	22.35	OS
4977.81	5004.50	97.27	23.23	OS
4977.92	5004.26	97.34	23.50	OS
4977.98	5004.14	97.44	23.62	REW
4977.99	5004.12	97.43	23.65	TOPO
4978.22	5003.62	97.52	24.20	TOPO
4978.31	5003.44	97.62	24.40	TOPO
4979.08	5001.82	98.45	26.19	TOPO
4979.29	5001.38	98.73	26.68	TOPO
4979.91	5000.08	98.79	28.12	TOPO

Table A-3. Reach C1, cross-section 1B point coordinates and descriptions.

Cross-Section 1B				
N (m)	**E (m)**	**Z (m)**	**X (m)**	**Description**
4940.30	5012.86	99.32	0.00	TOPO
4940.22	5013.32	99.05	0.47	TOPO
4937.21	5015.54	97.98	4.21	HW
4940.05	5014.26	97.79	7.33	TOPO
4940.48	5011.82	97.42	9.80	TOPO
4940.64	5010.94	97.29	10.70	LEW
4940.72	5010.45	97.08	11.20	OS
4941.16	5007.96	96.95	13.72	OS
4941.75	5004.65	96.82	17.08	OS
4942.26	5001.77	96.70	20.01	OS
4942.57	5000.01	96.67	21.80	OS
4943.16	4996.65	97.16	25.22	OS
4943.47	4994.86	97.26	27.03	OS
4943.50	4994.69	97.31	27.20	REW
4943.44	4995.03	97.40	27.55	TOPO
4943.52	4994.58	97.58	28.00	TOPO
4943.60	4994.12	97.86	28.47	TOPO
4943.75	4993.33	98.05	29.28	TOPO
4943.86	4992.66	98.37	29.95	TOPO
4944.37	4989.77	98.49	32.89	TOPO

Table A-4. Reach C1, cross-section 1C point coordinates and descriptions.

Cross-Section 1C				
N (m)	**E (m)**	**Z (m)**	**X (m)**	**Description**
4914.17	5021.70	99.06	0.00	TOPO
4914.46	5019.11	97.63	2.60	TOPO
4915.01	5014.35	97.27	7.39	TOPO
4915.44	5010.56	97.08	11.21	TOPO
4915.47	5010.35	96.99	11.43	LEW
4915.49	5010.14	96.94	11.64	OS
4915.77	5007.66	96.86	14.13	OS
4915.98	5005.87	96.72	15.93	OS
4916.13	5004.55	96.58	17.27	OS
4915.86	5006.87	96.37	19.60	OS
4915.94	5006.16	96.29	20.32	OS
4915.91	5006.50	96.75	20.66	OS
4916.16	5004.28	96.70	22.89	OS
4916.29	5003.13	96.46	24.05	OS
4916.09	5004.91	96.45	25.85	OS
4916.33	5002.77	96.66	28.00	OS
4916.20	5003.90	96.87	29.13	OS
4916.16	5004.26	97.07	29.49	REW
4915.65	5008.75	97.26	34.01	TOPO
4915.79	5007.49	97.13	35.28	TOPO
4915.91	5006.46	97.40	36.32	TOPO

Table A-5. Reach C1, cross-section 1D point coordinates and descriptions.

Cross-Section 1D				
N (m)	**E (m)**	**Z (m)**	**X (m)**	**Description**
4891.41	5025.58	98.96	0.00	TOPO
4891.09	5024.86	97.70	0.78	TOPO
4890.32	5023.12	97.31	2.68	TOPO
4890.12	5022.66	96.98	3.18	TOPO
4889.61	5021.50	96.85	4.46	TOPO
4889.57	5021.40	96.77	4.56	LEW
4889.59	5021.45	96.66	4.61	OS
4888.63	5019.28	96.44	6.99	OS
4888.15	5018.18	96.18	8.18	OS
4887.62	5016.98	96.19	9.50	OS
4886.76	5015.03	95.93	11.63	OS
4885.91	5013.12	95.82	13.72	OS
4884.85	5010.72	95.71	16.35	OS
4883.89	5008.54	95.72	18.72	OS
4883.12	5006.79	96.45	20.64	OS
4882.78	5006.01	96.64	21.49	OS
4882.70	5005.84	96.75	21.67	REW
4882.61	5005.62	96.90	21.91	TOPO
4882.10	5004.46	97.26	23.18	TOPO
4881.76	5003.70	97.44	24.01	TOPO
4881.48	5003.07	97.67	24.71	TOPO
4880.86	5001.67	97.81	26.23	TOPO

Table A-6. Reach C1, cross-section 2 point coordinates and descriptions.

Cross-Section 2				
N (m)	**E (m)**	**Z (m)**	**X (m)**	**Description**
4863.94	5038.44	99.35	0.00	XS2-LEP
4863.91	5038.40	99.35	0.05	TOPO
4863.84	5038.28	98.67	0.19	TOPO
4861.75	5034.71	96.87	4.33	TOPO
4861.71	5034.64	96.63	4.41	LEW
4861.64	5034.53	96.21	4.54	OS
4861.17	5033.72	96.06	5.47	OS
4860.81	5033.12	96.05	6.18	OS
4860.11	5031.92	95.92	7.57	OS
4858.47	5029.12	96.03	10.80	OS
4855.19	5023.52	96.17	17.30	OS
4853.01	5019.82	96.21	21.59	OS
4851.77	5017.69	96.44	24.06	OS
4851.65	5017.49	96.60	24.29	REW
4851.49	5017.22	96.77	24.61	TOPO
4851.08	5016.52	97.03	25.41	TOPO
4850.79	5016.03	97.43	25.99	TOPO
4849.86	5014.44	97.53	27.82	TOPO
4847.43	5010.30	97.59	32.63	TOPO
4847.47	5010.37	97.84	32.72	XS2-REP

Table A-7. Reach C1, cross-section 2A point coordinates and descriptions.

Cross-Section 2A				
N (m)	**E (m)**	**Z (m)**	**X (m)**	**Description**
4842.93	5064.43	98.09	0.00	TOPO
4841.64	5063.84	98.00	1.42	TOPO
4839.46	5062.82	97.16	3.83	TOPO
4838.43	5062.35	96.89	4.96	HW
4838.16	5062.22	96.77	5.25	TOPO
4838.09	5062.19	96.42	5.34	LEW
4838.08	5062.19	96.30	5.34	OS
4833.72	5060.16	95.96	10.15	OS
4830.25	5058.55	95.88	13.97	OS
4829.14	5058.04	95.85	15.20	OS
4828.61	5057.79	95.95	15.79	OS
4826.00	5056.58	96.08	18.66	OS
4822.13	5054.79	96.05	22.93	OS
4820.12	5053.85	96.19	25.15	OS
4817.81	5053.33	96.42	27.51	OS
4817.23	5051.86	96.40	29.09	OS
4815.77	5048.12	96.31	33.11	OS
4815.10	5046.43	96.30	34.93	OS
4814.74	5045.49	96.14	35.94	OS
4814.33	5044.44	96.15	37.07	OS
4813.87	5043.27	96.42	38.32	OS
4813.76	5043.01	96.56	38.61	REW
4812.57	5039.96	97.26	41.88	TOPO
4811.29	5036.69	97.19	45.38	TOPO

Table A-8. Reach C1, cross-section 2B point coordinates and descriptions.

Cross-Section 2B				
N (m)	**E (m)**	**Z (m)**	**X (m)**	**Description**
4833.12	5089.43	97.50	0.00	TOPO
4830.57	5087.81	96.68	3.02	TOPO
4829.35	5087.03	96.56	4.47	TOPO
4829.02	5086.82	96.06	4.86	TOPO
4828.70	5086.62	96.01	5.23	LEW
4827.50	5085.86	95.77	6.66	OS
4826.43	5085.18	95.73	7.92	OS
4825.25	5084.43	95.82	9.32	OS
4822.73	5082.83	95.85	12.31	OS
4818.70	5080.26	95.80	17.09	OS
4816.27	5078.72	95.53	19.96	OS
4815.40	5078.17	95.42	20.99	OS
4813.41	5076.90	95.40	23.35	OS
4811.95	5075.98	95.41	25.08	OS
4810.30	5074.93	95.72	27.04	OS
4809.50	5074.42	95.95	27.99	OS
4809.46	5074.39	96.14	28.03	EW
4809.35	5074.32	96.39	28.16	TOPO
4809.36	5074.33	96.35	28.16	TOPO
4805.76	5072.04	96.41	32.43	TOPO
4801.70	5069.46	96.63	37.24	TOPO
4797.93	5067.07	96.34	41.70	TOPO
4796.14	5065.93	96.11	43.82	TOPO
4793.18	5064.05	96.03	47.33	TOPO
4792.78	5063.79	95.87	47.80	EW
4791.29	5062.84	95.71	49.57	OS
4789.52	5061.72	95.63	51.67	OS
4788.95	5061.36	95.75	52.34	OS
4788.15	5060.85	95.83	53.29	OS
4788.20	5060.88	95.85	53.36	REW
4787.90	5060.69	96.22	53.71	TOPO
4787.50	5060.43	96.86	54.19	TOPO

Table A-9. Reach C1, cross-section 2C point coordinates and descriptions.

Cross-Section 2C				
N (m)	**E (m)**	**Z (m)**	**X (m)**	**Description**
4834.31	5100.61	98.08	0.00	TOPO
4828.87	5097.68	96.52	6.18	TOPO
4826.94	5096.64	96.30	8.37	TOPO
4826.65	5096.49	95.88	8.69	LEW
4825.04	5095.62	95.63	10.53	OS
4819.94	5092.88	95.68	16.31	OS
4814.20	5089.79	95.70	22.83	OS
4813.33	5089.32	95.78	23.82	OS
4810.21	5087.64	95.46	27.36	OS
4808.31	5086.61	95.47	29.53	OS
4806.61	5085.70	95.48	31.46	OS
4804.41	5084.51	95.73	33.96	OS
4803.86	5084.22	95.87	34.58	OS
4803.54	5084.05	96.04	34.94	EW
4802.83	5083.66	96.21	35.75	TOPO
4803.25	5083.89	96.07	36.23	TOPO
4801.33	5082.86	96.25	38.41	TOPO
4797.98	5080.42	96.23	42.55	TOPO
4794.86	5080.91	96.07	45.71	TOPO
4794.10	5081.03	95.99	46.48	TOPO
4793.81	5081.08	95.76	46.77	EW
4793.79	5081.08	95.61	46.79	OS
4793.34	5081.15	95.71	47.25	EW
4792.90	5081.22	95.77	47.69	TOPO
4792.81	5081.24	95.71	47.78	EW
4792.70	5081.25	95.35	47.89	OS
4791.01	5081.52	95.38	49.61	OS
4789.72	5081.72	95.43	50.90	OS
4788.23	5081.96	95.48	52.41	OS
4787.24	5082.12	95.74	53.42	REW
4785.84	5082.34	96.84	54.83	TOPO

Table A-10. Reach C1, cross-section 2D point coordinates and descriptions

Cross-Section 2D				
N (m)	**E (m)**	**Z (m)**	**X (m)**	**Description**
4829.44	5116.76	97.44	0.00	TOPO
4823.28	5115.44	95.99	6.30	TOPO
4821.39	5115.03	95.66	8.23	LEW
4819.76	5114.68	95.49	9.89	OS
4817.65	5114.23	95.28	12.05	OS
4816.27	5113.93	95.23	13.47	OS
4815.19	5113.70	95.34	14.57	OS
4813.65	5113.37	95.36	16.15	OS
4812.94	5113.21	95.57	16.87	OS
4812.45	5113.11	95.65	17.38	EW
4809.93	5112.57	95.88	19.95	TOPO
4809.93	5112.57	95.84	19.95	TOPO
4809.60	5112.49	95.57	20.29	EW
4808.62	5112.28	95.48	21.29	OS
4802.28	5110.92	95.34	27.78	OS
4800.20	5110.47	95.43	29.90	OS
4796.54	5109.68	95.34	33.66	OS
4793.82	5109.10	95.19	36.43	OS
4792.70	5109.15	95.05	37.55	OS
4793.80	5108.99	94.99	38.67	OS
4790.61	5109.43	95.48	41.90	OS
4790.77	5109.41	95.61	42.06	REW
4787.89	5109.81	96.66	44.96	TOPO

Table A-11. Reach C1, cross-section 2E point coordinates and descriptions.

Cross-Section 2E				
N (m)	**E (m)**	**Z (m)**	**X (m)**	**Description**
4825.02	5159.75	97.25	0.00	TOPO
4822.05	5158.69	95.76	3.15	TOPO
4820.98	5158.31	95.69	4.29	HW
4820.46	5158.13	95.55	4.84	TOPO
4819.76	5157.88	94.98	5.59	TOPO
4819.20	5157.68	94.82	6.18	LEW
4817.93	5157.23	94.68	7.53	OS
4815.88	5156.51	94.62	9.70	OS
4812.85	5155.43	94.72	12.92	OS
4810.65	5154.65	94.88	15.25	OS
4807.43	5153.51	94.80	18.66	OS
4804.04	5152.31	94.55	22.27	OS
4801.99	5151.58	94.19	24.44	OS
4799.48	5150.69	93.96	27.11	OS
4799.43	5150.68	93.99	27.15	OS
4798.27	5150.26	94.00	28.39	OS
4798.55	5150.36	94.28	28.70	OS
4797.86	5150.12	94.54	29.43	OS
4797.92	5150.14	94.74	29.50	REW
4798.27	5150.26	94.95	29.87	TOPO
4796.43	5149.61	96.04	31.82	TOPO
4795.30	5149.21	96.83	33.02	TOPO

Table A-12. Reach C1, cross-section 3 point coordinates and descriptions.

Cross-Section 3				
N (m)	**E (m)**	**Z (m)**	**X (m)**	**Description**
4820.44	5194.54	96.96	0.00	XS3-LEP
4820.49	5194.56	96.91	0.05	TOPO
4814.80	5191.94	96.71	6.31	TOPO
4811.11	5190.23	95.01	10.37	TOPO
4810.27	5189.84	94.57	11.30	LEW
4809.70	5189.58	94.47	11.92	OS
4807.32	5188.49	94.34	14.54	OS
4804.28	5187.08	94.33	17.90	OS
4800.88	5185.51	94.25	21.64	OS
4799.64	5184.94	94.12	23.01	OS
4798.17	5184.26	93.89	24.62	OS
4795.85	5183.19	93.95	27.18	OS
4793.66	5182.18	93.95	29.59	OS
4792.27	5181.54	94.06	31.12	OS
4790.87	5180.89	94.14	32.66	OS
4790.37	5180.66	94.27	33.21	OS
4790.11	5180.54	94.40	33.50	OS
4790.14	5180.56	94.56	33.54	REW
4790.11	5180.55	94.97	33.57	TOPO
4789.60	5180.31	95.30	34.13	TOPO
4787.77	5179.46	95.46	36.15	TOPO
4785.72	5178.52	97.16	38.41	TOPO
4784.83	5178.11	97.13	39.39	TOPO
4784.87	5178.13	97.20	39.43	XS3-REP

Table A-13. Reach C1, cross-section 3A point coordinates and descriptions.

Cross-Section 3A				
N (m)	**E (m)**	**Z (m)**	**X (m)**	**Description**
4806.83	5208.32	96.92	0.00	TOPO
4803.32	5206.69	94.87	3.87	HW
4803.09	5206.59	94.41	4.12	LEW
4803.07	5206.58	94.35	4.14	OS
4801.08	5205.65	94.14	6.33	OS
4798.16	5204.29	94.20	9.56	OS
4795.89	5203.24	94.09	12.06	OS
4793.79	5202.26	93.65	14.38	OS
4790.51	5200.74	93.76	17.99	OS
4790.04	5200.52	93.77	18.51	OS
4788.62	5199.86	93.96	20.08	OS
4785.53	5198.43	94.16	23.48	OS
4785.50	5198.41	94.32	23.52	OS
4785.34	5198.34	94.44	23.70	REW
4785.26	5198.30	94.59	23.78	TOPO
4783.88	5197.66	94.82	25.30	TOPO
4783.11	5197.30	95.02	26.16	TOPO
4780.51	5196.09	95.17	29.03	TOPO
4776.62	5194.28	96.68	33.32	TOPO

Table A-14. Reach C1, cross-section 3B point coordinates and descriptions.

Cross-Section 3B				
N (m)	**E (m)**	**Z (m)**	**X (m)**	**Description**
4794.33	5234.12	96.26	0.00	TOPO
4791.35	5232.59	94.27	3.36	LEW
4791.27	5232.55	93.99	3.44	OS
4789.00	5231.39	94.02	5.99	OS
4786.32	5230.02	93.82	9.00	OS
4784.91	5229.29	93.64	10.59	OS
4782.12	5227.86	93.68	13.73	OS
4779.87	5226.71	93.81	16.25	OS
4776.48	5224.97	93.95	20.06	OS
4774.30	5223.86	94.05	22.51	OS
4773.80	5223.60	94.16	23.08	OS
4773.61	5223.50	94.31	23.28	REW
4773.34	5223.37	94.42	23.59	TOPO
4771.92	5222.64	94.58	25.19	TOPO
4767.62	5220.43	94.96	30.02	TOPO
4765.93	5219.57	95.35	31.92	TOPO
4764.47	5218.82	95.53	33.55	TOPO
4762.25	5217.68	95.26	36.05	TOPO

Table A-15. Reach C1, cross-section 3C point coordinates and descriptions.

Cross-Section 3C				
N (m)	E (m)	Z (m)	X (m)	Description
4783.06	5261.61	95.99	0.00	TOPO
4781.04	5260.52	94.73	2.30	HW
4779.56	5259.73	94.15	3.97	LEW
4778.84	5259.34	93.91	4.79	OS
4777.44	5258.59	93.58	6.38	OS
4775.75	5257.69	93.46	8.29	OS
4774.50	5257.02	93.47	9.71	OS
4772.29	5255.83	93.59	12.22	OS
4771.89	5255.62	93.69	12.68	OS
4767.29	5253.15	93.76	17.89	OS
4763.94	5251.36	93.90	21.69	OS
4762.30	5250.48	94.12	23.56	REW
4760.03	5249.27	94.18	26.13	TOPO
4759.62	5249.05	94.29	26.59	TOPO
4753.01	5245.50	94.72	34.09	TOPO
4749.16	5243.44	95.39	38.46	TOPO

Table A-16. Reach C1, cross-section 3D point coordinates and descriptions.

Cross-Section 3D				
N (m)	E (m)	Z (m)	X (m)	Description
4773.67	5283.38	95.91	0.00	TOPO
4771.94	5282.59	94.90	1.90	TOPO
4771.03	5282.18	94.66	2.90	TOPO
4770.77	5282.06	93.97	3.19	LEW
4770.06	5281.74	93.87	3.97	OS
4768.93	5281.22	93.49	5.21	OS
4767.75	5280.68	93.35	6.51	OS
4766.42	5280.08	93.29	7.96	OS
4765.78	5279.79	93.22	8.67	OS
4762.60	5278.34	93.38	12.17	OS
4761.22	5277.71	93.54	13.68	OS
4756.61	5275.61	93.71	18.75	OS
4750.23	5272.70	93.66	25.76	OS
4749.83	5272.52	93.76	26.20	OS
4749.00	5272.15	93.83	27.11	OS
4748.92	5272.11	93.96	27.20	REW
4748.85	5272.08	94.08	27.27	TOPO
4746.21	5270.87	94.30	30.18	TOPO
4743.37	5269.58	94.27	33.30	TOPO
4742.66	5269.25	94.11	34.08	TOPO
4740.16	5268.11	94.63	36.83	TOPO
4737.83	5267.05	94.31	39.38	TOPO
4731.17	5264.02	95.31	46.70	TOPO

Table A-17. Reach C1, cross-section 4 point coordinates and descriptions.

Cross-Section 4				
N (m)	**E (m)**	**Z (m)**	**X (m)**	**Description**
4790.11	5303.74	95.94	0.00	XS4-LEP
4790.05	5303.72	95.84	0.06	TOPO
4785.98	5302.41	94.41	4.33	TOPO
4780.86	5300.77	94.45	9.71	TOPO
4778.74	5300.08	94.18	11.94	TOPO
4778.56	5300.03	93.90	12.13	LEW
4778.40	5299.97	93.87	12.30	OS
4777.16	5299.58	93.60	13.60	OS
4775.40	5299.01	93.26	15.45	OS
4773.45	5298.38	93.15	17.50	OS
4771.02	5297.60	93.19	20.05	OS
4766.79	5296.24	93.31	24.49	OS
4761.06	5294.40	93.51	30.51	OS
4745.06	5289.26	93.57	47.31	OS
4742.94	5288.58	93.57	49.54	OS
4742.39	5288.40	93.84	50.12	OS
4742.40	5288.41	93.92	50.14	REW
4742.47	5288.43	93.98	50.21	TOPO
4741.07	5287.98	94.24	51.68	TOPO
4740.08	5287.66	94.30	52.71	TOPO
4738.78	5287.24	94.03	54.08	TOPO
4731.91	5285.03	94.25	61.30	TOPO
4730.57	5284.60	95.09	62.71	TOPO
4729.28	5284.19	95.00	64.06	TOPO
4729.22	5284.17	95.08	64.12	XS4-REP

Table A-18. Reach C1, cross-section 4A point coordinates and descriptions.

Cross-Section 4A				
N (m)	E (m)	Z (m)	X (m)	Description
4761.96	5340.50	95.10	0.00	TOPO
4759.00	5339.62	93.94	3.08	HW
4757.87	5339.28	93.63	4.26	TOPO
4757.74	5339.24	93.57	4.40	LEW
4754.25	5338.20	93.47	8.04	OS
4753.59	5338.01	93.36	8.72	OS
4749.36	5336.75	93.18	13.14	OS
4746.40	5335.87	93.18	16.23	OS
4741.45	5334.40	93.41	21.40	OS
4740.40	5334.09	93.58	22.49	OS
4736.42	5332.90	93.37	26.64	OS
4731.50	5331.44	93.21	31.77	OS
4727.80	5330.34	93.11	35.63	OS
4726.13	5329.84	93.23	37.38	OS
4724.27	5329.29	93.09	39.31	OS
4722.94	5328.89	93.03	40.71	OS
4722.32	5328.71	93.27	41.35	OS
4722.27	5328.69	93.48	41.41	REW
4721.79	5328.55	93.74	41.90	TOPO
4720.21	5328.08	94.91	43.55	TOPO

Table A-19. Reach C1, cross-section 4B point coordinates and descriptions.

Cross-Section 4B				
N (m)	E (m)	Z (m)	X (m)	Description
4756.96	5373.24	95.11	0.00	TOPO
4756.48	5373.08	93.73	0.51	TOPO
4755.87	5372.88	93.40	1.15	TOPO
4755.21	5372.67	92.94	1.85	OS
4752.04	5371.64	92.71	5.18	OS
4748.59	5370.52	92.91	8.80	OS
4744.06	5369.04	92.75	13.57	OS
4739.92	5367.69	92.65	17.93	OS
4736.12	5366.46	92.81	21.92	OS
4732.36	5365.23	92.68	25.88	OS
4728.89	5364.10	92.66	29.52	OS
4726.64	5363.37	92.75	31.89	OS
4724.24	5362.59	92.62	34.41	OS
4721.56	5361.72	92.75	37.23	OS
4721.43	5361.68	92.93	37.37	OS
4721.51	5361.70	93.18	37.45	REW
4717.99	5360.56	94.72	41.16	TOPO

Table A-20. Reach C1, cross-section 4C point coordinates and descriptions.

Cross-Section 4C				
N (m)	**E (m)**	**Z (m)**	**X (m)**	**Description**
4747.97	5405.58	94.38	0.00	TOPO
4739.58	5402.18	91.08	9.05	TOPO
4739.16	5402.01	91.01	9.50	TOPO
4738.87	5401.89	90.81	9.81	LEW
4738.67	5401.81	90.60	10.03	OS
4736.78	5401.04	90.37	12.07	OS
4735.26	5400.42	90.22	13.72	OS
4733.97	5399.90	90.54	15.10	OS
4733.11	5399.55	90.83	16.03	EW
4731.94	5399.08	91.31	17.29	TOPO
4729.53	5398.10	91.33	19.90	TOPO
4728.30	5397.60	90.91	21.22	EW
4727.27	5397.18	90.61	22.34	OS
4724.86	5396.20	90.51	24.94	OS
4722.05	5395.06	90.02	27.97	OS
4718.59	5393.65	90.11	31.71	OS
4719.38	5393.98	90.72	32.56	OS
4718.60	5393.66	90.94	33.41	REW
4719.11	5393.87	91.11	33.97	TOPO
4717.22	5393.10	93.64	36.02	TOPO

Table A-21. Reach C1, cross-section 4D point coordinates and descriptions.

Cross-Section 4D				
N (m)	**E (m)**	**Z (m)**	**X (m)**	**Description**
4738.61	5419.81	93.53	0.00	TOPO
4734.16	5418.23	91.46	4.72	TOPO
4732.33	5417.57	90.96	6.67	TOPO
4732.45	5417.62	90.80	6.81	LEW
4732.47	5417.62	90.74	6.82	OS
4731.86	5417.40	90.61	7.47	OS
4730.98	5417.09	90.38	8.40	OS
4728.87	5416.34	90.41	10.65	OS
4726.23	5415.40	90.63	13.44	OS
4723.55	5414.44	90.53	16.29	OS
4720.12	5413.21	90.07	19.94	OS
4718.04	5412.47	90.07	22.14	OS
4715.34	5411.51	90.27	25.02	OS
4712.90	5410.64	90.79	27.60	REW
4710.62	5409.82	91.80	30.03	TOPO
4708.72	5409.14	92.37	32.04	TOPO

Table A-22. Reach C1, cross-section 5 point coordinates and descriptions.

Cross-Section 5				
N (m)	**E (m)**	**Z (m)**	**X (m)**	**Description**
4729.43	5445.44	93.46	0.00	XS5-LEP
4726.40	5444.08	90.64	3.33	LEW
4725.27	5443.57	90.37	4.56	OS
4722.97	5442.54	90.37	7.08	OS
4718.40	5440.50	90.36	12.09	OS
4715.06	5439.00	90.14	15.75	OS
4713.18	5438.16	90.00	17.81	OS
4711.84	5437.56	89.89	19.28	OS
4709.29	5436.42	89.90	22.07	OS
4707.89	5435.80	90.10	23.60	OS
4705.84	5434.87	90.35	25.85	OS
4704.54	5434.29	90.54	27.28	OS
4703.73	5433.93	90.62	28.16	REW
4703.53	5433.84	90.75	28.38	TOPO
4702.18	5433.24	91.31	29.86	TOPO
4701.68	5433.01	91.53	30.41	TOPO
4700.03	5432.27	91.72	32.22	TOPO
4695.41	5430.21	94.16	37.28	TOPO
4694.82	5429.94	94.25	37.92	TOPO
4694.73	5429.90	94.40	38.03	XS5-REP

STUDY REACH C2

Table A-23. Reach C2, cross-section 1 point coordinates and descriptions.

Cross-Section 1				
N (m)	**E (m)**	**Z (m)**	**X (m)**	**Description**
5653.15	5069.12	5007.70	0.00	TOPO
5650.44	5066.77	5005.61	3.58	LEW
5650.04	5066.42	5005.32	4.12	OS
5647.37	5064.11	5005.13	7.65	OS
5645.92	5062.85	5005.06	9.57	OS
5643.92	5061.12	5004.78	12.21	OS
5642.15	5059.58	5004.91	14.56	OS
5640.43	5058.09	5005.23	16.84	OS
5639.40	5057.20	5005.35	18.20	OS
5638.14	5056.10	5005.40	19.87	OS
5636.13	5054.36	5005.58	22.53	OS
5636.13	5054.36	5005.64	22.53	REW
5635.47	5053.79	5006.06	23.41	TOPO

Table A-24. Reach C2, cross-section 2 point coordinates and descriptions.

Cross-Section 2				
N (m)	**E (m)**	**Z (m)**	**X (m)**	**Description**
5638.18	5082.54	5007.36	0.00	TOPO
5636.55	5080.87	5005.56	2.33	LEW
5636.29	5080.60	5005.21	2.70	OS
5635.19	5079.47	5005.05	4.28	OS
5634.59	5078.86	5004.88	5.14	OS
5633.67	5077.92	5004.82	6.45	OS
5632.84	5077.07	5004.92	7.64	OS
5631.70	5075.90	5005.02	9.27	OS
5628.70	5072.83	5005.04	13.56	OS
5626.59	5070.67	5005.40	16.59	OS
5624.80	5068.84	5005.49	19.15	REW
5623.69	5067.70	5005.58	20.74	TOPO
5621.71	5065.68	5005.56	23.56	TOPO
5616.47	5060.31	5008.04	31.07	TOPO

Table A-25. Reach C2, cross-section 3 point coordinates and descriptions.

Cross-Section 3				
N (m)	**E (m)**	**Z (m)**	**X (m)**	**Description**
5612.22	5104.89	5007.11	0.00	TOPO
5609.44	5101.21	5005.24	4.61	LEW
5608.92	5100.52	5004.93	5.48	OS
5608.23	5099.60	5004.78	6.63	OS
5607.55	5098.71	5004.65	7.75	OS
5606.29	5097.04	5004.77	9.83	OS
5603.92	5093.90	5004.64	13.77	OS
5601.41	5090.56	5004.81	17.95	OS
5600.89	5089.88	5004.92	18.80	OS
5599.08	5087.48	5005.25	21.81	REW
5598.02	5086.07	5005.51	23.57	TOPO
5596.62	5084.21	5005.45	25.91	TOPO

Table A-26. Reach C2, cross-section 4 point coordinates and descriptions.

Cross-Section 4				
N (m)	**E (m)**	**Z (m)**	**X (m)**	**Description**
5580.48	5124.39	5005.07	0.00	LEW
5579.94	5123.43	5004.51	1.10	OS
5578.91	5121.64	5004.60	3.17	OS
5578.25	5120.49	5004.62	4.50	OS
5577.07	5118.43	5004.54	6.87	OS
5576.02	5116.61	5004.73	8.97	OS
5572.99	5111.32	5004.79	15.07	OS
5571.28	5108.35	5004.92	18.50	OS
5570.34	5106.71	5005.05	20.39	OS
5568.55	5103.58	5004.94	23.99	REW
5568.36	5103.24	5005.09	24.38	TOPO
5568.29	5103.12	5005.12	24.52	TOPO
5568.14	5102.86	5005.38	24.82	TOPO

Table A-27. Reach C2, cross-section 5 point coordinates and descriptions.

Cross-Section 5				
N (m)	**E (m)**	**Z (m)**	**X (m)**	**Description**
5559.06	5144.75	5006.83	0.00	TOPO
5556.07	5140.93	5004.86	4.85	LEW
5555.76	5140.53	5004.60	5.36	OS
5555.23	5139.84	5004.25	6.23	OS
5554.64	5139.09	5004.35	7.18	OS
5552.71	5136.62	5004.47	10.31	OS
5548.10	5130.72	5004.47	17.80	OS
5543.22	5124.48	5004.59	25.73	OS
5542.57	5123.65	5004.50	26.78	OS
5541.31	5122.03	5004.67	28.83	OS
5540.99	5121.62	5004.84	29.35	REW
5540.85	5121.44	5004.89	29.57	TOPO
5540.49	5120.98	5005.02	30.17	TOPO
5539.56	5119.79	5005.52	31.67	TOPO
5537.96	5117.74	5005.46	34.27	TOPO

Table A-28. Reach C2, cross-section 6 point coordinates and descriptions.

Cross-Section 6				
N (m)	**E (m)**	**Z (m)**	**X (m)**	**Description**
5541.36	5152.57	5004.71	0.00	LEW
5540.79	5151.74	5004.24	1.01	OS
5539.99	5150.58	5004.29	2.41	OS
5538.83	5148.88	5004.37	4.47	OS
5536.18	5145.02	5004.33	9.16	OS
5532.56	5139.74	5004.49	15.56	OS
5530.70	5137.03	5004.39	18.84	OS
5528.68	5134.09	5004.34	22.41	OS
5528.25	5133.45	5004.67	23.18	REW
5527.90	5132.94	5004.83	23.80	TOPO
5526.64	5131.10	5005.11	26.03	TOPO
5525.61	5129.61	5005.26	27.84	TOPO

Table A-29. Reach C2, cross-section 7 point coordinates and descriptions.

Cross-Section 7				
N (m)	**E (m)**	**Z (m)**	**X (m)**	**Description**
5529.77	5164.37	5004.71	0.00	LEW
5528.78	5163.38	5004.20	1.41	OS
5527.54	5162.13	5004.26	3.16	OS
5522.95	5157.54	5004.31	9.65	OS
5516.36	5150.94	5004.31	18.98	OS
5513.68	5148.25	5004.14	22.77	OS
5513.32	5147.89	5004.15	23.29	OS
5512.30	5146.87	5004.26	24.73	OS
5511.96	5146.53	5004.43	25.21	OS
5511.83	5146.40	5004.57	25.39	REW
5511.51	5146.08	5004.84	25.84	TOPO
5510.36	5144.93	5004.98	27.47	TOPO

Table A-30. Reach C2, cross-section 8 point coordinates and descriptions.

Cross-Section 8				
N (m)	**E (m)**	**Z (m)**	**X (m)**	**Description**
5501.92	5189.12	5005.05	0.00	TOPO
5500.82	5188.22	5004.57	1.43	TOPO
5501.10	5188.62	5004.23	1.92	LEW
5499.44	5185.96	5003.95	5.05	OS
5497.63	5182.96	5004.02	8.55	OS
5497.02	5182.34	5004.17	9.43	OS
5496.19	5181.26	5004.17	10.78	OS
5494.80	5179.39	5004.15	13.12	OS
5493.47	5177.75	5004.00	15.23	OS
5491.44	5174.66	5003.86	18.92	OS
5488.86	5171.67	5003.68	22.87	OS
5487.64	5170.36	5003.76	24.66	OS
5487.08	5169.49	5004.03	25.70	OS
5486.98	5169.48	5004.21	25.80	REW
5486.91	5169.23	5004.37	26.06	TOPO
5485.67	5167.51	5004.71	28.18	TOPO
5483.31	5164.65	5006.34	31.89	TOPO

Table A-31. Reach C2, cross-section 9 point coordinates and descriptions.

Cross-Section 9				
N (m)	**E (m)**	**Z (m)**	**X (m)**	**Description**
5493.22	5202.21	5004.91	0.00	TOPO
5492.25	5201.06	5004.80	1.50	HW
5490.46	5198.91	5004.42	4.30	TOPO
5490.50	5198.97	5004.17	4.37	LEW
5490.41	5198.86	5003.97	4.51	OS
5488.37	5196.42	5004.04	7.69	OS
5485.95	5193.53	5004.08	11.46	OS
5484.40	5191.69	5004.04	13.86	OS
5482.86	5189.85	5003.81	16.27	OS
5481.32	5188.01	5003.66	18.66	OS
5477.76	5183.77	5003.43	24.20	OS
5476.58	5182.36	5003.46	26.04	OS
5475.64	5181.24	5003.51	27.50	OS
5475.14	5180.64	5003.96	28.29	REW

Table A-32. Reach C2, cross-section 10 point coordinates and descriptions.

Cross-Section 10				
N (m)	E (m)	Z (m)	X (m)	Description
5466.65	5223.38	5005.88	0.00	TOPO
5466.56	5223.25	5005.72	0.15	TOPO
5462.64	5218.05	5003.77	6.66	LEW
5459.83	5214.32	5003.47	11.34	OS
5457.05	5210.61	5003.24	15.97	OS
5455.66	5208.77	5003.15	18.27	OS
5453.43	5205.81	5003.21	21.98	OS
5452.28	5204.28	5003.51	23.90	OS
5452.20	5204.17	5003.66	24.04	REW
5452.03	5203.95	5003.91	24.31	TOPO

Table A-33. Reach C2, cross-section 11 point coordinates and descriptions.

Cross-Section 11				
N (m)	E (m)	Z (m)	X (m)	Description
5441.84	5243.94	5003.78	0.00	TOPO
5440.79	5242.71	5003.31	1.62	LEW
5437.43	5238.77	5003.27	6.79	OS
5437.19	5238.48	5003.07	7.17	OS
5435.36	5236.32	5003.02	10.00	OS
5434.67	5235.51	5002.79	11.07	OS
5432.73	5233.23	5002.82	14.06	OS
5431.51	5231.80	5002.84	15.94	OS
5429.14	5229.02	5002.88	19.59	OS
5427.77	5227.40	5003.22	21.72	OS
5427.28	5226.82	5003.27	22.48	REW
5427.19	5226.72	5003.29	22.61	TOPO
5427.14	5226.66	5003.58	22.68	TOPO
5427.79	5227.42	5003.62	23.67	TOPO

A-34. Reach C2, cross-section 12 point coordinates and descriptions.

Cross-Section 12				
N (m)	**E (m)**	**Z (m)**	**X (m)**	**Description**
5420.80	5260.30	5003.40	0.00	TOPO
5420.22	5259.92	5003.15	0.70	LEW
5419.00	5257.67	5003.01	3.25	OS
5418.21	5256.48	5002.91	4.68	OS
5416.46	5254.02	5002.70	7.71	OS
5415.35	5252.64	5002.66	9.47	OS
5414.38	5251.37	5002.69	11.07	OS
5412.31	5248.91	5002.72	14.29	OS
5411.58	5248.18	5002.72	15.32	OS
5408.50	5244.93	5002.98	19.80	OS
5407.96	5244.35	5003.20	20.59	REW
5407.82	5244.15	5003.34	20.83	TOPO

A-35. Reach C2, cross-section 13 point coordinates and descriptions.

Cross-Section 13				
N (m)	**E (m)**	**Z (m)**	**X (m)**	**Description**
5398.18	5280.17	5003.62	0.00	TOPO
5396.68	5277.17	5003.36	3.36	TOPO
5395.67	5275.15	5003.27	5.61	TOPO
5395.54	5274.89	5003.03	5.90	LEW
5395.41	5274.64	5002.85	6.18	OS
5394.99	5273.79	5002.58	7.13	OS
5393.80	5271.42	5002.39	9.79	OS
5392.60	5269.02	5002.39	12.47	OS
5391.95	5267.73	5002.46	13.91	OS
5390.75	5265.33	5002.63	16.60	OS
5389.04	5261.91	5002.70	20.42	OS
5388.62	5261.07	5002.88	21.36	OS
5387.83	5259.50	5003.03	23.11	REW
5388.77	5261.37	5003.26	25.19	TOPO
5388.45	5260.74	5003.33	25.90	TOPO

A-36. Reach C2, cross-section 14 point coordinates and descriptions.

Cross-Section 14				
N (m)	**E (m)**	**Z (m)**	**X (m)**	**Description**
5376.63	5299.16	5005.08	0.00	TOPO
5372.28	5292.71	5003.36	7.78	TOPO
5371.22	5291.14	5003.27	9.67	TOPO
5370.70	5290.38	5002.99	10.60	TOPO
5370.58	5290.19	5002.84	10.83	LEW
5370.32	5289.80	5002.61	11.29	OS
5369.77	5288.99	5002.28	12.27	OS
5367.91	5286.24	5002.28	15.59	OS
5365.28	5282.34	5002.39	20.30	OS
5361.93	5277.38	5002.71	26.28	OS
5359.77	5274.18	5002.83	30.14	REW
5359.39	5273.62	5003.06	30.82	TOPO
5358.40	5272.16	5003.19	32.58	TOPO
5358.03	5271.61	5003.69	33.24	TOPO

A-37. Reach C2, cross-section 15 point coordinates and descriptions.

Cross-Section 15				
N (m)	**E (m)**	**Z (m)**	**X (m)**	**Description**
5337.24	5290.87	5004.26	0.00	TOPO
5341.19	5303.80	5002.95	13.52	TOPO
5340.91	5302.89	5002.28	14.47	LEW
5340.56	5301.72	5002.09	15.69	OS
5339.75	5299.09	5002.04	18.44	OS
5338.74	5295.79	5001.83	21.90	OS
5338.42	5294.73	5001.83	23.00	OS
5338.10	5293.70	5001.87	24.08	OS
5337.12	5290.49	5001.97	27.44	OS
5336.67	5289.01	5002.04	28.99	OS
5336.60	5288.78	5002.29	29.22	REW
5336.58	5288.74	5002.51	29.26	TOPO
5335.98	5286.76	5002.87	31.34	TOPO
5335.26	5284.41	5003.02	33.79	TOPO
5334.54	5282.08	5002.76	36.24	TOPO
5332.91	5276.74	5002.95	41.82	TOPO
5332.32	5274.82	5003.73	43.82	TOPO

Table A-38. Reach C2, cross-section 16 point coordinates and descriptions.

Cross-Section 16				
N (m)	E (m)	Z (m)	X (m)	Description
5282.48	5293.26	5004.21	0.00	TOPO
5287.69	5286.27	5002.29	8.72	LEW
5286.41	5287.99	5001.38	10.86	OS
5287.61	5286.39	5001.35	12.86	OS
5288.01	5285.84	5001.38	13.54	OS
5288.96	5284.57	5001.65	15.13	OS
5290.60	5282.37	5001.96	17.87	OS
5290.99	5281.85	5002.24	18.52	REW
5293.47	5278.51	5002.62	22.68	TOPO
5295.68	5275.55	5002.79	26.37	TOPO
5297.18	5273.53	5002.69	28.89	TOPO
5299.31	5270.67	5002.55	32.45	TOPO
5300.43	5269.18	5002.20	34.32	TOPO
5302.72	5266.10	5002.20	38.15	TOPO
5305.34	5262.58	5003.57	42.54	TOPO
5309.79	5256.61	5004.59	49.99	TOPO

Table A-39. Reach C2, cross-section 17 point coordinates and descriptions.

Cross-Section 17				
N (m)	E (m)	Z (m)	X (m)	Description
5262.47	5281.03	5004.06	0.00	TOPO
5265.73	5276.90	5002.16	5.26	LEW
5266.09	5276.44	5001.53	5.84	OS
5267.64	5274.47	5001.43	8.35	OS
5268.34	5273.58	5001.23	9.48	OS
5268.73	5273.09	5001.16	10.11	OS
5272.24	5268.63	5001.48	15.78	OS
5273.91	5266.52	5001.64	18.48	OS
5274.79	5265.40	5001.69	19.89	OS
5275.24	5264.83	5002.14	20.62	REW
5276.10	5263.74	5002.37	22.01	TOPO
5285.12	5252.29	5002.22	36.59	TOPO
5286.29	5250.82	5001.53	38.47	TOPO
5283.72	5254.08	5001.34	42.62	TOPO
5283.15	5254.79	5002.25	43.53	TOPO
5284.38	5253.23	5001.44	45.51	TOPO
5285.31	5252.06	5002.34	47.01	TOPO
5287.27	5249.57	5003.81	50.18	TOPO

Table A-40. Reach C2, cross-section 18 point coordinates and descriptions.

Cross-Section 18				
N (m)	**E (m)**	**Z (m)**	**X (m)**	**Description**
5225.48	5236.14	5003.52	0.00	TOPO
5229.77	5233.14	5001.98	5.23	LEW
5230.23	5232.82	5000.98	5.79	OS
5231.48	5231.95	5001.14	7.31	OS
5232.72	5231.09	5001.35	8.82	OS
5237.46	5227.78	5001.55	14.60	OS
5240.83	5225.43	5001.48	18.71	OS
5242.14	5224.51	5001.37	20.31	OS
5246.71	5221.32	5001.58	25.88	OS
5249.39	5219.45	5001.67	29.16	OS
5251.95	5217.67	5001.72	32.27	OS
5253.48	5216.59	5001.61	34.15	OS
5254.16	5216.12	5001.49	34.98	OS
5255.59	5215.12	5001.25	36.71	OS
5256.57	5214.44	5001.18	37.91	OS
5257.33	5213.91	5001.63	38.83	REW
5258.32	5213.22	5002.44	40.04	TOPO
5258.64	5213.00	5002.52	40.43	TOPO
5261.29	5211.15	5003.90	43.66	TOPO

STUDY REACH C3

Table A-41. Reach C3, cross-section 1 point coordinates and descriptions.

Cross-Section 1				
N (m)	**E (m)**	**Z (m)**	**X (m)**	**Description**
5200.12	5176.48	5003.48	0.00	TOPO
5209.51	5174.92	5001.38	9.52	LEW
5209.84	5174.87	5000.61	9.85	OS
5209.65	5174.90	5000.66	10.04	OS
5211.02	5174.67	5000.71	11.43	OS
5217.90	5173.53	5000.95	18.41	OS
5217.95	5173.52	5000.64	18.46	OS
5221.05	5173.00	5000.51	21.60	OS
5223.64	5172.58	5000.66	24.22	OS
5224.52	5172.43	5000.76	25.12	OS
5225.48	5172.27	5000.81	26.09	OS
5226.16	5172.16	5001.05	26.78	OS
5228.60	5171.75	5000.66	29.25	OS
5229.41	5171.62	5000.77	30.07	OS
5231.26	5171.31	5000.60	31.95	OS
5233.48	5170.94	5000.53	34.19	OS
5235.15	5170.67	5000.33	35.89	OS
5236.82	5170.39	5000.16	37.58	OS
5237.81	5170.22	5000.13	38.59	OS
5238.50	5170.11	5000.77	39.29	OS
5238.62	5170.09	5001.03	39.41	REW
5244.70	5169.08	5003.50	45.56	TOPO

Table A-42. Reach C3, cross-section 2 point coordinates and descriptions.

Cross-Section 2				
N (m)	**E (m)**	**Z (m)**	**X (m)**	**Description**
5203.86	5153.05	5002.32	0.00	TOPO
5204.89	5152.80	5001.37	1.06	HW
5207.63	5152.14	5000.46	3.88	LEW
5209.68	5151.65	5000.20	5.99	OS
5211.15	5151.29	5000.08	7.50	OS
5212.59	5150.94	4999.87	8.99	OS
5215.05	5150.35	5000.02	11.51	OS
5217.09	5149.86	5000.35	13.62	OS
5217.42	5149.78	5000.44	13.95	OS
5220.21	5149.11	5000.53	16.83	OS
5220.93	5148.93	5000.44	17.56	OS
5223.48	5148.32	5000.33	20.18	OS
5228.29	5147.16	5000.53	25.13	REW
5230.05	5146.74	5002.74	26.94	TOPO
5232.43	5146.16	5002.82	29.39	TOPO
5232.59	5146.12	5002.82	29.56	TOPO
5232.71	5146.09	5003.02	29.68	TOPO
5234.54	5145.65	5004.08	31.56	TOPO

Table A-43. Reach C3, cross-section 3 point coordinates and descriptions.

Cross-Section 3				
N (m)	**E (m)**	**Z (m)**	**X (m)**	**Description**
5189.00	5110.81	5002.30	0.00	TOPO
5193.34	5109.10	5000.40	4.66	LEW
5193.64	5108.98	5000.33	4.98	OS
5193.98	5108.85	5000.11	5.35	OS
5195.62	5108.20	4999.55	7.11	OS
5197.29	5107.55	4999.24	8.91	OS
5202.15	5105.63	4999.13	14.13	OS
5203.10	5105.26	4999.23	15.15	OS
5204.50	5104.71	4999.50	16.65	OS
5205.18	5104.44	4999.70	17.38	OS
5206.64	5103.86	4999.87	18.96	OS
5208.06	5103.31	5000.14	20.48	OS
5208.55	5103.11	5000.36	21.01	REW
5209.47	5102.75	5000.52	22.00	TOPO
5217.63	5099.54	5000.37	30.76	TOPO
5218.21	5099.31	5000.82	31.38	TOPO
5224.58	5096.81	5001.11	38.23	TOPO
5227.61	5095.61	5002.52	41.49	TOPO

Table A-44. Reach C3, cross-section 4 point coordinates and descriptions.

Cross-Section 4				
N (m)	**E (m)**	**Z (m)**	**X (m)**	**Description**
5159.65	5074.62	5001.83	0.00	TOPO
5165.98	5070.30	5000.54	7.66	TOPO
5167.52	5069.25	5000.24	9.53	LEW
5167.79	5069.06	5000.06	9.86	OS
5168.46	5068.61	4999.83	10.66	OS
5169.08	5068.19	4999.74	11.42	OS
5170.50	5067.22	4999.84	13.13	OS
5174.08	5064.78	4999.97	17.46	OS
5179.40	5061.16	4999.81	23.90	OS
5182.91	5058.77	4999.91	28.14	OS
5187.52	5055.63	4999.65	33.72	OS
5190.57	5053.55	4999.87	37.42	OS
5191.07	5053.21	4999.99	38.02	OS
5191.38	5053.00	5000.14	38.39	OS
5191.42	5052.97	5000.35	38.44	REW
5191.58	5052.86	5000.47	38.64	TOPO
5192.54	5052.21	5000.38	39.80	TOPO
5195.03	5050.51	5000.51	42.81	TOPO
5182.86	5058.80	5001.84	57.53	TOPO

Table A-45. Reach C3, cross-section 5 point coordinates and descriptions.

Cross-Section 5				
N (m)	**E (m)**	**Z (m)**	**X (m)**	**Description**
5146.54	5047.74	5000.26	0.00	TOPO
5147.50	5046.67	4999.95	1.44	TOPO
5148.15	5045.93	4999.96	2.43	TOPO
5148.70	5045.30	4999.91	3.26	LEW
5149.64	5044.24	4999.62	4.68	OS
5152.08	5041.49	4999.71	8.35	OS
5154.53	5038.71	4999.75	12.06	OS
5156.91	5036.02	4999.82	15.65	OS
5160.71	5031.73	4999.70	21.38	OS
5163.06	5029.06	4999.52	24.94	OS
5163.47	5028.60	4999.27	25.55	OS
5163.69	5028.35	4999.16	25.89	OS
5164.25	5027.72	4999.21	26.73	OS
5164.44	5027.51	4999.93	27.01	REW
5166.07	5025.66	5001.77	29.48	TOPO

Table A-46. Reach C3, cross-section 6 point coordinates and descriptions.

Cross-Section 6				
N (m)	**E (m)**	**Z (m)**	**X (m)**	**Description**
5062.96	5026.33	4999.70	0.00	TOPO
5063.14	5022.99	4999.24	3.35	LEW
5064.07	5006.13	4998.93	20.23	OS
5064.18	5004.29	4998.87	22.08	OS
5064.20	5003.92	4999.06	22.44	OS
5064.15	5004.79	4998.82	23.31	OS
5064.23	5003.25	4998.52	24.86	OS
5064.25	5002.96	4998.24	25.15	OS
5063.85	5010.11	4997.93	32.31	OS
5064.51	4998.20	4997.93	44.24	OS
5064.49	4998.66	4998.07	44.69	OS
5064.56	4997.43	4998.81	45.92	REW
5064.39	5000.45	5000.46	48.95	TOPO

Table A-47. Reach C3, cross-section 7 point coordinates and descriptions.

Cross-Section 7				
N (m)	**E (m)**	**Z (m)**	**X (m)**	**Description**
5040.96	5041.14	5000.50	0.00	TOPO
5037.97	5034.99	4998.95	6.84	TOPO
5034.40	5027.67	5000.40	14.98	TOPO
5032.28	5023.30	4998.94	19.84	TOPO
5029.45	5017.49	4998.65	26.30	LEW
5029.39	5017.36	4998.58	26.44	OS
5029.06	5016.69	4998.40	27.20	OS
5028.89	5016.35	4998.33	27.58	OS
5028.42	5015.37	4998.35	28.66	OS
5026.79	5012.03	4998.13	32.38	OS
5025.89	5010.19	4998.06	34.42	OS
5024.98	5008.32	4998.07	36.50	OS
5023.83	5005.95	4998.05	39.14	OS
5022.42	5003.06	4997.88	42.35	OS
5021.03	5000.19	4998.73	45.55	REW
5018.97	4995.97	4999.88	50.23	TOPO

Table A-48. Reach C3, cross-section 8 point coordinates and descriptions.

Cross-Section 8				
N (m)	E (m)	Z (m)	X (m)	Description
4996.20	4993.15	4999.71	0.00	TOPO
5001.68	5005.20	4998.73	13.24	TOPO
5001.67	5005.17	4998.60	13.27	LEW
5001.70	5005.25	4998.17	13.35	OS
5003.82	5009.89	4998.10	18.46	OS
5005.97	5014.61	4998.23	23.64	OS
5010.12	5023.75	4998.12	33.68	OS
5011.12	5025.95	4998.15	36.10	OS
5011.63	5027.07	4998.18	37.33	OS
5012.62	5029.25	4998.37	39.72	OS
5012.75	5029.52	4998.22	40.02	OS
5013.38	5030.90	4998.27	41.54	OS
5013.55	5031.29	4998.53	41.97	REW
5013.10	5030.30	4998.99	43.06	HW
5014.81	5034.05	4999.27	47.19	TOPO
5015.55	5035.68	4998.98	48.98	TOPO
5016.60	5037.99	4999.10	51.52	TOPO
5019.02	5043.29	5000.31	57.34	TOPO

Table A-49. Reach C3, cross-section 9 point coordinates and descriptions.

Cross-Section 9				
N (m)	E (m)	Z (m)	X (m)	Description
4984.89	5006.97	4999.56	0.00	TOPO
4986.12	5010.13	4998.33	2.50	LEW
4986.12	5010.13	4998.18	3.39	TOPO
4987.95	5014.83	4998.03	8.44	TOPO
4989.29	5018.29	4998.07	12.15	TOPO
4990.73	5021.99	4997.98	16.12	TOPO
4991.14	5023.03	4998.01	17.24	TOPO
4991.18	5023.13	4998.33	17.34	EW
4991.23	5023.26	4998.53	17.49	TOPO
4991.41	5023.73	4998.55	17.99	TOPO
4991.50	5023.95	4998.33	18.22	EW
4991.91	5025.02	4997.83	19.38	OS
4993.54	5029.21	4997.66	23.87	OS
4997.60	5039.64	4997.74	35.06	OS
4998.39	5041.67	4997.87	37.24	OS
4998.44	5041.78	4998.32	37.36	OS
4998.50	5041.94	4998.40	37.53	REW
4998.74	5042.56	4998.68	38.20	TOPO
5000.57	5047.25	4999.31	43.23	TOPO
5000.59	5047.32	4999.83	43.30	TOPO

Table A-50. Reach C3, cross-section 10 point coordinates and descriptions.

Cross-Section 10				
N (m)	**E (m)**	**Z (m)**	**X (m)**	**Description**
4954.47	5052.42	4999.44	0.00	TOPO
4953.62	5025.66	4997.89	26.77	TOPO
4953.68	5027.44	4997.54	28.55	LEW
4954.13	5041.65	4997.19	42.77	OS
4954.34	5048.28	4997.11	49.40	OS
4954.25	5045.29	4997.22	52.38	OS
4954.16	5042.59	4997.78	55.08	OS
4954.33	5047.96	4997.77	60.45	OS
4954.35	5048.55	4997.47	61.05	OS
4953.79	5030.97	4997.47	78.64	OS
4953.73	5029.14	4997.65	80.46	OS
4954.15	5042.29	4997.51	93.61	OS
4954.11	5040.87	4997.66	95.02	OS
4954.11	5040.98	4997.54	95.13	OS
4954.02	5038.16	4997.66	97.94	REW
4954.01	5037.95	4997.82	98.15	TOPO
4953.81	5031.73	4998.25	104.37	TOPO
4953.16	5011.38	4999.24	124.73	TOPO

Table A-51. Reach C3, cross-section 11 point coordinates and descriptions.

Cross-Section 11				
N (m)	**E (m)**	**Z (m)**	**X (m)**	**Description**
4904.35	5038.45	4998.44	0.00	TOPO
4904.17	5038.99	4997.52	0.56	TOPO
4904.11	5039.16	4997.17	0.75	LEW
4904.01	5039.43	4997.00	1.03	OS
4904.40	5038.31	4996.81	2.22	OS
4904.13	5039.08	4997.06	3.03	OS
4904.68	5037.49	4996.93	4.71	OS
4905.50	5035.10	4997.01	7.24	OS
4905.54	5035.00	4997.16	7.35	OS
4905.78	5034.29	4997.17	8.10	EW
4905.96	5033.77	4997.50	8.65	OS
4906.50	5032.22	4997.60	10.29	OS
4907.91	5028.10	4997.60	14.65	OS
4907.93	5028.04	4997.61	14.71	OS
4908.50	5026.39	4997.33	16.46	OS
4908.36	5026.80	4997.08	16.90	EW
4908.60	5026.10	4996.63	17.64	OS
4910.22	5021.40	4996.78	22.61	OS
4910.57	5020.38	4996.94	23.69	OS
4910.79	5019.73	4996.78	24.38	OS
4911.65	5017.23	4996.70	27.02	OS
4913.40	5012.14	4996.95	32.40	OS
4913.65	5011.43	4997.17	33.16	REW
4914.88	5007.86	4998.20	36.94	TOPO

Table A-52. Reach C3, cross-section 12 point coordinates and descriptions.

Cross-Section 12

N (m)	E (m)	Z (m)	X (m)	Description
4861.76	5027.21	4998.16	0.00	TOPO
4862.98	5025.31	4997.33	2.26	TOPO
4864.36	5023.14	4997.30	4.83	LEW
4864.53	5022.87	4996.93	5.15	OS
4865.38	5021.55	4996.67	6.72	OS
4866.75	5019.41	4996.53	9.26	OS
4869.43	5015.22	4996.73	14.23	OS
4872.33	5010.67	4996.82	19.63	OS
4873.00	5009.63	4996.95	20.87	OS
4874.04	5008.01	4996.61	22.79	OS
4876.40	5004.31	4996.68	27.18	OS
4877.66	5002.34	4996.28	29.51	OS
4879.75	4999.07	4996.23	33.40	OS
4879.97	4998.73	4996.32	33.80	OS
4880.92	4997.24	4996.75	35.57	OS
4881.11	4996.95	4996.98	35.92	REW
4881.78	4995.89	4997.30	37.17	TOPO
4878.36	5001.25	4998.51	43.52	TOPO

Table A-53. Reach C3, cross-section 13 point coordinates and descriptions.

Cross-Section 13				
N (m)	**E (m)**	**Z (m)**	**X (m)**	**Description**
4816.25	4989.10	4998.15	0.00	TOPO
4824.08	4983.87	4996.60	9.42	LEW
4825.15	4983.16	4996.37	10.70	OS
4827.12	4981.84	4996.32	13.07	OS
4828.62	4980.85	4996.44	14.87	OS
4828.97	4980.61	4996.66	15.29	EW
4829.20	4980.46	4996.67	15.57	TOPO
4833.02	4977.91	4996.63	20.17	TOPO
4832.73	4978.10	4996.63	20.52	EW
4833.09	4977.87	4996.38	20.95	OS
4834.27	4977.08	4996.24	22.37	OS
4834.62	4976.84	4996.10	22.80	OS
4835.75	4976.09	4995.95	24.16	OS
4837.14	4975.16	4995.91	25.82	OS
4839.08	4973.86	4995.72	28.16	OS
4842.72	4971.44	4995.77	32.53	OS
4844.26	4970.41	4995.99	34.39	OS
4845.98	4969.26	4996.21	36.45	OS
4849.14	4967.15	4996.33	40.26	OS
4849.12	4967.16	4996.46	40.28	REW
4849.26	4967.08	4996.64	40.44	TOPO
4851.33	4965.69	4998.09	42.94	TOPO

Table A-54. Reach C3, cross-section 14 point coordinates and descriptions.

Cross-Section 14				
N (m)	E (m)	Z (m)	X (m)	Description
4827.05	4902.60	4997.70	0.00	TOPO
4818.00	4907.19	4996.45	10.15	TOPO
4816.78	4907.81	4996.13	11.51	LEW
4816.59	4907.91	4995.79	11.72	OS
4814.14	4909.15	4995.67	14.47	OS
4808.76	4911.88	4995.57	20.50	OS
4804.29	4914.14	4995.61	25.52	OS
4803.03	4914.78	4995.39	26.93	OS
4801.15	4915.74	4995.66	29.04	OS
4800.87	4915.88	4996.12	29.35	OS
4797.62	4917.53	4996.05	32.99	OS
4796.96	4917.86	4995.88	33.74	OS
4796.27	4918.21	4995.77	34.51	OS
4794.15	4919.28	4995.99	36.88	OS
4791.40	4920.68	4995.76	39.97	OS
4789.26	4921.77	4995.86	42.37	OS
4788.59	4922.10	4996.13	43.12	REW
4787.68	4922.57	4996.12	44.14	TOPO
4783.69	4924.59	4998.08	48.62	TOPO

Table A-55. Reach C3, cross-section 15 point coordinates and descriptions.

Cross-Section 15				
N (m)	E (m)	Z (m)	X (m)	Description
4772.49	4890.06	4998.66	0.00	TOPO
4774.39	4888.39	4995.84	2.53	LEW
4774.83	4888.00	4995.46	3.12	OS
4775.69	4887.24	4995.31	4.26	OS
4777.50	4885.63	4995.05	6.69	OS
4778.18	4885.03	4995.26	7.60	OS
4779.90	4883.51	4995.42	9.89	OS
4786.09	4878.03	4995.63	18.16	OS
4791.03	4873.66	4995.26	24.75	OS
4792.61	4872.26	4995.35	26.86	OS
4794.44	4870.64	4995.70	29.30	OS
4794.62	4870.48	4995.80	29.55	REW
4797.88	4867.59	4996.12	33.91	TOPO
4808.21	4858.46	4997.52	47.69	TOPO

Table A-56. Reach C3, cross-section 16 point coordinates and descriptions.

Cross-Section 16				
N (m)	E (m)	Z (m)	X (m)	Description
4749.13	4863.41	4997.02	0.00	TOPO
4750.14	4861.83	4995.80	1.88	TOPO
4753.34	4856.83	4995.42	7.81	LEW
4753.59	4856.43	4995.33	8.28	OS
4753.79	4856.12	4994.98	8.65	OS
4754.76	4854.61	4994.73	10.45	OS
4755.74	4853.08	4994.73	12.26	OS
4758.17	4849.27	4994.97	16.78	OS
4761.64	4843.84	4995.20	23.23	OS
4763.65	4840.70	4995.27	26.96	OS
4764.21	4839.82	4995.42	28.00	OS
4765.47	4837.86	4995.13	30.33	OS
4766.28	4836.58	4995.23	31.84	OS
4766.47	4836.28	4995.44	32.20	REW
4766.65	4836.01	4995.72	32.52	TOPO
4767.69	4834.37	4995.59	34.46	TOPO
4770.80	4829.51	4997.50	40.23	TOPO

STUDY REACH R1

Table A-57. Reach R1, cross-section 5A point coordinates and descriptions.

Cross-Section 5A				
N (m)	E (m)	Z (m)	X (m)	Description
8087.36	7914.78	8001.39	0.00	TOPO
8084.28	7913.76	8000.91	3.25	TOPO
8084.33	7913.78	8000.70	3.31	TOPO
8083.55	7913.52	8000.14	4.12	LEW
8083.53	7913.52	8000.11	4.15	OS
8081.47	7912.83	8000.03	6.32	OS
8078.72	7911.93	7999.94	9.21	OS
8077.22	7911.43	7999.69	10.79	OS
8071.79	7909.64	7999.75	16.51	OS
8068.08	7908.42	7999.53	20.42	OS
8064.26	7907.16	7999.62	24.44	OS
8064.43	7907.21	7999.72	24.61	OS
8061.95	7906.39	8000.26	27.23	REW
8061.03	7906.09	8001.34	28.20	TOPO
8057.12	7904.80	8001.42	32.31	TOPO

Table A-58. Reach R1, cross-section 5B point coordinates and descriptions.

Cross-Section 5B				
N (m)	**E (m)**	**Z (m)**	**X (m)**	**Description**
8072.84	7950.71	8000.57	0.00	TOPO
8070.86	7949.29	8000.50	2.44	TOPO
8070.39	7948.96	8000.11	3.01	TOPO
8070.12	7948.77	7999.81	3.35	TOPO
8070.07	7948.73	7999.67	3.41	LEW
8069.97	7948.66	7999.62	3.54	OS
8069.80	7948.54	7999.54	3.74	OS
8069.39	7948.25	7999.39	4.24	OS
8067.45	7946.86	7999.18	6.62	OS
8065.42	7945.42	7999.08	9.12	OS
8063.89	7944.32	7999.20	11.00	OS
8061.72	7942.78	7999.18	13.66	OS
8060.33	7941.79	7999.05	15.37	OS
8058.80	7940.70	7999.11	17.24	OS
8056.70	7939.20	7999.38	19.82	OS
8054.25	7937.46	7999.72	22.83	REW
8053.25	7936.74	7999.89	24.07	TOPO
8052.36	7936.11	8000.29	25.16	TOPO
8050.42	7934.72	8000.64	27.54	TOPO
8046.52	7931.95	8000.83	32.33	TOPO

Table A-59. Reach R1, cross-section 5 point coordinates and descriptions.

Cross-Section 5				
N (m)	**E (m)**	**Z (m)**	**X (m)**	**Description**
8055.19	7978.17	8000.82	0.00	XS5-LEP
8054.59	7977.70	8000.67	0.76	TOPO
8053.53	7976.86	8000.60	2.12	TOPO
8052.09	7975.73	8000.09	3.94	TOPO
8051.15	7974.98	7999.85	5.15	TOPO
8049.50	7973.68	7999.65	7.25	TOPO
8049.03	7973.32	7999.31	7.84	LEW
8048.53	7972.92	7998.41	8.47	OS
8047.80	7972.34	7998.21	9.41	OS
8047.74	7972.30	7998.14	9.48	OS
8046.38	7971.23	7998.28	11.22	OS
8044.91	7970.07	7998.55	13.08	OS
8042.68	7968.32	7998.88	15.92	OS
8041.64	7967.50	7999.24	17.24	OS
8040.06	7966.25	7999.36	19.25	OS
8038.68	7965.16	7999.48	21.02	OS
8037.32	7964.09	7999.52	22.75	OS
8036.21	7963.22	7999.44	24.16	OS
8034.45	7961.83	7999.50	26.40	OS
8033.07	7960.75	7999.55	28.15	OS
8032.61	7960.38	7999.61	28.75	REW
8032.49	7960.29	7999.64	28.89	TOPO
8030.26	7958.53	7999.71	31.73	TOPO
8029.67	7958.07	7999.75	32.48	TOPO
8027.41	7956.29	7999.82	35.36	TOPO
8024.79	7954.23	7999.94	38.69	TOPO
8022.63	7952.52	8000.18	41.45	TOPO
8019.06	7949.71	8000.29	45.99	TOPO
8019.11	7949.75	8000.47	46.05	XS5-REP

Table A-60. Reach R1, cross-section 4A point coordinates and descriptions.

Cross-Section 4A				
N (m)	**E (m)**	**Z (m)**	**X (m)**	**Description**
8008.29	8002.23	8000.18	0.00	TOPO
8008.40	8001.18	8000.03	1.05	TOPO
8008.37	8001.53	7999.90	1.40	TOPO
8008.39	8001.31	7999.74	1.62	TOPO
8008.47	8000.54	7999.70	2.38	TOPO
8008.56	7999.70	7999.55	3.24	TOPO
8008.54	7999.83	7999.34	3.37	TOPO
8008.56	7999.65	7999.20	3.55	LEW
8008.58	7999.52	7999.05	3.69	OS
8008.53	7999.97	7999.01	4.15	OS
8008.54	7999.85	7998.51	4.27	OS
8008.69	7998.41	7998.18	5.72	OS
8009.32	7992.46	7998.05	11.70	OS
8009.28	7992.81	7998.08	12.06	OS
8009.22	7993.44	7998.25	12.69	OS
8009.25	7993.08	7998.30	13.05	OS
8009.68	7988.99	7998.79	17.16	OS
8009.78	7988.08	7998.84	18.08	OS
8009.98	7986.17	7998.76	19.99	OS
8010.20	7984.09	7998.81	22.09	OS
8010.54	7980.83	7999.20	25.37	REW
8010.50	7981.24	7999.37	25.78	TOPO
8010.88	7977.57	7999.35	29.47	TOPO
8011.30	7973.59	7999.69	33.47	TOPO
8011.58	7970.95	7999.70	36.13	TOPO
8012.10	7965.99	7999.85	41.11	TOPO

Table A-61. Reach R1, cross-section 4B point coordinates and descriptions.

Cross-Section 4B				
N (m)	**E (m)**	**Z (m)**	**X (m)**	**Description**
7977.18	7990.32	7999.66	0.00	TOPO
7977.82	7989.54	7999.58	1.01	TOPO
7978.12	7989.22	7999.53	1.44	TOPO
7978.27	7989.09	7999.45	1.65	TOPO
7978.86	7988.51	7999.29	2.47	TOPO
7979.59	7987.64	7999.26	3.61	TOPO
7980.45	7986.63	7999.15	4.93	TOPO
7980.71	7986.27	7999.21	5.38	TOPO
7980.93	7986.06	7999.33	5.68	TOPO
7981.12	7985.74	7999.25	6.06	TOPO
7981.30	7985.53	7999.07	6.33	LEW
7981.42	7985.48	7998.96	6.46	OS
7981.98	7984.47	7998.67	7.62	OS
7982.72	7983.72	7998.52	8.68	OS
7984.36	7982.29	7998.53	10.85	OS
7985.66	7980.79	7998.57	12.83	OS
7986.33	7980.18	7998.71	13.73	OS
7988.43	7977.26	7998.82	17.34	OS
7990.41	7974.73	7998.70	20.54	OS
7991.83	7972.93	7998.77	22.84	OS
7994.64	7969.80	7998.94	27.05	OS
7995.27	7968.93	7999.01	28.12	OS
7995.48	7968.68	7999.08	28.44	REW
7995.95	7968.12	7999.10	29.18	TOPO
7996.66	7967.39	7999.30	30.20	TOPO
7998.87	7965.31	7999.50	33.23	TOPO
8001.97	7961.54	7999.81	38.11	TOPO
8004.52	7959.21	7999.96	41.56	TOPO

Table A-62. Reach R1, cross-section 4C point coordinates and descriptions.

Cross-Section 4C				
N (m)	E (m)	Z (m)	X (m)	Description
7947.84	7967.34	7999.50	0.00	TOPO
7951.24	7964.73	7999.26	4.29	TOPO
7952.34	7963.88	7999.13	5.68	TOPO
7953.38	7963.08	7998.76	6.99	TOPO
7953.37	7963.09	7998.71	7.00	TOPO
7953.64	7962.88	7998.64	7.33	LEW
7955.66	7961.33	7998.47	9.88	OS
7956.94	7960.34	7998.36	11.50	OS
7960.05	7957.95	7998.33	15.42	OS
7961.91	7956.51	7998.25	17.77	OS
7962.90	7955.75	7998.15	19.03	OS
7963.28	7955.46	7998.07	19.50	OS
7964.01	7954.90	7997.97	20.42	OS
7964.80	7954.29	7998.06	21.42	OS
7966.65	7952.87	7998.06	23.75	OS
7968.74	7951.25	7998.19	26.40	OS
7969.86	7950.40	7998.66	27.80	REW
7970.00	7950.29	7998.71	27.99	TOPO
7970.20	7950.14	7999.03	28.23	TOPO
7970.34	7950.03	7999.74	28.41	TOPO
7970.70	7949.75	7999.85	28.87	TOPO

Table A-63. Reach R1, cross-section 4 point coordinates and descriptions.

Cross-Section 4				
N (m)	**E (m)**	**Z (m)**	**X (m)**	**Description**
7927.87	7959.57	7999.27	0.00	TOPO
7927.87	7959.59	7999.08	0.02	TOPO
7927.76	7959.13	7998.82	0.49	HW
7927.45	7957.84	7998.58	1.82	TOPO
7926.77	7954.97	7998.72	4.76	TOPO
7926.49	7953.78	7998.61	5.99	TOPO
7926.36	7953.24	7998.52	6.54	TOPO
7926.26	7952.81	7998.40	6.98	TOPO
7926.20	7952.56	7998.34	7.24	LEW
7926.16	7952.40	7998.28	7.41	OS
7926.08	7952.06	7998.30	7.75	OS
7925.99	7951.69	7998.34	8.13	OS
7926.09	7952.10	7998.27	8.55	OS
7925.91	7951.35	7998.35	9.31	OS
7925.93	7951.42	7998.21	9.39	OS
7925.47	7949.47	7997.64	11.39	OS
7925.05	7947.71	7997.44	13.20	OS
7924.02	7943.41	7997.04	17.63	OS
7922.36	7936.41	7996.88	24.82	OS
7921.99	7934.87	7997.35	26.41	OS
7921.87	7934.36	7998.29	26.93	REW
7921.69	7933.58	7999.11	27.72	TOPO
7921.60	7933.21	8000.08	28.11	TOPO
7920.88	7930.16	8000.54	31.24	TOPO
7918.49	7920.12	8000.28	41.56	XS4-REP

Table A-64. Reach R1, cross-section 3A point coordinates and descriptions.

Cross-Section 3A				
N (m)	**E (m)**	**Z (m)**	**X (m)**	**Description**
7896.90	7984.71	7998.75	0.00	TOPO
7896.48	7984.42	7998.72	0.50	TOPO
7896.24	7984.24	7998.58	0.81	TOPO
7895.73	7983.89	7998.47	1.42	TOPO
7895.47	7983.70	7998.21	1.75	HW
7894.98	7983.36	7998.00	2.34	TOPO
7894.89	7983.30	7997.88	2.45	LEW
7893.68	7982.44	7997.68	3.94	OS
7892.75	7981.79	7997.68	5.07	OS
7891.35	7980.81	7997.81	6.78	OS
7890.52	7980.22	7997.77	7.80	OS
7889.75	7979.68	7997.59	8.74	OS
7888.99	7979.15	7997.60	9.66	OS
7887.18	7977.87	7997.29	11.88	OS
7884.41	7975.93	7997.20	15.27	OS
7882.23	7974.40	7997.73	17.93	OS
7880.58	7973.24	7997.84	19.94	OS
7880.43	7970.58	7997.91	22.60	OS
7881.57	7967.46	7997.61	25.93	OS
7882.75	7964.26	7997.67	29.34	OS
7884.01	7960.80	7997.63	33.02	OS
7884.34	7959.90	7997.68	33.98	OS
7885.72	7956.14	7997.73	37.98	OS
7886.91	7952.90	7997.91	41.44	OS
7887.28	7951.88	7997.94	42.52	OS
7887.31	7951.79	7998.02	42.62	OS
7887.32	7951.77	7998.07	42.63	REW
7887.73	7950.65	7998.97	43.83	TOPO
7888.99	7947.20	7999.02	47.50	TOPO
7889.51	7945.78	7998.84	49.01	TOPO
7890.10	7944.19	7998.35	50.71	TOPO
7890.40	7943.37	7998.13	51.58	EW
7890.39	7943.38	7998.04	51.60	OS
7890.81	7942.24	7998.13	52.81	EW
7891.25	7941.05	7998.37	54.08	TOPO
7892.55	7937.50	7998.15	57.86	TOPO
7893.50	7934.90	7998.79	60.63	TOPO
7894.19	7933.02	7999.35	62.63	TOPO
7894.87	7931.17	7999.48	64.61	TOPO

Table A-65. Reach R1, cross-section 3B point coordinates and descriptions.

Cross-Section 3B				
N (m)	E (m)	Z (m)	X (m)	Description
7876.07	8017.01	7998.41	0.00	TOPO
7875.13	8015.44	7998.43	1.83	TOPO
7875.04	8015.29	7998.14	2.01	TOPO
7874.46	8014.33	7998.16	3.13	TOPO
7874.44	8014.29	7998.06	3.17	HW
7873.67	8013.00	7997.72	4.67	TOPO
7873.62	8012.92	7997.58	4.77	LEW
7873.60	8012.88	7997.46	4.81	OS
7873.13	8012.09	7997.20	5.74	OS
7872.31	8010.72	7996.99	7.33	OS
7871.71	8009.71	7996.79	8.51	OS
7870.67	8007.97	7997.23	10.53	OS
7869.77	8006.46	7997.39	12.29	OS
7868.36	8004.11	7997.39	15.03	OS
7867.55	8002.74	7997.18	16.62	OS
7866.02	8000.18	7997.21	19.61	OS
7864.86	7998.24	7997.33	21.87	OS
7864.72	7998.01	7997.56	22.13	OS
7864.52	7997.66	7997.66	22.54	EW
7862.93	7995.01	7998.50	25.63	TOPO
7857.37	7987.12	7998.46	35.28	TOPO
7856.44	7979.59	7998.87	42.87	TOPO
7856.17	7977.40	7998.07	45.08	TOPO
7855.39	7971.07	7997.83	51.45	TOPO
7855.07	7968.53	7997.74	54.01	TOPO
7854.77	7966.07	7997.65	56.49	TOPO
7854.71	7965.57	7997.73	56.99	TOPO
7854.62	7964.86	7997.58	57.71	EW
7854.46	7963.54	7997.47	59.04	OS
7854.22	7961.64	7997.29	60.95	OS
7853.62	7956.78	7997.17	65.85	OS
7853.12	7952.75	7997.27	69.92	OS
7852.97	7951.54	7997.37	71.13	OS
7853.27	7953.98	7997.59	73.58	LEW
7852.98	7951.56	7998.06	76.02	TOPO
7853.35	7954.57	7998.64	79.06	TOPO

Table A-66. Reach R1, cross-section 3 point coordinates and descriptions.

Cross-Section 3				
N (m)	**E (m)**	**Z (m)**	**X (m)**	**Description**
7849.91	8050.59	7998.07	0.00	XS3-LEP
7847.16	8041.93	7998.07	9.09	TOPO
7846.50	8039.85	7998.07	11.27	TOPO
7846.51	8039.88	7997.97	11.30	TOPO
7846.15	8038.75	7997.83	12.49	TOPO
7845.44	8036.52	7997.23	14.83	TOPO
7845.48	8036.64	7997.15	14.95	LEW
7844.87	8034.70	7996.56	16.99	OS
7844.85	8034.63	7996.56	17.05	OS
7844.21	8032.62	7996.67	19.17	OS
7843.98	8031.91	7996.87	19.91	OS
7843.05	8028.96	7996.64	23.00	OS
7842.48	8027.18	7996.75	24.87	OS
7841.78	8024.99	7996.75	27.17	OS
7840.93	8022.31	7996.78	29.98	OS
7840.51	8020.97	7996.87	31.39	OS
7840.06	8019.56	7996.82	32.87	OS
7839.71	8018.45	7997.08	34.03	OS
7839.16	8016.74	7997.08	35.82	OS
7838.93	8016.00	7997.15	36.60	EW
7838.37	8014.24	7997.48	38.45	TOPO
7838.01	8013.12	7997.64	39.62	TOPO
7837.18	8010.49	7998.02	42.38	TOPO
7836.41	8008.06	7998.21	44.94	TOPO
7834.58	8002.31	7998.58	50.97	TOPO
7830.85	7990.57	7998.24	63.29	TOPO
7828.82	7984.16	7998.05	70.01	TOPO
7827.78	7980.91	7998.25	73.43	TOPO
7826.56	7977.07	7997.69	77.45	TOPO
7826.34	7976.37	7997.41	78.18	EW
7825.81	7974.69	7997.15	79.95	OS
7825.12	7972.53	7997.18	82.21	OS
7824.10	7969.31	7996.97	85.59	OS
7823.57	7967.63	7996.94	87.36	OS
7823.20	7966.46	7997.02	88.58	OS
7822.20	7963.32	7997.19	91.87	OS
7821.09	7959.83	7997.36	95.53	REW
7820.88	7959.18	7997.42	96.23	TOPO
7820.58	7958.23	7997.77	97.22	TOPO
7819.98	7956.32	7997.98	99.22	TOPO
7819.04	7953.38	7997.88	102.30	TOPO
7818.65	7952.14	7998.07	103.60	TOPO
7818.62	7952.06	7998.06	103.69	TOPO
7818.19	7950.70	7997.53	105.11	TOPO
7817.82	7949.52	7997.35	106.35	EW
7817.78	7949.39	7997.28	106.49	OS
7817.72	7949.21	7997.36	106.68	EW
7817.50	7948.52	7997.70	107.41	TOPO
7817.48	7948.47	7997.82	107.46	TOPO
7817.51	7948.56	7997.84	107.54	TOPO
7816.97	7946.86	7998.02	109.33	TOPO
7817.41	7948.25	7998.24	110.79	TOPO
7816.34	7944.88	7998.70	114.31	XS3-REP

Table A-67. Reach R1, cross-section 2A point coordinates and descriptions.

Cross-Section 2A				
N (m)	E (m)	Z (m)	X (m)	Description
7795.97	8040.46	7997.72	0.00	TOPO
7796.99	8037.99	7997.58	2.68	TOPO
7797.87	8035.87	7997.16	4.97	TOPO
7798.50	8034.34	7996.98	6.62	LEW
7799.25	8032.53	7996.44	8.58	OS
7800.01	8030.69	7996.38	10.58	OS
7800.43	8029.66	7996.22	11.68	OS
7801.20	8027.78	7996.29	13.72	OS
7801.39	8027.32	7996.48	14.22	OS
7803.04	8023.34	7996.37	18.52	OS
7803.18	8022.99	7996.59	18.90	OS
7803.83	8021.42	7996.62	20.60	OS
7803.93	8021.19	7996.86	20.86	OS
7804.57	8019.61	7996.94	22.55	OS
7804.91	8018.79	7996.72	23.44	OS
7805.38	8017.67	7996.84	24.65	OS
7805.49	8017.39	7996.98	24.96	OS
7805.97	8016.23	7997.05	26.22	EW
7806.41	8015.17	7997.24	27.37	TOPO
7807.09	8013.52	7997.64	29.15	TOPO
7807.56	8012.37	7997.65	30.39	TOPO
7809.07	8000.48	7997.61	42.37	TOPO
7805.92	7985.14	7998.04	58.03	TOPO
7805.86	7984.83	7997.74	58.35	TOPO
7805.40	7982.60	7997.51	60.63	TOPO
7805.52	7983.18	7997.39	61.22	TOPO
7805.42	7982.70	7997.25	61.71	EW
7804.83	7979.84	7997.11	64.63	OS
7804.73	7979.34	7996.91	65.14	OS
7804.91	7980.23	7996.95	66.04	OS
7804.56	7978.54	7996.82	67.77	OS
7804.74	7979.38	7996.87	68.63	OS
7804.61	7978.77	7996.99	69.24	OS
7804.58	7978.63	7996.92	69.39	OS
7803.87	7975.14	7996.79	72.95	OS
7803.67	7974.18	7996.95	73.93	OS
7803.10	7971.40	7996.97	76.77	OS
7802.90	7970.41	7997.08	77.78	OS
7802.43	7968.16	7997.08	80.08	OS
7802.08	7966.43	7996.97	81.84	OS
7801.83	7965.20	7997.12	83.10	OS
7801.54	7963.81	7997.14	84.51	OS
7800.79	7960.15	7997.24	88.26	OS
7800.65	7959.46	7997.36	88.96	OS
7800.63	7959.39	7997.35	89.03	OS
7800.10	7956.77	7997.36	91.71	OS
7799.42	7953.49	7997.84	95.05	REW
7799.21	7952.45	7998.20	96.11	TOPO

Table A-68. Reach R1, cross-section 2B point coordinates and descriptions.

Cross-Section 2B				
N (m)	E (m)	Z (m)	X (m)	Description
7766.65	7961.65	7997.51	0.00	TOPO
7767.26	7963.34	7997.09	1.80	HW
7767.79	7964.84	7996.65	3.39	TOPO
7767.83	7964.96	7996.42	3.51	LEW
7768.20	7965.98	7996.22	4.60	OS
7769.10	7968.53	7996.26	7.30	OS
7770.46	7972.33	7996.03	11.34	OS
7771.06	7974.03	7996.10	13.14	OS
7772.07	7976.85	7995.98	16.14	OS
7773.01	7979.51	7996.31	18.96	OS
7773.30	7980.32	7996.38	19.83	OS
7773.51	7980.90	7996.48	20.44	EW
7773.72	7981.48	7996.81	21.05	TOPO
7773.88	7981.93	7997.06	21.53	TOPO
7773.87	7981.92	7997.37	21.55	TOPO
7775.24	7985.76	7997.71	25.63	TOPO
7776.23	7996.61	7997.87	36.53	TOPO
7774.34	8004.42	7997.65	44.56	TOPO
7772.97	8010.11	7996.57	50.40	EW
7774.56	8003.53	7996.14	57.17	OS
7774.04	8005.68	7996.20	59.37	OS
7773.61	8007.45	7996.22	61.20	OS
7773.33	8008.62	7996.22	62.40	OS
7772.33	8012.76	7996.23	66.66	OS
7771.91	8014.51	7996.19	68.46	OS
7771.55	8015.97	7996.18	69.96	OS
7771.02	8018.15	7995.81	72.21	OS
7770.64	8019.75	7995.99	73.84	OS
7770.23	8021.44	7996.33	75.58	OS
7770.14	8021.80	7996.57	75.96	REW
7770.14	8021.83	7996.68	75.98	TOPO
7769.72	8023.54	7997.12	77.75	HW
7768.41	8028.98	7997.50	83.34	TOPO

Table A-69. Reach R1, cross-section 2C point coordinates and descriptions.

Cross-Section 2C				
N (m)	**E (m)**	**Z (m)**	**X (m)**	**Description**
7720.60	7990.47	7996.98	0.00	TOPO
7720.84	7990.60	7996.58	0.27	TOPO
7723.30	7991.96	7996.25	3.08	TOPO
7723.89	7992.29	7996.20	3.76	TOPO
7724.71	7992.74	7995.92	4.69	TOPO
7724.89	7992.84	7995.79	4.89	LEW
7724.88	7992.84	7995.65	4.90	OS
7725.23	7993.03	7995.67	5.29	OS
7726.79	7993.90	7995.33	7.09	OS
7727.72	7994.41	7995.17	8.15	OS
7729.20	7995.23	7995.16	9.83	OS
7731.08	7996.27	7995.48	11.98	OS
7731.93	7996.74	7995.56	12.96	OS
7732.39	7997.00	7995.25	13.49	OS
7732.38	8000.38	7995.11	16.87	OS
7732.97	8009.29	7995.18	25.80	OS
7733.19	8012.66	7995.26	29.17	OS
7733.17	8012.33	7995.26	29.51	OS
7732.92	8008.60	7995.28	33.24	OS
7732.61	8003.89	7995.19	37.96	OS
7732.90	8008.34	7995.42	42.43	OS
7733.00	8009.74	7995.48	43.83	OS
7733.04	8010.45	7995.61	44.54	OS
7733.04	8010.39	7995.73	44.60	OS
7733.00	8009.82	7995.73	45.17	REW
7733.03	8010.24	7995.78	45.59	TOPO
7732.98	8009.47	7995.89	46.36	TOPO
7732.96	8009.21	7996.08	46.62	TOPO
7733.46	8016.65	7996.24	54.06	TOPO
7733.66	8019.77	7996.65	57.20	TOPO
7733.83	8022.33	7997.30	59.76	TOPO

Table A-70. Reach R1, cross-section 2 point coordinates and descriptions.

Cross-Section 2				
N (m)	**E (m)**	**Z (m)**	**X (m)**	**Description**
7722.63	8023.31	7997.49	0.00	XS2-LEP
7720.60	8019.66	7996.48	4.18	TOPO
7719.40	8017.51	7995.85	6.64	TOPO
7719.01	8016.82	7995.63	7.43	LEW
7718.46	8015.82	7995.41	8.57	OS
7717.86	8014.75	7995.36	9.80	OS
7717.24	8013.63	7995.41	11.08	OS
7716.64	8012.56	7995.28	12.31	OS
7715.77	8011.00	7995.24	14.09	OS
7715.37	8010.28	7995.11	14.91	OS
7713.81	8007.48	7994.90	18.12	OS
7712.75	8005.56	7994.96	20.31	OS
7711.80	8003.85	7994.80	22.27	OS
7710.29	8001.16	7994.99	25.36	OS
7709.65	8000.00	7995.29	26.68	OS
7709.49	7999.72	7995.54	27.00	REW
7709.51	7999.76	7997.25	27.04	TOPO
7708.81	7998.50	7997.37	28.48	TOPO
7708.06	7997.14	7996.53	30.04	TOPO
7707.74	7996.57	7997.07	30.69	TOPO
7706.42	7994.21	7997.10	33.40	TOPO
7706.44	7994.24	7997.24	33.44	XS2-REP

Table A-71. Reach R1, cross-section 1A point coordinates and descriptions.

Cross-Section 1A				
N (m)	**E (m)**	**Z (m)**	**X (m)**	**Description**
7707.91	8037.99	7996.92	0.00	TOPO
7708.38	8038.52	7996.21	0.70	TOPO
7708.48	8038.63	7995.91	0.86	TOPO
7707.81	8037.88	7995.77	1.86	TOPO
7707.75	8037.81	7995.68	1.95	TOPO
7705.95	8035.80	7995.58	4.65	TOPO
7705.77	8035.59	7996.34	4.93	TOPO
7704.48	8034.14	7995.99	6.87	TOPO
7703.48	8033.02	7995.58	8.37	TOPO
7703.22	8032.73	7995.48	8.75	LEW
7702.74	8032.18	7995.41	9.49	OS
7702.02	8031.38	7995.45	10.56	OS
7701.38	8030.66	7995.49	11.53	OS
7699.80	8028.88	7995.12	13.91	OS
7698.86	8027.83	7995.13	15.31	OS
7698.01	8026.88	7995.06	16.59	OS
7697.38	8026.16	7995.10	17.55	OS
7696.40	8025.06	7994.94	19.03	OS
7695.13	8023.64	7994.80	20.93	OS
7693.17	8021.43	7994.95	23.88	OS
7691.63	8019.70	7994.83	26.20	OS
7690.79	8018.76	7995.00	27.46	OS
7689.87	8017.73	7994.86	28.84	OS
7688.60	8016.30	7995.02	30.75	OS
7688.04	8015.68	7995.35	31.59	OS
7687.51	8015.07	7995.52	32.40	REW
7687.23	8014.76	7995.68	32.82	TOPO
7686.74	8014.22	7995.87	33.54	TOPO
7685.63	8012.96	7996.65	35.22	TOPO
7683.99	8011.12	7996.86	37.68	TOPO

Table A-72. Reach R1, cross-section 1B point coordinates and descriptions.

Cross-Section 1B				
N (m)	**E (m)**	**Z (m)**	**X (m)**	**Description**
7691.77	8055.99	7996.44	0.00	TOPO
7690.84	8054.84	7995.81	1.47	TOPO
7689.91	8053.68	7995.45	2.96	TOPO
7689.40	8053.05	7995.32	3.77	TOPO
7688.77	8052.26	7995.36	4.78	TOPO
7688.26	8051.63	7995.16	5.59	TOPO
7687.27	8050.39	7995.03	7.18	LEW
7686.45	8049.37	7994.99	8.49	OS
7685.35	8048.00	7994.78	10.25	OS
7684.67	8047.16	7994.88	11.32	OS
7683.17	8045.29	7995.06	13.72	OS
7682.98	8045.06	7994.93	14.03	OS
7681.12	8042.75	7994.78	16.99	OS
7680.63	8042.14	7994.71	17.77	OS
7680.22	8041.62	7994.62	18.43	OS
7679.39	8040.59	7994.26	19.76	OS
7676.26	8036.70	7994.52	24.75	OS
7675.78	8036.10	7994.69	25.52	OS
7674.57	8034.60	7994.93	27.45	OS
7674.49	8034.50	7995.21	27.58	REW
7674.38	8034.36	7995.40	27.75	TOPO
7673.50	8033.27	7995.49	29.15	TOPO
7672.47	8031.99	7995.98	30.79	TOPO
7671.91	8031.29	7996.51	31.69	TOPO
7671.48	8030.76	7996.66	32.37	TOPO
7670.61	8029.67	7997.23	33.76	TOPO

Table A-73. Reach R1, cross-section 1C point coordinates and descriptions.

Cross-Section 1C				
N (m)	**E (m)**	**Z (m)**	**X (m)**	**Description**
7654.69	8068.68	7996.73	0.00	TOPO
7654.06	8065.89	7996.61	2.86	TOPO
7654.06	8065.91	7995.68	2.88	TOPO
7653.85	8065.00	7995.33	3.82	TOPO
7653.75	8064.57	7994.89	4.26	LEW
7653.50	8063.43	7994.63	5.43	OS
7653.35	8062.77	7994.49	6.11	OS
7653.09	8061.65	7994.34	7.26	OS
7652.78	8060.27	7994.07	8.67	OS
7652.96	8061.07	7994.01	9.50	OS
7652.48	8058.96	7994.12	11.67	OS
7651.87	8056.30	7994.30	14.39	OS
7650.95	8052.25	7994.61	18.55	OS
7650.95	8052.22	7994.71	18.58	OS
7650.02	8048.13	7994.75	22.77	OS
7650.00	8048.03	7994.84	22.87	REW
7649.94	8047.78	7994.95	23.13	TOPO
7649.72	8046.83	7995.12	24.10	TOPO
7649.63	8046.41	7995.27	24.53	TOPO

Table A-74. Reach R1, cross-section 1 point coordinates and descriptions.

Cross-Section 1				
N (m)	**E (m)**	**Z (m)**	**X (m)**	**Description**
7607.89	8066.02	7995.76	0.00	XS1-LEP
7608.45	8065.21	7995.81	0.98	TOPO
7608.96	8064.47	7995.83	1.88	TOPO
7608.99	8064.42	7994.94	1.94	TOPO
7609.51	8063.67	7994.66	2.85	TOPO
7611.03	8061.46	7994.70	5.53	TOPO
7612.02	8060.03	7994.70	7.27	TOPO
7612.41	8059.46	7994.59	7.96	LEW
7612.63	8059.14	7994.53	8.35	OS
7613.46	8057.93	7994.04	9.81	OS
7614.89	8055.85	7993.72	12.35	OS
7616.10	8054.09	7993.83	14.47	OS
7617.29	8052.36	7994.09	16.58	OS
7618.56	8050.52	7994.26	18.82	OS
7620.36	8047.90	7994.29	21.99	OS
7620.80	8047.27	7994.55	22.76	REW
7620.90	8047.12	7994.64	22.95	TOPO
7621.42	8046.36	7994.80	23.86	TOPO
7622.92	8044.18	7994.88	26.51	TOPO
7623.58	8043.23	7994.84	27.67	TOPO
7624.11	8042.45	7994.54	28.61	EW
7624.75	8041.53	7994.39	29.72	OS
7625.05	8041.09	7994.56	30.27	EW
7625.09	8041.03	7994.59	30.34	TOPO
7625.28	8040.76	7994.70	30.66	TOPO
7625.56	8040.35	7994.83	31.16	TOPO
7626.11	8039.55	7994.93	32.14	TOPO
7626.63	8038.79	7995.12	33.05	TOPO
7627.01	8038.24	7995.42	33.72	TOPO
7627.36	8037.73	7995.70	34.34	TOPO
7628.65	8035.87	7995.86	36.60	TOPO
7629.92	8034.02	7996.16	38.85	TOPO
7633.02	8029.51	7996.54	44.32	XS1-REP

STUDY REACH R2

Table A-75. Reach R2, cross-section 1 point coordinates and descriptions.

Cross-Section 1				
N (m)	**E (m)**	**Z (m)**	**X (m)**	**Description**
5768.97	47379.61	1747.96	0.00	TOPO
5777.05	47383.29	1748.02	8.87	HW
5777.11	47383.32	1747.60	8.94	TOPO
5778.12	47383.78	1747.41	10.05	LEW
5778.74	47384.06	1747.17	10.73	OS
5779.98	47384.62	1746.90	12.09	OS
5783.29	47386.13	1746.82	15.73	OS
5786.25	47387.48	1746.86	18.98	OS
5789.52	47388.97	1746.92	22.58	OS
5796.15	47391.99	1747.03	29.86	OS
5798.27	47392.95	1746.98	32.19	OS
5799.46	47393.49	1747.36	33.49	REW
5800.27	47393.86	1747.84	34.39	TOPO
5800.46	47393.95	1748.27	34.60	TOPO
5801.35	47394.36	1748.23	35.58	TOPO

Table A-76. Reach R2, cross-section 2 point coordinates and descriptions.

Cross-Section 2				
N (m)	**E (m)**	**Z (m)**	**X (m)**	**Description**
5788.32	47354.84	1747.71	0.00	TOPO
5791.00	47355.33	1747.33	2.72	TOPO
5791.19	47355.37	1747.15	2.92	LEW
5791.16	47355.36	1746.93	2.96	OS
5791.40	47355.41	1746.84	3.21	OS
5792.85	47355.68	1746.63	4.68	OS
5796.42	47356.34	1746.70	8.31	OS
5803.28	47357.61	1746.78	15.28	OS
5804.32	47357.80	1746.67	16.35	OS
5809.87	47358.83	1746.77	21.98	OS
5811.76	47359.18	1746.64	23.91	OS
5813.26	47359.45	1747.08	25.43	REW
5813.82	47359.56	1747.35	26.00	TOPO
5814.05	47359.60	1747.62	26.24	TOPO
5815.76	47359.91	1748.15	27.97	TOPO
5818.45	47360.41	1748.21	30.71	TOPO

Table A-77. Reach R2, cross-section 3 point coordinates and descriptions.

Cross-Section 3				
N (m)	E (m)	Z (m)	X (m)	Description
5782.78	47339.70	1747.68	0.00	TOPO
5789.18	47338.63	1747.34	6.49	TOPO
5791.34	47338.27	1746.89	8.67	LEW
5791.73	47338.20	1746.76	9.07	OS
5798.79	47337.02	1746.61	16.24	OS
5799.82	47336.85	1746.42	17.27	OS
5801.21	47336.62	1746.56	18.68	OS
5805.37	47335.92	1746.16	22.91	OS
5808.03	47335.48	1746.62	25.60	OS
5813.26	47334.60	1746.49	30.90	OS
5815.81	47334.18	1746.94	33.49	REW
5816.69	47334.03	1747.65	34.38	TOPO
5820.51	47333.39	1747.90	38.25	TOPO

Table A-78. Reach R2, cross-section 4 point coordinates and descriptions.

Cross-Section 4				
N (m)	E (m)	Z (m)	X (m)	Description
5767.27	47325.68	1747.28	0.00	TOPO
5770.26	47318.37	1746.76	7.90	TOPO
5772.39	47313.14	1746.23	13.54	LEW
5772.95	47311.78	1746.07	15.02	OS
5774.95	47306.88	1745.87	20.31	OS
5776.45	47303.19	1745.82	24.30	OS
5778.48	47298.20	1745.28	29.68	OS
5779.01	47296.91	1744.86	31.07	OS
5781.04	47291.93	1745.74	36.46	OS
5781.51	47290.78	1746.06	37.70	REW
5781.62	47290.51	1746.95	37.99	TOPO

Table A-79. Reach R2, cross-section 5 point coordinates and descriptions.

Cross-Section 5				
N (m)	**E (m)**	**Z (m)**	**X (m)**	**Description**
5744.66	47318.60	1746.97	0.00	TOPO
5746.08	47313.07	1746.90	5.72	TOPO
5745.78	47314.24	1746.65	6.93	TOPO
5746.21	47312.57	1746.41	8.65	TOPO
5746.31	47312.17	1746.04	9.06	LEW
5746.57	47311.17	1745.85	10.09	OS
5746.73	47310.57	1745.69	10.72	OS
5747.06	47309.25	1745.63	12.08	OS
5747.72	47306.71	1745.75	14.70	OS
5748.68	47302.97	1745.85	18.56	OS
5749.37	47300.30	1745.84	21.32	OS
5750.15	47297.27	1745.78	24.45	OS
5750.82	47294.67	1745.96	27.14	OS
5751.10	47293.58	1745.99	28.26	OS
5751.22	47293.12	1746.20	28.73	EW
5751.20	47293.19	1746.37	28.80	TOPO
5751.69	47291.30	1746.25	30.74	EW
5752.77	47287.11	1746.04	35.08	OS
5753.34	47284.87	1746.15	37.39	OS
5753.62	47283.80	1745.84	38.49	OS
5754.16	47281.67	1745.68	40.69	OS
5755.05	47278.24	1745.73	44.23	OS
5755.76	47275.47	1745.89	47.09	OS
5756.26	47273.55	1746.17	49.07	REW
5756.72	47271.75	1746.32	50.93	TOPO
5758.26	47265.75	1746.74	57.13	TOPO
5758.87	47263.38	1746.66	59.58	TOPO
5760.40	47257.47	1746.62	65.68	TOPO
5759.31	47261.69	1746.59	70.04	TOPO

Table A-80. Reach R2, cross-section 6 point coordinates and descriptions.

Cross-Section 6				
N (m)	**E (m)**	**Z (m)**	**X (m)**	**Description**
5679.07	47310.33	1745.95	0.00	TOPO
5681.44	47306.80	1745.94	4.25	TOPO
5682.84	47304.73	1745.74	6.75	TOPO
5683.48	47303.78	1745.32	7.89	TOPO
5683.69	47303.46	1745.10	8.28	LEW
5683.93	47303.11	1744.87	8.70	OS
5684.64	47302.06	1744.42	9.97	OS
5685.32	47301.04	1744.39	11.20	OS
5685.85	47300.25	1744.27	12.15	OS
5686.29	47299.60	1744.38	12.93	OS
5687.30	47298.09	1744.59	14.74	OS
5688.07	47296.96	1744.72	16.11	OS
5689.34	47295.06	1744.93	18.40	OS
5690.53	47293.30	1745.09	20.53	OS
5691.99	47291.12	1745.23	23.15	OS
5693.03	47289.58	1745.05	25.00	OS
5694.22	47287.81	1745.06	27.14	OS
5695.27	47286.25	1745.02	29.02	OS
5696.28	47284.74	1745.31	30.84	EW
5697.73	47282.58	1745.61	33.44	TOPO
5701.63	47276.79	1746.09	40.42	TOPO
5711.10	47262.72	1746.06	57.38	TOPO
5717.93	47252.55	1746.03	69.63	TOPO
5722.86	47246.58	1746.14	77.38	TOPO
5725.71	47245.31	1745.70	80.49	TOPO
5726.10	47245.14	1745.50	80.92	EW
5726.58	47244.93	1745.23	81.44	OS
5727.67	47244.44	1745.18	82.64	OS
5730.26	47243.29	1745.28	85.47	OS
5731.84	47242.58	1745.51	87.20	REW
5733.41	47241.89	1745.91	88.92	TOPO
5735.38	47241.01	1746.25	91.07	TOPO
5748.71	47235.08	1746.24	105.67	TOPO

Table A-81. Reach R2, cross-section 7 point coordinates and descriptions.

Cross-Section 7				
N (m)	**E (m)**	**Z (m)**	**X (m)**	**Description**
5650.89	47290.86	1745.68	0.00	TOPO
5657.10	47287.03	1745.63	7.29	TOPO
5659.61	47285.48	1745.47	10.24	TOPO
5660.01	47285.23	1745.24	10.71	XS8 HW
5660.01	47285.23	1744.92	10.71	LEW
5660.72	47284.80	1744.54	11.54	OS
5660.97	47284.64	1744.43	11.84	OS
5662.58	47283.65	1744.17	13.73	OS
5664.17	47282.67	1744.28	15.60	OS
5665.46	47281.87	1744.42	17.12	OS
5668.30	47280.11	1744.56	20.46	OS
5671.32	47278.26	1744.58	24.00	OS
5675.14	47275.90	1744.52	28.49	OS
5676.76	47274.89	1744.65	30.40	OS
5678.63	47273.74	1744.87	32.59	EW
5683.99	47270.43	1745.14	38.90	TOPO
5690.69	47266.30	1745.46	46.77	TOPO
5694.64	47263.86	1745.78	51.40	TOPO
5706.01	47256.84	1745.88	64.77	TOPO
5716.53	47250.35	1745.91	77.13	TOPO
5721.87	47247.06	1746.03	83.41	TOPO
5725.24	47244.98	1746.14	87.36	TOPO
5725.82	47244.62	1745.87	88.04	TOPO
5727.27	47243.72	1745.49	89.75	EW
5727.55	47243.55	1745.21	90.08	OS
5728.38	47243.04	1745.28	91.05	OS
5728.95	47242.69	1745.20	91.72	OS
5729.62	47242.28	1745.32	92.51	OS
5730.85	47241.52	1745.35	93.95	OS
5731.42	47241.16	1745.50	94.63	REW
5731.83	47240.91	1745.66	95.11	TOPO
5732.49	47240.50	1745.94	95.88	TOPO
5734.85	47239.05	1746.21	98.65	TOPO
5738.78	47236.62	1746.26	103.27	TOPO
5744.76	47232.93	1746.29	110.30	TOPO

Table A-82. Reach R2, cross-section 8 point coordinates and descriptions.

Cross-Section 8				
N (m)	E (m)	Z (m)	X (m)	Description
5639.80	47247.05	1745.39	0.00	TOPO
5642.91	47246.55	1745.41	3.15	TOPO
5639.64	47247.07	1744.51	6.46	LEW
5638.12	47247.32	1744.20	8.01	OS
5640.85	47246.88	1743.81	10.78	OS
5645.36	47246.15	1743.67	15.35	OS
5647.79	47245.76	1743.77	17.81	OS
5651.01	47245.24	1743.95	21.07	OS
5650.76	47245.28	1744.25	21.33	OS
5650.52	47245.32	1744.25	21.57	OS
5649.91	47245.42	1744.24	22.19	OS
5650.25	47245.36	1744.33	22.54	OS
5650.63	47245.30	1744.50	22.93	EW
5651.55	47245.16	1744.96	23.85	TOPO
5653.59	47244.83	1745.32	25.92	TOPO
5660.36	47243.73	1745.71	32.79	TOPO
5682.19	47240.21	1745.76	54.90	TOPO
5676.14	47241.19	1745.94	61.03	TOPO
5684.28	47239.88	1746.04	69.28	TOPO
5691.12	47238.77	1745.73	76.21	TOPO
5696.87	47237.85	1745.50	82.04	TOPO
5698.66	47237.56	1745.35	83.85	EW
5703.25	47236.82	1745.15	88.49	OS
5706.42	47236.31	1745.08	91.71	OS
5708.31	47236.00	1745.19	93.62	OS
5709.56	47235.80	1745.33	94.89	REW
5711.44	47235.50	1745.73	96.79	TOPO
5716.72	47234.65	1746.15	102.14	TOPO
5725.20	47233.28	1746.21	110.72	TOPO
5742.79	47230.44	1746.27	128.55	TOPO

Table A-83. Reach R2, cross-section 9 point coordinates and descriptions.

Cross-Section 9				
N (m)	E (m)	Z (m)	X (m)	Description
5643.69	47193.46	1745.44	0.00	TOPO
5643.83	47193.50	1744.90	0.15	TOPO
5650.66	47195.80	1745.01	7.36	TOPO
5651.09	47195.94	1744.78	7.80	TOPO
5652.05	47196.26	1744.55	8.81	LEW
5654.55	47197.11	1743.59	11.46	OS
5656.02	47197.60	1743.57	13.01	OS
5661.29	47199.37	1743.64	18.57	OS
5666.36	47201.07	1744.10	23.91	OS
5668.27	47201.72	1744.29	25.93	OS
5672.01	47202.98	1744.71	29.88	OS
5673.10	47203.34	1744.40	31.02	OS
5674.11	47203.68	1744.40	32.09	OS
5675.10	47204.01	1744.52	33.14	EW
5681.22	47206.07	1745.42	39.59	TOPO
5701.68	47206.00	1745.54	60.06	TOPO
5717.91	47205.65	1745.54	76.28	TOPO
5720.51	47204.95	1745.04	78.97	TOPO
5720.32	47204.98	1744.78	79.16	EW
5720.95	47204.88	1744.51	79.81	OS
5724.18	47204.35	1744.45	83.07	OS
5726.29	47204.01	1744.36	85.22	OS
5728.75	47203.60	1744.59	87.71	OS
5727.33	47203.84	1744.77	89.15	REW
5727.44	47203.82	1745.00	89.27	TOPO
5730.92	47203.25	1745.43	92.79	TOPO
5730.32	47203.35	1745.64	93.40	TOPO

Table A-84. Reach R2, cross-section 10 point coordinates and descriptions.

Cross-Section 10				
N (m)	**E (m)**	**Z (m)**	**X (m)**	**Description**
5686.51	47141.90	1745.17	0.00	TOPO
5688.58	47143.40	1744.34	2.56	LEW
5689.12	47144.16	1743.85	3.49	OS
5692.22	47145.94	1743.80	7.07	OS
5694.70	47147.16	1743.83	9.83	OS
5696.48	47147.80	1743.70	11.72	OS
5696.97	47148.15	1743.87	12.32	OS
5699.75	47150.08	1743.89	15.71	OS
5701.68	47151.15	1743.75	17.92	OS
5702.63	47151.50	1743.62	18.93	OS
5704.06	47152.64	1743.91	20.76	OS
5705.66	47153.87	1744.01	22.78	OS
5706.56	47154.43	1744.37	23.83	EW
5706.61	47154.56	1744.50	23.97	TOPO
5709.85	47157.26	1745.35	28.19	TOPO
5724.35	47163.79	1745.48	44.10	TOPO
5730.88	47167.12	1745.51	51.43	TOPO
5731.08	47167.15	1744.76	51.63	EW
5731.21	47167.30	1744.51	51.83	OS
5736.96	47170.18	1744.52	58.26	OS
5739.36	47171.85	1744.65	61.18	OS
5741.71	47173.79	1744.35	64.22	OS
5741.59	47173.76	1744.41	64.34	REW
5743.59	47175.23	1745.10	66.82	TOPO
5745.74	47176.75	1745.54	69.46	TOPO

Table A-85. Reach R2, cross-section 11 point coordinates and descriptions.

Cross-Section 11				
N (m)	**E (m)**	**Z (m)**	**X (m)**	**Description**
5698.01	47116.71	1745.04	0.00	TOPO
5697.66	47116.59	1744.91	0.37	TOPO
5700.47	47117.57	1744.13	3.35	LEW
5703.58	47118.65	1743.80	6.64	OS
5706.81	47119.78	1743.66	10.06	OS
5707.74	47120.10	1743.67	11.05	OS
5709.17	47120.60	1743.65	12.56	OS
5713.02	47121.94	1743.72	16.64	OS
5716.06	47123.00	1743.67	19.85	OS
5720.38	47124.51	1743.60	24.43	OS
5720.68	47124.62	1743.39	24.75	OS
5722.41	47125.22	1743.21	26.58	OS
5726.37	47126.60	1743.37	30.77	OS
5729.00	47127.52	1743.80	33.57	OS
5729.00	47127.52	1744.05	33.57	EW
5729.01	47127.52	1744.05	33.58	TOPO
5733.34	47129.03	1744.87	38.17	TOPO
5737.42	47130.45	1745.31	42.49	TOPO
5740.87	47131.65	1745.40	46.14	TOPO
5739.93	47131.33	1745.04	47.14	TOPO
5743.61	47132.61	1744.43	51.04	TOPO
5743.45	47132.55	1744.15	51.20	EW
5758.75	47137.89	1743.71	67.40	OS
5760.32	47138.44	1744.09	69.06	OS
5760.37	47138.45	1744.11	69.11	EW
5761.34	47138.79	1744.74	70.14	TOPO
5763.46	47139.53	1745.53	72.38	TOPO
5764.07	47139.74	1745.66	73.03	TOPO
5763.57	47139.57	1745.69	73.55	TOPO

Table A-86. Reach R2, cross-section 12 point coordinates and descriptions.

Cross-Section 12				
N (m)	**E (m)**	**Z (m)**	**X (m)**	**Description**
5684.47	47081.74	1744.92	0.00	TOPO
5691.65	47083.61	1744.77	7.42	HW
5705.73	47087.28	1744.76	21.97	TOPO
5708.01	47087.88	1744.03	24.33	TOPO
5711.50	47088.79	1743.65	27.94	TOPO
5711.97	47088.91	1743.91	28.42	TOPO
5712.97	47089.17	1744.38	29.45	TOPO
5714.79	47089.64	1744.69	31.33	TOPO
5716.40	47090.06	1744.41	33.00	TOPO
5718.95	47090.72	1743.76	35.63	TOPO
5719.21	47090.79	1743.37	35.90	LEW
5719.23	47090.80	1743.20	35.92	OS
5720.61	47091.16	1743.21	37.35	OS
5724.16	47092.08	1743.32	41.02	OS
5731.79	47094.07	1742.91	48.90	OS
5734.92	47094.89	1742.68	52.14	OS
5737.74	47095.62	1742.76	55.05	OS
5739.81	47096.16	1742.68	57.20	OS
5742.70	47096.91	1742.96	60.17	OS
5749.46	47098.68	1743.14	67.17	OS
5748.34	47098.39	1743.23	68.32	OS
5747.96	47098.29	1743.48	68.72	REW
5747.82	47098.25	1743.61	68.86	TOPO
5736.46	47095.29	1744.09	80.60	TOPO
5736.23	47095.23	1744.61	80.84	TOPO
5721.25	47091.33	1745.29	96.32	TOPO

Table A-87. Reach R2, cross-section 13 point coordinates and descriptions.

Cross-Section 13				
N (m)	**E (m)**	**Z (m)**	**X (m)**	**Description**
5724.13	47052.24	1744.58	0.00	TOPO
5724.73	47052.39	1744.09	0.62	TOPO
5726.16	47052.76	1743.36	2.10	LEW
5727.43	47053.09	1743.22	3.41	OS
5727.39	47053.08	1743.30	3.46	OS
5727.49	47053.10	1743.17	3.56	OS
5731.23	47054.06	1743.00	7.42	OS
5733.12	47054.55	1742.77	9.38	OS
5735.01	47055.03	1742.96	11.33	OS
5736.85	47055.50	1742.96	13.22	OS
5740.02	47056.31	1742.91	16.50	OS
5743.52	47057.21	1742.91	20.11	OS
5746.86	47058.07	1742.97	23.56	OS
5748.00	47058.36	1743.37	24.73	OS
5748.28	47058.44	1743.44	25.03	REW
5748.58	47058.51	1743.66	25.34	TOPO
5751.79	47059.33	1744.20	28.65	TOPO

Table A-88. Reach R2, cross-section 14 point coordinates and descriptions.

Cross-Section 14				
N (m)	E (m)	Z (m)	X (m)	Description
5728.36	47033.03	1744.13	0.00	TOPO
5728.38	47033.03	1743.64	0.01	HW
5728.27	47033.02	1742.99	0.12	LEW
5728.22	47033.01	1742.76	0.18	OS
5729.80	47033.20	1742.56	1.77	OS
5732.22	47033.49	1742.65	4.21	OS
5734.90	47033.80	1742.46	6.91	OS
5739.63	47034.36	1742.44	11.67	OS
5740.60	47034.48	1742.69	12.64	OS
5740.36	47034.45	1742.69	12.88	OS
5741.84	47034.62	1742.85	14.38	OS
5739.32	47034.32	1742.91	16.92	OS
5743.73	47034.85	1742.91	21.37	OS
5743.46	47034.81	1742.69	21.64	OS
5747.71	47035.32	1742.48	25.91	OS
5751.13	47035.72	1742.55	29.36	OS
5753.27	47035.97	1742.55	31.52	OS
5755.24	47036.20	1742.26	33.50	OS
5755.09	47036.19	1742.15	33.65	OS
5753.51	47036.00	1742.12	35.24	OS
5751.53	47035.77	1742.44	37.23	OS
5751.30	47035.74	1742.65	37.47	OS
5750.85	47035.69	1742.71	37.93	REW
5747.40	47035.28	1743.45	41.39	TOPO

Table A-89. Reach R2, cross-section 15 point coordinates and descriptions.

Cross-Section 15				
N (m)	E (m)	Z (m)	X (m)	Description
5727.12	47006.91	1743.27	0.00	HW
5718.12	47010.86	1744.11	9.83	TOPO
5719.85	47010.10	1742.75	11.72	TOPO
5720.79	47009.69	1742.69	12.74	TOPO
5722.54	47008.92	1742.34	14.65	LEW
5724.81	47007.93	1741.90	17.13	OS
5726.40	47007.23	1741.61	18.87	OS
5735.64	47003.18	1741.26	28.96	OS
5736.60	47002.76	1741.65	30.00	OS
5737.68	47002.29	1742.33	31.18	REW
5739.08	47001.67	1742.69	32.71	TOPO
5739.94	47001.30	1743.23	33.64	TOPO
5742.10	47000.35	1743.90	36.01	TOPO
5739.97	47001.28	1743.59	38.34	TOPO

Table A-90. Reach R2, cross-section 16 point coordinates and descriptions.

Cross-Section 16				
N (m)	E (m)	Z (m)	X (m)	Description
5701.66	46986.47	1743.40	0.00	TOPO
5703.17	46984.59	1743.09	2.41	HW
5707.03	46981.10	1742.66	7.61	TOPO
5708.68	46980.44	1742.32	9.39	LEW
5710.49	46978.10	1742.06	12.35	OS
5714.93	46974.16	1741.67	18.28	OS
5715.99	46972.77	1741.25	20.03	OS
5717.98	46970.41	1740.87	23.12	OS
5718.53	46969.62	1741.11	24.09	OS
5719.91	46968.95	1741.65	25.62	OS
5720.40	46968.61	1742.34	26.21	REW
5720.43	46968.53	1742.51	26.30	TOPO
5722.17	46967.00	1743.57	28.61	TOPO
5723.37	46965.86	1743.74	30.27	TOPO

Table A-91. Reach R2, cross-section 17 point coordinates and descriptions.

Cross-Section 17				
N (m)	E (m)	Z (m)	X (m)	Description
5683.44	46987.75	1742.32	0.00	TOPO
5683.26	46985.19	1743.18	2.56	RRLEP1
5683.91	46994.56	1743.08	11.95	TOPO
5684.16	46998.07	1742.41	15.47	LEW
5684.30	47000.10	1742.41	17.50	OS
5684.17	46998.20	1742.25	19.41	OS
5683.95	46995.07	1742.11	22.54	OS
5683.15	46983.71	1741.78	33.93	OS
5681.97	46966.86	1741.48	50.82	OS
5680.75	46949.42	1741.20	68.31	OS
5680.41	46944.46	1741.24	73.27	OS
5680.43	46944.80	1741.54	73.62	OS
5680.51	46945.93	1742.31	74.75	REW
5680.47	46945.40	1742.85	75.28	TOPO
5680.41	46944.55	1743.04	76.13	TOPO
5680.50	46945.85	1743.07	77.44	RRREP1

Table A-92. Reach R2, cross-section 18 point coordinates and descriptions.

Cross-Section 18				
N (m)	**E (m)**	**Z (m)**	**X (m)**	**Description**
5641.00	47007.91	1743.31	0.00	RRLEP2
5638.00	47002.65	1743.22	6.05	TOPO
5637.91	47002.48	1743.01	6.25	TOPO
5637.80	47002.30	1742.95	6.46	HW
5636.44	46999.91	1742.37	9.21	TOPO
5635.55	46998.36	1742.29	11.00	LEW
5634.51	46996.53	1741.78	13.11	OS
5634.17	46995.94	1741.49	13.78	OS
5633.40	46994.58	1741.72	15.34	OS
5630.94	46990.29	1741.82	20.29	OS
5628.38	46985.79	1741.80	25.47	OS
5627.45	46984.16	1741.65	27.34	OS
5626.29	46982.13	1741.75	29.69	OS
5624.08	46978.26	1741.68	34.14	OS
5622.46	46975.43	1742.31	37.40	EW
5620.99	46972.85	1742.66	40.37	TOPO
5620.07	46971.24	1742.14	42.22	EW
5619.96	46971.05	1741.89	42.44	OS
5619.49	46970.22	1741.93	43.40	OS
5618.09	46967.77	1741.91	46.22	OS
5617.56	46966.84	1742.20	47.29	REW
5617.73	46967.15	1742.40	47.64	TOPO
5617.83	46967.32	1742.52	47.84	TOPO
5613.11	46959.04	1742.57	57.37	RRREP2

Table A-93. Reach R2, cross-section 19 point coordinates and descriptions.

Cross-Section 19				
N (m)	**E (m)**	**Z (m)**	**X (m)**	**Description**
5619.00	47034.93	1743.65	0.00	RRLEP-3
5617.22	47031.17	1743.50	4.16	TOPO
5613.90	47024.15	1742.85	11.92	HW
5616.16	47028.93	1742.73	17.21	TOPO
5615.74	47028.04	1742.55	18.20	TOPO
5615.62	47027.79	1742.21	18.47	LEW
5615.51	47027.56	1741.96	18.72	OS
5615.05	47026.58	1741.66	19.81	OS
5614.37	47025.16	1741.57	21.38	OS
5613.33	47022.96	1741.63	23.82	OS
5611.88	47019.89	1741.73	27.21	OS
5608.58	47012.90	1741.76	34.94	OS
5607.18	47009.95	1741.77	38.20	OS
5606.69	47008.91	1742.00	39.36	OS
5605.53	47006.46	1742.02	42.07	OS
5605.07	47005.47	1742.22	43.16	EW
5603.82	47002.84	1742.52	46.07	TOPO
5601.77	46998.50	1742.70	50.87	TOPO
5601.44	46997.81	1742.90	51.63	TOPO
5598.13	46990.80	1742.83	59.39	TOPO
5594.52	46983.16	1742.08	67.84	TOPO
5594.36	46982.84	1742.03	68.19	TOPO
5593.81	46981.68	1741.96	69.48	TOPO
5593.28	46980.55	1741.95	70.73	TOPO
5592.03	46977.90	1741.87	73.66	TOPO
5591.48	46976.74	1741.65	74.94	EW
5590.29	46974.23	1741.19	77.71	OS
5589.57	46972.70	1740.99	79.41	OS
5589.03	46971.55	1741.18	80.68	OS
5588.64	46970.74	1741.62	81.58	REW
5588.56	46970.56	1741.97	81.78	TOPO
5588.46	46970.36	1742.47	82.00	TOPO
5587.08	46967.43	1742.42	85.24	RRREP3

Table A-94. Reach R2, cross-section 20 point coordinates and descriptions.

Cross-Section 20				
N (m)	**E (m)**	**Z (m)**	**X (m)**	**Description**
5574.30	47050.14	1743.17	0.00	RRLEP4
5575.98	47041.72	1743.12	8.58	TOPO
5576.27	47040.28	1741.78	10.05	LEW
5576.30	47040.14	1741.39	10.19	OS
5576.51	47039.08	1741.39	11.27	OS
5576.57	47038.80	1741.16	11.57	OS
5577.16	47035.85	1741.05	14.58	OS
5577.41	47034.62	1741.19	15.82	OS
5577.80	47032.68	1741.38	17.81	OS
5578.10	47031.19	1741.62	19.32	OS
5578.62	47028.60	1741.77	21.97	OS
5578.87	47027.32	1741.64	23.27	OS
5578.87	47024.14	1741.96	26.45	OS
5578.73	47023.31	1742.03	27.29	OS
5578.46	47021.67	1742.39	28.95	OS
5578.82	47023.85	1742.79	31.16	OS
5577.71	47017.18	1742.71	37.92	OS
5577.03	47013.11	1742.15	42.04	OS
5576.68	47011.06	1741.77	44.12	OS
5575.93	47006.57	1741.61	48.68	OS
5575.33	47002.99	1741.39	52.30	OS
5574.56	46998.41	1741.40	56.95	OS
5573.61	46992.72	1741.27	62.72	OS
5571.88	46982.35	1741.18	73.23	OS
5571.79	46981.82	1741.62	73.77	REW
5572.36	46985.27	1742.33	77.26	RRREP4

Table A-95. Reach R2, cross-section 21 point coordinates and descriptions.

Cross-Section 21				
N (m)	**E (m)**	**Z (m)**	**X (m)**	**Description**
5539.60	47035.27	1742.59	0.00	RRLEP5
5542.63	47027.17	1742.60	8.65	TOPO
5543.19	47025.66	1742.26	10.25	HW
5542.56	47027.36	1741.98	12.07	TOPO
5542.77	47026.79	1741.45	12.67	LEW
5543.71	47024.27	1740.91	15.36	OS
5545.25	47020.15	1740.62	19.76	OS
5546.32	47017.27	1740.50	22.83	OS
5547.94	47012.95	1740.95	27.45	OS
5549.09	47009.88	1741.22	30.73	OS
5550.27	47006.71	1741.21	34.11	OS
5550.49	47006.12	1741.46	34.75	EW
5550.85	47005.16	1741.69	35.76	TOPO
5553.45	46998.19	1741.98	43.21	TOPO
5554.25	46996.05	1742.30	45.49	TOPO
5554.08	46996.50	1741.48	45.97	TOPO
5553.98	46996.77	1741.27	46.26	EW
5554.88	46994.36	1740.88	48.83	OS
5555.03	46993.97	1740.69	49.25	OS
5555.34	46993.14	1741.08	50.14	OS
5555.34	46993.13	1741.28	50.14	REW
5555.62	46992.40	1741.52	50.93	TOPO
5556.24	46990.72	1742.40	52.72	TOPO
5559.40	46982.26	1742.34	61.75	TOPO

Table A-96. Reach R2, cross-section 22 point coordinates and descriptions.

Cross-Section 22				
N (m)	E (m)	Z (m)	X (m)	Description
5520.40	46999.33	1742.21	0.00	RRLEP6
5524.00	46996.92	1742.03	4.34	TOPO
5524.79	46996.39	1741.65	5.29	HW
5525.10	46996.18	1741.56	5.66	TOPO
5525.64	46995.82	1741.17	6.31	LEW
5527.22	46994.76	1740.86	8.22	OS
5530.61	46992.49	1740.15	12.29	OS
5531.88	46991.64	1740.04	13.82	OS
5534.18	46990.10	1740.38	16.59	OS
5536.00	46988.88	1740.73	18.78	OS
5539.48	46986.55	1741.22	22.97	REW
5540.45	46985.90	1741.35	24.14	TOPO
5541.45	46985.23	1741.62	25.34	TOPO
5546.84	46981.62	1741.74	31.83	TOPO
5547.32	46981.30	1742.23	32.41	TOPO
5549.35	46979.93	1742.24	34.86	RRREP6

Table A-97. Reach R2, cross-section 23 point coordinates and descriptions.

Cross-Section 23				
N (m)	E (m)	Z (m)	X (m)	Description
5471.73	46970.27	1741.36	0.00	TOPO
5480.60	46966.94	1741.00	9.48	LEW
5485.93	46964.94	1740.65	15.17	OS
5487.37	46964.40	1740.45	16.71	OS
5489.80	46963.48	1740.29	19.31	OS
5492.67	46962.41	1740.51	22.37	OS
5493.28	46962.17	1740.65	23.03	EW
5496.26	46961.06	1739.03	26.20	TOPO
5500.01	46959.65	1739.09	30.21	TOPO
5500.19	46959.58	1741.09	30.40	REW
5502.27	46958.80	1740.82	32.63	TOPO
5502.83	46958.59	1740.49	33.23	TOPO
5505.94	46957.42	1740.52	36.55	TOPO
5511.39	46955.37	1740.78	42.37	TOPO
5514.46	46954.22	1740.82	45.65	TOPO
5518.97	46952.52	1740.58	50.47	TOPO
5525.45	46950.09	1740.87	57.39	TOPO
5531.29	46947.90	1740.57	63.63	TOPO
5532.99	46947.25	1741.10	65.45	TOPO
5534.46	46946.70	1740.63	67.01	TOPO
5539.76	46944.71	1741.61	72.67	TOPO

STUDY REACH R3

Table A-98. Reach R3, cross-section 1 point coordinates and descriptions.

Cross-Section 1				
N (m)	**E (m)**	**Z (m)**	**X (m)**	**Description**
4245.45	3963.36	4002.52	0.00	TOPO
4246.17	3961.49	4002.29	2.00	TOPO
4246.72	3960.07	4001.36	3.53	TOPO
4246.71	3960.08	4001.25	3.55	LEW
4247.07	3959.15	4000.99	4.55	OS
4247.12	3959.02	4000.90	4.69	OS
4247.26	3958.65	4000.89	5.08	OS
4247.37	3958.39	4000.91	5.36	OS
4248.03	3956.66	4000.85	7.21	OS
4249.56	3952.71	4000.73	11.45	OS
4249.77	3952.18	4000.60	12.02	OS
4250.07	3951.39	4000.60	12.87	OS
4250.48	3950.33	4000.70	14.01	OS
4250.73	3949.68	4000.67	14.70	OS
4250.91	3949.22	4000.84	15.20	OS
4251.72	3947.11	4000.95	17.45	OS
4252.57	3944.94	4000.86	19.79	OS
4253.62	3942.21	4000.80	22.71	OS
4253.76	3941.85	4000.94	23.10	OS
4253.99	3941.26	4001.09	23.73	OS
4253.99	3941.25	4001.21	23.74	REW
4254.09	3940.98	4001.37	24.03	TOPO
4254.37	3940.26	4001.54	24.80	TOPO
4254.65	3939.54	4001.77	25.58	TOPO
4255.11	3938.34	4001.95	26.86	TOPO
4255.70	3936.83	4002.00	28.48	TOPO

Table A-99. Reach R3, cross-section 2 point coordinates and descriptions.

Cross-Section 2				
N (m)	**E (m)**	**Z (m)**	**X (m)**	**Description**
4210.38	3945.47	4002.21	0.00	TOPO
4210.22	3945.92	4001.94	0.47	TOPO
4210.27	3945.78	4001.72	0.62	TOPO
4210.27	3945.79	4001.59	0.62	TOPO
4210.29	3945.73	4001.49	0.69	TOPO
4210.61	3944.80	4001.21	1.67	TOPO
4210.96	3943.80	4001.07	2.73	TOPO
4211.34	3942.70	4001.05	3.89	TOPO
4212.17	3940.33	4000.96	6.40	LEW
4212.91	3938.20	4000.79	8.65	OS
4213.85	3935.48	4000.69	11.54	OS
4213.93	3935.25	4000.66	11.77	OS
4214.55	3933.47	4000.56	13.66	OS
4214.86	3932.57	4000.32	14.61	OS
4215.41	3931.01	4000.21	16.26	OS
4216.04	3929.18	4000.16	18.20	OS
4217.73	3924.32	4000.39	23.35	OS
4217.84	3924.02	4000.55	23.67	OS
4217.93	3923.74	4000.75	23.96	REW
4217.91	3923.81	4000.85	24.03	TOPO
4218.04	3923.42	4000.99	24.43	TOPO
4218.24	3922.84	4001.11	25.04	TOPO
4218.48	3922.18	4001.26	25.75	TOPO
4218.78	3921.31	4001.43	26.66	TOPO
4220.17	3917.29	4001.48	30.92	TOPO
4221.07	3914.70	4001.96	33.66	TOPO

Table A-100. Reach R3, cross-section 3 point coordinates and descriptions.

Cross-Section 3				
N (m)	**E (m)**	**Z (m)**	**X (m)**	**Description**
4195.14	3947.39	4001.86	0.00	TOPO
4195.02	3946.58	4001.62	0.82	TOPO
4194.04	3939.83	4001.24	7.64	TOPO
4194.09	3940.18	4001.14	7.99	TOPO
4193.50	3936.10	4001.00	12.11	TOPO
4192.92	3932.11	4000.97	16.14	TOPO
4192.66	3930.25	4000.65	18.02	LEW
4192.66	3930.28	4000.39	18.04	OS
4192.45	3928.82	3999.95	19.52	OS
4192.33	3927.97	3999.81	20.38	OS
4192.26	3927.48	3999.58	20.87	OS
4191.90	3925.01	3999.45	23.37	OS
4191.04	3919.10	3999.35	29.34	OS
4191.05	3919.17	3999.65	29.41	OS
4191.04	3919.05	3999.80	29.53	OS
4190.63	3916.25	4000.50	32.35	OS
4190.61	3916.10	4000.66	32.51	REW
4190.53	3915.59	4000.82	33.03	TOPO
4190.66	3916.47	4001.36	33.92	TOPO
4190.72	3916.89	4001.56	34.34	TOPO
4190.71	3916.82	4001.73	34.40	TOPO
4190.75	3917.10	4001.95	34.69	TOPO
4190.95	3918.48	4002.18	36.08	TOPO

Table A-101. Reach R3, cross-section 4 point coordinates and descriptions.

Cross-Section 4				
N (m)	**E (m)**	**Z (m)**	**X (m)**	**Description**
4179.14	3954.90	4001.59	0.00	XS4-LEP
4177.37	3949.38	4001.46	5.80	TOPO
4176.05	3945.26	4001.31	10.13	TOPO
4175.29	3942.89	4001.05	12.61	TOPO
4173.72	3938.01	4000.78	17.74	TOPO
4172.09	3932.93	4000.61	23.08	LEW
4171.03	3929.61	4000.34	26.57	OS
4170.38	3927.58	4000.22	28.69	OS
4169.88	3926.03	3999.89	30.33	OS
4169.75	3925.62	3999.76	30.75	OS
4169.35	3924.38	3999.67	32.05	OS
4168.97	3923.20	3999.70	33.30	OS
4168.05	3920.33	4000.02	36.31	OS
4167.93	3919.95	4000.61	36.70	REW
4167.92	3919.92	4000.74	36.74	TOPO
4167.68	3919.17	4001.22	37.52	HW
4167.67	3919.12	4001.81	37.57	TOPO
4167.52	3918.65	4001.98	38.07	TOPO
4166.65	3915.95	4001.88	40.91	TOPO
4164.83	3910.26	4002.04	46.89	XS4-REP

Table A-102. Reach R3, cross-section 5 point coordinates and descriptions.

Cross-Section 5				
N (m)	**E (m)**	**Z (m)**	**X (m)**	**Description**
4167.07	3954.01	4001.41	0.00	TOPO
4165.52	3951.25	4001.16	3.17	TOPO
4164.41	3949.28	4000.89	5.42	TOPO
4162.54	3945.94	4000.59	9.26	LEW
4159.44	3940.42	4000.28	15.59	OS
4158.92	3939.48	4000.13	16.65	OS
4157.98	3937.80	3999.82	18.58	OS
4156.71	3935.54	3999.50	21.18	OS
4155.99	3934.26	3999.45	22.64	OS
4155.04	3932.57	3999.73	24.59	OS
4153.92	3930.56	4000.07	26.89	OS
4153.15	3929.20	4000.05	28.45	OS
4153.15	3929.19	4000.59	28.45	REW
4152.88	3928.71	4001.21	29.01	TOPO
4152.51	3928.05	4001.40	29.77	TOPO
4151.09	3925.51	4001.61	32.68	TOPO
4148.03	3920.06	4001.66	38.93	TOPO

Table A-103. Reach R3, cross-section 6 point coordinates and descriptions.

Cross-Section 6				
N (m)	**E (m)**	**Z (m)**	**X (m)**	**Description**
4155.79	3975.88	4001.58	0.00	TOPO
4153.32	3974.59	4001.48	2.79	TOPO
4152.54	3974.19	4000.82	3.66	TOPO
4152.28	3974.05	4000.74	3.95	TOPO
4151.87	3973.84	4000.61	4.42	TOPO
4151.13	3973.45	4000.61	5.25	TOPO
4149.85	3972.78	4000.47	6.69	LEW
4146.80	3971.18	4000.46	10.14	OS
4146.15	3970.84	4000.29	10.87	OS
4143.67	3969.54	4000.32	13.68	OS
4142.39	3968.87	4000.38	15.12	OS
4140.74	3968.00	3999.83	16.99	OS
4139.48	3967.35	3999.65	18.41	OS
4138.32	3966.74	3999.66	19.71	OS
4136.55	3965.81	3999.63	21.71	OS
4134.40	3964.69	3999.89	24.14	OS
4132.79	3963.84	4000.26	25.96	OS
4132.83	3963.86	4000.52	26.01	REW
4132.53	3963.70	4001.33	26.35	TOPO
4131.38	3963.10	4001.42	27.65	TOPO
4130.97	3962.89	4001.49	28.11	TOPO

Table A-104. Reach R3, cross-section 7 point coordinates and descriptions.

Cross-Section 7				
N (m)	**E (m)**	**Z (m)**	**X (m)**	**Description**
4148.20	3997.97	4001.67	0.00	TOPO
4147.44	3997.59	4001.65	0.85	TOPO
4147.11	3997.43	4001.58	1.22	TOPO
4147.09	3997.42	4001.34	1.24	TOPO
4146.16	3996.96	4001.05	2.27	TOPO
4144.50	3996.13	4000.74	4.13	TOPO
4143.14	3995.46	4000.43	5.65	LEW
4141.93	3994.86	4000.41	6.99	OS
4141.44	3994.62	4000.21	7.55	OS
4137.95	3992.89	4000.09	11.44	OS
4136.41	3992.13	4000.20	13.16	OS
4132.96	3990.42	4000.17	17.01	OS
4130.26	3989.08	4000.72	20.02	OS
4130.14	3989.02	4000.47	20.16	OS
4128.60	3988.26	4000.36	21.87	OS
4129.05	3988.48	3999.68	22.37	OS
4126.36	3987.15	3999.84	25.37	OS
4125.42	3986.69	3999.95	26.42	OS
4126.10	3987.02	4000.41	27.17	REW
4125.96	3986.95	4000.73	27.32	TOPO
4125.62	3986.78	4001.01	27.70	TOPO
4125.15	3986.55	4001.34	28.22	TOPO
4123.31	3985.64	4001.41	30.28	TOPO

Table A-105. Reach R3, cross-section 8 point coordinates and descriptions.

Cross-Section 8				
N (m)	**E (m)**	**Z (m)**	**X (m)**	**Description**
4122.56	4035.43	4001.28	0.00	TOPO
4119.77	4031.85	4001.29	4.54	TOPO
4117.14	4028.48	4000.06	8.81	LEW
4116.28	4027.37	3999.40	10.22	OS
4115.16	4025.94	3999.16	12.03	OS
4114.54	4025.14	3999.17	13.05	OS
4113.70	4024.06	3999.40	14.42	OS
4112.52	4022.55	3999.70	16.33	OS
4111.50	4021.24	3999.97	17.99	OS
4110.20	4019.58	4000.07	20.09	REW
4109.42	4018.58	4000.26	21.36	TOPO
4105.32	4013.32	4000.41	28.03	TOPO
4100.68	4007.36	4000.60	35.58	TOPO
4100.51	4007.15	4000.68	35.86	TOPO
4099.88	4006.33	4000.73	36.89	TOPO
4098.02	4003.95	4000.83	39.91	TOPO
4097.99	4003.92	4000.95	39.96	TOPO

Table A-106. Reach R3, cross-section 9 point coordinates and descriptions.

Cross-Section 9				
N (m)	**E (m)**	**Z (m)**	**X (m)**	**Description**
4081.79	4059.34	4000.86	0.00	LXS9-LEP
4084.90	4046.39	4000.74	13.32	TOPO
4084.99	4045.99	4000.07	13.73	LEW
4084.98	4046.03	3999.46	13.78	OS
4085.18	4045.20	3999.24	14.63	OS
4085.68	4043.14	3999.30	16.75	OS
4085.84	4042.46	3999.12	17.45	OS
4086.18	4041.04	3998.95	18.90	OS
4086.23	4040.84	3998.66	19.11	OS
4086.77	4038.57	3999.75	21.45	OS
4086.88	4038.12	4000.04	21.91	REW
4087.05	4037.43	4000.26	22.62	TOPO
4089.48	4027.29	4000.67	33.05	TOPO
4089.03	4029.16	4000.62	34.97	TOPO
4090.80	4021.76	4000.36	42.58	TOPO
4092.10	4016.37	4000.43	48.12	TOPO
4092.44	4014.92	4000.52	49.61	TOPO
4093.56	4010.27	4000.71	54.40	TOPO
4094.19	4007.64	4000.71	57.10	TOPO
4094.66	4005.70	4000.62	59.10	TOPO
4094.82	4005.01	4000.70	59.80	TOPO
4095.35	4002.79	4000.71	62.09	TOPO
4095.61	4001.70	4000.79	63.20	TOPO
4095.69	4001.36	4000.88	63.55	HW
4095.76	4001.10	4000.90	63.83	TOPO
4096.17	3999.38	4001.13	65.59	TOPO
4096.19	3999.30	4001.19	65.68	TOPO
4096.40	3998.42	4001.20	66.58	XS9-REP

Table A-107. Reach R3, cross-section 10 point coordinates and descriptions.

Cross-Section 10				
N (m)	**E (m)**	**Z (m)**	**X (m)**	**Description**
4052.27	4038.84	4000.86	0.00	TOPO
4055.70	4035.80	4000.66	4.58	TOPO
4055.73	4035.77	4000.00	4.62	LEW
4055.80	4035.71	3999.73	4.72	OS
4056.29	4035.28	3999.47	5.37	OS
4057.06	4034.59	3999.60	6.40	OS
4058.60	4033.23	3999.76	8.46	OS
4060.56	4031.50	3999.78	11.07	OS
4061.30	4030.84	3999.73	12.06	OS
4062.43	4029.85	3999.55	13.57	OS
4063.42	4028.96	3999.20	14.90	OS
4064.92	4027.64	3999.41	16.89	OS
4066.26	4026.46	3999.59	18.68	OS
4067.30	4025.54	3999.80	20.07	OS
4067.52	4025.34	3999.76	20.37	OS
4068.56	4024.42	3999.12	21.75	OS
4069.34	4023.73	3999.08	22.80	OS
4070.33	4022.85	3999.79	24.12	REW
4070.36	4022.83	3999.90	24.16	TOPO
4070.53	4022.67	3999.98	24.39	TOPO
4071.05	4022.22	4000.01	25.08	TOPO
4074.03	4019.58	4000.20	29.06	TOPO
4078.38	4015.72	4000.30	34.88	TOPO
4082.11	4012.43	4000.50	39.85	TOPO
4084.42	4010.38	4000.66	42.93	TOPO
4088.03	4007.19	4000.59	47.76	TOPO
4089.94	4005.50	4000.51	50.31	TOPO
4092.97	4002.81	4000.72	54.35	TOPO
4093.01	4002.78	4000.81	54.41	TOPO
4094.08	4001.83	4000.92	55.84	TOPO
4096.41	3999.77	4001.20	58.95	XS9-REP

Table A-108. Reach R3, cross-section 11 point coordinates and descriptions.

Cross-Section 11				
N (m)	**E (m)**	**Z (m)**	**X (m)**	**Description**
4039.25	4018.62	4000.99	0.00	TOPO
4040.00	4017.79	4000.92	1.13	TOPO
4040.13	4017.65	3999.88	1.32	TOPO
4040.73	4016.98	3999.74	2.21	LEW
4040.90	4016.80	3999.52	2.46	OS
4042.26	4015.29	3999.37	4.49	OS
4042.98	4014.50	3999.14	5.56	OS
4043.91	4013.47	3999.08	6.95	OS
4044.88	4012.40	3999.11	8.40	OS
4046.01	4011.15	3999.06	10.08	OS
4047.62	4009.37	3999.20	12.48	OS
4048.55	4008.34	3999.39	13.87	OS
4049.77	4006.99	3999.45	15.69	OS
4050.79	4005.86	3999.47	17.21	OS
4051.83	4004.72	3999.58	18.76	OS
4053.31	4003.08	3999.75	20.96	REW
4053.60	4002.76	3999.91	21.40	TOPO
4054.85	4001.38	4000.10	23.26	TOPO
4055.29	4000.89	4000.28	23.92	TOPO
4055.78	4000.35	4000.47	24.65	TOPO
4056.15	3999.95	4000.79	25.19	TOPO
4058.04	3997.85	4000.98	28.01	TOPO

Table A-109. Reach R3, cross-section 12 point coordinates and descriptions.

Cross-Section 12				
N (m)	**E (m)**	**Z (m)**	**X (m)**	**Description**
4019.33	4010.20	4000.63	0.00	TOPO
4021.15	4008.64	4000.40	2.40	TOPO
4021.44	4008.39	4000.27	2.78	TOPO
4022.03	4007.88	4000.15	3.56	TOPO
4022.33	4007.61	3999.95	3.97	TOPO
4023.17	4006.89	3999.79	5.07	TOPO
4024.37	4005.86	3999.71	6.65	LEW
4026.82	4003.74	3999.53	9.89	OS
4029.39	4001.52	3999.29	13.29	OS
4032.49	3998.84	3999.32	17.39	OS
4034.12	3997.44	3999.15	19.53	OS
4035.88	3995.91	3999.14	21.86	OS
4036.85	3995.08	3999.05	23.14	OS
4037.92	3994.15	3999.07	24.56	OS
4038.78	3993.41	3999.23	25.69	OS
4040.04	3992.32	3999.61	27.36	REW
4040.34	3992.06	3999.79	27.76	TOPO
4041.67	3990.92	4000.10	29.51	TOPO
4043.06	3989.71	4000.51	31.35	TOPO
4043.46	3989.37	4000.80	31.88	TOPO
4045.22	3987.85	4001.06	34.20	TOPO

Table A-110. Reach R3, cross-section 13 point coordinates and descriptions.

Cross-Section 13				
N (m)	**E (m)**	**Z (m)**	**X (m)**	**Description**
4013.47	4007.48	4000.87	0.00	TOPO
4013.22	4008.83	4000.35	1.37	TOPO
4014.41	4002.33	4000.00	7.97	TOPO
4014.28	4003.06	3999.86	8.71	TOPO
4014.72	4000.64	3999.83	11.18	TOPO
4014.89	3999.70	3999.60	12.13	TOPO
4015.25	3997.74	3999.45	14.12	LEW
4015.20	3998.06	3999.16	14.44	OS
4015.61	3995.78	3998.92	16.76	OS
4016.05	3993.40	3998.41	19.18	OS
4016.92	3988.65	3998.27	24.01	OS
4017.14	3987.50	3998.62	25.18	OS
4017.54	3985.32	3999.10	27.39	OS
4018.01	3982.75	3999.45	30.01	REW
4018.23	3981.52	3999.70	31.26	TOPO
4018.22	3981.61	4000.13	31.34	TOPO
4018.29	3981.22	4000.27	31.74	TOPO
4018.63	3979.34	4000.52	33.65	TOPO
4018.91	3977.84	4000.71	35.17	TOPO
4019.61	3974.05	4000.85	39.03	TOPO

Table A-111. Reach R3, cross-section 14 point coordinates and descriptions.

Cross-Section 14				
N (m)	**E (m)**	**Z (m)**	**X (m)**	**Description**
4002.97	4016.05	4000.74	0.00	XS14-LEP
4001.79	4013.25	4000.32	3.04	TOPO
4001.07	4011.53	4000.15	4.90	TOPO
3999.80	4008.53	4000.10	8.17	TOPO
3999.15	4006.98	3999.86	9.84	TOPO
3997.22	4002.42	3999.95	14.80	TOPO
3996.38	4000.42	3999.96	16.96	TOPO
3995.86	3999.19	3999.43	18.30	LEW
3995.48	3998.27	3998.88	19.29	OS
3994.64	3996.28	3998.74	21.45	OS
3994.13	3995.09	3998.45	22.75	OS
3994.04	3994.87	3998.59	22.99	OS
3993.43	3993.41	3998.73	24.57	OS
3991.08	3987.85	3998.84	30.61	OS
3989.96	3985.20	3999.35	33.48	OS
3989.20	3983.39	3999.43	35.45	REW
3988.68	3982.16	3999.66	36.78	TOPO
3988.59	3981.94	4000.52	37.02	TOPO
3988.58	3981.92	4000.52	37.04	HW
3988.01	3980.57	4000.68	38.50	TOPO
3987.14	3978.51	4000.86	40.74	XS14-REP

Table A-112. Reach R3, cross-section 15 point coordinates and descriptions.

Cross-Section 15				
N (m)	**E (m)**	**Z (m)**	**X (m)**	**Description**
3983.62	4017.81	4000.67	0.00	TOPO
3983.33	4017.40	4000.62	0.50	TOPO
3983.25	4017.29	4000.52	0.64	TOPO
3983.02	4016.96	4000.47	1.04	TOPO
3982.97	4016.88	3999.74	1.13	TOPO
3982.66	4016.44	3999.59	1.67	TOPO
3981.63	4014.98	3999.61	3.46	TOPO
3981.47	4014.75	3999.37	3.74	TOPO
3981.19	4014.35	3999.26	4.22	LEW
3980.74	4013.71	3999.21	5.00	OS
3980.54	4013.43	3999.07	5.35	OS
3979.12	4011.39	3999.06	7.84	OS
3978.27	4010.19	3999.12	9.31	OS
3977.17	4008.61	3998.96	11.23	OS
3976.06	4007.03	3998.52	13.17	OS
3974.99	4005.49	3998.26	15.04	OS
3974.02	4004.12	3998.36	16.72	OS
3973.04	4002.72	3998.59	18.42	OS
3972.64	4002.15	3998.93	19.12	OS
3972.15	4001.44	3998.97	19.99	OS
3971.68	4000.77	3999.25	20.80	EOW
3971.50	4000.51	3999.48	21.13	TOPO
3970.20	3998.66	3999.54	23.38	TOPO
3969.64	3997.85	3999.40	24.37	EOW
3968.69	3996.50	3999.17	26.02	OS
3967.94	3995.43	3999.23	27.32	OS
3967.95	3995.44	3999.42	27.34	REW
3967.70	3995.09	4000.46	27.77	TOPO
3966.53	3993.43	4000.32	29.80	TOPO

Table A-113. Reach R3, cross-section 16 point coordinates and descriptions.

Cross-Section 16				
N (m)	**E (m)**	**Z (m)**	**X (m)**	**Description**
3965.30	4036.34	4000.27	0.00	TOPO
3963.42	4033.88	4000.23	3.10	TOPO
3963.46	4033.94	3999.55	3.18	TOPO
3962.95	4033.27	3999.29	4.01	TOPO
3962.68	4032.91	3999.12	4.47	LEW
3962.15	4032.22	3998.94	5.34	OS
3959.94	4029.34	3998.75	8.97	OS
3959.01	4028.11	3998.82	10.51	OS
3956.97	4025.45	3998.75	13.87	OS
3955.78	4023.89	3998.82	15.82	OS
3955.25	4023.21	3998.93	16.69	OS
3954.53	4022.26	3998.80	17.88	OS
3953.64	4021.10	3998.78	19.34	OS
3951.77	4018.66	3998.69	22.42	OS
3950.37	4016.82	3998.71	24.73	OS
3950.33	4016.78	3999.22	24.78	REW
3950.29	4016.73	3999.58	24.85	TOPO
3949.68	4015.92	3999.78	25.86	TOPO
3948.34	4014.17	3999.74	28.06	TOPO
3948.05	4013.79	3999.90	28.55	HW
3947.20	4012.67	4000.29	29.95	TOPO

Table A-114. Reach R3, cross-section 17 point coordinates and descriptions.

Cross-Section 17				
N (m)	E (m)	Z (m)	X (m)	Description
3946.69	4055.60	4000.35	0.00	TOPO
3944.49	4052.44	4000.36	3.84	TOPO
3944.47	4052.40	4000.29	3.89	TOPO
3943.80	4051.45	4000.18	5.05	TOPO
3943.58	4051.13	3999.88	5.44	TOPO
3941.56	4048.23	3999.39	8.98	TOPO
3941.45	4048.06	3999.16	9.18	TOPO
3941.27	4047.81	3998.96	9.49	TOPO
3940.97	4047.38	3998.94	10.01	LEW
3940.56	4046.79	3998.88	10.73	OS
3940.17	4046.22	3998.42	11.42	OS
3939.66	4045.49	3998.31	12.31	OS
3938.49	4043.81	3998.30	14.36	OS
3938.08	4043.21	3998.24	15.09	OS
3935.91	4040.09	3998.49	18.89	OS
3935.40	4039.36	3998.65	19.77	OS
3934.50	4038.07	3998.77	21.34	OS
3933.30	4036.34	3998.87	23.45	OS
3932.19	4034.75	3998.96	25.39	REW
3931.41	4033.61	3999.13	26.77	TOPO
3930.23	4031.93	3999.15	28.83	TOPO
3930.19	4031.86	3999.21	28.91	TOPO
3930.07	4031.69	3999.23	29.11	TOPO
3930.07	4031.69	3999.33	29.11	TOPO
3929.49	4030.86	3999.44	30.12	TOPO
3929.26	4030.53	3999.64	30.53	TOPO
3928.62	4029.60	3999.89	31.66	HW
3927.99	4028.70	4000.19	32.75	TOPO

Table A-115. Reach R3, cross-section 18 point coordinates and descriptions.

Cross-Section 18				
N (m)	**E (m)**	**Z (m)**	**X (m)**	**Description**
3896.26	4068.43	4000.09	0.00	XS18-LEP
3895.96	4064.03	3999.99	4.41	TOPO
3895.83	4062.08	3999.93	6.37	TOPO
3895.80	4061.57	3999.77	6.87	TOPO
3895.50	4057.01	3999.61	11.45	TOPO
3895.41	4055.76	3999.37	12.70	TOPO
3895.34	4054.60	3999.24	13.87	TOPO
3895.37	4055.12	3998.92	14.39	LEW
3895.32	4054.42	3998.51	15.10	OS
3895.21	4052.70	3998.11	16.82	OS
3894.76	4045.99	3998.09	23.55	OS
3894.76	4045.91	3998.11	23.63	OS
3894.41	4040.73	3998.15	28.82	OS
3894.20	4037.44	3998.25	32.12	OS
3894.18	4037.22	3998.41	32.34	OS
3894.05	4035.19	3998.38	34.37	OS
3894.05	4035.27	3998.37	34.45	OS
3894.09	4035.78	3998.73	34.97	OS
3894.20	4037.51	3998.89	36.70	REW
3894.04	4035.11	3999.03	39.10	TOPO
3894.24	4038.07	3999.18	42.07	TOPO
3894.11	4036.09	3999.50	44.06	TOPO
3894.34	4039.65	3999.66	47.63	HW
3894.27	4038.63	3999.75	48.66	TOPO
3894.22	4037.87	3999.78	49.42	TOPO
3894.29	4038.78	3999.78	50.33	TOPO
3894.67	4044.64	3999.83	56.21	TOPO
3894.84	4047.09	3999.77	58.67	TOPO
3894.71	4045.24	3999.77	60.52	TOPO
3893.85	4032.19	4000.30	73.60	XS18-REP

Table A-116. Reach R3, cross-section 19 point coordinates and descriptions.

Cross-Section 19				
N (m)	**E (m)**	**Z (m)**	**X (m)**	**Description**
3871.53	4073.31	3999.90	0.00	TOPO
3870.90	4070.42	3999.84	2.96	TOPO
3870.80	4069.97	3999.62	3.42	TOPO
3870.75	4069.74	3999.45	3.66	TOPO
3870.70	4069.54	3999.21	3.86	TOPO
3870.66	4069.35	3998.94	4.05	TOPO
3870.66	4069.34	3998.81	4.07	LEW
3870.29	4067.65	3998.65	5.79	OS
3870.22	4067.33	3998.52	6.12	OS
3869.52	4064.14	3998.25	9.39	OS
3869.45	4063.82	3998.17	9.72	OS
3869.20	4062.67	3998.33	10.90	OS
3869.05	4062.00	3998.17	11.58	OS
3868.93	4061.42	3998.24	12.18	OS
3868.36	4058.83	3998.27	14.83	OS
3867.79	4056.22	3998.32	17.49	OS
3867.62	4055.47	3998.31	18.26	OS
3867.35	4054.21	3998.34	19.56	OS
3867.07	4052.96	3998.41	20.83	OS
3866.49	4050.32	3998.37	23.54	OS
3866.40	4049.87	3998.53	24.00	OS
3866.27	4049.31	3998.78	24.57	REW
3866.18	4048.90	3998.91	24.99	TOPO
3865.98	4047.96	3999.32	25.96	TOPO
3865.99	4048.01	3999.32	26.02	TOPO
3865.95	4047.81	3999.42	26.22	TOPO
3865.80	4047.13	3999.52	26.93	TOPO
3865.67	4046.56	3999.70	27.51	TOPO
3865.52	4045.86	3999.85	28.22	TOPO
3865.29	4044.82	3999.95	29.29	TOPO

Table A-117. Reach R3, cross-section 20 point coordinates and descriptions.

Cross-Section 20				
N (m)	**E (m)**	**Z (m)**	**X (m)**	**Description**
3861.22	4109.66	3999.67	0.00	TOPO
3860.68	4109.29	3999.67	0.66	TOPO
3860.62	4109.25	3999.61	0.73	TOPO
3852.47	4103.67	3999.23	10.61	TOPO
3847.80	4100.48	3999.08	16.27	TOPO
3845.60	4098.97	3998.89	18.93	TOPO
3844.36	4098.13	3998.93	20.43	TOPO
3843.56	4097.58	3999.13	21.40	TOPO
3842.22	4096.66	3999.10	23.02	TOPO
3840.51	4095.49	3999.10	25.10	TOPO
3838.85	4094.36	3998.94	27.11	TOPO
3836.97	4093.07	3998.71	29.38	LEW
3836.30	4092.61	3998.62	30.20	OS
3835.52	4092.08	3998.53	31.15	OS
3833.58	4090.75	3998.37	33.50	OS
3832.62	4090.10	3998.23	34.65	OS
3831.20	4089.13	3997.91	36.37	OS
3829.38	4087.88	3997.92	38.59	OS
3828.42	4087.22	3997.98	39.74	OS
3826.23	4085.72	3997.90	42.40	OS
3823.32	4083.73	3997.63	45.93	OS
3821.27	4082.33	3998.00	48.41	OS
3819.62	4081.20	3998.24	50.41	OS
3818.96	4080.75	3998.61	51.21	OS
3818.83	4080.66	3998.71	51.37	REW
3818.76	4080.62	3998.91	51.45	TOPO
3818.23	4080.25	3999.10	52.10	TOPO
3816.98	4079.40	3999.34	53.60	TOPO
3815.92	4078.67	3999.49	54.89	TOPO
3814.91	4077.98	3999.58	56.12	TOPO

Table A-118. Reach R3, cross-section 21 point coordinates and descriptions.

Cross-Section 21				
N (m)	**E (m)**	**Z (m)**	**X (m)**	**Description**
3861.67	4105.53	3999.70	0.00	TOPO
3857.51	4106.07	3999.50	4.20	TOPO
3852.05	4106.77	3999.20	9.71	TOPO
3844.55	4107.73	3998.92	17.26	TOPO
3843.92	4107.81	3999.12	17.90	TOPO
3842.24	4108.02	3999.10	19.59	TOPO
3841.85	4108.07	3998.98	19.99	TOPO
3841.60	4108.11	3999.06	20.24	TOPO
3840.76	4108.21	3999.17	21.09	TOPO
3839.15	4108.42	3999.15	22.71	TOPO
3838.36	4108.52	3999.12	23.51	TOPO
3837.01	4108.70	3998.96	24.87	TOPO
3835.88	4108.84	3998.83	26.01	TOPO
3835.49	4108.89	3998.70	26.39	LEW
3834.84	4108.97	3998.63	27.06	OS
3834.35	4109.04	3998.61	27.55	OS
3833.83	4109.10	3998.84	28.07	OS
3833.49	4109.15	3998.64	28.41	OS
3833.19	4109.18	3998.33	28.72	OS
3831.31	4109.43	3998.13	30.62	OS
3830.13	4109.58	3997.96	31.80	OS
3828.50	4109.79	3997.52	33.44	OS
3826.11	4110.09	3997.38	35.86	OS
3823.34	4110.45	3997.37	38.65	OS
3822.08	4110.61	3997.59	39.92	OS
3821.48	4110.69	3997.81	40.53	OS
3820.12	4110.86	3997.91	41.89	OS
3818.46	4111.07	3998.13	43.57	OS
3816.62	4111.31	3998.10	45.42	OS
3815.13	4111.50	3998.10	46.93	OS
3814.39	4111.60	3998.49	47.68	OS
3814.45	4111.59	3998.71	47.74	REW
3814.23	4111.62	3999.48	47.95	TOPO
3810.82	4112.05	3999.47	51.39	TOPO

Table A-119. Reach R3, cross-section 22 point coordinates and descriptions.

Cross-Section 22				
N (m)	**E (m)**	**Z (m)**	**X (m)**	**Description**
3852.38	4124.65	3999.58	0.00	XS22-LEP
3851.47	4124.82	3999.57	0.92	TOPO
3850.77	4124.94	3999.41	1.63	TOPO
3848.77	4125.30	3999.13	3.67	TOPO
3842.87	4126.36	3998.88	9.66	TOPO
3841.66	4126.57	3998.86	10.88	TOPO
3840.71	4126.74	3998.68	11.85	LEW
3840.34	4126.81	3998.58	12.23	OS
3839.90	4126.89	3998.55	12.67	OS
3839.28	4127.00	3998.25	13.30	OS
3835.41	4127.69	3998.20	17.23	OS
3834.22	4127.91	3998.05	18.44	OS
3830.64	4128.55	3998.01	22.08	OS
3827.22	4129.16	3997.89	25.56	OS
3823.55	4129.82	3997.82	29.29	OS
3820.68	4130.33	3997.84	32.20	OS
3817.73	4130.86	3998.43	35.20	OS
3816.80	4131.03	3998.58	36.14	OS
3816.68	4131.05	3998.69	36.26	REW
3816.62	4131.06	3998.76	36.32	TOPO
3816.34	4131.11	3998.81	36.61	TOPO
3815.54	4131.25	3999.07	37.42	TOPO
3814.76	4131.40	3999.27	38.22	TOPO
3812.32	4131.83	3999.35	40.70	HW
3806.53	4132.87	3999.32	46.58	XS22-REP

APPENDIX B: POINTS POSITIONS FOR THALWEG SURVEYS, AND SUBSEQUENT BED ELEVATION AND RESIDUAL DEPTH ANALYSIS

STUDY REACH C1

Table B-1. Coordinates for streambed and water surface points in reach C1 thalweg surveys.

Thalweg Streambed Surface Points				Thalweg Water Surface Points			
N (m)	E (m)	Z (m)	X (m)	N (m)	E (m)	Z (m)	X (m)
4990.20	5025.18	96.98	0.00	4990.12	5025.23	97.70	0.00
4984.93	5023.10	96.99	5.67	4984.93	5023.03	97.65	5.64
4980.52	5020.67	97.05	10.70	4980.56	5020.53	97.51	10.66
4976.57	5019.00	96.65	14.99	4976.59	5018.84	97.50	14.98
4972.17	5016.24	96.57	20.18	4972.26	5016.03	97.44	20.14
4966.93	5013.74	96.62	25.99	4966.98	5013.71	97.41	25.91
4959.50	5010.86	96.63	33.96	4959.40	5010.85	97.43	34.01
4950.48	5007.25	96.79	43.67	4950.49	5007.18	97.39	43.65
4940.96	5003.22	96.84	54.01	4940.97	5003.08	97.31	54.01
4932.34	5000.19	96.80	63.15	4932.33	5000.08	97.23	63.16
4927.65	4999.74	96.47	67.86	4927.72	4999.63	97.21	67.79
4921.88	4999.86	96.52	73.63	4921.96	4999.78	97.13	73.55
4916.07	4999.93	96.44	79.44	4916.07	4999.70	96.97	79.44
4910.44	4999.72	95.93	85.08	4910.32	4999.51	96.86	85.19
4905.39	5001.48	95.48	90.42	4905.37	5001.27	96.81	90.45
4900.60	5003.05	95.59	95.47	4900.46	5002.55	96.77	95.52
4894.58	5005.98	95.49	102.16	4894.18	5005.36	96.75	102.40
4891.94	5006.62	95.50	104.87	4891.85	5006.04	96.76	104.83
4886.12	5009.74	95.57	111.48	4886.10	5009.13	96.77	111.36
4886.48	5009.95	95.59	111.90	4885.94	5009.35	96.76	111.63
4879.72	5012.52	96.01	119.13	4879.62	5012.45	96.77	118.67
4880.86	5013.08	95.94	120.41	4880.88	5013.06	96.74	120.06
4875.72	5016.80	96.15	126.76	4875.77	5016.77	96.72	126.38
4867.82	5022.53	96.15	136.51	4867.87	5022.51	96.67	136.14
4856.20	5029.92	96.02	150.28	4856.13	5030.01	96.59	150.07
4846.93	5038.38	96.01	162.83	4846.97	5038.42	96.59	162.51
4839.21	5046.69	95.87	174.18	4839.15	5046.74	96.52	173.93
4831.98	5054.90	95.87	185.12	4831.94	5054.87	96.45	184.80
4826.80	5058.82	96.00	191.62	4827.33	5057.14	96.41	189.93
4823.24	5060.58	95.91	195.58	4823.20	5060.54	96.22	195.29
4819.57	5063.40	95.71	200.21	4819.58	5063.35	96.10	199.86
4816.90	5062.41	95.30	203.06	4816.89	5062.46	96.14	202.70
4816.66	5066.26	95.35	206.91	4816.42	5066.12	96.18	206.38
4814.21	5068.12	95.12	209.98	4814.16	5067.99	96.14	209.32
4813.84	5070.49	95.09	212.38	4811.39	5075.00	96.09	216.85
4811.46	5075.03	95.39	217.51	4808.03	5083.65	96.03	226.14
4808.04	5083.74	95.49	226.87	4804.98	5089.70	96.02	232.91
4805.06	5089.87	95.51	233.68	4801.25	5097.62	95.90	241.66
4801.29	5097.69	95.50	242.37	4796.31	5105.49	95.72	250.96

4796.34	5105.64	95.43	251.73	4793.92	5109.98	95.55	256.04
4794.22	5110.10	95.15	256.67	4793.02	5114.25	95.34	260.41
4793.21	5114.31	94.83	261.00	4793.94	5116.92	95.30	263.23
4794.17	5117.06	94.59	263.91	4795.49	5119.52	95.07	266.26
4795.53	5119.52	94.76	266.72	4798.00	5122.98	95.17	270.53
4798.15	5123.15	94.75	271.20	4800.77	5127.42	95.01	275.76
4800.85	5127.55	94.78	276.36	4803.32	5131.98	94.93	280.99
4803.64	5132.12	94.06	281.71	4803.56	5136.54	94.91	285.56
4803.74	5136.60	94.04	286.20	4802.14	5141.60	94.86	290.82
4802.13	5141.76	93.94	291.60	4800.94	5146.31	94.85	295.67
4801.14	5146.47	94.11	296.42	4800.13	5152.36	94.77	301.78
4800.33	5152.37	93.97	302.37	4799.40	5157.51	94.68	306.97
4799.61	5157.75	93.69	307.79	4799.06	5161.95	94.65	311.44
4799.41	5162.14	93.75	312.19	4799.04	5167.15	94.62	316.64
4799.22	5167.22	93.79	317.27	4798.23	5174.27	94.64	323.80
4798.25	5174.41	93.78	324.53	4796.81	5182.86	94.59	332.50
4796.67	5183.15	93.95	333.41	4795.11	5189.49	94.56	339.35
4794.91	5189.74	93.87	340.24	4792.65	5199.18	94.45	349.34
4792.58	5199.46	93.81	350.23	4788.39	5211.94	94.34	362.80
4788.22	5211.82	93.65	363.34	4784.06	5225.03	94.33	376.59
4783.98	5225.06	93.62	377.24	4780.38	5239.64	94.24	391.65
4780.35	5239.72	93.66	392.34	4777.98	5249.54	94.17	401.84
4778.10	5249.48	93.51	402.36	4773.60	5261.14	94.10	414.24
4773.74	5261.13	93.39	414.80	4772.45	5263.45	94.10	416.82
4772.61	5263.57	93.13	417.49	4770.45	5269.24	93.99	422.94
4770.54	5269.39	93.30	423.66	4765.84	5277.27	93.97	432.21
4765.97	5277.32	93.24	432.82	4762.66	5285.93	93.96	441.43
4762.68	5286.19	93.21	442.27	4759.93	5292.43	93.95	448.48
4760.01	5292.42	93.08	449.05	4757.05	5302.08	93.93	458.56
4757.10	5302.05	93.27	459.11	4753.75	5311.06	93.93	468.11
4753.83	5311.07	93.09	468.70	4750.63	5314.66	93.90	472.89
4750.60	5314.48	93.42	473.40	4746.13	5318.18	93.85	478.59
4746.22	5318.11	93.49	479.09	4741.03	5321.18	93.76	484.51
4741.04	5321.11	93.39	485.07	4733.44	5325.24	93.63	493.12
4733.45	5325.14	93.17	493.67	4729.10	5332.40	93.42	501.50
4729.11	5332.46	93.05	502.19	4728.98	5338.90	93.25	508.00
4729.03	5339.15	92.73	508.88	4729.57	5341.80	93.29	510.96
4729.07	5341.75	92.48	511.47	4729.13	5348.84	93.23	518.01
4728.51	5348.87	92.33	518.61	4728.19	5356.34	93.23	525.56
4728.19	5356.18	92.43	525.93	4728.35	5361.96	93.26	531.19
4728.36	5362.05	92.49	531.80	4728.42	5364.46	93.23	533.69
4728.53	5364.56	92.70	534.32				

Table B-2. Results of bed elevation differencing applied to thalweg data from study reach C1.

Bed Elevation Differencing Data

Z (m)	X (m)	Δ Z (m)	Series	Z (m)	X (m)	Δ Z (m)	Series
96.98	0.00	0.06	1	94.76	269.99	-0.48	10
97.04	10.06	-0.47	2	94.28	280.12	-0.31	10
96.58	19.85	0.05	3	93.97	290.03	0.05	11
96.63	29.99	0.11	3	94.03	299.99	-0.30	12
96.73	39.94	0.09	3	93.72	310.06	0.07	13
96.82	49.95	-0.01	4	93.79	320.09	0.10	13
96.81	60.03	-0.32	4	93.89	329.97	-0.01	14
96.49	70.06	-0.11	4	93.88	340.00	-0.07	14
96.38	80.07	-0.87	4	93.81	350.03	-0.12	14
95.51	90.10	0.01	5	93.69	360.10	-0.05	14
95.52	100.08	0.04	5	93.64	369.98	-0.01	14
95.56	109.97	0.40	5	93.63	380.04	0.03	15
95.96	119.95	0.19	5	93.66	390.08	-0.12	16
96.15	130.03	-0.03	6	93.54	400.10	-0.11	16
96.12	139.92	-0.10	6	93.43	409.94	-0.24	16
96.02	150.00	-0.01	6	93.20	420.10	0.06	17
96.01	160.02	-0.09	6	93.26	429.89	-0.04	18
95.92	170.14	-0.05	6	93.21	439.98	-0.12	18
95.87	179.90	0.10	7	93.09	449.97	0.16	19
95.97	189.86	-0.26	8	93.25	459.91	-0.07	20
95.71	200.06	-0.59	8	93.18	469.99	0.29	21
95.12	209.98	0.30	9	93.48	479.99	-0.22	22
95.42	219.89	0.08	9	93.26	490.00	-0.18	22
95.50	229.95	0.00	9	93.08	499.96	-0.46	22
95.50	239.93	-0.06	10	92.62	510.03	-0.27	22
95.44	250.09	-0.54	10	92.35	520.05	0.12	23
94.90	260.00	-0.14	10	92.47	530.06		

Table B-3. Results of bedform designation in study reach C1.

Bedform Designation by Bed Elevation Differencing Method	
STDEV of Δ Z	Δ Z Threshold
0.28	0.21

Series Analysis

Series	Ei (m)	Z (m)	X (m)	Bedform Designation
1	0.06	97.04	10.06	RIFFLE
2	-0.47	96.58	19.85	POOL
3	0.25	96.82	49.95	RIFFLE
4	-1.31	95.51	90.10	POOL
5	0.64	96.15	130.03	RIFFLE
6	-0.28	95.87	179.90	ND
7	0.10	95.97	189.86	ND
8	-0.85	95.12	209.98	POOL
9	0.38	95.50	239.93	RIFFLE
10	-1.53	93.97	290.03	ND
11	0.05	94.03	299.99	ND
12	-0.30	93.72	310.06	ND
13	0.17	93.89	329.97	ND
14	-0.26	93.63	380.04	ND
15	0.03	93.66	390.08	ND
16	-0.46	93.20	420.10	ND
17	0.06	93.26	429.89	ND
18	-0.16	93.09	449.97	POOL
19	0.16	93.25	459.91	ND
20	-0.07	93.18	469.99	ND
21	0.29	93.48	479.99	RIFFLE
22	-1.13	92.35	520.05	POOL
23	0.12	92.47	530.06	ND

Table B-4. Longitudinal characteristics calculated using the residual depth method in study reach C1.

Longitudinal Measurements Calculated by Residual Depth Method

Pool Length (m)	Distance to Next Pool (m)	Riffle Length (m)	Distance to Next Riffle (m)	Riffle Gradient	Length-Weighted Riffle Gradient	Relative Length-Weighted Riffle Gradient
41.35	70.14	2.62	43.96	0.067	0.00060	1.68
53.54	118.60	28.79	82.33	0.024	0.0023	
32.40	202.33	65.06	97.46	0.0095	0.0021	
75.38	105.28	169.93	245.30	0.012	0.0068	
25.29		29.91	55.20	0.026	0.0026	

STUDY REACH C2

Table B-5. Coordinates for streambed and water surface points in reach C2 thalweg surveys.

Thalweg Streambed Surface Points				Thalweg Water Surface Points			
N (m)	E (m)	Z (m)	X (m)	N (m)	E (m)	Z (m)	X (m)
5645.89	5057.74	5004.61	0.00	5645.92	5057.68	5005.60	0.00
5642.74	5062.51	5004.88	5.72	5642.82	5062.36	5005.56	5.60
5639.95	5068.84	5005.01	12.64	5642.82	5062.36	5005.41	12.80
5637.47	5076.02	5004.95	20.28	5636.90	5076.17	5005.50	20.57
5630.92	5080.91	5004.88	28.45	5630.87	5080.85	5005.41	28.21
5624.20	5086.08	5004.77	36.93	5624.29	5086.05	5005.35	36.60
5616.99	5091.08	5004.60	45.70	5617.06	5091.08	5005.25	45.40
5611.23	5094.77	5004.57	52.55	5611.05	5094.75	5005.28	52.44
5606.01	5098.22	5004.76	58.80	5606.06	5098.27	5005.21	58.55
5601.88	5102.97	5004.60	65.10	5601.90	5102.89	5005.19	64.77
5592.95	5110.55	5004.78	76.81	5593.03	5110.56	5005.19	76.49
5583.75	5117.46	5004.63	88.32	5583.77	5117.49	5005.10	88.05
5572.55	5125.72	5004.54	102.23	5572.48	5125.67	5005.06	102.00
5565.82	5128.13	5004.53	109.39	5565.82	5128.17	5004.99	109.12
5556.25	5135.88	5004.38	121.69	5543.63	5146.89	5004.71	138.44
5543.84	5146.76	5004.37	137.90	5529.64	5156.41	5004.61	155.37
5529.58	5156.41	5004.27	155.12	5519.14	5159.43	5004.51	166.29
5519.16	5159.47	5004.23	165.98	5513.25	5160.44	5004.44	172.26
5513.18	5160.30	5004.16	172.02	5504.83	5161.63	5004.32	180.77
5504.74	5161.55	5003.92	180.55	5498.26	5162.55	5004.31	187.41
5498.33	5162.41	5003.83	187.01	5491.17	5169.09	5004.30	197.05
5491.11	5168.91	5003.67	196.73	5474.42	5188.00	5003.91	222.32
5473.84	5186.87	5003.35	221.64	5464.85	5196.70	5003.81	235.25
5464.94	5196.63	5003.25	234.86	5456.34	5206.06	5003.71	247.90
5456.37	5206.08	5003.15	247.61	5444.92	5216.10	5003.57	263.11
5444.90	5216.16	5002.90	262.88	5440.85	5220.04	5003.46	268.77
5440.95	5220.08	5002.88	268.45	5431.78	5230.09	5003.32	282.31
5431.87	5230.04	5002.82	281.93	5423.67	5241.52	5003.22	296.33
5423.70	5241.51	5002.63	296.01	5414.95	5251.98	5003.18	309.94
5415.02	5251.96	5002.67	309.59	5404.26	5262.70	5003.09	325.08
5404.26	5262.63	5002.53	324.75	5394.15	5271.65	5003.06	338.58
5394.19	5271.54	5002.40	338.19	5384.66	5278.89	5003.02	350.52
5384.67	5278.89	5002.32	350.22	5379.70	5282.21	5002.98	356.49
5379.68	5282.11	5002.39	356.16	5367.55	5288.53	5002.88	370.18
5367.60	5288.52	5002.33	369.83	5356.50	5293.69	5002.74	382.37
5356.54	5293.64	5002.29	382.02	5350.10	5295.14	5002.70	388.94
5350.02	5295.12	5002.27	388.71	5339.79	5297.13	5002.36	399.44
5339.68	5297.00	5001.95	399.21	5328.02	5299.64	5002.32	411.47
5328.07	5299.64	5001.61	411.13	5335.04	5305.74	5002.36	420.77

5334.83	5305.75	5001.99	420.24	5329.63	5304.20	5002.26	426.39
5329.60	5304.08	5001.76	425.74	5322.28	5301.97	5002.21	434.07
5322.30	5302.04	5001.58	433.32	5317.19	5299.36	5002.10	439.79
5316.75	5299.13	5001.33	439.58	5311.55	5296.79	5002.10	445.99
5311.45	5296.85	5001.29	445.35	5302.99	5293.79	5002.07	455.06
5302.64	5293.92	5001.22	454.64	5296.95	5291.85	5002.09	461.40
5296.53	5292.01	5001.07	461.03	5286.31	5286.11	5002.03	473.50
5286.15	5286.15	5001.09	472.96	5276.84	5280.11	5001.99	484.70
5276.66	5280.00	5001.10	484.26	5264.87	5269.80	5001.96	500.50
5264.64	5269.87	5001.07	499.99	5256.44	5262.64	5002.00	511.56
5256.41	5262.73	5001.18	510.89	5249.97	5255.45	5001.99	521.23
5249.90	5255.55	5001.27	520.57	5240.99	5244.32	5001.96	535.54
5241.06	5244.40	5001.38	534.80	5235.96	5237.80	5001.91	543.77
5236.02	5237.85	5001.43	543.06				

Table B-6. Results of bed elevation differencing applied to thalweg data from study reach C2.

Bed Elevation Differencing Data							
Z (m)	**X (m)**	**Δ Z (m)**	**Series**	**Z (m)**	**X (m)**	**Δ Z (m)**	**Series**
5004.61	0.00	0.35	1.00	5002.83	280.00	-0.11	6.00
5004.96	10.07	0.00	2.00	5002.71	290.00	-0.07	6.00
5004.96	19.94	-0.10	2.00	5002.64	299.96	0.03	7.00
5004.86	30.04	-0.15	2.00	5002.66	310.11	-0.09	8.00
5004.71	40.02	-0.13	2.00	5002.58	319.97	-0.10	8.00
5004.58	49.96	0.15	3.00	5002.48	330.08	-0.09	8.00
5004.73	60.11	-0.05	4.00	5002.39	340.01	-0.06	8.00
5004.68	69.98	0.06	5.00	5002.32	349.95	0.05	9.00
5004.74	80.00	-0.12	6.00	5002.38	359.93	-0.04	10.00
5004.62	90.01	-0.07	6.00	5002.33	370.03	-0.04	10.00
5004.56	99.93	-0.04	6.00	5002.30	380.04	-0.05	10.00
5004.52	109.93	-0.12	6.00	5002.24	389.92	-0.31	10.00
5004.40	119.90	-0.03	6.00	5001.93	400.10	-0.28	10.00
5004.37	130.15	-0.02	6.00	5001.66	410.10	0.32	11.00
5004.35	139.95	-0.06	6.00	5001.97	420.11	-0.33	12.00
5004.30	149.91	-0.05	6.00	5001.64	430.01	-0.31	12.00
5004.25	160.04	-0.06	6.00	5001.33	440.04	-0.07	12.00
5004.19	170.05	-0.24	6.00	5001.26	449.97	-0.16	12.00
5003.94	179.93	-0.16	6.00	5001.10	459.95	-0.02	12.00
5003.79	190.01	-0.15	6.00	5001.08	469.95	0.01	13.00
5003.63	199.89	-0.13	6.00	5001.10	479.92	0.00	14.00
5003.50	209.99	-0.13	6.00	5001.09	489.95	-0.02	14.00
5003.38	219.99	-0.09	6.00	5001.07	500.03	0.09	15.00
5003.29	230.06	-0.08	6.00	5001.16	509.96	0.10	15.00
5003.21	239.98	-0.10	6.00	5001.26	519.88	0.08	15.00
5003.11	250.00	-0.16	6.00	5001.34	530.14	0.07	15.00
5002.95	259.89	-0.08	6.00	5001.41	540.00		

5002.88	269.98	-0.05	6.00

Table B-7. Results of bedform designation in study reach C2.

Bedform Designation by Bed Elevation Differencing Method

STDEV of Δ Z	Δ Z Threshold
0.11	0.08

Series Analysis

Series	Ei (m)	Z (m)	X (m)	Bedform Designation
1	0.35	5004.96	10.07	Riffle
2	-0.37	5004.58	49.96	Pool
3	0.15	5004.73	60.11	Riffle
4	-0.05	5004.68	69.98	
5	0.06	5004.74	80.00	
6	-2.10	5002.64	299.96	
7	0.03	5002.66	310.11	
8	-0.34	5002.32	349.95	
9	0.05	5002.38	359.93	
10	-0.44	5001.66	410.10	Pool
11	0.32	5001.97	420.11	Riffle
12	-0.89	5001.08	469.95	Pool
13	0.01	5001.10	479.92	
14	-0.02	5001.07	500.03	
15	0.34	5001.41	540.00	Riffle

Table B-8. Longitudinal characteristics calculated using the residual depth method in study reach C2.

Longitudinal Measurements Calculated by Residual Depth Method

Pool Length (m)	Distance to Next Pool (m)	Riffle Length (m)	Distance to Next Riffle (m)	Riffle Gradient	Length-Weighted Riffle Gradient	Relative Length-Weighted Riffle Gradient
28.03	349.25	36.04	64.07	0.0063	0.00060	1.18
22.41	39.14	321.22	343.62	0.0087	0.007	
106.09		16.73	122.82	0.033	0.0015	

STUDY REACH C3

Table B-9. Coordinates for streambed and water surface points in reach C3 thalweg surveys.

Thalweg Streambed Points				Thalweg Water Surface Points			
N (m)	E (m)	Z (m)	X (m)	N (m)	E (m)	Z (m)	X (m)
5212.95	5184.66	5000.82	0.00	5212.97	5184.72	5001.24	0.00
5211.93	5176.40	5000.76	8.32	5211.96	5176.46	5001.23	8.32
5211.76	5171.08	5000.74	13.64	5211.64	5171.17	5000.98	13.62
5211.62	5165.09	5000.25	19.63	5211.71	5165.19	5000.87	19.60
5212.01	5162.72	5000.21	22.04	5212.06	5163.07	5000.70	21.75
5212.32	5160.57	5000.08	24.21	5212.48	5160.66	5000.56	24.19
5212.56	5153.07	4999.93	31.71	5212.57	5153.06	5000.55	31.79
5213.85	5147.17	4999.91	37.75	5213.90	5147.26	5000.44	37.75
5212.89	5143.09	4999.64	41.94	5212.99	5143.37	5000.30	41.74
5211.27	5139.03	4999.40	46.31	5211.52	5139.10	5000.24	46.26
5209.34	5132.91	4999.21	52.73	5209.46	5132.85	5000.27	52.84
5206.71	5125.83	4999.15	60.28	5206.89	5125.89	5000.23	60.26
5204.43	5116.38	4998.94	70.01	5204.82	5116.39	5000.28	69.98
5197.97	5102.43	4999.33	85.37	5197.91	5102.38	5000.29	85.61
5192.55	5089.37	4999.48	99.51	5192.48	5089.41	5000.28	99.66
5187.37	5077.53	4999.58	112.43	5187.34	5077.58	5000.27	112.56
5181.89	5064.48	4999.85	126.60	5181.83	5064.53	5000.23	126.73
5180.89	5058.89	4999.86	132.27	5180.81	5058.95	5000.22	132.40
5179.03	5048.17	4999.70	143.15	5179.03	5048.08	5000.20	143.41
5172.42	5036.21	4999.62	156.82	5172.47	5036.09	5000.10	157.08
5163.02	5027.58	4999.15	169.57	5163.28	5027.49	5000.00	169.67
5158.30	5024.27	4999.03	175.34	5158.50	5024.06	4999.78	175.55
5155.57	5022.54	4999.05	178.57	5155.60	5022.24	4999.78	178.98
5150.99	5020.95	4998.96	183.42	5151.05	5020.70	4999.53	183.78
5146.33	5020.68	4998.57	188.09	5146.33	5020.47	4999.17	188.51
5140.36	5018.83	4998.31	194.34	5140.36	5018.47	4999.11	194.80
5133.53	5015.85	4998.35	201.79	5133.55	5015.82	4999.07	202.11
5130.30	5014.28	4998.31	205.38	5130.37	5014.23	4998.98	205.67
5124.17	5012.23	4998.39	211.85	5124.09	5012.24	4998.88	212.26
5122.15	5007.23	4998.31	217.24	5122.17	5007.24	4998.85	217.61
5110.46	5003.32	4998.19	229.57	5110.51	5003.44	4998.72	229.88
5097.26	5000.36	4998.04	243.09	5097.26	5000.47	4998.70	243.45
5086.03	4999.23	4997.87	254.38	5086.20	4999.19	4998.62	254.59
5076.80	4998.03	4997.75	263.69	5076.79	4998.07	4998.66	264.06
5070.56	4997.51	4997.61	269.95	5070.40	4997.36	4998.64	270.49
5060.64	4997.35	4997.63	279.88	5060.77	4997.32	4998.65	280.12
5047.48	4997.93	4997.83	293.04	5047.56	4997.83	4998.61	293.35
5033.28	4999.26	4997.94	307.31	5033.29	4999.24	4998.61	307.68
5023.91	5003.34	4997.96	317.53	5012.22	5006.87	4998.53	330.09
5012.21	5006.88	4998.06	329.75	5001.71	5011.82	4998.46	341.71

5001.70	5011.88	4998.04	341.39	4992.23	5017.96	4998.34	353.00
4992.22	5017.93	4998.07	352.64	4986.73	5023.08	4998.21	360.52
4986.80	5023.08	4997.98	360.12	4979.39	5029.34	4998.09	370.16
4979.38	5029.33	4997.70	369.81	4970.27	5033.64	4998.05	380.25
4970.23	5033.69	4997.51	379.95	4963.70	5035.72	4997.98	387.13
4963.69	5035.62	4997.59	386.77	4948.63	5034.97	4997.87	402.22
4948.63	5035.02	4997.63	401.84	4944.50	5031.88	4997.81	407.39
4944.52	5031.84	4997.59	407.03	4937.30	5028.81	4997.72	415.21
4937.31	5028.80	4997.30	414.86	4926.27	5027.53	4997.47	426.32
4926.29	5027.46	4997.21	425.96	4916.17	5023.54	4997.13	437.18
4916.13	5023.49	4996.77	436.87	4904.30	5018.24	4996.95	450.17
4904.25	5018.26	4996.58	449.85	4890.90	5009.89	4996.84	465.96
4890.90	5009.81	4996.54	465.65	4886.21	5005.24	4996.82	472.57
4886.28	5005.26	4996.23	472.13	4876.92	4998.59	4996.76	483.99
4876.99	4998.53	4996.30	483.61	4866.61	4992.04	4996.61	496.21
4866.62	4992.01	4996.22	495.86	4862.75	4990.80	4996.48	500.26
4862.70	4990.81	4996.14	499.95	4860.11	4988.68	4996.45	503.65
4859.83	4988.92	4995.55	503.39	4854.17	4987.13	4996.30	509.79
4853.81	4987.19	4995.29	509.65	4846.50	4979.71	4996.33	520.46
4846.46	4979.75	4995.53	520.11	4837.89	4970.27	4996.30	533.24
4837.83	4970.21	4995.70	532.98	4828.62	4962.25	4996.20	545.49
4828.71	4962.29	4995.96	545.05	4826.36	4960.81	4996.18	548.17
4826.38	4960.81	4995.74	547.82	4824.25	4956.82	4996.14	552.68
4824.20	4956.83	4995.52	552.36	4820.05	4949.58	4996.10	561.06
4820.01	4949.60	4995.35	560.71	4813.89	4937.33	4996.07	574.77
4814.03	4937.33	4995.21	574.36	4810.67	4930.75	4996.08	582.09
4810.77	4930.65	4995.20	581.79	4805.29	4918.88	4996.07	595.13
4805.41	4918.92	4995.38	594.70	4802.34	4910.70	4996.04	603.82
4802.32	4910.79	4995.61	603.39	4800.35	4900.57	4995.95	614.14
4800.38	4900.51	4995.66	613.85	4797.01	4890.16	4995.91	625.08
4797.04	4890.14	4995.63	624.75	4794.34	4879.80	4995.81	635.78
4794.31	4879.83	4995.43	635.42	4791.54	4873.79	4995.66	642.40
4791.59	4873.70	4995.27	642.12	4787.22	4867.96	4995.51	649.66
4787.28	4867.94	4995.06	649.32	4777.50	4857.27	4995.50	664.11
4777.49	4857.31	4994.90	663.76	4765.75	4848.79	4995.49	678.61
4765.80	4848.84	4995.01	678.20	4765.23	4850.67	4995.45	680.56
4765.19	4850.62	4995.14	680.08	4760.82	4850.16	4995.34	685.00
4760.83	4850.11	4995.14	684.47	4754.79	4849.91	4995.30	691.04
4754.79	4849.87	4994.73	690.52				

Table B-10. Results of bed elevation differencing applied to thalweg data from study reach C3.

Bed Elevation Differencing Data

Z (m)	X (m)	Δ Z (m)	Series	Z (m)	X (m)	Δ Z (m)	Series
5000.82	0	-0.06	1	4998.06	350	-0.08	9
5000.76	10	-0.52	1	4997.98	360	-0.28	9
5000.24	20	-0.27	1	4997.70	370	-0.19	9
4999.97	30	-0.20	1	4997.51	380	0.09	10
4999.77	40	-0.48	1	4997.60	390	0.02	10
4999.29	50	-0.14	1	4997.62	400	-0.14	11
4999.15	60	-0.21	1	4997.48	410	-0.22	11
4998.94	70	0.25	2	4997.26	420	-0.21	11
4999.19	80	0.19	2	4997.05	430	-0.33	11
4999.38	90	0.10	2	4996.72	440	-0.14	11
4999.48	100	0.08	2	4996.58	450	-0.03	11
4999.56	110	0.16	2	4996.55	460	-0.22	11
4999.72	120	0.13	2	4996.33	470	-0.06	11
4999.85	130	-0.11	3	4996.28	480	-0.02	11
4999.75	140	-0.09	3	4996.26	490	-0.13	11
4999.66	150	-0.15	3	4996.13	500	-0.83	11
4999.50	160	-0.36	3	4995.30	510	0.23	12
4999.14	170	-0.12	3	4995.52	520	0.13	12
4999.02	180	-0.54	3	4995.66	530	0.20	12
4998.48	190	-0.14	3	4995.85	540	-0.22	13
4998.34	200	0.02	4	4995.63	550	-0.27	13
4998.36	210	-0.08	5	4995.37	560	-0.11	13
4998.29	220	-0.10	5	4995.25	570	-0.05	13
4998.19	230	-0.11	5	4995.20	580	0.11	14
4998.08	240	-0.14	5	4995.31	590	0.21	14
4997.93	250	-0.14	5	4995.52	600	0.12	14
4997.79	260	-0.18	5	4995.64	610	0.00	14
4997.61	270	0.02	6	4995.64	620	-0.11	15
4997.63	280	0.16	6	4995.53	630	-0.21	15
4997.79	290	0.10	6	4995.32	640	-0.27	15
4997.89	300	0.06	6	4995.05	650	-0.10	15
4997.94	310	0.03	6	4994.94	660	0.04	16
4997.98	320	0.08	6	4994.99	670	0.15	16
4998.06	330	-0.02	7	4995.13	680	-0.37	17
4998.04	340	0.02	8	4994.76	690		

Table B-11. Results of bedform designation in study reach C3.

Bedform Designation by Bed Elevation Differencing Method

STDEV of Δ Z	Δ Z Threshold
0.19	0.14

Series Analysis

Series	Ei (m)	Z (m)	X (m)	Bedform Designation
1	-1.88	4998.94	70.01	POOL
2	0.92	4999.85	129.97	RIFFLE
3	-1.51	4998.34	200.12	ND
4	0.02	4998.36	209.89	ND
5	-0.75	4997.61	269.95	POOL
6	0.45	4998.06	329.91	RIFFLE
7	-0.02	4998.04	339.87	ND
8	0.02	4998.06	350.09	ND
9	-0.55	4997.51	379.95	ND
10	0.11	4997.62	399.90	ND
11	-2.33	4995.30	509.85	POOL
12	0.56	4995.85	540.20	RIFFLE
13	-0.65	4995.20	580.13	POOL
14	0.44	4995.64	620.01	RIFFLE
15	-0.70	4994.94	659.91	POOL
16	0.19	4995.13	680.00	RIFFLE
17	-0.37	4994.76	690.02	POOL

Table B-12. Longitudinal characteristics calculated using the residual depth method in study reach C3.

Longitudinal Measurements Calculated by Residual Depth Method

Pool Length (m)	Distance to Next Pool (m)	Riffle Length (m)	Distance to Next Riffle (m)	Riffle Gradient	Length-Weighted Riffle Gradient	Relative Length-Weighted Riffle Gradient
93.52	202.66	38.59	220.47	0.024	0.003	2.08
111.33	260.09	109.14	192.38	0.016	0.005	
43.62	48.35	148.76	69.06	0.014	0.006	
64.33	97.37	4.73	66.07	0.059	0.001	
33.03		33.03		0.016	0.002	

STUDY REACH R1

Table B-13. Coordinates for streambed and water surface points in reach R1 thalweg surveys.

Thalweg Streambed Surface Points				Thalweg Water Surface Points			
N (m)	E (m)	Z (m)	X (m)	N (m)	E (m)	Z (m)	X (m)
8078.92	7908.48	7999.97	0.00	8078.91	7908.49	8000.23	0.00
8074.72	7914.94	7999.72	7.71	8074.91	7915.09	8000.12	7.72
8072.68	7920.12	7999.49	13.27	8072.65	7920.14	8000.04	13.26
8071.10	7926.14	7999.32	19.50	8071.14	7926.05	7999.87	19.35
8069.24	7933.75	7999.16	27.34	8069.27	7933.68	7999.77	27.21
8065.90	7942.36	7999.19	36.57	8066.06	7942.39	7999.69	36.49
8062.13	7951.18	7999.04	46.16	8062.09	7951.18	7999.63	46.14
8060.53	7953.69	7998.76	49.14	8060.55	7953.43	7999.57	48.86
8058.78	7958.72	7998.55	54.46	8058.90	7958.83	7999.45	54.51
8055.26	7963.49	7998.32	60.39	8055.48	7963.66	7999.34	60.43
8052.28	7966.65	7998.41	64.74	8052.39	7966.91	7999.34	64.92
8047.07	7971.68	7998.14	71.98	8047.41	7971.98	7999.28	72.02
8042.30	7976.63	7998.15	78.85	8042.91	7977.26	7999.26	78.95
8034.51	7982.19	7998.30	88.43	8034.62	7982.31	7999.20	88.66
8028.02	7986.62	7998.36	96.28	8027.95	7986.58	7999.17	96.58
8019.92	7990.47	7998.43	105.25	8020.07	7990.49	7999.14	105.38
8014.55	7993.51	7998.11	111.42	8014.10	7994.38	7999.19	112.51
8007.50	7994.90	7998.06	118.61	8007.60	7994.94	7999.18	119.03
7998.91	7993.03	7998.23	127.40	7999.12	7992.82	7999.20	127.77
7991.73	7987.15	7998.50	136.68	7991.78	7987.12	7999.19	137.06
7985.80	7982.17	7998.51	144.42	7985.87	7982.23	7999.11	144.73
7982.43	7980.27	7998.37	148.29	7982.49	7980.39	7998.95	148.59
7977.04	7975.76	7998.20	155.32	7977.37	7975.53	7998.84	155.64
7970.47	7970.37	7998.07	163.82	7970.63	7970.27	7998.81	164.19
7965.78	7964.48	7998.13	171.34	7965.84	7964.45	7998.73	171.72
7960.45	7956.41	7998.16	181.01	7960.31	7956.44	7998.67	181.46
7959.10	7951.67	7997.91	185.95	7959.14	7951.76	7998.63	186.29
7957.45	7952.66	7998.08	187.88	7954.94	7948.90	7998.59	191.37
7954.95	7948.67	7997.95	192.59	7952.27	7946.48	7998.52	194.97
7952.22	7946.52	7998.05	196.07	7946.83	7942.64	7998.45	201.63
7946.94	7942.69	7997.96	202.59	7942.74	7939.80	7998.40	206.61
7942.84	7939.86	7997.69	207.57	7938.11	7938.29	7998.36	211.48
7937.75	7938.72	7997.40	212.78	7934.07	7938.23	7998.26	215.52
7934.15	7938.59	7997.39	216.38	7931.35	7938.22	7998.24	218.24
7930.96	7938.81	7997.29	219.58	7929.66	7942.00	7998.24	222.38
7929.51	7941.35	7997.30	222.51	7925.71	7943.09	7998.21	226.48
7925.46	7942.21	7997.03	226.65	7919.63	7942.92	7998.33	232.56
7920.25	7943.11	7997.09	231.94	7918.59	7944.51	7998.21	234.46
7918.57	7944.67	7997.01	234.23	7916.40	7946.93	7998.23	237.73
7916.53	7947.23	7996.92	237.50	7913.60	7948.50	7998.25	240.93

7913.82	7948.75	7997.49	240.61	7911.75	7951.40	7998.21	244.37
7911.73	7951.41	7997.44	243.99	7908.68	7953.34	7998.19	248.00
7908.45	7953.35	7997.59	247.81	7903.22	7959.62	7998.13	256.33
7903.22	7959.63	7997.49	255.98	7898.30	7966.32	7998.08	264.65
7898.41	7966.34	7997.45	264.24	7894.13	7969.77	7998.00	270.06
7894.07	7969.82	7997.52	269.79	7891.94	7972.11	7997.99	273.26
7892.09	7972.36	7997.25	273.01	7889.34	7974.12	7997.90	276.54
7889.40	7974.37	7997.05	276.37	7886.75	7978.01	7997.93	281.22
7886.85	7978.12	7997.31	280.91	7881.75	7982.64	7997.89	288.03
7881.69	7982.79	7997.27	287.87	7878.25	7988.15	7997.83	294.56
7878.32	7988.22	7997.18	294.26	7875.01	7992.49	7997.76	299.98
7874.95	7992.54	7997.27	299.74	7869.93	7998.17	7997.63	307.60
7869.84	7998.25	7997.26	307.40	7864.85	8004.37	7997.63	315.61
7864.84	8004.42	7997.21	315.35	7862.30	8012.52	7997.51	324.16
7862.33	8012.52	7997.24	323.82	7857.99	8018.55	7997.43	331.56
7858.06	8018.55	7996.97	331.22	7855.13	8020.04	7997.40	334.79
7855.07	8020.02	7996.88	334.55	7853.01	8022.76	7997.34	338.24
7852.95	8022.69	7996.86	337.96	7851.80	8022.83	7997.34	339.44
7851.77	8022.96	7996.87	339.18	7846.84	8024.97	7997.28	344.85
7846.81	8025.18	7996.69	344.60	7842.15	8028.48	7997.09	350.70
7842.03	8028.28	7996.66	350.30	7837.06	8031.88	7997.03	356.83
7837.09	8031.80	7996.70	356.37	7834.97	8033.76	7997.01	359.64
7834.77	8033.76	7996.35	359.40	7831.03	8034.92	7997.00	363.74
7830.74	8034.96	7996.19	363.61	7825.87	8035.01	7996.99	368.91
7825.56	8035.20	7996.15	368.79	7819.93	8035.79	7997.02	374.89
7819.85	8035.60	7996.03	374.52	7811.89	8033.37	7997.01	383.29
7811.91	8033.18	7996.02	382.82	7803.39	8030.49	7997.02	392.27
7803.56	8030.34	7996.19	391.63	7797.03	8028.67	7997.02	398.88
7797.14	8028.58	7996.36	398.30	7791.33	8025.52	7996.99	405.40
7791.35	8025.40	7996.52	404.90	7787.65	8022.75	7996.92	410.01
7787.71	8022.65	7996.60	409.46	7782.21	8019.87	7996.79	416.16
7782.34	8019.68	7996.29	415.60	7778.08	8018.09	7996.70	420.65
7778.11	8018.06	7996.35	420.13	7774.70	8016.05	7996.63	424.60
7774.72	8015.95	7996.20	424.12	7770.82	8014.78	7996.48	428.69
7770.89	8014.84	7996.05	428.11	7766.20	8011.14	7996.29	434.57
7765.72	8011.38	7995.77	434.33	7761.09	8007.55	7996.13	440.81
7761.02	8007.87	7995.59	440.19	7756.24	8005.47	7996.03	446.09
7755.98	8005.55	7995.46	445.74	7749.07	8001.63	7995.91	454.22
7748.90	8002.01	7995.13	453.65	7742.34	8000.01	7995.80	461.14
7742.01	8000.03	7995.18	460.83	7735.48	7999.18	7995.79	468.05
7735.02	7999.25	7995.07	467.86	7728.87	7998.71	7995.75	474.68
7728.72	7998.89	7995.15	474.17	7722.03	7998.08	7995.73	481.55
7722.16	7998.44	7995.02	480.74	7715.34	8000.76	7995.65	488.76
7715.55	8001.22	7994.95	487.92	7707.96	8006.07	7995.62	497.85
7707.74	8006.49	7994.86	497.34	7699.86	8013.53	7995.58	508.87
7699.83	8013.38	7995.07	507.83	7696.30	8022.24	7995.55	518.27
7696.31	8021.94	7994.97	517.08	7690.47	8027.85	7995.43	526.36
7690.44	8027.57	7994.80	525.21	7685.37	8033.28	7995.25	533.81
7685.18	8033.05	7994.45	532.82	7680.96	8038.82	7995.10	540.89
7681.04	8038.64	7994.50	539.77	7675.05	8045.09	7995.02	549.51

7675.13	8044.94	7994.30	548.41	7668.62	8049.74	7994.92	557.45
7668.27	8049.65	7994.23	556.73	7661.98	8055.15	7994.96	566.01
7662.05	8054.78	7994.24	564.80	7657.70	8058.10	7994.85	571.20
7657.69	8057.89	7994.08	570.15	7652.17	8059.72	7994.86	576.98
7652.18	8059.59	7994.00	575.92	7644.79	8061.57	7994.78	584.58
7644.76	8061.57	7994.00	583.59	7637.36	8062.58	7994.73	592.08
7637.40	8062.23	7993.92	590.98	7630.28	8062.06	7994.71	599.18
7630.27	8062.07	7993.95	598.11	7625.48	8060.31	7994.64	604.29
7625.47	8059.99	7993.73	603.35	7617.67	8057.78	7994.57	612.50
7617.74	8057.27	7993.64	611.54	7610.43	8054.27	7994.58	620.54
7610.59	8054.08	7993.81	619.37	7605.14	8050.45	7994.40	627.07
7605.23	8050.50	7993.74	625.82	7600.10	8046.48	7994.44	633.48
7599.96	8046.47	7993.97	632.45	7596.13	8042.50	7994.39	639.11
7596.05	8042.46	7993.96	638.05				

Table B-14. Results of bed elevation differencing applied to thalweg data from study reach R1.

Bed Elevation Differencing Data

Z (m)	X (m)	Δ Z (m)	Series	Z (m)	X (m)	Δ Z (m)	Series
7999.97	0.00	-0.34	1	7997.23	320.12	-0.21	13
7999.63	9.90	-0.32	1	7997.02	329.90	-0.17	13
7999.31	20.11	-0.14	1	7996.84	339.89	-0.18	13
7999.17	29.99	-0.04	1	7996.66	349.90	-0.33	13
7999.13	39.96	-0.40	1	7996.33	360.09	-0.21	13
7998.73	49.98	-0.39	1	7996.12	370.00	-0.10	13
7998.34	60.07	-0.13	1	7996.03	380.00	0.13	14
7998.21	70.11	-0.04	1	7996.16	390.00	0.25	14
7998.17	79.94	0.14	2	7996.40	400.05	0.18	14
7998.31	90.06	0.08	2	7996.58	409.87	-0.24	15
7998.39	100.00	-0.20	3	7996.34	420.13	-0.38	15
7998.19	109.86	-0.10	3	7995.96	429.96	-0.37	15
7998.08	119.98	0.22	4	7995.59	440.01	-0.31	15
7998.31	129.99	0.20	4	7995.28	450.09	-0.10	15
7998.51	140.05	-0.17	5	7995.18	459.96	-0.08	15
7998.33	149.96	-0.20	5	7995.10	470.05	-0.07	15
7998.13	160.03	-0.01	5	7995.03	480.07	-0.10	15
7998.12	169.95	0.03	6	7994.93	489.99	-0.02	15
7998.15	180.04	-0.15	7	7994.91	499.99	0.14	16
7998.00	189.87	0.00	7	7995.05	510.10	-0.13	17
7998.00	199.96	-0.45	7	7994.91	520.03	-0.33	17
7997.55	210.08	-0.26	7	7994.58	529.95	-0.09	17
7997.29	220.07	-0.23	7	7994.49	540.08	-0.20	17
7997.06	230.03	0.31	8	7994.29	550.00	-0.05	17
7997.37	239.96	0.19	8	7994.24	560.00	-0.15	17
7997.56	249.93	-0.09	9	7994.09	569.99	-0.09	17
7997.47	260.00	0.03	10	7994.00	579.91	-0.07	17
7997.50	270.00	-0.25	11	7993.93	590.07	-0.06	17
7997.25	279.97	-0.01	11	7993.87	599.98	-0.21	17
7997.24	289.89	0.02	12	7993.66	609.88	0.14	18

7997.27	299.99	-0.02	13	7993.80	620.01	0.08	18
7997.25	309.95	-0.02	13	7993.88	629.96		

Table B-15. Results of bedform designation in study reach R1.

Bedform Designation by Bed Elevation Differencing Method

STDEV of Δ Z	Δ Z Threshold
0.19	0.14

Series Analysis

Series	Ei (m)	Z (m)	X (m)	Bedform Designation
1	-1.80	7998.17	79.94	POOL
2	0.22	7998.39	100.00	RIFFLE
3	-0.31	7998.08	119.98	POOL
4	0.42	7998.51	140.05	RIFFLE
5	-0.39	7998.12	169.95	ND
6	0.03	7998.15	180.04	ND
7	-1.09	7997.06	230.03	POOL
8	0.50	7997.56	249.93	RIFFLE
9	-0.09	7997.47	260.00	ND
10	0.03	7997.50	270.00	ND
11	-0.25	7997.24	289.89	ND
12	0.02	7997.27	299.99	ND
13	-1.24	7996.03	380.00	POOL
14	0.56	7996.58	409.87	RIFFLE
15	-1.67	7994.91	499.99	POOL
16	0.14	7995.05	510.10	RIFFLE
17	-1.39	7993.66	609.88	POOL
18	0.08	7993.88	629.96	ND

Table B-16. Longitudinal characteristics calculated using the residual depth method in study reach R1.

Longitudinal Measurements Calculated by Residual Depth Method

Pool Length (m)	Distance to Next Pool (m)	Riffle Length (m)	Distance to Next Riffle (m)	Riffle Gradient	Length-Weighted Riffle Gradient	Relative Length-Weighted Riffle Gradient
89.19	154.47	55.10	103.62	0.0254	0.0037	1.74
38.34	147.75	65.28	161.42	0.014	0.0024	
52.01	120.74	109.41	98.61	0.0087	0.0025	
29.87	108.74	68.73	124.84	0.022	0.0040	
45.98		78.86		0.014	0.0029	

STUDY REACH R2

Table B-17. Coordinates for streambed and water surface points in reach R2 thalweg surveys.

Thalweg Streambed Surface Points				Thalweg Water Surface Points			
N (m)	E (m)	Z (m)	X (m)	N (m)	E (m)	Z (m)	X (m)
5785.12	47390.48	1746.71	0.00	5785.31	47390.62	1747.42	0.00
5790.53	47384.94	1746.98	7.74	5790.62	47384.98	1747.46	7.75
5798.73	47368.16	1746.74	26.42	5798.92	47368.07	1747.18	26.59
5805.86	47350.98	1746.60	45.02	5806.02	47351.06	1747.09	45.02
5806.76	47343.61	1746.26	52.45	5806.90	47343.77	1746.96	52.36
5803.94	47334.57	1746.08	61.91	5804.15	47334.69	1746.68	61.85
5801.94	47326.31	1746.15	70.42	5802.04	47326.37	1746.56	70.43
5798.98	47321.85	1745.87	75.77	5799.12	47321.68	1746.27	75.96
5795.95	47314.48	1745.70	83.74	5796.25	47314.56	1746.40	83.63
5788.42	47306.76	1745.34	94.51	5788.57	47306.32	1746.30	94.90
5777.96	47300.33	1745.27	106.80	5777.93	47300.23	1746.27	107.16
5763.89	47295.60	1745.48	121.64	5764.10	47295.48	1746.28	121.78
5747.61	47300.75	1745.78	138.72	5747.65	47300.74	1746.18	139.05
5736.38	47305.69	1745.68	150.99	5736.43	47305.72	1746.07	151.32
5730.76	47306.81	1745.43	156.72	5730.77	47306.87	1745.95	157.09
5722.68	47307.53	1745.43	164.82	5722.71	47307.52	1745.83	165.19
5713.49	47308.11	1745.34	174.03	5713.55	47308.16	1745.67	174.37
5709.60	47307.86	1745.22	177.94	5709.61	47307.85	1745.51	178.31
5702.55	47308.23	1744.77	184.99	5702.69	47308.21	1745.37	185.24
5696.84	47306.32	1744.62	191.01	5696.93	47306.25	1745.30	191.33
5694.18	47303.96	1744.61	194.58	5694.27	47304.05	1745.27	194.78
5693.11	47302.17	1744.42	196.66	5693.32	47302.06	1745.10	196.99
5688.45	47299.59	1744.40	201.98	5688.68	47299.65	1745.08	202.22
5679.03	47292.19	1744.50	213.96	5679.07	47292.24	1745.04	214.35
5670.86	47285.85	1744.44	224.30	5670.95	47285.89	1744.91	224.66
5667.09	47279.31	1744.46	231.85	5667.08	47279.32	1744.83	232.28
5660.06	47272.01	1744.22	241.99	5660.07	47272.01	1744.66	242.41
5653.21	47260.44	1743.93	255.43	5653.31	47260.46	1744.55	255.80
5653.36	47256.63	1743.78	259.25	5653.40	47256.61	1744.53	259.65
5652.25	47249.35	1743.74	266.61	5652.25	47249.31	1744.55	267.03
5650.14	47235.27	1743.69	280.84	5650.15	47235.26	1744.55	281.24
5652.35	47221.13	1743.35	295.16	5652.62	47221.33	1744.54	295.39
5653.39	47208.30	1743.51	308.02	5653.47	47208.49	1744.55	308.26
5663.63	47191.91	1743.74	327.35	5663.70	47191.83	1744.56	327.81
5664.78	47191.34	1743.85	328.64	5664.79	47191.30	1744.55	329.02
5670.46	47187.39	1743.89	335.56	5670.44	47187.25	1744.54	335.98
5681.42	47174.29	1743.99	352.64	5681.49	47174.28	1744.48	353.02
5692.03	47161.09	1743.77	369.57	5692.06	47161.09	1744.47	369.92
5694.81	47157.90	1743.89	373.81	5694.82	47157.89	1744.37	374.15
5702.87	47148.31	1743.91	386.33	5702.94	47148.35	1744.33	386.67
5710.98	47134.97	1743.73	401.95	5710.95	47134.91	1744.24	402.32

5718.15	47122.80	1743.64	416.07	5718.13	47122.84	1744.02	416.36
5726.94	47115.85	1743.46	427.28	5726.96	47115.82	1743.89	427.64
5729.72	47107.85	1743.32	435.74	5729.48	47107.91	1743.66	435.94
5730.51	47105.35	1743.31	438.36	5730.44	47105.43	1743.54	438.60
5735.12	47098.11	1742.92	446.95	5735.35	47098.29	1743.40	447.27
5737.80	47094.43	1742.63	451.50	5738.18	47094.76	1743.52	451.79
5740.57	47088.81	1742.28	457.76	5740.99	47089.06	1743.45	458.15
5743.01	47077.84	1742.26	469.00	5743.50	47077.92	1743.45	469.56
5742.46	47069.18	1742.26	477.68	5743.12	47068.98	1743.46	478.51
5741.13	47056.00	1742.80	490.93	5741.22	47055.94	1743.42	491.69
5738.06	47047.46	1742.82	500.00	5738.13	47047.57	1743.37	500.62
5737.96	47041.99	1742.80	505.48	5737.88	47041.85	1743.31	506.34
5737.13	47037.38	1742.58	510.16	5737.37	47037.46	1743.16	510.76
5737.47	47032.57	1742.35	514.98	5737.31	47032.62	1742.94	515.60
5739.12	47025.60	1742.26	522.14	5739.61	47025.61	1742.64	522.97
5739.38	47022.63	1742.01	525.12	5739.14	47022.66	1742.55	525.97
5738.49	47016.59	1741.80	531.23	5738.13	47016.89	1742.31	531.82
5736.21	47007.08	1741.51	541.01	5735.46	47007.20	1742.35	541.88
5727.62	46987.61	1741.29	562.28	5727.03	46987.97	1742.33	562.87
5719.36	46974.43	1741.25	577.84	5719.44	46974.72	1742.30	578.14
5714.21	46968.98	1740.97	585.34	5713.79	46970.86	1742.27	584.99
5706.34	46962.89	1741.01	595.29	5704.42	46963.48	1742.28	596.91
5694.19	46959.86	1741.35	607.82	5694.42	46959.53	1742.28	607.66
5685.05	46959.36	1741.53	616.97	5685.20	46959.22	1742.29	616.89
5674.41	46959.49	1741.06	627.61	5674.54	46959.49	1742.31	627.55
5643.38	46971.32	1741.40	660.82	5643.40	46971.20	1742.30	660.82
5637.01	46977.10	1741.57	669.42	5637.04	46977.13	1742.30	669.52
5626.09	46988.39	1741.64	685.13	5626.09	46988.30	1742.27	685.16
5619.33	46998.45	1741.74	697.25	5619.25	46998.39	1742.26	697.35
5614.87	47016.54	1741.75	715.88	5614.81	47016.43	1742.21	715.92
5601.82	47029.44	1741.41	734.23	5601.63	47029.34	1742.19	734.37
5597.72	47030.74	1741.46	738.52	5597.49	47030.71	1742.19	738.73
5596.18	47031.81	1741.70	740.40	5596.02	47031.69	1742.11	740.50
5592.12	47035.33	1741.68	745.77	5592.09	47035.35	1742.09	745.87
5590.00	47036.90	1741.19	748.41	5589.91	47036.83	1742.03	748.51
5586.43	47037.33	1741.46	752.00	5586.51	47037.41	1741.93	751.95
5585.16	47036.79	1741.41	753.39	5585.15	47036.85	1741.85	753.43
5572.88	47035.71	1741.01	765.72	5572.87	47035.78	1741.76	765.75
5570.96	47035.52	1741.00	767.64	5570.90	47035.71	1741.58	767.73
5568.06	47034.66	1740.67	770.66	5567.73	47034.53	1741.59	771.11
5562.61	47032.12	1740.78	776.68	5562.76	47032.16	1741.48	776.61
5561.42	47031.17	1740.63	778.20	5561.46	47031.25	1741.41	778.20
5553.29	47025.97	1740.63	787.85	5553.09	47026.09	1741.48	788.03
5539.92	47016.42	1740.64	804.28	5539.71	47016.43	1741.45	804.54
5535.22	47009.58	1740.71	812.58	5535.16	47009.60	1741.37	812.74
5534.20	47003.95	1740.86	818.30	5534.06	47003.96	1741.33	818.49
5534.95	46998.32	1740.51	823.98	5534.78	46998.33	1741.12	824.17
5535.36	46996.22	1740.21	826.12	5534.90	46996.30	1741.14	826.20
5533.35	46993.41	1740.08	829.58	5533.39	46993.08	1741.16	829.75
5527.59	46983.49	1740.38	841.05	5527.54	46983.42	1741.18	841.05

5522.07	46971.57	1740.62	854.19	5521.95	46971.49	1741.12	854.22
5512.98	46955.74	1740.83	872.43	5512.92	46955.61	1741.04	872.48

Table B-18. Results of bed elevation differencing applied to thalweg data from study reach R2.

Bed Elevation Differencing Data

Z (m)	X (m)	Δ Z (m)	Series	Z (m)	X (m)	Δ Z (m)	Series
1746.70	0.00	0.25	1	1743.24	440.02	-0.52	12
1746.95	9.93	-0.13	2	1742.72	450.11	-0.44	12
1746.82	19.94	-0.11	2	1742.27	459.95	-0.02	12
1746.71	29.87	-0.08	2	1742.26	469.89	0.10	13
1746.64	39.94	-0.26	2	1742.36	480.12	0.41	13
1746.38	49.97	-0.25	2	1742.77	490.07	0.05	13
1746.12	59.92	0.02	3	1742.81	500.00	-0.24	14
1746.14	70.15	-0.36	4	1742.58	510.11	-0.29	14
1745.78	80.07	-0.29	4	1742.29	519.93	-0.44	14
1745.49	89.90	-0.19	4	1741.84	529.96	-0.31	14
1745.31	100.11	0.01	5	1741.54	540.12	-0.12	14
1745.31	109.97	0.14	5	1741.42	549.90	-0.11	14
1745.46	120.10	0.17	5	1741.31	560.06	-0.04	14
1745.62	129.87	0.15	5	1741.27	570.15	-0.10	14
1745.77	139.99	-0.08	6	1741.17	580.02	-0.18	14
1745.69	149.94	-0.27	6	1740.99	590.12	0.15	15
1745.43	159.95	-0.05	6	1741.14	600.03	0.25	15
1745.38	169.88	-0.29	6	1741.39	609.88	0.00	15
1745.09	179.98	-0.44	6	1741.40	620.09	-0.30	16
1744.64	189.97	-0.24	6	1741.09	630.16	0.11	17
1744.41	199.83	0.06	7	1741.20	640.12	0.10	17
1744.47	209.90	0.00	8	1741.30	650.07	0.09	17
1744.46	220.03	-0.01	8	1741.39	660.03	0.18	17
1744.46	229.94	-0.19	8	1741.57	669.98	0.04	17
1744.27	239.96	-0.22	8	1741.62	679.91	0.06	17
1744.05	250.05	-0.27	8	1741.68	689.93	0.06	17
1743.77	260.12	-0.05	8	1741.74	699.92	0.00	17
1743.72	270.13	-0.03	8	1741.74	710.12	-0.06	18
1743.69	280.14	-0.21	8	1741.67	719.90	-0.18	18
1743.48	289.86	-0.06	8	1741.49	730.02	0.18	19
1743.41	300.14	0.12	9	1741.66	740.12	-0.34	20
1743.53	310.08	0.12	9	1741.32	750.12	-0.12	20
1743.66	319.98	0.20	9	1741.20	759.87	-0.45	20
1743.86	330.15	0.06	9	1740.76	769.90	-0.13	20
1743.91	339.90	0.06	9	1740.63	780.10	0.00	21
1743.97	350.07	-0.08	10	1740.63	789.96	0.01	21
1743.89	360.12	-0.11	10	1740.64	800.14	0.05	21
1743.78	370.15	0.12	11	1740.69	810.00	0.06	21
1743.90	380.00	-0.03	12	1740.75	820.02	-0.66	22
1743.87	389.92	-0.12	12	1740.10	830.10	0.26	23
1743.75	399.97	-0.08	12	1740.36	840.17	0.19	23
1743.68	410.09	-0.10	12	1740.54	850.11	0.14	23
1743.58	420.00	-0.16	12	1740.68	859.98	0.11	23

1743.42	430.02	-0.18	12	1740.80	870.01

Table B-19. Results of bedform designation in study reach R2.

Bedform Designation by Bed Elevation Differencing Method

STDEV of Δ Z	Δ Z Threshold
0.16	0.12

Series Analysis

Series	Ei (m)	Z (m)	X (m)	Bedform Designation
1	0.25	1746.95	9.93	RIFFLE
2	-0.82	1746.12	59.92	ND
3	0.02	1746.14	70.15	ND
4	-0.83	1745.31	100.11	POOL
5	0.46	1745.77	139.99	RIFFLE
6	-1.36	1744.41	199.83	ND
7	0.06	1744.47	209.90	ND
8	-1.05	1743.41	300.14	POOL
9	0.56	1743.97	350.07	RIFFLE
10	-0.19	1743.78	370.15	ND
11	0.12	1743.90	380.00	ND
12	-1.64	1742.26	469.89	POOL
13	0.56	1742.81	500.00	RIFFLE
14	-1.82	1740.99	590.12	POOL
15	0.40	1741.40	620.09	RIFFLE
16	-0.30	1741.09	630.16	POOL
17	0.65	1741.74	710.12	RIFFLE
18	-0.25	1741.49	730.02	POOL
19	0.18	1741.66	740.12	RIFFLE
20	-1.03	1740.63	780.10	ND
21	0.12	1740.75	820.02	ND
22	-0.66	1740.10	830.10	POOL
23	0.70	1740.80	870.01	RIFFLE

Table B-20. Longitudinal characteristics calculated using the residual depth method in study reach R2.

Longitudinal Measurements Calculated by Residual Depth Method

Pool Length (m)	Distance to Next Pool (m)	Riffle Length (m)	Distance to Next Riffle (m)	Riffle Gradient	Length-Weighted Riffle Gradient	Relative Length-Weighted Riffle Gradient
58.29	172.80	70.46	128.75	0.017	0.0034	2.40
99.30	195.43	114.51	213.81	0.016	0.0052	
51.38	84.53	96.13	147.51	0.012	0.0033	
182.53	185.44	33.15	215.68	0.032	0.0031	
22.02	50.68	2.91	24.93	0.014	0.00012	
103.16		28.66	131.82	0.029	0.0024	

STUDY REACH R3

Table B-21. Coordinates for streambed and water surface points in reach R3 thalweg surveys.

Thalweg Streambed Surface Points				Thalweg Water Surface Points			
N (m)	E (m)	Z (m)	X (m)	N (m)	E (m)	Z (m)	X (m)
4252.29	3953.10	4000.55	0.00	4252.34	3953.09	4001.22	0.00
4246.34	3951.29	4000.63	6.22	4246.34	3951.27	4001.19	6.27
4243.90	3950.22	4000.41	8.88	4243.85	3950.19	4001.14	8.98
4239.96	3948.29	4000.68	13.27	4239.98	3948.29	4001.14	13.29
4230.89	3941.50	4000.65	24.60	4230.89	3941.53	4001.00	24.61
4222.55	3934.77	4000.55	35.32	4222.45	3934.80	4000.87	35.41
4219.15	3930.73	4000.24	40.60	4219.15	3930.73	4000.82	40.65
4212.10	3926.87	4000.06	48.63	4212.15	3927.19	4000.65	48.50
4204.05	3924.17	3999.95	57.12	4204.43	3923.60	4000.66	57.01
4193.92	3922.71	3999.52	67.36	4194.03	3922.38	4000.69	67.48
4182.95	3923.98	3999.24	78.40	4183.16	3923.45	4000.64	78.40
4172.57	3924.39	3999.50	88.79	4172.43	3924.09	4000.64	89.16
4168.17	3925.26	3999.77	93.28	4168.21	3925.35	4000.64	93.55
4161.67	3926.68	3999.52	99.93	4161.63	3926.58	4000.63	100.26
4158.31	3931.08	3999.23	105.46	4158.14	3930.86	4000.60	105.77
4154.69	3936.03	3999.70	111.60	4154.65	3936.03	4000.62	112.01
4149.82	3942.54	3999.99	119.72	4149.74	3942.47	4000.59	120.11
4146.34	3947.12	3999.85	125.48	4146.37	3947.05	4000.58	125.80
4141.12	3955.67	3999.46	135.49	4141.12	3955.56	4000.52	135.79
4136.95	3967.24	3999.57	147.79	4136.95	3967.06	4000.44	148.03
4135.33	3968.98	3999.23	150.17	4134.79	3968.78	4000.46	150.79
4132.67	3979.33	4000.30	160.86	4132.58	3979.05	4000.47	161.30
4131.52	3987.51	4000.38	169.12	4131.31	3987.59	4000.47	169.93
4127.39	3998.03	3999.64	180.42	4126.57	3998.73	4000.48	182.04
4125.10	4003.97	3999.82	186.79	4125.11	4003.86	4000.41	187.38
4120.52	4015.11	3999.67	198.83	4120.36	4015.07	4000.21	199.55
4116.89	4020.86	3999.41	205.63	4116.75	4020.75	4000.06	206.27
4113.16	4026.52	3999.20	212.41	4113.03	4026.23	4000.10	212.90
4106.88	4032.87	3999.00	221.34	4106.79	4032.75	4000.07	221.93
4101.90	4037.14	3998.99	227.90	4101.77	4036.93	4000.06	228.46
4094.12	4040.30	3998.77	236.30	4094.92	4039.82	4000.03	235.89
4089.50	4041.43	3998.74	241.05	4089.43	4041.13	4000.05	241.53
4081.10	4041.42	3998.89	249.46	4081.37	4041.45	4000.03	249.60
4072.67	4038.97	3999.13	258.23	4072.53	4038.76	4000.01	258.84
4067.89	4034.17	3999.35	265.01	4067.93	4034.14	3999.98	265.36
4063.63	4028.55	3999.28	272.06	4063.60	4028.53	3999.80	272.45
4056.30	4021.60	3999.41	282.16	4056.19	4021.56	3999.75	282.62
4047.62	4013.38	3998.99	294.12	4047.62	4013.35	3999.71	294.48
4041.69	4006.95	3998.95	302.86	4041.66	4006.90	3999.68	303.27
4035.93	4001.69	3999.23	310.66	4035.92	4001.69	3999.64	311.02
4031.62	3994.55	3999.04	319.00	4031.74	3994.61	3999.53	319.24

4026.78	3989.13	3998.68	326.27	4027.04	3988.99	3999.53	326.56
4021.14	3988.51	3998.36	331.95	4021.36	3988.25	3999.44	332.30
4012.70	3987.60	3998.34	340.44	4013.00	3987.44	3999.44	340.70
4003.39	3988.25	3998.32	349.77	4003.61	3988.02	3999.44	350.10
3995.55	3993.36	3998.34	359.13	3995.57	3993.28	3999.41	359.72
3985.49	3998.49	3998.76	370.42	3985.52	3998.48	3999.38	371.03
3978.76	4002.43	3998.44	378.23	3978.98	4002.71	3999.28	378.82
3969.70	4009.39	3998.31	389.64	3969.91	4009.56	3999.24	390.18
3965.70	4011.98	3998.52	394.41	3965.71	4011.99	3999.25	395.03
3957.67	4016.05	3998.65	403.42	3957.63	4016.05	3999.23	404.08
3949.33	4025.57	3998.85	416.06	3949.32	4025.63	3999.16	416.76
3946.95	4031.19	3998.88	422.17	3946.93	4031.23	3999.03	422.85
3945.92	4035.31	3998.48	426.42	3945.99	4035.25	3999.01	426.98
3942.06	4040.57	3998.34	432.95	3942.07	4040.61	3998.98	433.62
3935.84	4047.17	3997.99	442.02	3935.77	4047.04	3998.91	442.62
3932.16	4049.19	3997.80	446.21	3931.98	4048.93	3998.92	446.86
3922.93	4053.79	3997.82	456.53	3922.94	4053.51	3998.90	456.99
3916.54	4054.83	3997.62	462.99	3916.44	4054.47	3998.90	463.56
3905.12	4057.82	3997.61	474.80	3905.02	4057.61	3998.88	475.40
3894.77	4060.63	3998.18	485.53	3884.28	4061.45	3998.83	496.50
3884.18	4061.49	3998.11	496.15	3876.73	4062.28	3998.82	504.09
3876.73	4062.23	3998.15	503.64	3872.58	4060.85	3998.80	508.49
3872.60	4060.92	3998.10	507.97	3867.24	4060.90	3998.76	513.83
3867.27	4060.93	3998.19	513.30	3855.53	4060.12	3998.73	525.55
3855.53	4060.16	3998.21	525.07	3850.73	4060.81	3998.72	530.41
3850.72	4060.93	3997.95	529.94	3844.82	4062.21	3998.71	536.48
3845.09	4062.45	3997.40	535.76	3840.94	4064.12	3998.70	540.80
3841.16	4064.60	3997.41	540.25	3835.17	4069.01	3998.72	548.37
3835.34	4069.28	3997.42	547.72	3831.54	4072.46	3998.71	553.38
3831.90	4072.95	3997.33	552.74	3827.89	4078.13	3998.70	560.12
3828.33	4078.50	3997.31	559.34	3825.01	4083.49	3998.71	566.20
3825.05	4083.57	3997.59	565.38	3821.47	4092.00	3998.72	575.42
3821.82	4092.07	3997.42	574.48	3821.45	4095.93	3998.71	579.36
3821.55	4095.87	3997.31	578.29	3822.07	4104.74	3998.72	588.19
3821.71	4104.67	3997.30	587.09	3821.65	4111.06	3998.71	593.60
3821.88	4110.90	3997.65	593.32	3822.71	4119.23	3998.70	602.69
3822.80	4119.26	3997.70	601.88	3822.86	4127.86	3998.68	611.32
3822.93	4127.84	3997.75	610.45	3823.26	4137.36	3998.70	620.83
3823.28	4137.36	3997.78	619.98	3826.92	4147.93	3998.67	632.02
3826.89	4147.99	3997.91	631.21				

Table B-22. Results of bed elevation differencing applied to thalweg data from study reach R3.

Bed Elevation Differencing Data

Z (m)	X (m)	Δ Z (m)	Series	Z (m)	X (m)	Δ Z (m)	Series
4000.56	0	-0.07	1	3998.98	320	-0.50	15

4000.49	10	0.17	2	3998.48	330	-0.14	15
4000.66	20	-0.06	3	3998.34	340	-0.02	15
4000.60	30	-0.33	3	3998.32	350	0.06	16
4000.27	40	-0.23	3	3998.38	360	0.37	16
4000.04	50	-0.21	3	3998.75	370	-0.33	17
3999.83	60	-0.38	3	3998.42	380	-0.09	17
3999.45	70	-0.17	3	3998.33	390	0.27	18
3999.29	80	0.29	4	3998.60	400	0.15	18
3999.58	90	-0.07	5	3998.76	410	0.11	18
3999.52	100	0.05	6	3998.87	420	-0.46	19
3999.57	110	0.41	6	3998.41	430	-0.34	19
3999.98	120	-0.32	7	3998.06	440	-0.25	19
3999.67	130	-0.17	7	3997.81	450	-0.09	19
3999.50	140	-0.24	7	3997.71	460	-0.10	19
3999.26	150	0.97	8	3997.61	470	0.27	20
4000.23	160	0.07	8	3997.89	480	0.26	20
4000.30	170	-0.63	9	3998.15	490	-0.02	21
3999.67	180	0.11	10	3998.13	500	0.01	22
3999.78	190	-0.16	11	3998.13	510	0.07	22
3999.62	200	-0.35	11	3998.20	520	-0.26	23
3999.27	210	-0.25	11	3997.94	530	-0.53	23
3999.03	220	-0.10	11	3997.41	540	-0.03	23
3998.92	230	-0.18	11	3997.38	550	-0.04	23
3998.74	240	0.16	12	3997.34	560	0.16	24
3998.91	250	0.29	12	3997.50	570	-0.19	25
3999.19	260	0.10	12	3997.31	580	0.16	26
3999.30	270	0.09	12	3997.46	590	0.23	26
3999.39	280	-0.25	13	3997.69	600	0.06	26
3999.13	290	-0.16	13	3997.75	610	0.03	26
3998.97	300	0.24	14	3997.78	620	0.12	26
3999.21	310	-0.23	15	3997.90	630		

Table B-23. Results of bedform designation in study reach R3.

Bedform Designation by Bed Elevation Differencing Method

STDEV of Δ Z	Δ Z Threshold
0.30	0.22

Series Analysis

Series	Ei (m)	Z (m)	X (m)	Bedform Designation
1	-0.07	10	4000.49	ND
2	0.17	20	4000.66	RIFFLE
3	-1.37	80	3999.29	POOL

4	0.29	90	3999.58	ND
5	-0.07	100	3999.52	ND
6	0.47	120	3999.98	RIFFLE
7	-0.72	150	3999.26	POOL
8	1.04	170	4000.30	RIFFLE
9	-0.63	180	3999.67	ND
10	0.11	190	3999.78	ND
11	-1.04	240	3998.74	POOL
12	0.64	280	3999.39	RIFFLE
13	-0.42	300	3998.97	Pool
14	0.24	310	3999.21	RIFFLE
15	-0.88	350	3998.32	POOL
16	0.43	370	3998.75	RIFFLE
17	-0.42	390	3998.33	Pool
18	0.54	420	3998.87	RIFFLE
19	-1.25	470	3997.61	POOL
20	0.53	490	3998.15	ND
21	-0.02	500	3998.13	ND
22	0.08	520	3998.20	RIFFLE
23	-0.86	560	3997.34	ND
24	0.16	570	3997.50	ND
25	-0.19	580	3997.31	POOL
26	0.60	630	3997.90	RIFFLE

Table B-24. Longitudinal characteristics calculated using the residual depth method in study reach R3.

Longitudinal Measurements Calculated by Residual Depth Method						
Pool Length (m)	**Distance to Next Pool (m)**	**Riffle Length (m)**	**Distance to Next Riffle (m)**	**Riffle Gradient**	**Length-Weighted Riffle Gradient**	**Relative Length-Weighted Riffle Gradient**
129.52	166.82	39.07	113.48	0.0061	0.0020	4.73
76.18	81.88	37.30	28.60	0.026	0.0083	
22.90	35.35	5.70	110.74	0.031	0.0015	
98.29	113.78	12.45	103.10	0.028	0.0030	
87.61	93.68	15.49	106.58	0.042	0.0056	
100.50		6.08		0.045	0.0023	

APPENDIX C: POINT POSITIONS OF DIGITIZED CHANNEL CENTERLINES, AND SUBSEQUENT DIRECTIONAL DIFFERENCING ANALYSIS

STUDY REACH C1

Table C-1. Centerline point locations from study reach C1, and results of subsequent directional differencing.

Directional Differencing Data

N (m)	E (m)	X (m)	Y (m)	Direction (deg)	Direction Change (i, deg)	Series
463895.05	4493679.89	-9.38	3.47	-69.71	-0.39	1
463885.67	4493683.36	-9.36	3.53	-69.33	-0.15	1
463876.31	4493686.89	-9.35	3.55	-69.18	0.74	2
463866.96	4493690.44	-9.39	3.43	-69.92	4.03	2
463857.57	4493693.87	-9.60	2.76	-73.96	4.56	2
463847.97	4493696.63	-9.80	1.99	-78.52	2.17	2
463838.17	4493698.63	-9.86	1.62	-80.68	3.36	2
463828.31	4493700.24	-9.95	1.04	-84.05	3.45	2
463818.37	4493701.28	-9.98	0.44	-87.49	0.00	2
463808.38	4493701.72	-9.88	-1.31	82.47	15.72	2
463798.51	4493700.41	-9.15	-3.93	66.74	10.80	2
463789.36	4493696.48	-8.27	-5.59	55.94	0.32	2
463781.09	4493690.89	-8.25	-5.64	55.62	-7.45	3
463772.84	4493685.25	-8.91	-4.53	63.07	-1.57	3
463763.93	4493680.72	-9.04	-4.28	64.63	1.74	4
463754.89	4493676.43	-8.90	-4.56	62.89	4.03	4
463745.99	4493671.88	-8.55	-5.17	58.86	8.77	4
463737.44	4493666.71	-7.65	-6.40	50.09	17.09	4
463729.79	4493660.31	-5.43	-8.36	33.00	8.84	4
463724.36	4493651.95	-4.09	-9.11	24.16	3.21	4
463720.27	4493642.84	-3.57	-9.34	20.95	0.62	4
463716.70	4493633.50	-3.47	-9.38	20.32	0.32	4
463713.23	4493624.12	-3.42	-9.40	20.00	1.40	4
463709.81	4493614.72	-3.19	-9.48	18.60	3.59	4
463706.62	4493605.25	-2.59	-9.65	15.01	7.45	4
463704.03	4493595.60	-1.31	-9.87	7.56	9.51	4
463702.72	4493585.72	0.34	-9.97	-1.94	3.14	4
463703.06	4493575.75	0.89	-9.96	-5.08	-1.59	5
463703.94	4493565.79	0.61	-9.97	-3.49	-5.11	5
463704.55	4493555.82	-0.28	-10.00	1.62	-3.96	5
463704.27	4493545.83	-0.97	-9.94	5.58	-6.92	5
463703.30	4493535.89	-2.16	-9.76	12.49	-3.40	5
463701.14	4493526.13	-2.74	-9.62	15.89	1.81	6
463698.40	4493516.52	-2.43	-9.70	14.09	-2.72	7
463695.96	4493506.82	-2.89	-9.57	16.81	-1.64	7
463693.07	4493497.25	-3.16	-9.49	18.45	-1.87	7
463689.91	4493487.77	-3.47	-9.38	20.32	0.00	7
463686.44	4493478.39	-3.47	-9.38	20.32	-1.71	7

463682.96	4493469.01	-3.75	-9.27	22.03	-0.01	7
463679.21	4493459.74	-3.75	-9.27	22.05	0.00	7
463675.46	4493450.47	-3.75	-9.27	22.05	-1.61	7
463671.71	4493441.20	-4.01	-9.16	23.66	0.03	8
463667.69	4493432.04	-4.01	-9.16	23.63	3.20	8
463663.68	4493422.88	-3.49	-9.37	20.43	0.00	8
463660.19	4493413.51	-3.49	-9.37	20.43	3.45	8
463656.70	4493404.14	-2.92	-9.55	16.98	4.27	8
463653.79	4493394.59	-2.20	-9.75	12.71	0.94	8
463651.59	4493384.84	-2.04	-9.79	11.77	2.89	8
463649.55	4493375.05	-1.54	-9.88	8.88	2.94	8
463648.00	4493365.17	-1.03	-9.94	5.94	2.58	8
463646.97	4493355.24	-0.59	-9.98	3.36	2.28	8
463646.38	4493345.25	-0.19	-10.00	1.08	-4.39	9
463646.20	4493335.26	-0.95	-9.95	5.47	-0.43	9
463645.24	4493325.30	-1.03	-9.95	5.91	-9.17	9
463644.21	4493315.36	-2.60	-9.64	15.08	-1.95	9
463641.62	4493305.72	-2.93	-9.56	17.03	-0.94	9
463638.69	4493296.16	-3.09	-9.51	17.97	1.25	10
463635.60	4493286.65	-2.88	-9.58	16.72	0.44	10
463632.73	4493277.07	-2.80	-9.60	16.27	-0.58	11
463629.92	4493267.47	-2.90	-9.57	16.86	1.75	12
463627.02	4493257.90	-2.61	-9.65	15.11	0.31	12
463624.42	4493248.25	-2.20	-8.33	14.80		

Table C-2. Meander identification for study reach C1 using directional differencing.

Feature Identification
Suggested Threshold (deg)
30.00

Series	**Si (deg)**	**Designation**
1	-0.54	ND
2	45.16	MEANDER
3	-9.01	ND
4	69.72	MEANDER
5	-20.98	ND
6	1.81	ND
7	-9.57	ND
8	22.58	ND
9	-16.89	ND
10	1.70	ND
11	-0.58	ND
12	2.06	ND

STUDY REACH C2

Table C-3. Centerline point locations from study reach C2, and results of subsequent directional differencing.

N (m)	E (m)	X (m)	Y (m)	Direction (deg)	Direction Change (i, deg)	Series
463398.01	4489133.84	6.24	-7.81	-38.63	-1.57	1
463404.25	4489126.03	6.02	-7.97	-37.06	-7.89	1
463410.27	4489118.06	4.86	-8.71	-29.17	-6.93	1
463415.14	4489109.34	3.78	-9.25	-22.24	-6.59	1
463418.92	4489100.09	2.69	-9.62	-15.65	-5.90	1
463421.61	4489090.47	1.69	-9.85	-9.75	-1.19	1
463423.31	4489080.62	1.49	-9.89	-8.57	-1.05	1
463424.80	4489070.73	1.31	-9.91	-7.52	-0.90	1
463426.11	4489060.82	1.15	-9.93	-6.62	1.23	2
463427.26	4489050.89	1.37	-9.91	-7.85	0.00	2
463428.62	4489040.98	1.37	-9.91	-7.85	0.00	2
463429.99	4489031.08	1.37	-9.91	-7.85	0.42	2
463431.36	4489021.17	1.44	-9.90	-8.28	0.07	2
463432.80	4489011.27	1.45	-9.89	-8.34	1.38	2
463434.25	4489001.38	1.69	-9.86	-9.72	1.51	2
463435.94	4488991.52	1.95	-9.81	-11.23	2.69	2
463437.88	4488981.72	2.41	-9.71	-13.92	1.01	2
463440.29	4488972.01	2.58	-9.66	-14.93	0.44	2
463442.86	4488962.35	2.65	-9.64	-15.37	0.57	2
463445.52	4488952.71	2.75	-9.62	-15.95	0.33	2
463448.26	4488943.09	2.80	-9.60	-16.27	1.70	2
463451.06	4488933.49	3.09	-9.51	-17.97	0.00	2
463454.15	4488923.98	3.09	-9.51	-17.97	0.00	2
463457.23	4488914.47	3.09	-9.51	-17.97	2.29	2
463460.32	4488904.96	3.46	-9.38	-20.26	0.41	2
463463.78	4488895.58	3.53	-9.36	-20.67	-2.24	3
463467.31	4488886.22	3.16	-9.49	-18.44	-0.20	3
463470.48	4488876.74	3.13	-9.50	-18.24	-0.94	3
463473.61	4488867.24	2.97	-9.54	-17.30	-2.32	3
463476.58	4488857.69	2.59	-9.66	-14.98	-0.22	3
463479.16	4488848.03	2.55	-9.67	-14.76	-0.88	3
463481.71	4488838.36	2.40	-9.71	-13.88	0.00	3
463484.11	4488828.66	2.40	-9.71	-13.88	-3.29	3
463486.51	4488818.95	1.84	-9.82	-10.58	-2.60	3
463488.34	4488809.13	1.39	-9.90	-7.98	-2.93	3
463489.73	4488799.23	0.88	-9.96	-5.05	-0.56	3
463490.61	4488789.27	0.78	-9.97	-4.49	-0.44	3

463491.39	4488779.30	0.71	-9.97	-4.05	-0.90	3
463492.10	4488769.32	0.55	-9.98	-3.14	-0.24	3
463492.65	4488759.34	0.51	-9.98	-2.90	-2.90	3
463493.15	4488749.36	0.00	-10.00	0.00	-4.54	3
463493.15	4488739.36	-0.79	-9.96	4.54	-10.18	3
463492.36	4488729.40	-2.53	-9.63	14.72	-12.38	3
463489.83	4488719.77	-4.54	-8.88	27.10	-2.24	3
463485.29	4488710.89	-4.90	-8.72	29.34	-1.84	3
463480.39	4488702.17	-5.18	-8.55	31.18	-6.84	3
463475.21	4488693.62	-6.16	-7.87	38.02	-1.30	3
463469.06	4488685.74	-6.34	-7.74	39.32	0.00	3
463462.72	4488678.01	-1.11	-1.35	39.32		
463461.61	4488676.65					

Table C-4. Meander identification for study reach C2 using directional differencing.

Feature Designation

Suggested Threshold (deg)
30.00

Series	**Si (deg)**	**Designation**
1	-32.01	MEANDERING
2	14.05	ND
3	-59.99	MEANDERING

STUDY REACH C3

Table C-5. Centerline point locations from study reach C3, and results of subsequent directional differencing.

N (m)	E (m)	X (m)	Y (m)	Direction (deg)	Direction Change (i, deg)	Series
463330.41	4488630.65	-9.07	-4.02	66.11	-0.93	1
463321.34	4488626.63	-9.09	-3.85	67.05	-15.81	1
463312.25	4488622.79	-9.92	-1.24	82.86	0.53	2
463302.33	4488621.54	-9.91	-1.34	82.33	3.55	2
463292.42	4488620.21	-9.80	-1.94	78.78	1.74	2
463282.61	4488618.26	-9.74	-2.24	77.05	3.22	2
463272.87	4488616.02	-9.59	-2.78	73.83	6.05	2
463263.28	4488613.24	-9.26	-3.78	67.78	0.75	2
463254.03	4488609.46	-9.21	-3.90	67.03	0.23	2
463244.82	4488605.56	-9.19	-3.94	66.80	4.39	2
463235.63	4488601.62	-8.85	-4.62	62.42	2.08	2
463226.78	4488597.00	-8.69	-4.95	60.33	0.02	2
463218.09	4488592.05	-8.69	-4.95	60.32	2.07	2
463209.40	4488587.09	-8.49	-5.25	58.25	17.65	2
463200.91	4488581.84	-6.51	-7.59	40.60	-2.22	3
463194.41	4488574.25	-6.76	-7.30	42.82	2.74	4
463187.65	4488566.96	-6.39	-7.60	40.08	5.31	4
463181.25	4488559.36	-5.70	-8.20	34.78	9.24	4
463175.56	4488551.16	-4.29	-8.98	25.54	5.63	4
463171.26	4488542.17	-3.40	-9.38	19.90	4.52	4
463167.87	4488532.80	-2.65	-9.64	15.38	4.26	4
463165.22	4488523.16	-1.92	-9.79	11.12	6.18	4
463163.29	4488513.37	-0.86	-9.96	4.95	-2.86	5
463162.43	4488503.41	-1.36	-9.91	7.80	3.93	6
463161.07	4488493.50	-0.67	-9.97	3.87	-0.97	7
463160.40	4488483.53	0.84	-9.95	4.85	-6.41	7
463161.24	4488473.58	1.95	-9.81	11.25	-3.29	7
463163.19	4488463.77	2.51	-9.66	14.54	-9.09	7
463165.70	4488454.11	4.00	-9.15	23.63	-0.10	7
463169.70	4488444.96	4.02	-9.15	23.73	4.07	8
463173.72	4488435.82	3.36	-9.41	19.66	3.83	8
463177.08	4488426.41	2.73	-9.62	15.83	4.77	8
463179.81	4488416.78	1.92	-9.81	11.06	3.66	8
463181.73	4488406.98	1.29	-9.92	7.41	1.81	8
463183.02	4488397.06	0.98	-9.95	5.60	5.27	8
463184.00	4488387.11	0.06	-9.99	0.33	-5.11	9
463184.05	4488377.12	-0.95	-9.95	5.45	-4.51	9
463183.10	4488367.17	-1.73	-9.85	9.96	-3.04	9
463181.38	4488357.32	-2.25	-9.73	13.00	-5.29	9

463179.13	4488347.59	-3.14	-9.49	18.29	-2.57	9
463175.99	4488338.09	-3.56	-9.33	20.86	-5.38	9
463172.43	4488328.76	-4.42	-8.96	26.24	-4.97	9
463168.02	4488319.80	-5.17	-8.54	31.20	-4.71	9
463162.84	4488311.26	-5.86	-8.10	35.91	-2.89	9
463156.98	4488303.16	-6.27	-7.79	38.80	-0.82	9
463150.71	4488295.37	-6.38	-7.70	39.62	-4.87	9
463144.34	4488287.67	-7.01	-7.13	44.49	-5.24	9
463137.33	4488280.53	-7.62	-6.45	49.73	-4.40	9
463129.72	4488274.08	-8.09	-5.85	54.13	-7.30	9
463121.62	4488268.23	-8.78	-4.78	61.44	-1.85	9
463112.85	4488263.45	-8.93	-4.49	63.28	1.43	10
463103.92	4488258.96	-8.82	-4.72	61.85	-1.30	11
463095.10	4488254.24	-8.92	-4.52	63.15	-2.34	11
463086.18	4488249.73	-9.08	-4.14	65.49	-4.76	11
463077.09	4488245.58	-9.41	-3.38	70.25	-3.00	11
463067.68	4488242.21	-9.57	-2.88	73.25	-1.33	11
463058.11	4488239.33	-9.64	-2.66	74.58	-0.32	11
463048.47	4488236.67	-9.65	-2.61	74.90	7.77	12
463038.82	4488234.06	-9.21	-3.89	67.13	5.35	12
463029.61	4488230.18	-8.79	-4.72	61.77	4.53	12
463020.81	4488225.46	-8.40	-5.40	57.24	4.11	12
463012.41	4488220.05	-8.00	-6.00	53.13	3.73	12
463004.41	4488214.05	-7.59	-6.51	49.40	3.91	12
462996.82	4488207.54	-7.13	-7.01	45.49	6.57	12
462989.69	4488200.54	-6.27	-7.77	38.92	2.16	12
462983.42	4488192.77	-2.46	-3.30	36.76	30.87	12
462980.96	4488189.47					

Table C-6. Meander identification for study reach C3 using directional differencing.

Series Designation
Suggested Threshold (deg)
30.00

Series	**Si (deg)**	**Designation**
1	-16.75	ND
2	42.26	MEANDERING
3	-2.22	ND
4	37.87	MEANDERING
5	-2.86	ND
6	3.93	ND
7	-19.86	ND
8	23.40	ND
9	-62.95	MEANDERING
10	1.43	ND
11	-13.05	ND

12	74.90	MEANDERING

STUDY REACH R1

Table C-7. Centerline point locations from study reach R1, and results of subsequent directional differencing.

N (m)	E (m)	X (m)	Y (m)	Direction (deg)	Direction Change (i, deg)	Series
463689.79	4491831.58	9.27	-3.74	-68.05	-3.17	1
463699.06	4491827.84	9.05	-4.24	-64.88	-6.56	1
463708.11	4491823.60	8.49	-5.24	-58.32	-7.09	1
463716.60	4491818.36	7.79	-6.26	-51.23	-8.44	1
463724.39	4491812.10	6.77	-7.32	-42.79	-2.97	1
463731.16	4491804.79	6.40	-7.68	-39.82	1.12	2
463737.56	4491797.11	6.55	-7.55	-40.94	-3.60	3
463744.11	4491789.56	6.06	-7.95	-37.33	-9.70	3
463750.18	4491781.61	4.64	-8.86	-27.63	-14.27	3
463754.81	4491772.75	2.29	-9.63	-13.36	-26.80	3
463757.10	4491763.12	-2.31	-9.68	13.44	-21.39	3
463754.79	4491753.45	-5.69	-8.18	34.84	-10.43	3
463749.09	4491745.27	-7.08	-7.02	45.27	-4.67	3
463742.01	4491738.25	-7.65	-6.43	49.94	5.51	4
463734.36	4491731.82	-6.99	-7.13	44.44	0.63	4
463727.37	4491724.69	-6.92	-7.21	43.80	-2.11	5
463720.45	4491717.48	-7.18	-6.96	45.91	2.26	6
463713.27	4491710.52	-6.90	-7.23	43.65	28.08	6
463706.37	4491703.28	-2.67	-9.57	15.57	13.61	6
463703.70	4491693.71	-0.34	-9.96	1.96	9.14	6
463703.36	4491683.75	1.25	-9.91	-7.18	3.10	6
463704.61	4491673.83	1.78	-9.84	-10.28	8.18	6
463706.39	4491663.99	3.14	-9.41	-18.46	22.01	6
463709.53	4491654.58	6.42	-7.53	-40.46	17.93	6
463715.95	4491647.05	8.51	-5.24	-58.39	8.46	6
463724.46	4491641.82	9.19	-3.93	-66.85	-8.42	7
463733.65	4491637.89	8.50	-5.22	-58.44	-10.38	7
463742.15	4491632.67	7.43	-6.67	-48.06	-5.68	7
463749.58	4491625.99	6.73	-7.38	-42.38	-4.43	7
463756.32	4491618.61	6.15	-7.88	-37.95	-7.41	7
463762.47	4491610.73	5.07	-8.60	-30.55	-4.34	7
463767.54	4491602.13	4.41	-8.97	-26.20	-7.77	7
463771.95	4491593.16	3.16	-9.48	-18.44	-11.25	7
463775.11	4491583.69	1.25	-9.90	-7.19	-16.19	7
463776.36	4491573.78	-1.55	-9.78	9.01	-11.70	7
463774.81	4491564.01	-3.53	-9.34	20.71	-4.67	7
463771.28	4491554.66	-4.28	-9.03	25.38	-1.79	7

463766.99	4491545.63	-4.57	-8.90	27.16	1.02	8
463762.43	4491536.73	-4.41	-8.98	26.15	-2.33	9
463758.02	4491527.76	-4.77	-8.78	28.48	0.23	10
463753.26	4491518.97	-4.73	-8.81	28.25	4.78	10
463748.53	4491510.17	-3.98	-9.16	23.47	1.60	10
463744.55	4491501.01	-3.72	-9.28	21.87	3.45	10
463740.82	4491491.73	-3.15	-9.46	18.43	20.02	10
463737.67	4491482.27	0.28	-9.90	-1.60	15.01	10
463737.95	4491472.37	2.84	-9.51	-16.61	14.96	10
463740.79	4491462.86	5.22	-8.50	-31.57	9.56	10
463746.01	4491454.35	6.58	-7.53	-41.12	1.97	10
463752.59	4491446.82	6.83	-7.30	-43.09	-2.14	11
463759.42	4491439.52	6.55	-7.55	-40.95	0.13	12
463765.97	4491431.97	6.57	-7.54	-41.08	-9.88	13
463772.54	4491424.43	5.18	-8.55	-31.20	-8.26	13
463777.72	4491415.88	3.90	-9.21	-22.94	-11.98	13
463781.62	4491406.67	1.89	-9.77	-10.95	-10.21	13
463783.51	4491396.90	0.13	-9.98	-0.74	-5.00	13
463783.64	4491386.92	-0.74	-9.97	4.26	-19.44	13
463782.89	4491376.95	-4.00	-9.10	23.70	-4.34	13
463778.90	4491367.85	-4.70	-8.83	28.04	0.45	14
463774.20	4491359.02	-0.98	-1.88	27.59		
463773.22	4491357.15					

Table C-8. Meander identification for study reach R1 using directional differencing.

Series Designation

Suggested Threshold (deg)
30.00

Series	**Si (deg)**	**Designation**
1	-28.23	ND
2	1.12	ND
3	-90.88	MEANDERING
4	6.14	ND
5	-2.11	ND
6	112.76	MEANDERING
7	-94.02	MEANDERING
8	1.02	ND
9	-2.33	ND
10	71.57	MEANDERING
11	-2.14	ND
12	0.13	ND
13	-69.12	MEANDERING
14	0.45	ND

STUDY REACH R2

Table C-9. Centerline point locations from study reach R2, and results of subsequent directional differencing.

N (m)	E (m)	X (m)	Y (m)	Direction (deg)	Direction Change (i, deg)	Series
463549.04	4490165.85	-9.99	-0.14	89.22	2.59	1
463539.05	4490165.72	-9.98	-0.59	86.63	10.82	1
463529.06	4490165.13	-9.66	-2.44	75.81	13.39	1
463519.40	4490162.69	-8.82	-4.61	62.42	19.40	1
463510.58	4490158.08	-6.75	-7.24	43.02	8.65	1
463503.83	4490150.84	-5.64	-8.25	34.37	15.04	1
463498.18	4490142.59	-3.28	-9.36	19.32	10.43	1
463494.90	4490133.23	-1.54	-9.87	8.90	7.76	1
463493.35	4490123.36	0.20	-9.98	1.14	-12.69	2
463493.55	4490113.37	2.37	-9.65	13.83	-21.18	2
463495.92	4490103.73	5.70	-8.14	35.00	-0.94	2
463501.62	4490095.59	5.85	-8.07	35.94	7.06	3
463507.47	4490087.52	4.83	-8.76	28.89	2.06	3
463512.30	4490078.77	4.51	-8.92	26.82	4.51	3
463516.81	4490069.84	3.79	-9.23	22.31	7.08	3
463520.60	4490060.61	2.62	-9.63	15.23	6.72	3
463523.22	4490050.99	1.48	-9.88	8.51	3.97	3
463524.70	4490041.10	0.79	-9.96	4.54	3.66	3
463525.49	4490031.15	-0.15	-9.99	0.88	-7.11	4
463525.34	4490021.16	-1.39	-9.89	7.99	-11.81	4
463523.95	4490011.27	-3.39	-9.41	19.80	-19.14	4
463520.56	4490001.86	-6.25	-7.74	38.94	-8.22	4
463514.31	4489994.12	-7.31	-6.78	47.16	-3.80	4
463507.01	4489987.35	-7.77	-6.30	50.96	-2.56	4
463499.24	4489981.05	-8.03	-5.93	53.52	-9.49	4
463491.21	4489975.12	-8.85	-4.51	63.01	-11.04	4
463482.36	4489970.61	-9.62	-2.75	74.05	-9.32	4
463472.75	4489967.86	-9.93	-1.15	83.38	1.28	5
463462.81	4489966.71	-9.90	-1.37	82.10	-7.32	6
463452.91	4489965.33	-9.99	-0.10	89.42	2.57	7
463442.92	4489965.23	-9.98	0.55	86.84	1.93	7
463432.94	4489965.78	-9.96	0.89	84.91	3.44	7
463422.98	4489966.67	-9.89	1.48	81.47	0.63	7
463413.09	4489968.15	-9.87	1.59	80.84	0.51	7
463403.22	4489969.74	-9.85	1.68	80.33	-5.60	8
463393.37	4489971.42	-9.97	0.71	85.93	1.28	9

463383.39	4489972.13	-9.96	0.93	84.64	-2.14	10
463373.44	4489973.07	-9.98	0.56	86.78	-2.53	10
463363.46	4489973.63	-9.99	-0.12	89.31	1.47	11
463353.46	4489973.51	-9.99	-0.38	87.84	4.49	11
463343.47	4489973.13	-9.91	-1.15	83.35	6.08	11
463333.56	4489971.97	-9.74	-2.20	77.27	6.22	11
463323.82	4489969.77	-9.45	-3.24	71.05	3.65	11
463314.37	4489966.53	-9.23	-3.84	67.40	-3.46	12
463305.14	4489962.69	-9.41	-3.26	70.86	-8.79	12
463295.73	4489959.42	-9.83	-1.79	79.65	0.74	13
463285.90	4489957.63	-9.79	-1.92	78.91	13.66	13
463276.11	4489955.71	-9.01	-4.16	65.24	28.66	13
463267.10	4489951.55	-5.90	-7.95	36.58	5.21	13
463261.20	4489943.60	-5.21	-8.54	31.37	-0.07	14
463255.99	4489935.07	-5.22	-8.53	31.44	1.02	15
463250.78	4489926.53	-5.06	-8.61	30.43	5.13	15
463245.72	4489917.92	-4.27	-9.04	25.30	2.16	15
463241.44	4489908.88	-3.93	-9.19	23.14	10.04	15
463237.51	4489899.69	-2.24	-9.62	13.11	-3.39	16
463235.27	4489890.07	2.83	-9.55	16.50	-16.23	16
463238.10	4489880.51	5.39	-8.39	32.73	1.39	17
463243.50	4489872.12	5.20	-8.54	31.34	-1.93	18
463248.70	4489863.58	5.48	-8.36	33.27	-9.71	18
463254.18	4489855.22	6.75	-7.24	42.98	-15.42	18
463260.93	4489847.98	8.44	-5.19	58.40	-9.80	18
463269.37	4489842.78	9.27	-3.71	68.20	-8.96	18
463278.64	4489839.08	9.73	-2.22	77.16	-2.96	18
463288.37	4489836.86	9.85	-1.72	80.12	-0.72	18
463298.23	4489835.14	9.87	-1.59	80.84	0.00	18
463308.10	4489833.55	9.87	-1.59	80.84	2.62	19
463317.97	4489831.96	9.79	-2.04	78.22	5.24	19
463327.76	4489829.92	9.55	-2.92	72.98	12.72	19
463337.31	4489826.99	8.64	-4.94	60.26	23.04	19
463345.95	4489822.06	6.04	-7.95	37.22	9.44	19
463351.99	4489814.10	4.64	-8.81	27.78	12.72	19
463356.63	4489805.29	2.59	-9.61	15.06	10.53	19
463359.22	4489795.68	0.79	-9.96	4.53	3.79	19
463360.01	4489785.72	-0.13	-10.00	0.74	-15.14	20
463359.88	4489775.73	-2.69	-9.47	15.88	-29.77	20
463357.19	4489766.26	-7.12	-6.96	45.65	-5.63	20
463350.06	4489759.30	-7.80	-6.25	51.29	-3.86	20
463342.26	4489753.05	-8.20	-5.71	55.15	2.53	21
463334.06	4489747.33	-7.94	-6.07	52.61	5.99	21
463326.12	4489741.27	-7.25	-6.85	46.62	7.53	21
463318.87	4489734.41	-6.29	-7.74	39.09	4.08	21
463312.58	4489726.67	-5.03	-7.19	35.01		
463307.54	4489719.49					

Table C-10. Meander identification for study reach R2 using directional differencing.

Feature Designation		
Suggested Threshold (deg)		
30.00		
Series	**Si (deg)**	**Designation**
1	88.08	MEANDERING
2	-34.81	MEANDERING
3	35.06	MEANDERING
4	-82.49	MEANDERING
5	1.28	ND
6	-7.32	ND
7	9.08	ND
8	-5.60	ND
9	1.28	ND
10	-4.67	ND
11	21.91	ND
12	-12.25	ND
13	48.28	MEANDERING
14	-0.07	ND
15	18.34	ND
16	-19.62	ND
17	1.39	ND
18	-49.50	MEANDERING
19	80.10	MEANDERING
20	-54.40	MEANDERING
21	20.14	ND

STUDY REACH R3

Table C-11. Centerline point locations from study reach R3, and results of subsequent directional differencing.

N (m)	E (m)	X (m)	Y (m)	Direction (deg)	Direction Change (i, deg)	Series
461842.74	4482729.62	-9.96	0.85	85.14	1.22	1
461832.78	4482730.47	-9.94	1.06	83.92	-0.58	2
461822.83	4482731.53	-9.95	0.96	84.50	-1.82	2
461812.88	4482732.48	-9.97	0.64	86.32	-1.24	2
461802.91	4482733.12	-9.99	-0.43	87.56	3.03	3
461792.93	4482732.70	-9.95	-0.95	84.53	6.66	3
461782.98	4482731.74	-9.76	-2.10	77.87	13.58	3
461773.22	4482729.65	-8.99	-4.33	64.29	12.59	3
461764.22	4482725.32	-7.77	-6.13	51.70	17.25	3
461756.46	4482719.18	-5.64	-8.22	34.45	11.22	3
461750.82	4482710.96	-3.93	-9.17	23.22	11.47	3
461746.88	4482701.79	-2.02	-9.73	11.76	8.82	3
461744.86	4482692.06	0.51	-9.99	2.93	1.00	3
461745.37	4482682.08	0.34	-9.99	1.93	0.70	3
461745.71	4482672.08	0.21	-10.00	1.23	0.69	3
461745.92	4482662.08	-0.10	-10.00	0.54	-1.26	4
461745.83	4482652.09	-0.32	-9.99	1.81	-4.88	4
461745.51	4482642.09	-1.16	-9.90	6.69	-4.04	4
461744.35	4482632.19	-1.86	-9.83	10.73	-5.74	4
461742.49	4482622.37	-2.83	-9.59	16.47	-24.93	4
461739.65	4482612.78	-6.53	-7.41	41.39	-18.65	4
461733.12	4482605.37	-8.60	-4.96	60.04	-7.47	4
461724.53	4482600.41	-9.24	-3.83	67.51	-3.51	4
461715.29	4482596.59	-9.44	-3.25	71.02	-12.66	4
461705.84	4482593.34	-9.84	-1.09	83.68	4.82	5
461696.00	4482592.25	-9.79	1.93	78.86	6.01	5
461686.21	4482594.18	-9.55	2.95	72.86	2.85	5
461676.66	4482597.12	-9.40	3.42	70.01	0.00	5
461667.26	4482600.54	-9.40	3.42	70.00	-13.01	6
461657.86	4482603.96	-9.92	1.22	83.01	0.38	7
461647.94	4482605.18	-9.90	-1.28	82.63	13.06	7
461638.05	4482603.90	-9.32	-3.47	69.57	19.08	7
461628.72	4482600.43	-7.61	-6.27	50.49	12.04	7
461621.11	4482594.15	-6.22	-7.83	38.46	3.27	7
461614.90	4482586.32	-5.76	-8.17	35.19	-2.44	8

461609.13	4482578.15	-6.11	-7.92	37.63	4.55	9
461603.03	4482570.23	-5.43	-8.33	33.07	11.89	9
461597.60	4482561.90	-3.61	-9.31	21.19	0.70	9
461593.99	4482552.59	-3.50	-9.36	20.49	-8.03	10
461590.50	4482543.23	-4.77	-8.77	28.52	-4.82	10
461585.73	4482534.46	-5.49	-8.35	33.34	-7.82	10
461580.24	4482526.11	-6.58	-7.52	41.16	-3.59	10
461573.66	4482518.58	-7.04	-7.10	44.75	-2.37	10
461566.62	4482511.48	-7.31	-6.79	47.12	-11.85	10
461559.31	4482504.69	-8.55	-5.15	58.97	-2.94	10
461550.75	4482499.54	-8.82	-4.71	61.91	0.07	11
461541.93	4482494.84	-8.82	-4.72	61.84	1.67	11
461533.11	4482490.12	-8.66	-4.97	60.17	5.87	11
461524.45	4482485.15	-8.12	-5.83	54.30	10.53	11
461516.33	4482479.32	-6.85	-7.15	43.77	15.61	11
461509.48	4482472.16	-4.71	-8.79	28.16	5.14	11
461504.78	4482463.37	-3.91	-9.20	23.02	5.66	11
461500.87	4482454.17	-2.97	-9.50	17.36	12.35	11
461497.90	4482444.67	0.85	-9.69	5.00	-25.92	12
461498.75	4482434.98	5.11	-8.53	30.92	2.92	13
461503.86	4482426.45	4.69	-8.82	28.00	7.21	13
461508.55	4482417.62	3.55	-9.34	20.79	6.26	13
461512.10	4482408.28	2.51	-9.68	14.53	-3.55	14
461514.61	4482398.60	2.88	-8.82	18.08	18.08	15
461517.49	4482389.78					

Table C-12. Meander identification for study reach R3 using directional differencing.

Feature Designation

Suggested Threshold (deg)
30

Series	**Si (deg)**	**Designation**
1	1	ND
2	-3.64	ND
3	87.01	MEANDERING
4	-83.14	MEANDERING
5	13.67	ND
6	-13.01	ND
7	47.82	MEANDERING
8	-2.44	ND
9	17.14	ND
10	-41.42	MEANDERING
11	56.91	MEANDERING
12	-25.92	ND
13	16.39	ND

14	-3.55	ND
15	18.08	ND

APPENDIX D: POINT COUNT DATA FOR INDIVIDUAL FACIES, AND SUBSEQUENT AREA-WEIGHTED DISTRIBUTION FOR EACH REACH

STUDY REACH C1

Table D-1. Surface point count data gathered in riffles and pools in study reach C1.

Riffle Point Counts

	Number Finer Than				
Grainsize (mm)	**Sample 1**	**Sample 2**	**Sample 3**	**Riffle Point Count Totals**	**Percent Finer Than Size**
4	0	5	0	5	2
8	0	0	3	3	2
11	0	0	0	0	2
16	0	0	1	1	3
23	1	1	1	3	4
32	2	3	5	10	7
45	7	6	6	19	13
64	11	13	12	36	24
90	27	12	20	59	42
128	27	37	29	93	71
180	11	17	11	39	83
256	19	11	15	45	97
362	5	3	2	10	100

Pool Point Counts

	Number Finer Than				
Grainsize (mm)	**Sample 1**	**Sample 2**	**Sample 3**	**Pool Point Count Totals**	**Percent Finer Than Size**
4	1	0	0	1	0
8	0	0	2	2	1
11	0	0	0	0	1
16	5	0	0	5	3
23	4	0	0	4	4
32	4	1	4	9	7
45	7	5	0	12	10
64	9	10	7	26	19
90	17	20	14	51	35
128	23	34	29	86	62
180	8	11	20	39	74
256	19	14	31	64	94
362	3	5	7	15	99
512	2	0	0	2	100
724	1	0	0	1	100

Table D-2. Results of area-weighting on determining grain size fractions in study reach C1.

Graphically Determined Grain Size Fractions	
Riffle	**Size (mm)**
D_{16}	50
D_{50}	100
D_{84}	180
Pool	
D_{16}	59
D_{50}	105
D_{84}	205

Facies Area Determinations	
Total Reach Area (m^2)	13855
Total Riffle Area (m^2)	**Total Pool Area (m^2)**
7071	6784
Reach Fraction of Riffles	**Reach Fraction of Pools**
0.51	0.49
Area-Weighted Reach Average Grainsize Fractions (mm)	
D_{16}	54
D_{50}	102
D_{84}	192

STUDY REACH C2

Table D-3. Surface point count data gathered in riffles and pools in study reach C2.

Riffle Point Counts

	Number Finer Than			
Grainsize (mm)	**Sample 1**	**Sample 2**	**Riffle Point Count Totals**	**Percent Finer Than Size**
4	0	0	0	0
8	0	0	0	0
11	0	0	0	0
16	0	2	2	1
23	1	3	4	3
32	5	2	7	6
45	4	4	8	10
64	10	6	16	18
90	20	17	37	37
128	16	21	37	55
180	24	22	46	78
256	20	17	37	96
362	2	4	6	99
512	0	2	2	100

Riffle Point Counts

	Number Finer Than			
Grainsize (mm)	**Sample 1**	**Sample 2**	**Riffle Point Count Totals**	**Percent Finer Than Size**
4	0	4	4	2
8	0	0	0	2
11	0	0	0	2
16	0	1	1	2
23	5	1	6	5
32	8	2	10	10
45	5	6	11	15
64	15	8	23	27
90	17	23	40	46
128	29	26	55	72
180	15	20	35	89
256	6	13	19	99
362	1	0	1	99
512	0	1	1	100
724	0	1	1	100

Table D-4. Results of area-weighting on determining grain size fractions in study reach C2.

Graphically Determined Grain Size Fractions	
Riffle	**Size (mm)**
D_{16}	60
D_{50}	105
D_{84}	150
Pool	
D_{16}	48
D_{50}	93
D_{84}	140

Facies Area Determinations	
Total Reach Area (m^2)	8924
Total Riffle Area (m^2)	**Total Pool Area (m^2)**
7171	1753
Reach Fraction of Riffles	**Reach Fraction of Pools**
0.80	0.20

Area-Weighted Reach Average Grainsize Fractions (mm)	
D_{16}	58
D_{50}	103
D_{84}	148

STUDY REACH C3

Table D-5. Surface point count data gathered in riffles and pools in study reach C3.

Riffle Point Counts

	Number Finer Than				
Grainsize (mm)	**Sample 1**	**Sample 2**	**Sample 3**	**Riffle Point Count Totals**	**Percent Finer Than Size**
4	0	0	0	0	0
8	0	0	1	1	0
11	0	0	1	1	1
16	0	0	0	0	1
23	2	0	1	3	2
32	2	0	2	4	3
45	8	2	7	17	8
64	12	10	10	32	19
90	23	20	17	60	38
128	43	39	18	100	70
180	10	16	20	46	85
256	9	12	20	41	98
362	1	1	3	5	100

Pool Point Counts

	Number Finer Than				
Grainsize (mm)	**Sample 1**	**Sample 2**	**Sample 3**	**Pool Point Count Totals**	**Percent Finer Than Size**
4	0	10	4	14	4
8	0	0	0	0	4
11	0	0	0	0	4
16	0	0	0	0	4
23	0	2	0	2	5
32	3	5	2	10	8
45	16	10	11	37	20
64	31	11	30	72	43
90	26	24	19	69	65
128	22	20	22	64	86
180	13	10	3	26	94
256	1	7	10	18	100
362	0	0	0	0	100

Table D-6. Results of area-weighting on determining grain size fractions in study reach C3.

Graphically Determined Grain Size Fractions

Riffle	Size (mm)
D_{16}	60
D_{50}	100
D_{84}	180
Pool	
D_{16}	40
D_{50}	70
D_{84}	120

Facies Area Determinations

Total Reach Area (m^2)	15180

Total Riffle Area (m^2)	Total Pool Area (m^2)
7570	7610

Reach Fraction of Riffles	Reach Fraction of Pools
0.50	0.50

Area-Weighted Reach Average Grainsize Fractions (mm)

D_{16}	50
D_{50}	85
D_{84}	150

STUDY REACH R1

Table D-7. Surface point count data gathered in riffles and pools in study reach R1.

Riffle Point Counts

Grainsize (mm)	Number Finer Than Sample 1	Sample 2	Riffle Point Count Totals	Percent Finer Than Size
4	0	0	0	0
8	0	0	0	0
11	1	0	1	0
16	1	2	3	2
23	1	0	1	2
32	8	3	11	8
45	14	7	21	18
64	19	16	35	34
90	28	31	59	62
128	21	28	49	86
180	8	8	16	93
256	3	5	8	97
362	3	3	6	100

Pool Point Counts

Grainsize (mm)	Number Finer Than Sample 1	Sample 2	Sample 3	Pool Point Count Totals	Percent Finer Than Size
4	2	4	2	8	3
8	1	3	3	7	5
11	1	1	2	4	6
16	4	1	1	6	8
23	3	1	3	7	10
32	7	3	3	13	15
45	9	7	12	28	24
64	20	13	11	44	38
90	23	20	23	66	59
128	22	24	20	66	81
180	8	15	16	39	93
256	4	8	4	16	98
362	2	0	2	4	100
512	0	1	0	1	100

Table D-8. Results of area-weighting on determining grain size fractions in study reach R1.

Graphically Determined Grain Size Fractions

Riffle	Size (mm)
D_{16}	41
D_{50}	77
D_{84}	130
Pool	
D_{16}	32
D_{50}	77
D_{84}	120

Facies Area Determinations

Total Reach Area (m^2)	13477

Total Riffle Area (m^2)	Total Pool Area (m^2)
4957	8520

Reach Fraction of Riffles	Reach Fraction of Pools
0.37	0.63

Area-Weighted Reach Average Grainsize Fractions (mm)	
D_{16}	35
D_{50}	77
D_{84}	124

STUDY REACH R2

Table D-9. Surface point count data gathered in riffles and pools in study reach R2.

Riffle Point Counts

	Number Finer Than				
Grainsize (mm)	**Sample 1**	**Sample 2**	**Sample 3**	**Riffle Point Count Totals**	**Percent Finer Than Size**
4	0	2	1	3	1
8	0	0	0	0	1
11	0	0	0	0	1
16	0	1	0	1	1
23	2	5	1	8	4
32	4	2	5	11	8
45	11	7	11	29	17
64	12	13	14	39	30
90	25	28	15	68	53
128	25	17	22	64	74
180	10	12	15	37	86
256	7	9	13	29	96
362	2	4	2	8	98
512	1	0	0	1	99
724	1	1	0	2	99
1024	0	2	0	2	100

Pool Point Counts

	Number Finer Than				
Grainsize (mm)	**Sample 1**	**Sample 2**	**Sample 3**	**Pool Point Count Totals**	**Percent Finer Than Size**
4	19	0	23	42	14
8	4	0	2	6	16
11	2	0	0	2	16
16	9	0	1	10	20
23	13	0	4	17	25
32	5	3	9	17	31
45	7	11	16	34	42
64	21	29	18	68	64
90	13	32	16	61	84
128	4	18	6	28	93
180	1	8	3	12	97
256	2	1	6	9	100
362	0	0	1	1	100

Table D-10. Results of area-weighting on determining grain size fractions in study reach R2.

Graphically Determined Grain Size Fractions	
Riffle	**Size (mm)**
D_{16}	42
D_{50}	91
D_{84}	170
Pool	
D_{16}	10
D_{50}	50
D_{84}	94

Facies Area Determinations	
Total Reach Area (m^2)	17193
Total Riffle Area (m^2)	**Total Pool Area (m^2)**
7026	10167
Reach Fraction of Riffles	**Reach Fraction of Pools**
0.41	0.59

Area-Weighted Reach Average Grainsize Fractions (mm)	
D_{16}	23
D_{50}	67
D_{84}	125

STUDY REACH R3

Table D-11. Surface point count data gathered in riffles and pools in study reach R3.

Riffle Point Counts

	Number Finer Than			
Grainsize (mm)	**Sample 1**	**Sample 2**	**Riffle Point Count Totals**	**Percent Finer Than Size**
4	9	16	25	11
8	0	1	1	12
11	1	0	1	12
16	2	2	4	14
23	0	5	5	16
32	2	7	9	20
45	10	8	18	28
64	14	19	33	43
90	22	24	46	63
128	31	17	48	85
180	15	3	18	93
256	4	4	8	96
362	0	0	0	96
512	4	4	8	100

Pool Point Counts

	Number Finer Than			
Grainsize (mm)	**Sample 1**	**Sample 2**	**Pool Point Count Totals**	**Percent Finer Than Size**
4	16	19	35	18
8	1	0	1	18
11	1	0	1	19
16	2	2	4	21
23	7	2	9	25
32	6	7	13	32
45	17	11	28	46
64	17	19	36	64
90	20	13	33	80
128	10	21	31	96
180	4	4	8	100

Table D-12. Results of area-weighting on determining grain size fractions in study reach R3.

Graphically Determined Grain Size Fractions	
Riffle	**Size (mm)**
D_{16}	22
D_{50}	71
D_{84}	103
Pool	
D_{16}	4
D_{50}	49
D_{84}	96

Facies Area Determinations	
Total Reach Area (m^2)	7988
Total Riffle Area (m^2)	**Total Pool Area (m^2)**
1181	6807
Reach Fraction of Riffles	**Reach Fraction of Pools**
0.15	0.85
Area-Weighted Reach Average Grainsize Fractions (mm)	
D_{16}	7
D_{50}	52
D_{84}	97